



University of HUDDERSFIELD

University of Huddersfield Repository

Hussain, Talib

The application of microwave formulation and isothermal titration calorimetry for pharmaceutical compounds

Original Citation

Hussain, Talib (2014) The application of microwave formulation and isothermal titration calorimetry for pharmaceutical compounds. Doctoral thesis, University of Huddersfield.

This version is available at <http://eprints.hud.ac.uk/23397/>

The University Repository is a digital collection of the research output of the University, available on Open Access. Copyright and Moral Rights for the items on this site are retained by the individual author and/or other copyright owners. Users may access full items free of charge; copies of full text items generally can be reproduced, displayed or performed and given to third parties in any format or medium for personal research or study, educational or not-for-profit purposes without prior permission or charge, provided:

- The authors, title and full bibliographic details is credited in any copy;
- A hyperlink and/or URL is included for the original metadata page; and
- The content is not changed in any way.

For more information, including our policy and submission procedure, please contact the Repository Team at: E.mailbox@hud.ac.uk.

<http://eprints.hud.ac.uk/>

The application of microwave formulation
and isothermal titration calorimetry for
pharmaceutical compounds

Talib Hussain

A thesis submitted in partial fulfillment of the requirements for the degree of
Doctor of Philosophy

The University of Huddersfield

2014

Abstract

Solid dispersions are commonly used to overcome bioavailability issues of poorly water soluble drugs. Various preparation methods along with carrier systems have been used to develop solid dispersions. However, this study investigates the application of microwave heating methods in formulation development alongside associated analytical investigations. Formulations of poorly soluble drugs, namely, fenofibrate, gemfibrozil, ibuprofen, ibuprofen (+) S and phenylbutazone were prepared using a microwave technique and compared with standard formulation techniques. Mesoporous silicas and polyethylene glycol were used as excipients. Then in vitro dissolution analysis was carried out for the performance evaluation of the resultant formulations. It was found that effective products were produced as a result of microwave processing compared with the traditional techniques. Analytical techniques such as differential scanning calorimetry (DSC), X-ray diffraction (XRD), scanning electron microscopy (SEM) and Fourier transform infrared spectroscopy ((FTIR) were employed to determine the solid state properties, i.e. thermal stability, crystalline state, physical appearance and chemical stability of developed formulations. The overall findings indicate that successful formulation can be achieved using microwave heating.

Isothermal titration calorimetry (ITC) was used to probe the interactions of model drugs, namely, caffeine, diprophylline, etofylline, paracetamol and theophylline with excipients such as sodium dodecyl sulphate (SDS), sodium deoxycholate (NaDC) and PEG. Thermodynamic data suggests the successful use of ITC to investigate drug-excipient interactions. In summary, the potential of microwave heating in formulation development and ITC to characterise drug-excipient interactions was thoroughly investigated and both found as potential alternatives to more traditional techniques.

Dedication

This thesis is dedicated to my grandfather and mother, without their
love, support and encouragement,
this would not have been possible.

Acknowledgements

I would like to say my humble gratitude and appreciation to almighty ALLAH for all His blessings to accomplish this work. I also would like to express my sincere appreciation to my supervisors, Dr Laura Waters and Dr Gareth Parkes, whose guidance, motivation and understanding make this research experience wonderful and memorable for me.

I would also like to thank the University of Huddersfield for providing me a fee-waiver scholarship to pursue doctoral degree at the School of Applied Sciences. I would also like to thank the University of Huddersfield Graduate Centre for providing me with the much needed conference presentation funds throughout the duration of my PhD.

I would like to extend my thanks to all my colleagues who work in W1/28 and XG/04 for creating a friendly working environment, as well as to the technical staff of the School of Applied Sciences for their laboratory assistance.

I would especially like to thank my grandfather and parents for their patience and moral support.

Finally, I would like to take the opportunity to thank all my sisters, fiancé and uncle for their incredible support and encouragement.

Table of Contents

Abstract	ii
Dedication	iii
Acknowledgements	iv
Table of Contents	v
List of Figures	xi
List of Tables	xvii
Chapter 1: Introduction	1
1.1. Introduction	1
1.2. Formulation development and drug dissolution.....	1
1.3. Strategies to enhance dissolution	6
1.3.1. Salt formation.....	7
1.3.2. Prodrug formation.....	7
1.3.3. Alteration of the solvent system	8
1.3.4. Physical modification.....	8
1.3.5. Particle size reduction	9
1.3.6. Carrier systems.....	11
1.4. Solid dispersion based formulations	13
1.4.1. Classification of solid dispersions	14
1.4.2. Advantages of solid dispersions.....	20
1.4.3. Common problems with solid dispersions.....	21

1.4.4.	Methods for preparing solid dispersions.....	22
1.5.	Drug-excipient interactions	28
1.6.	Isothermal titration calorimetry (ITC).....	31
1.6.1.	ITC instrumentation	32
1.6.2.	General operation of ITC	33
1.6.3.	ITC experiment analysis	34
1.7.	Aims and objectives	38
	References	39
Chapter 2:	Materials and methods.....	52
2.1.	Chemicals	52
2.2.	Methods.....	56
2.2.1.	Mesoporous silica based formulations.....	57
2.2.1.1.	Conventional melt formulation.....	57
2.2.1.2.	Multi-mode microwave processed formulation.....	58
2.2.1.3.	Single-mode microwave processed formulation	59
2.2.2.	Polyethylene glycol 6000 (PEG) based formulations	60
2.2.2.1.	Conventional formulation method.....	60
2.2.2.2.	Microwave formulation method	61
2.3.	Characterisation techniques.....	61
2.3.1.	Dissolution testing	62
2.3.1.1.	In vitro dissolution of mesoporous silica based formulations	62

2.3.1.2.	In vitro dissolution of PEG based formulations	63
2.3.2.	Solid state characterisation	64
2.3.2.1.	X-ray diffraction (XRD).....	64
2.3.2.2.	Differential scanning calorimetry (DSC)	64
2.3.2.3.	Fourier-transform infrared spectroscopy (FTIR).....	65
2.3.2.4.	Scanning electron microscopy (SEM).....	65
2.3.3.	Isothermal titration calorimetry (ITC)	65
	References	71
Chapter 3:	Mesoporous silica based formulations	72
3.1.	Introduction	72
3.2.	Results and discussion.....	74
3.2.1.	In-vitro dissolution of fenofibrate	74
3.2.1.1.	Dissolution studies of Core Shell silica based formulations.....	74
3.2.1.2.	Dissolution studies of Core Shell rehydrox based formulations	77
3.2.1.3.	Dissolution studies of SBA-15 based formulations.....	79
3.2.1.4.	Dissolution studies of Syloid AL-1 based formulations.....	81
3.2.1.5.	Dissolution studies of silica gel based formulations	83
3.2.1.6.	Dissolution studies of Stober based formulations	85
3.2.1.7.	Summary.....	87
3.2.2.	Solid state characterisation	88
3.2.2.1.	Differential scanning calorimetry (DSC) and X-ray diffraction (XRD)	88

3.2.2.2.	Scanning electron microscopy (SEM).....	95
3.2.2.3.	Fourier transform infrared spectroscopy (FTIR).....	98
3.3.	Conclusions.....	101
	References.....	102
Chapter 4: Microwave processed formulations of gemfibrozil using non-ordered mesoporous silica.....		
		104
4.1.	Introduction.....	104
4.2.	Results and discussion.....	105
4.2.1.	In vitro dissolution.....	105
4.2.1.1.	Dissolution studies of Syloid AL-1 based formulations.....	105
4.2.1.2.	Dissolution studies of Syloid 72 based formulations.....	107
4.2.1.3.	Dissolution studies of Syloid 244 based formulations.....	108
4.2.1.4.	Summary.....	109
4.2.2.	Solid state characterisation.....	111
4.2.2.1.	Differential scanning calorimetry (DSC) and X-ray diffraction (XRD) ..	111
4.2.2.2.	Scanning electron microscopy (SEM).....	121
4.2.2.3.	Fourier transform infrared spectroscopy (FTIR).....	122
4.3.	Conclusions.....	125
	References.....	126
Chapter 5: Microwave assisted formulation in the presence of a hydrophilic carrier		
		127
5.1.	Introduction.....	127
5.2.	Results and discussion.....	129

5.2.1.	In vitro dissolution	129
5.2.1.1.	Dissolution studies of ibuprofen.....	129
5.2.1.2.	Dissolution studies of ibuprofen (+) S.....	129
5.2.1.3.	Dissolution studies of fenofibrate.....	133
5.2.1.4.	Dissolution studies of phenylbutazone	135
5.2.1.5.	Summary.....	137
5.2.2.	Solid state characterisation	138
5.2.2.2.	Differential scanning calorimetry (DSC)	142
5.2.2.3.	Scanning electron microscopy (SEM).....	147
5.2.2.4.	Fourier transform infrared spectroscopy (FTIR)	149
5.3.	Conclusions	153
	References	154
Chapter 6:	Drug-exipient interactions: Saturation and micellisation studies of surfactant	
	using isothermal titration calorimetry (ITC).....	156
6.1.	Introduction	156
6.2.	Results and discussion.....	160
6.2.1.	Saturation limit of SDS	160
6.2.2.	Micellisation protocol for surfactants using ITC	163
6.2.3.	Sodium dodecyl sulfate (SDS) micellisation in the presence of model drugs and PEG	166
6.2.4.	Sodium deoxycholate (NaDC) micellisation in the presence of model drugs and PEG	178

6.3. Conclusions	185
References	186
Chapter 7: Conclusions and future work.....	189
Appendix 1: DSC curves of Core Shell (CS), Core Shell rehydrox (CSR) and silica gel (SG) based dry microwave formulations	194
Appendix 2: XRD Patterns for fenofibrate along with Core Shell (CS), Core Shell rehydrox (CSR) and silica gel (SG) based dry microwave formulations	195
Appendix 3: DSC curves of fenofibrate (FF) along with Stober (ST) based physical mixtures and dry microwave (DM) formulations	196
Appendix 4: XRD Patterns for fenofibrate along with Stober (ST) based physical mixtures (PM) and dry microwave (DM) formulations	197
Appendix 5: XRD Patterns for ibuprofen IBU (+) S along with PEG based physical mixtures (PM) and conventionally heated (CH) formulations	198
Appendix 6: XRD Patterns for fenofibrate (FF) along with PEG based physical mixtures (PM) and conventionally heated (CH) formulations	199
Appendix 7: XRD Patterns for phenylbutazone (PB) along with PEG based physical mixtures (PM) and conventionally heated (CH) formulations	200
Appendix 8.....	201

List of Figures

Figure 1.1: The drug research process	2
Figure 1.2: The fate of a drug administered via the oral route depicting the various biochemical and enzymatic factors responsible for poor bioavailability	3
Figure 1.3: The Biopharmaceutical Classification system (BCS)	4
Figure 1.4: Surfactant micellisation and demicellisation.....	13
Figure 1.5: Phase diagram of a eutectic system	14
Figure 1.6: Schematic of a) substitutional crystalline solid solution and b) an interstitial crystalline solid solution.	15
Figure 1.7: An amorphous solid solution.....	16
Figure 1.8: Isothermal titration calorimetry instrumentation	32
Figure 2.1: Schematic view of the single-mode microwave system.....	57
Figure 2.2: Example of processing of fenofibrate and Core Shell (1:1) using the multi-mode microwave system.....	59
Figure 2.3: Example of processing of fenofibrate and Core Shell (1:5) using the single mode microwave system.....	60
Figure 2.4: Dissolution apparatus used for analysing formulations	62
Figure 2.5: A MicroCal VP-ITC used in this study to investigate the thermodynamics of drug-excipient interactions.....	66
Figure 2.6: ITC calibration of barium (Ba^{+2}) and 18-crown-6	67
Figure 3.1: Fenofibrate release profiles for pure fenofibrate along with Core Shell (CS) based formulations	76
Figure 3.2: Fenofibrate release profiles for pure fenofibrate (FF) along with Core Shell rehdrox (CSR) based formulations	78

Figure 3.3: Fenofibrate release profiles for pure fenofibrate (FF) along with SBA-15 (SBA) based formulations	80
Figure 3.4: Fenofibrate release profiles for pure fenofibrate (FF) along with Syloid AL-1 (SYL 1) based formulations	82
Figure 3.5: Fenofibrate release profiles for pure fenofibrate (FF) along with silica gel (SG) based formulations	84
Figure 3.6: Fenofibrate release profiles for pure fenofibrate (FF) along with Stober (ST) based formulations	86
Figure 3.7: DSC curves for fenofibrate (FF) along with SBA-15 (SBA).....	89
Figure 3.8: DSC curves for fenofibrate (FF) along with Syloid AL-1 (SYL 1).....	90
Figure 3.9: XRD pattern for fenofibrate (FF) and SBA-15 (SBA).....	93
Figure 3.10: XRD pattern of fenofibrate (FF) and Syloid AL-1 (SYL 1)	94
Figure 3.11: SEM images of (a) Core Shell, (b) Core Shell rehdrox, (c) SBA-15, (d) silica gel, (e) Syloid AL-1, (f) Stober.....	95
Figure 3.12: SEM images of (a) fenofibrate, (b) a physical mix of CS and FF (1:1), (c) TH formulation of CS and FF (5:1), (d) WM formulation of CS and FF (5:1) and DM formulation CS/FF at ratios of (e) 1:1 and (f) 5:1.....	96
Figure 3.13: SEM images of (a) SBA-15, (b) DM SBA-15/FF (5:1), (c) Silica gel, (d) DM Silica gel/FF (5:1)	97
Figure 3.14: FTIR spectra of pure fenofibrate, Core Shell and SBA-15 silica.....	99
Figure 3.15: FTIR spectra of fenofibrate (FF) along with Core Shell (CS), Core Shell Rehydrox (CSR), SBA-15 (SBA), Syloid AL-1 (SYL 1), Silica gel (SG) and Stober (ST)...	100
Figure 4.1: Gemfibrozil release profiles for pure gemfibrozil (GF) along with Syloid AL-1 ...	106

Figure 4.2: Gemfibrozil release profiles for pure gemfibrozil (GF) along with Syloid 72	107
Figure 4.3: Gemfibrozil release profiles for pure gemfibrozil (GF) along with Syloid 244	109
Figure 4.4: DSC profiles for gemfibrozil (GF) along with Syloid AL-1.....	112
Figure 4.5: DSC profiles for gemfibrozil (GF) along with Syloid 72	114
Figure 4.6: DSC profiles for gemfibrozil (GF) along with Syloid 244	115
Figure 4.7: XRD pattern of gemfibrozil (GF) and Syloid AL-1.....	117
Figure 4.8: XRD pattern of gemfibrozil (GF) and Syloid 72	119
Figure 4.9: XRD pattern of gemfibrozil (GF) and Syloid 244	120
Figure 4.10: SEM images of (a) gemfibrozil, (b) Syloid AL-1, (c) a physical mix of Syloid AL-1 and gemfibrozil (1:1), (d) microwave formulation of Syloid AL-1 and gemfibrozil (1:1)	121
Figure 4.11: SEM images of (a) Syloid 72, (b) microwave formulation of Syloid 72 and gemfibrozil (1:1), (c) Syloid 244, (d) microwave formulation of Syloid 244 and gemfibrozil (1:1).....	122
Figure 4.12: FTIR spectra of pure gemfibrozil and Syloid 244 silica	123
Figure 4.13: FTIR spectra of Syloid 72, Syloid 244 and Syloid AL-1.....	124
Figure 5.1: Ibuprofen release profiles for pure ibuprofen (IBU) along with PEG based formulations	131
Figure 5.2: Ibuprofen (+) S release profiles for pure ibuprofen (+) S (IBU S) along with PEG based formulations	132
Figure 5.3: Fenofibrate release profiles for pure fenofibrate (FF) along with PEG based formulations	134

Figure 5.4: Phenylbutazone release profiles for pure phenylbutazone (PB) along with PEG based formulations	136
Figure 5.5: XRD patterns for ibuprofen (IBU) and physically mixed (PM), conventionally heated and dry microwave (MW) based formulations.....	139
Figure 5.6: XRD patterns for PEG with microwave (MW) formulations of ibuprofen (+) S (a), fenofibrate (FF) (b) and phenylbutazone (PB) (c) at 5:1 and 1:1 ratios along with each pure drug	141
Figure 5.7: DSC profiles for ibuprofen (IBU) and PEG along with PEG based physical mixtures (PM), conventionally heated (CH) products and microwave (MW* and MW) formulations all at PEG / drug ratios of 1:1 and 5:1	143
Figure 5.8: DSC profiles for ibuprofen (+) S (IBU S) and PEG along with PEG based physical mixtures (PM), conventionally heated (CH) products and microwave (MW) formulations all at PEG / drug ratios of 1:1 and 5:1	144
Figure 5.9: DSC profiles for PEG, fenofibrate (FF) and phenylbutazone (PB) along with PEG based microwave (MW) formulations all at PEG / drug ratios of 1:1 and 5:1.....	146
Figure 5.10: SEM images (magnification x 1000) of (a) PEG, (b) pure ibuprofen (IBU), (c) a physical mix of PEG and IBU (5:1), (d) conventionally heated formulation of PEG and IBU (5:1), (e) microwave processed (MW*) product of PEG and IBU (5:1), (f) microwave processed (MW) product of PEG and IBU (5:1)	148
Figure 5.11: SEM images (magnification x 1000) of (a) pure ibuprofen (+) S (IBU S), (b) microwave processed (MW*) formulation of PEG and IBU S (5:1), (c) microwave processed (MW) formulation of PEG and IBU S (5:1), (d) pure fenofibrate (FF), (e) microwave processed (MW*) formulation of PEG and FF, (f) microwave processed (MW) formulation of PEG and FF, (g) pure phenylbutazone (PB), (h) microwave processed (MW*) formulation of PEG and PB and (i) microwave processed (MW) formulation of PEG and PB	149

Figure 5.12: FTIR spectrum of pure PEG, ibuprofen (IBU), ibuprofen (+) S (IBU S), phenylbutazone (PB) and fenofibrate (FF)	151
Figure 5.13: FTIR spectra of microwave formulations (MW) of ibuprofen (IBU), ibuprofen (+) S (IBU S), phenylbutazone (PB) and fenofibrate (FF)	152
Figure 6.1: Transformation of micelles into different shapes on increasing surfactant	157
Figure 6.2: Chemical structure of NaDC, $R_1 = H$ and $R_2 = OH$ with hydrophobic and hydrophilic surfaces	159
Figure 6.3: Raw ITC data for the saturation of SDS micelles with caffeine at 298 K	161
Figure 6.4: Schematic representation of a typical demicellisation experiment	165
Figure 6.5: Raw ITC data and subsequent data analysis to determine the CMC of SDS in aqueous solution at 298 K	167
Figure 6.6: Raw ITC data and subsequent data analysis to determine the CMC of SDS in the presence of Paracetamol at 298 K	168
Figure 6.7: Raw ITC data and subsequent data analysis to determine the CMC of SDS in the presence of PEG-6000 at 298 K	173
Figure 6.8: The effect upon micellisation of SDS in the presence of PEG and five model compounds	175
Figure 6.9: Enthalpy change for the titration of 200 mM SDS into deionised water or 0.02 mM PEG at 298 K	177
Figure 6.10: Integrated ITC heat data indicating the micellisation point of (a) NaDC alone (CMC 1 and 2) and (b) in the presence of PEG at 298 K	179
Figure 6.11: Raw ITC data for the titration of 50 mM NaDC into a 60 mM paracetamol solution at (a) 298 K, (b) 304 K and (c) 310 K	182

Figure 6.12: Enthalpy change for titration of 50 mM NaDC into deionised water and 0.02 mM PEG at 298 K.....183

List of Tables

Table 2.1: Physicochemical properties of chemicals	53
Table 2.2: Physicochemical properties of mesoporous silica	55
Table 4.1: Physical characteristics of mesoporous silica	105
Table 6.1: Molecular ratios and associated enthalpic values for the micellar saturation of SDS in the presence of five drugs at T = 298 K and 310 K.....	162
Table 6.2: Critical micellar concentrations and thermodynamic values associated with the micellisation of SDS in the presence of five model compounds at 298, 304 and 310 K.....	169
Table 6.3: Critical micellar concentrations and thermodynamic values associated with the micellisation of SDS in the presence of PEG and five model compounds at 298, 304 and 310 K.....	174
Table 6.4: Critical micellar concentrations and thermodynamic values associated with the micellisation of NaDC in the presence of five model compounds at 298, 304 and 310 K....	180
Table 6.5: Critical micellar concentrations and thermodynamic values associated with the micellisation of NaDC in the presence of PEG and five model compounds at 298, 304 and 310 K.....	184

Chapter 1: Introduction

1.1. Introduction

Advances in combinatorial chemistry and high-throughput screening have facilitated the development of highly potent and versatile new chemical entities. In spite of having such incredible properties, very few of these compounds reach the market because of their poor aqueous solubility and associated bioavailability. Drugs need to be fully dissolved in the gastrointestinal (GI) tract to be absorbed into general circulation to produce a pharmacological response. Various approaches have been used to circumvent such issues utilising excipients that can enhance the solubility of an active pharmaceutical ingredient (API). There are several proposed mechanisms by which excipients can increase the dissolution rate of insoluble APIs. For example, the solubilising effect of surfactants, inclusion complexes with cyclodextrins, API-excipient binding through covalent or hydrogen-bonding and adsorption of the API onto excipient. However, a judicious choice of excipients could also possibly decrease the adverse effects associated with the drug delivery system. The choice of a suitable excipient is a combination of its physicochemical properties and interaction with the drug. Therefore, designing an optimised formulation requires a thorough investigation into API-excipient interactions.

1.2. Formulation development and drug dissolution

Drugs have traditionally been administered in several forms, namely, ingestion, inhalation, injection, infusion, and topical application (Fasinu et al., 2011). Oral delivery is the most preferred route of drug administration, accounting for more than a 50 % share of the global drug delivery market. The convenience of drug administration and patient compliance

make it the most frequent and suitable drug delivery route (Desai et al., 2012). However, this route of delivery is not devoid of challenges which can result in poor bioavailability (Alam et al., 2013, Henchoz et al., 2009). Investigating a potential drug candidate is a complex, time-consuming and costly procedure which is divided into two phases, namely drug discovery and drug development as depicted in Figure 1.1. An inappropriate pharmacokinetic profile has been recognised as one of the key factors leading to the rejection of chemical entities during drug development. Therefore, rigorous studies are conducted to select a pharmaceutical compound that has significant potency and a suitable pharmacokinetic profile (Henchoz et al., 2009, Alam et al., 2013, Kerns, 2001).

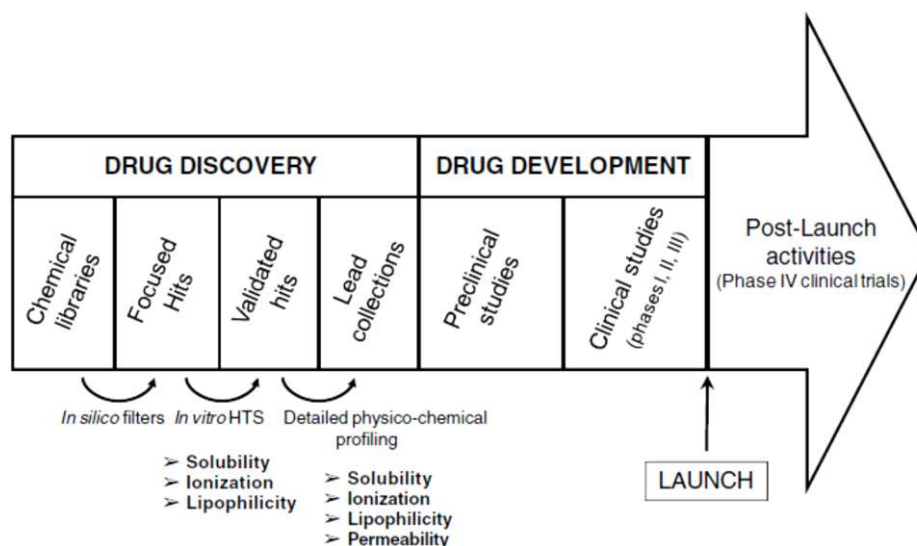


Figure 1.1: The drug research process: adapted from (Henchoz et al., 2009).

Among physicochemical properties, solubility is a parameter of prime importance in drug development as poor aqueous solubility limits the efficacy of compounds. To achieve optimal success with oral administration, drug molecules need to dissolve and permeate through the gastrointestinal tract (Alam et al., 2013). The extent of oral bioavailability is also affected by physiological factors, including, luminal degradation (Granero and Amidon, 2006), ionisation of the compounds (Kostewicz et al., 2004), intestinal mucosal metabolism (Lown et al., 1997,

Choi et al., 2011, S. Darwich et al., 2010), hepatic metabolism (Zhu et al., 2010), a narrow absorption window and active influx/efflux transporters (Murphy et al., 2012, Lown et al., 1997, Choi et al., 2011). In general, it can be stated that the rate of absorption, and therefore extent of clinical effect, are determined by the dissolution of the drug and subsequent transport into general blood circulation (Alam et al., 2013) as illustrated in Figure 1.2.

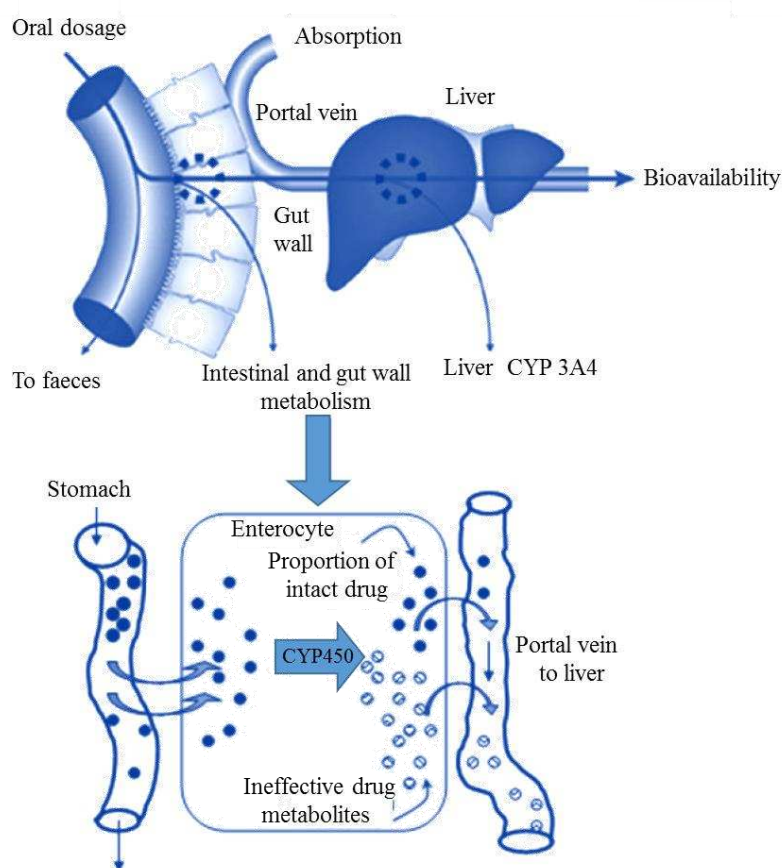


Figure 1.2: The fate of a drug administered via the oral route depicting the various biochemical and enzymatic factors responsible for poor bioavailability (Fasinu et al., 2011).

The pharmacokinetic profile of an orally administered drug is based on interacting parameters associated with absorption, distribution, metabolism, and excretion (ADME). The absorption component of this cascade can be assessed in the context of Fick's First law (Eq. 1.1), where the flux (J) of a drug through the GI wall depends on the permeability coefficient

(P) of the GI barrier for the drug and the drug concentration (C) in the gastrointestinal lumen (assuming sink conditions) (Brouwers et al., 2009):

$$J = PC \quad (\text{Eq. 1.1})$$

Combining these two parameters, namely, solubility and permeability explains the basis of the biopharmaceutical classification system (BCS) (Amidon et al., 1995). The BCS is an important tool, providing a better understanding of physicochemical and biopharmaceutical properties of drugs and is used in decision making when developing formulations (Kawabata et al., 2011, Amidon et al., 1995). According to the BCS, four different drug groups are specified (Figure 1.3).

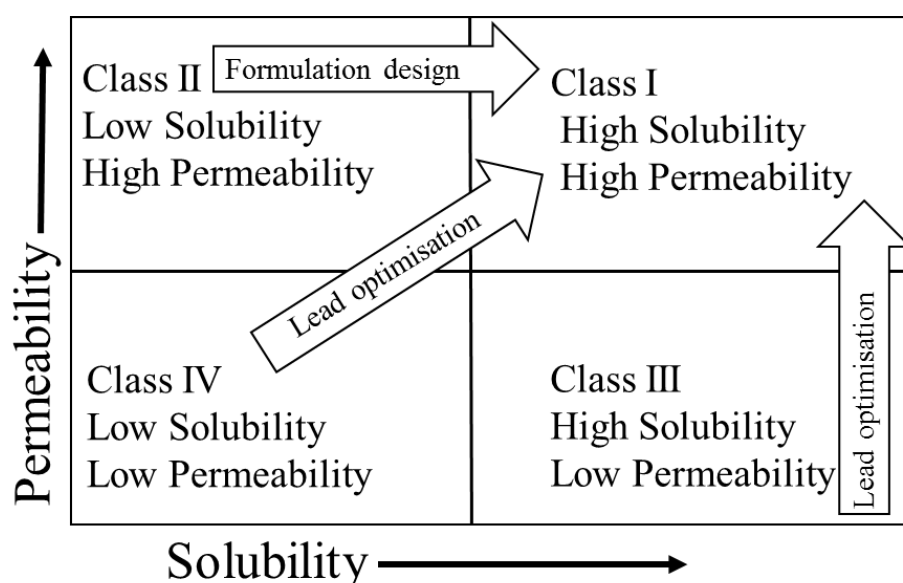


Figure 1.3: The Biopharmaceutical Classification system (BCS) (Amidon et al., 1995).

Definitions for the BCS are (Langham, 2011, Alam et al., 2013);

1. A drug is classed as poorly soluble if the highest dose strength of the immediate release product is not soluble in 250 mL or less of aqueous media over the pH range of 1 to 7.5.

2. A drug is classed as having low intestinal permeability when the extent of absorption in humans is less than 90 % of the administered dose based on a mass - balance determination or in comparison with an intravenous dose.
3. A drug is classed as rapidly dissolving if ≥ 85 % of the immediate release dissolves within 30 minutes with either USP dissolution apparatus I at 100 rpm or USP dissolution apparatus II at 50 rpm in ≤ 900 mL of 1 N HCl, or simulated gastric fluid, or pH 4.5 and pH 6.8 buffer, or simulated intestinal fluid.

Drugs need to dissolve in gastrointestinal fluids to permeate the gut wall, passing through the liver without being inactivated and reaching systemic blood circulation to produce a pharmacological response which requires good aqueous solubility. However, the majority of newly developed compounds are lipophilic in nature resulting in poor dissolution profiles owing to their low aqueous solubility (Janssens and Van den Mooter, 2009). Therefore, the rate of dissolution is the most influential factor controlling the bioavailability of drugs.

The chemists Arthur Noyes and Willis Whitney published a mathematical expression for dissolution in a paper entitled “The rate of solution of solid substances in their own solution” (Noyes and Whitney, 1897). A modified form of the Noyes-Whitney equation highlights important factors affecting the dissolution profile of poorly soluble drugs, (Leuner and Dressman, 2000, Alam et al., 2013, Janssens and Van den Mooter, 2009) as expressed in Eq. (1.2):

$$\frac{\partial C}{\partial t} = \frac{AD(C_s - C)}{h} \quad (\text{Eq. 1.2})$$

where $\partial C/\partial t$ is the rate of dissolution, A is the surface area available for dissolution, D is the diffusion coefficient of the compound, C_s is the solubility of compound in the dissolution medium, C is the concentration of drug in the medium at time t and h is the thickness of the diffusion boundary layer adjacent to the surface of dissolving compound.

Using parameters outlined in the Noyes-Whitney equation leads to the following possibilities for improving the solubility of poorly water soluble drugs (Leuner and Dressman, 2000):

1. Increasing the surface area by reducing the particle size of compound, i.e. increasing A
2. Improving the wetting properties of the compound
3. Reducing the boundary-layer thickness, i.e. reducing h
4. Ensuring sink conditions are maintained
5. Enhancing drug solubility in the physiological relevant dissolution media, i.e. increasing C_s

Hence, the following three approaches could be considered for the development of an enhanced effective drug delivery system (Fasinu et al., 2011):

1. Modification of the physicochemical properties of the drug molecule (for example, modifying lipophilicity and enzyme susceptibility)
2. Addition of novel functionality (e.g. receptor recognition or cell permeability)
3. The use of an innovative drug delivery system

1.3. Strategies to enhance dissolution

There are six common strategies used to enhance the dissolution and bioavailability of drugs, namely, salt formation, prodrug formation, solvent modification, physical modification, particle size reduction and carrier systems.

1.3.1. Salt formation

An enhanced dissolution profile of a solid oral dosage form can sometimes be achieved through salt formation (Nelson, 1957, Nelson, 1958). This is the most common technique in the pharmaceutical industry for ionisable drugs because stable ionic bonds can be formed when the ionisable group on the drug and the salt's counter-ion have a difference in pK_a values of at least three units thus preventing dissociation (Bowker, 2002, Childs et al., 2007). According to the Henderson-Hasselbalch equation, the aqueous solubility of ionisable drugs is highly dependent on pH which can be altered through salt formation (Avdeef, 2007). For example, celecoxib (in the form of the sodium salt) displayed an enhanced dissolution rate and oral bioavailability compared with the corresponding free acid form (Guzman et al., 2007). Another example is the solubility of haloperidol mesylate which is significantly higher than that of its hydrochloride salt at a lower pH (Li et al., 2005). In summary, an appropriate salt form can possibly help enhance solubility depending upon the physicochemical properties of the drug under investigation.

1.3.2. Prodrug formation

The concept of a “prodrug” was introduced by Adrian Albert in 1958 to describe compounds that undergo biotransformation prior to eliciting their pharmacological effect, i.e. “therapeutic agents that are inactive but can be transformed into one or more active metabolites” (Albert, 1958). Forming a prodrug has become an established technique and a powerful tool in optimising pharmacologically potent structures and overcoming physicochemical, pharmaceutical and biopharmaceutical barriers to a drug's usefulness (Stella and Nti-Addae, 2007, Fleisher et al., 1996, Rautio et al., 2008). To develop a successful prodrug, there must be a suitable functional group on the compound along with a mechanistic

pathway in the body to transform the prodrug into an active metabolite after administration (Stella and Nti-Addae, 2007).

1.3.3. Alteration of the solvent system

A change in pH significantly affects the solubility of poorly water soluble drugs having functional groups that can be protonated or deprotonated. pH modification can be used for both oral and parenteral administrations. To evaluate the appropriateness of this approach for a particular formulation, the buffer capacity and suitability of the selected pH must be considered. The extent of solubility of drugs changes as the pH increases from stomach to intestine (Lachman et al., 1986, Venkatesh et al., 1996). Furthermore, the pK_a value of a compound is an important factor to be considered when changing the pH of the solvent when improving the solubility of a drug (McMorland et al., 1986, Jain et al., 2004). pH adjustment is also used with co-solvents to enhance the solubility of poorly soluble drugs (Vemula et al., 2010).

1.3.4. Physical modification

Many drug-like compounds can exist in several different solid forms ranging from disordered amorphous materials to ordered crystalline materials. Materials having the same chemical composition but different lattice structures are known as polymorphs and this phenomenon is polymorphism (Kawabata et al., 2011, Rodríguez-Spong et al., 2004). The physicochemical properties of polymorphs, including solubility, physical stability, melting point, density and compatibility make them potential candidates for pharmaceutical research (Brittain, 1999, Kawabata et al., 2011). Previous studies have reported that metastable forms

of polymorphs are more soluble than thermodynamically stable forms (Blagden et al., 2007) and this difference in solubility can be significant (Pudipeddi and Serajuddin, 2005).

The formation of polymorphs is an effective strategy to improve the dissolution profile for poorly soluble drugs. However, it is necessary to monitor for further polymorphic transformations during both manufacturing and storage of dosage forms to ensure reproducibility. This is because metastable forms will eventually transform into thermodynamically stable forms which may exhibit variations in bioavailability (Kawabata et al., 2011).

In recent years, considerable attention has been given to co-crystals to increase the dissolution rate of poorly water-soluble drugs. These are defined as crystalline materials comprised of at least two different components (Schultheiss and Newman, 2009). Pharmaceutical co-crystals are formed with an API and a guest molecule (co-crystal former) without any proton transfer but in many cases, requires hydrogen bonding to make a stable co-crystal. Generally, pK_a is an indicator for distinguishing between salts and co-crystals (Kawabata et al., 2011). There have been several studies claiming an improved dissolution rate and oral bioavailability by co-crystal formation (Jung et al., 2010, McNamara et al., 2006). One such example is AMG-517 (Amgen) which is a potent and selective VR1 antagonist. It is a base and the co-crystals with ascorbic acid demonstrated a higher dissolution rate in the fasted state simulated intestinal fluid compared with the original form (Bak et al., 2008).

1.3.5. Particle size reduction

Dissolution is intrinsically related to particle size as reducing the size of particles provides a larger surface area resulting in an increased rate of dissolution owing to the

improved solvation of the solute (Savjani Ketan et al., 2012). Therefore, this approach is widely used to increase the dissolution rate of a drug (Hörter and Dressman, 2001). According to the Prandtl boundary layer equation, a decrease of the diffusion layer thickness by reducing particle size, particularly down to $< 5 \mu\text{m}$, results in accelerated dissolution (Mosharraf and Nyström, 1995). The micronisation approach to enhance the bioavailability of poorly water-soluble drugs such as griseofulvin, digoxin, and felodipine has proven successful (Atkinson et al., 1962, Jounela et al., 1975, Scholz et al., 2002). The micronised drug particles are obtained through mechanical pulverisation while jet milling, ball milling and pin milling are also commonly used. Micronisation of drug particles sometimes results in agglomeration which can decrease the dissolution rate by reducing the available surface area. Surfactants have previously been employed to avoid such issues (Kawabata et al., 2011).

Nanocrystal formation is an attractive technique for poorly water soluble drugs, used to reduce particle size to a nano-meter range ($< 1 \mu\text{m}$). An increase in dissolution can be observed by decreasing particle size to less than $1 \mu\text{m}$, as described by Ostwald-Freundlich's equation (Müller and Peters, 1998). Nanocrystal formulations are commonly produced by wet-milling with beads, high-pressure homogenisation, or controlled precipitation (Shegokar and Müller, 2010). Nanocrystals are obtained after dispersing drug particles into inert carriers followed by a drying process such as spray drying or freeze drying. Most importantly for stabilised nanocrystals, hydrophilic polymers and/or surfactants are also used. These products can be defined as a crystalline solid dispersion (CSD). There have been numerous studies demonstrating an enhanced oral bioavailability of pharmaceuticals and nutraceuticals by nanocrystal technologies (Xia et al., 2010, Wu et al., 2004, Sylvestre et al., 2011, Fakes et al., 2009). Nanocrystal formulations of either neutral or acidic compounds such as danazol (Liversidge and Cundy, 1995), cilostazol (Jinno et al., 2006), tranilast (Kawabata et al., 2010)

and curcumin (Onoue et al., 2010) have been found to exhibit enhanced pharmacokinetic profiles compared with basic compounds through using nanocrystal technologies.

1.3.6. Carrier systems

Drugs have been incorporated with a range of carrier systems as a technique to enhance dissolution. For example, complexation of drugs with cyclodextrin has been achieved using different methods, including kneading (Swarbirck and Boylan, 2001), co-precipitation (Baboota et al., 2005), solvent evaporation (Parikh et al., 2005), lyophilisation (Chiou and Riegelman, 1971) and microwave irradiation (Charman, 2000). Cyclodextrins are oligosaccharides containing a hydrophilic exterior and hydrophobic core in which appropriate sized drug molecules can form non-covalent complexes resulting in improved aqueous solubility and chemical stability (Loftsson and Brewster, 1996). Cyclodextrins and their derivatives have been extensively used in pharmaceutical research to enhance the dissolution rate of poorly soluble drugs and currently more than ten solid dosage forms containing cyclodextrins are available on the market (Kawabata et al., 2011).

In recent years, self-emulsification drug-delivery systems (SEDDS) have been utilised to enhance the oral bioavailability of poorly water soluble drugs, especially highly lipophilic drugs. A SEDDS is an isotropic mixture of oil, surfactant, co-solvent, and solubilised drug (Neslihan Gursoy and Benita, 2004). These formulations are further classified into self-microemulsifying drug delivery systems (SMEDDS) and self-nanoemulsifying drug delivery systems (SNEDDS) according to the size range of the oil droplets (Kohli et al., 2010). Improved oral bioavailability, and subsequently higher plasma concentrations of drugs, is attributed to the rapid emulsification of these formulations whereas the droplet size of the emulsion has a pronounced effect on the extent of absorption. Neoral[®], a cyclosporin SNEDDS

formulation, is a good example of the effectiveness of the utilisation of droplets of a smaller size. Neoral[®] has an increased maximum plasma concentration (C_{max}) and absorption area under the curve (AUC) compared with Sandimmune[®], a coarse SMEDDS formulation, in humans (Mueller et al., 1994). The intrinsic lipophilicity of a drug is the prime requirement of a SEDDS as the API must be dissolved in a limited amount of oil within the formulation. (Kawabata et al., 2011).

Surfactants have been used to improve the solubility of water-insoluble drugs for many years (Gharaei-Fathabad, 2011). Surfactants have the ability to form micelles at a certain concentration known as the critical micelle concentration (CMC) and the phenomenon is called micellisation (Figure 1.4). Micellisation results from a delicate balance of intermolecular forces, including hydrophobic, steric, electrostatic, hydrogen bonding and Van der Waals interactions. The hydrophobic effect associated with the nonpolar surfactant tail is the main attractive force whereas the main opposing force results from steric and electrostatic repulsion between the surfactant polar heads (Rangel-Yagui et al., 2005b, Torchilin, 2007). Micelles reduce surface tension and increase solubility by entrapping drug molecules inside the hydrophobic core (Emara et al., 2002a), i.e. they have an ability to increase the solubility of drugs in water (Hosseinzadeh et al., 2009). Therefore, the utilisation of micelles can be advantageous for drug delivery purposes with the possibility of improving bioavailability, reducing toxicity and enhancing permeability across physiological barriers (Torchilin, 2007). Drug interactions with micelles can induce changes in the physiochemical properties of drugs (solubility, spectroscopic and acid-base properties) and these can be used to quantify the degree of drug-micelle interaction, expressed as the drug-micelle binding constant and micelle-water partition coefficient (Čudina et al., 2005).

Often non-ionic surfactants are used, including polysorbates, polyoxyethylated castor oil, polyoxyethylated glycerides, lauroyl macroglycerides, and mono- and di-fatty acid esters of low molecular weight polyethylene glycols, to stabilise micro emulsions and suspensions into which drugs are dissolved (Rangel-Yagui et al., 2005).

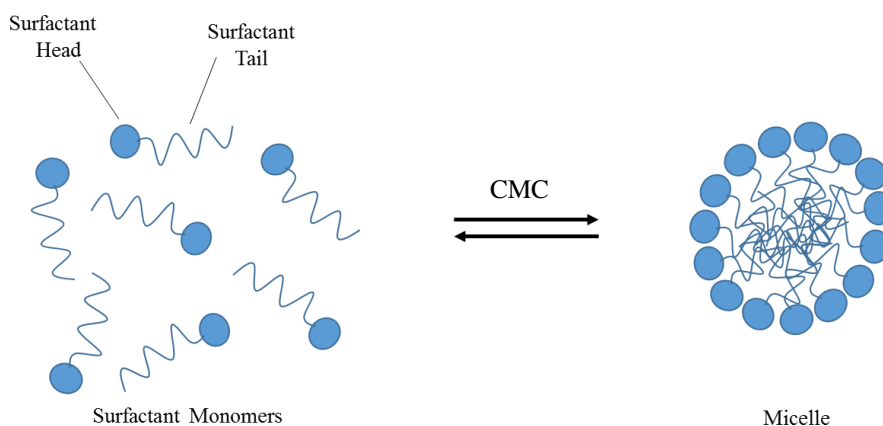


Figure 1.4: Surfactant micellisation and demicellisation.

1.4. Solid dispersion based formulations

Solid dispersion has been considered one of the major developments in overcoming bioavailability issues of poorly water soluble drugs with several successfully marketed products (Vo et al., 2013). These have been defined as a dispersion of one or more pharmaceutically active ingredients in an inert carrier or matrix in the solid state prepared by solvent, melting or solvent-melting methods (Chiou and Riegelman, 1971; Janssens and Van den Mooter, 2009).

Several studies on solid dispersions have been published, confirming the advantageous properties of solid dispersions in increasing the solubility and dissolution rate of poorly water soluble drugs. Solid dispersions tend to reduce particle size, possibly to a molecular level, and

change the crystalline state of drugs, thereby promoting their solubility (Vasconcelos et al., 2007; Vo et al., 2013).

1.4.1. Classification of solid dispersions

First generation solid dispersions are known as crystalline solid dispersions. Sekiguchi and Obi prepared solid dispersions for the first time using urea as a carrier to form a eutectic mixture with sulphathiazole (Sekiguchi and Obi, 1961). The eutectic (or monotectic) mixture is formed when a crystalline drug is dispersed within a crystalline carrier (Chiou and Riegelman, 1971). The melting temperature of the eutectic mixture is lower than the API and carrier as both the drug and carrier are crystallised simultaneously in the cooling process, resulting in a dispersed state, thus improving the dissolution rate (Figure 1.5) (Leuner and Dressman, 2000). Moreover, if the system is not specifically at a eutectic composition, the solid dispersion will comprise of a blend of the microfine dispersion and another constituent as a distinct phase because one component will be progressively crystalline until the eutectic point is reached.

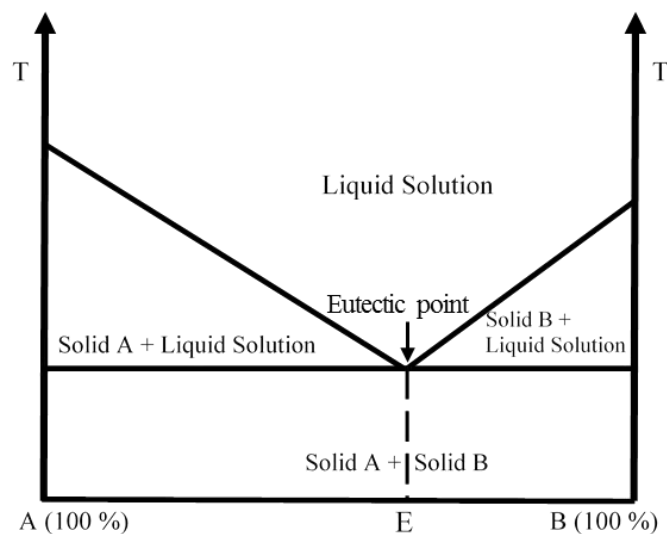


Figure 1.5: Phase diagram of a eutectic system (Leuner and Dressman, 2000).

An API can exist as a substitutional crystalline solid solution (where drug molecules can substitute carrier molecules in the crystal lattice) or an interstitial crystalline solid solution (where drug resides in interstitial spaces between the solvent molecules) in the crystal lattice (Figure 1.6) (Leuner and Dressman, 2000).

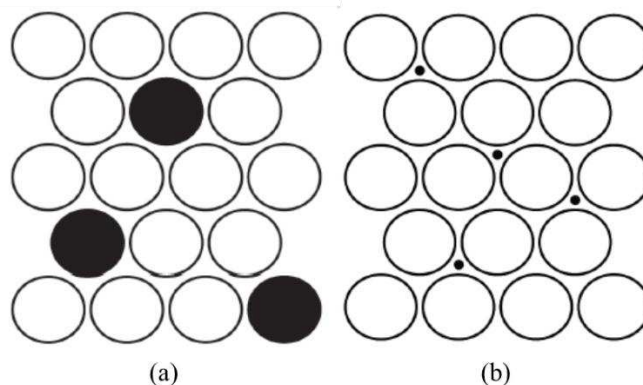


Figure 1.6: Schematic of a) substitutional crystalline solid solution and b) an interstitial crystalline solid solution. Solvent molecules are represented as open circles, and filled circles indicate solute molecules (Leuner and Dressman, 2000).

Urea (Sekiguchi and Obi, 1961) and sugars such as sorbitol and mannitol (Jachowicz, 1987) are crystalline carriers generally used in first generation solid dispersions. The small particle size, improved wettability and polymorphic change are the leading factors for enhancing drug solubility and dissolution. The results of mannitol-based solid dispersions using nifedipine as a model drug revealed significant enhancement in the dissolution rate of nifedipine compared with the physical mixture, despite retaining the crystalline state (Zajc et al., 2005). Okonogiet and co-workers (1997) developed a solid dispersion of ofloxacin with urea and mannitol. The urea based solid dispersions exhibited a higher solubility and dissolution rate than mannitol because of a greater reduction in the degree of crystallinity as revealed by X-ray diffraction and differential scanning calorimetry. The prominent drawback of crystalline solid dispersions is the high thermodynamic stability of the carriers that decreases their dissolution rate compared with amorphous solid dispersions.

In the late sixties (Simonelli et al., 1969; Chiou and Riegelman, 1969), second generation solid dispersions appeared containing amorphous carriers, also known as amorphous solid dispersions (Figure 1.7). These can be classified into amorphous solid solutions (glass solutions), amorphous solid suspensions or mixtures of both, according to the physical state of the drug (Vo et al., 2013).

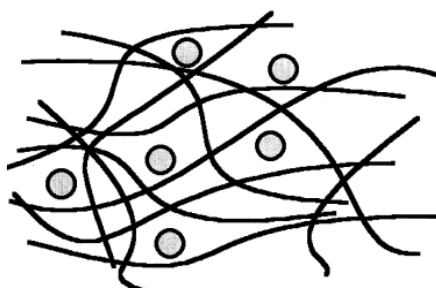


Figure 1.7: An amorphous solid solution (Leuner and Dressman, 2000).

In amorphous solid solutions, the drug and amorphous carrier are miscible to form a molecularly consistent mixture while an amorphous solid suspension comprises of two distinct phases, formed with drugs having a high melting point or limited solubility in the excipient (Van Drooge et al., 2006). When an API is dissolved and/or suspended in the carrier, a heterogeneous system is obtained with mixed properties of amorphous solid solutions and amorphous solid suspensions, respectively (Vasconcelos et al., 2007). In amorphous solid dispersions, drug molecules are dispersed in an amorphous carrier (Tanaka et al., 2006) which promotes wettability and dispersibility of drugs along with an inhibition of precipitation when solid dispersions are dissolved in water (Chauhan et al., 2013, Crowley et al., 2007).

Amorphous carriers are divided into synthetic and natural polymers. Examples of synthetic polymers include povidone (PVP) (Taylor and Zografi, 1997), polyethylene glycol (PEG) (Bley et al., 2010), crospovidone (PVP-CL) (Shin et al., 1998), polyvinylpyrrolidone-

co-vinyl acetate (PVPVA) (Bley et al., 2010) and polymethacrylate (Huang et al., 2006). Natural polymers include cellulose derivatives such as hydroxypropylmethyl cellulose (HPMC), hydroxypropylcellulose (HPC), hydroxypropylmethylcellulose phthalate (HPMCP) (Miyazaki et al., 2011), hydroxypropylmethylcellulose acetate succinate (HPMCAS) (Zhang et al., 2012), starch (corn starch, potato starch) (Bialleck and Rein, 2011) and sugar glass (trehalose, sucrose, inulin) (Van Drooge et al., 2004). Among them, HPMC, PEG and PVP are extensively used (Bialleck and Rein, 2011). In contrast to the amorphous polymers listed above, PEG has a semi-crystalline structure with a very low melting point (below 65 °C) regardless of its molecular weight. Therefore, it is possible to formulate solid dispersions using the melting method, particularly suited to heat-sensitive drugs (Vo et al., 2013).

All polymers discussed previously have excellent solubility profiles in a wide range of solvents, making them ideal candidates for solid dispersions by the solvent method plus the greater aqueous solubility improves the wettability of drugs. The solubility and viscosity of these polymers is dependent on molecular weight, which is important in selecting an appropriate polymer as a carrier. For example, the recrystallisation of drugs during preparation, storage and dissolution can be prevented using high viscosity polymers but at the same time, these can hinder the release of drug in water during dissolution (Vo et al., 2013). PEG with molecular weights of 1500-20000 and PVP with molecular weights of 2500-50000 (K12 to K30) are commonly used polymers in developing solid dispersions (Leuner and Dressman, 2000).

An investigation of albendazole solid dispersions using HPMC and HPMCP as carriers indicated an improved dissolution profile along with inhibition of crystallisation in a neutral medium for eight hours (Crowley et al., 2007) In fact, HPMC and its derivatives have been

successfully applied in many marketed solid dispersion products. Similarly, sugar glasses such as trehalose, sucrose and inulin are used to formulate solid dispersions owing to their fast dissolution rate, which sometimes leads to precipitation of drugs (Van Drooge et al., 2004). Inulin dissolves more gradually than sucrose and trehalose because of its oligomeric nature; therefore, the precipitation and crystallisation rate of inulin based solid dispersions in water is lower than trehalose and sucrose based solid dispersions (Visser et al., 2010, Vo et al., 2013).

To overcome precipitation and recrystallisation issues, carriers having surface activity or self-emulsifying properties were later introduced, known as third generation solid dispersions. These are composed of surfactants or combinations of amorphous polymer and surfactants, intended to achieve the highest possible degree of bioavailability of poorly soluble drugs (Vo et al., 2013, Vasconcelos et al., 2007). Moreover, surfactants are capable of improving wettability and hinder drug precipitation which further enhances dissolution profiles as well as the physical and chemical stability of drugs.

Examples of carriers include inutec SP1 (Van den Mooter et al., 2006), poloxamer (Passerini et al., 2002), compritol 888 ATO (Li et al., 2006a), gelucire 44/14 (Karataş et al., 2005; Yüksel et al., 2003) and soluplus (Kalivoda et al., 2012) (proven to be effective in producing enhanced bioavailability). A solid dispersion of PEG and polysorbate 80 containing a model drug was evaluated to acquire information regarding bioavailability and dissolution enhancement. A 10-fold increased bioavailability (compared with dry micronised drug) was observed, with physical and chemical stability for at least 16 months (Dannenfelser et al., 2004). Solid dispersions of ketoprofen and ibuprofen with poloxamer 407 and 188 demonstrated higher levels of drug release as a result of hydrogen bonding between drug and carrier, indicated by fourier transform infrared spectroscopy (FTIR) studies (Ali et al., 2010).

Additional surfactants used as additives in solid dispersions include sodium dodecyl sulphate (SDS) (Moes et al., 2011), Tween 80 (Joshi et al., 2004), polyoxyethylene hydrogenated castor oil (Won et al., 2005) and sucrose laurate (Szűts et al., 2011).

The principal objective of fourth generation solid dispersions was to improve solubility along with the release of drug in a controlled fashion, therefore, they are more commonly known as controlled release solid dispersions (CRSD). The significant increase in solubility is achieved through a dispersion of drug in the carrier while a swellable polymer is used to delay the drug release in the dissolution media (Huang et al., 2006). Thus an effective amount of drug is delivered for a prolonged period of time, increasing patient compliance by reducing dose frequency and decreased side effects (Desai et al., 2006). Retarding polymers used in CRSD include ethyl cellulose (EC) (Desai et al., 2006), Eudragit RS and RL (Cui et al., 2003), polyethylene oxide (PEO) and carboxyvinyl polymer (Carbopol) (Ozeki et al., 2000). Diffusion and erosion profiles dictate the release mechanisms of drug from CRSD systems (Vo et al., 2013).

Cui and co-workers (2003) developed nitrendipine controlled release solid dispersions, containing HPMCP55 and aerosil as the solid dispersion agents with Eudragit RS, PEO and EC as retarding agents. The results of these studies revealed a more effective absorption profile and improved bioavailability compared with the reference tablets (Baypress TM) and conventional tablets.

1.4.2. Advantages of solid dispersions

Solid dispersions are considered one of the most successful techniques used to enhance the dissolution of poorly water soluble drugs. In comparison with other techniques, such as those addressed earlier i.e. salt formation, prodrug formation, solubilisation and micronisation, solid dispersion presents several advantages. The particle size of a drug can be reduced to a molecular level in solid dispersions while a size limit around 2-5 μm is obtained by conventional techniques, i.e. accelerating the chances of agglomeration upon dissolution and during storage of formulation (Karavas et al., 2006, Pouton, 2006). Drugs are therefore released in a supersaturated state i.e. as high energy drug particles, which subsequently improves bioavailability. Additionally, drug-polymer interactions can avoid agglomeration of drug particles by maintaining the size of particles to a sub-micron level resulting in improved dissolution rates (Leuner and Dressman, 2000, Serajuddin, 1999).

The process to develop solid dispersions is relatively simple compared with other techniques such as salt formation or nanoparticle preparation. Solid oral dosage forms are more acceptable to patients than liquid formulations developed through solubilisation techniques (Karavas et al., 2006, Serajuddin, 1999). The improved wettability and polymorphic changes are some of the unique properties of solid dispersions. Recently, Zhang and co-workers (2012) developed amorphous solid dispersions of fenofibrate using a thin film freezing technique. The results showed a significant increase in surface area, which dramatically enhanced the dissolution rate and bioavailability of fenofibrate. Several other studies on solid dispersions confirmed a change in the polymorphic state of drugs from a crystalline to amorphous form, thus increasing the solubility of the drug (Taylor and Zografi, 1997). This polymorphic change is highly dependent upon the preparation process and underlying drug carrier interactions (Vo et al., 2013).

1.4.3. Common problems with solid dispersions

Stability related issues frequently limit the commercial use of solid dispersions. The most commonly encountered problem with solid dispersions is recrystallisation of drug during preparation (as well as during storage), which results in a decreased dissolution rate. The recrystallisation mechanism involving nucleation followed by crystal growth, leads to disruption in the arrangement of drug molecules (Baird and Taylor, 2012). Physical stability is based on molecular mobility, which is divided into global mobility (α -relaxations) and local mobility (β -relaxations) (Van den Mooter, 2012). The physical stability of a drug is highly influenced by the storage conditions, such as moisture and temperature. Higher water content and elevated temperature can enhance drug mobility, which quickly recrystallises the drug in solid dispersions (Duddu and Sokoloski, 1995). These issues are the main hurdles in the bench to market scalability of solid dispersion (Vasconcelos et al., 2007). Some common issues for solid dispersion based formulations include: thermal instability of drugs and carriers using the melt method, solvent residues using the solvent method, the recrystallisation of drugs in the developing process, the low in vivo-in vitro correlation and the precipitation of drugs in dissolution media owing to supersaturation (Vo et al., 2013). Ayenew and co-workers (2012) evaluated tablet compression on the miscibility of naproxen-PVP K25 solid dispersions. It was found that the amorphous-amorphous phase separation at a compression pressure beyond 565.05 MPa could be the result of intermolecular hydrogen bond disruption between drug and polymer.

To avoid phase separation and recrystallisation, a polymer has to be miscible with the drug to form strong intermolecular hydrogen bonds and reduce molecular mobility (Vasanthavada et al., 2004, Vasanthavada et al., 2005). This is possible using polymers with a

glass transition temperature (T_g) higher than the T_g of the drug (Taylor and Zografi, 1997) (Yoshioka et al., 1994).

Vasanthavada and co-workers (2005) studied factors affecting the solid solubility and phase separation kinetics in griseofulvin-PVP and indoprofen-PVP solid dispersions. Indoprofen miscibility with polymer under accelerated study conditions for three months was around 13 % w/w while griseofulvin was completely insoluble in the polymer. The author's findings indicated that strong hydrogen bonding between indoprofen and PVP could explain the higher miscibility, which was confirmed by FTIR results while no such H-bonding was observed in the case of griseofulvin-PVP. Therefore, it was concluded that phase separations were proportional to drug-polymer interactions and the drug content of dispersions. In many studies, drugs retain their crystallinity even in a solid dispersion, displaying a significant improvement in bioavailability in comparison with the physical mixture and having good stability (Ali et al., 2010, Yan et al., 2012). Furthermore, the addition of surface active agents as an additive in the formulation can reduce the rate of recrystallisation, improve wettability and inhibit precipitation by developing micelles to encapsulate drugs (Vo et al., 2013).

1.4.4. Methods for preparing solid dispersions

a. Solvent evaporation method

The solvent evaporation technique involves dissolving drug and carrier in a common solvent to form a homogenised solution followed by evaporation of the solvent (Chiou and Riegelman, 1971). This is a method of choice, particularly for thermo-labile drugs (Janssens and Van den Mooter, 2009, Vo et al., 2013, Vasconcelos et al., 2007). Tachibana and Nakamura (1965) developed solid dispersions using the solvent evaporation approach to solubilise β -

carotene and polyvinylpyrrolidone (PVP) in a common solvent, namely chloroform. The physical state of drug in the resultant solid dispersion is often determined by the rate of solidification; hence rapid solidification guarantees the amorphous content of drug, which can be achieved by the fast removal of solvent (Vo et al., 2013). Several techniques of solvent removal are used in practice including heating on a hot plate (Desai et al., 2006), vacuum drying (Won et al., 2005), rotary evaporation (Ceballos et al., 2005), spray drying (Li et al., 2011), freeze drying (García-Rodríguez et al., 2011), spray freeze drying (Lim et al., 2010) and ultra-rapid freezing (Overhoff et al., 2007). Solvents used in solid dispersions may include methanol, ethanol, ethyl acetate, methylene chloride, acetone and water or mixtures of these solvents (Hoshino et al., 2007), however, toxicity of several organic solvents is a major limitation of this technique. Furthermore, the plasticising effect of residual solvent can provoke phase separation; resulting in physical instability of solid dispersions. Environmental issues, high cost of production (as it requires extra facilities for solvent removal) and protection against an explosion, affect its suitability and frequent use to produce solid dispersions (Vo et al., 2013, Janssens and Van den Mooter, 2009)

b. Melting or fusion method

Solid dispersions are generally prepared by melting methods i.e. melting an API and a carrier above their melting points, followed by mixing and cooling (Sekiguchi and Obi, 1961, Chiou and Riegelman, 1971). The resultant solid mass is then subjected to crushing, sieving and pulverising to reduce the particle size without milling (Owusu-Ababio et al., 1998). Sources of heating can be a laboratory hot-plate, specialised equipment i.e. a hot melt extruder or a microwave unit.

The drug-polymer incompatibility, as well as the slow cooling process, can cause phase separation, which can be controlled by the addition of a suitable surfactant and processing through spray congealing (Passerini et al., 2006, Vo et al., 2013). APIs having low thermal stability can be suspended in a previously molten carrier to reduce drug heating time and thermal degradation (Vippagunta et al., 2007, Karataş et al., 2005). A pluronic-tadalafil solid dispersion is an example of such a formulation approach (Mehanna et al., 2010). Differential scanning calorimetry (DSC), X-ray diffraction (XRD) and scanning electron microscopy (SEM) demonstrated the formation of a microcrystalline uniform dispersion of tadalafil in the pluronic system. A dramatic enhancement in the dissolution rate of pluronic-tadalafil solid dispersions was observed, compared with their physical mix.

Hot melt extrusion is an appropriate method to prepare solid dispersions at a manufacturing scale. In recent years, this strategy has gained prominence to formulate solid dispersions (Bruce et al., 2007, Nollenberger et al., 2009). The drug and carrier are simultaneously subjected to intense mixing and agitation followed by a heating cycle which results in a homogeneous dispersion (Verhoeven et al., 2009, Crowley et al., 2007). The reduced residence time of the drug and carrier at elevated temperatures in the extruder make it a superior method for thermo-labile drugs (Leuner and Dressman, 2000). Additional benefits of this approach include effectiveness, easy scale up and thermodynamically stable products compared with other methods (Williams et al., 2010). Hot melt extrusion and its advanced technology, for example, Meltrex™, are the most successful approaches to prepare solid dispersions with many marketed products such as Cesamet®, Rezulin®, Kaletra® (Meltrex™), Novir® (Meltrex™) and Isotip® (Meltrex™) (Maniruzzaman et al., 2012, Vo et al., 2013).

Despite several advantages, hot melt extrusion also faces challenges to produce solid dispersions of thermo-labile compounds. The use of plasticisers can mitigate thermal degradation, but this approach is not applicable for all formulations as variable processing is required for different components. Furthermore, optimisation of different operational variables such as the feed rate, screw speed and extrusion temperature makes it a lengthy process (Langham, 2011).

The use of microwave technology in pharmaceutical processing is categorised on the basis of thermal and non-thermal effects of microwaves. Microwave drying of pharmaceuticals is a result of thermal effects whereas microwave energy is used to induce a heating process in the system. Apart from heating and drying applications, microwaves offer an avenue for the modification of the physicochemical properties of materials via specific microwave-material interactions, which have been considered as non-thermal in nature (Ku et al., 2002). These are exploited primarily for the design of controlled release dosage forms. Microwave technology has been employed to develop controlled drug delivery formulations based on natural polymers such as alginate, chitosan and pectin (Wong et al., 2002, Nurjaya and Wong, 2005, Wong et al., 2005). In these studies, a laboratory scale microwave was used to prepare polymer beads and microspheres followed by characterisation using DSC and fourier transform infra-red (FTIR) spectroscopy. The results indicated the effective formation of crosslinkages, resulting in a strong polymer-polymer and drug-polymer complexation in matrices. These matrices were highly efficient in controlling the release of sulphathiazole and sodium diclofenac without affecting the chemical stabilities of drug and the polymer. It appeared that selection of appropriate microwave conditions, along with polymer structural arrangement, influence the matrices' effectiveness. Several other studies have been made to encapsulate drugs in synthetic polymers such as poly (methyl vinyl ether-co-maleic acid) using a microwave to achieve better

results (Wong et al., 2008). However, varying degrees of success were achieved with different polymers.

After exploring the utility of microwaves in designing controlled release dosage forms, researchers started investigating the potential of microwaves to enhance solubility and bioavailability of poorly soluble drugs via the formation of solid dispersions and nanocomposite materials. Kerc and co-workers (1998) used microwave heating to prepare a binary solid mixture of felodipine and amorphous silicon dioxide or crystalline sodium chloride. The conversion of crystalline felodipine to its amorphous or microcrystalline state is evident from the results obtained using differential scanning calorimetry and X-ray diffraction. The dissolution properties of the formulation were influenced by the exposure time of the material to microwaves.

In another study, the microwave technique was employed to develop solid dispersions of ibuprofen and polyvinylpyrrolidone-vinyl acetate copolymer or hydroxypropyl- β -cyclodextrin (Moneghini et al., 2008). The significant enhancement in the in vitro dissolution rate was achieved in the microwave treated solid dispersions as compared with the pure drug. Bergese and co-worker (2003) developed nanocomposites of crospovidone or β -cyclodextrin carrying ibuprofen, nimesulide or nifedipine in an embedded form. A remarkable reduction in crystallinity was produced under the influence of microwave treatment.

In recent times, solid dispersions of a water insoluble drug, tibolone, in a polyethylene glycol matrix were formulated by both conventional and microwave-induced melt mixing (Papadimitriou et al., 2008). The unaffected tibolone stability was confirmed by the results of liquid chromatography. The penetrative and volumetric heating of microwaves induced the

rapid production of solid dispersions in comparison with conventional heating methods. Additionally, the drug was dispersed uniformly as fine particles in a carrier which was confirmed by the results of scanning electron microscopy (SEM). In summary, an elevated dissolution rate of tibolone melt dispersions was developed through microwave techniques.

Microwaves are part of the electromagnetic spectrum, the frequency range of which is 300MHz to 300GHz. Microwave processing of material is through direct interaction of material with microwave radiation and a range of parameters dictate the extent of material heating, but the dielectric properties of materials have a particular relevance. Therefore, microwaves may confer several advantages for suitable systems over conventional heating (Solanki et al., 2011, Waters et al., 2011) including:

- Uniform and deep heating of material in contrast to surface heating through conventional heating.
- Rapid heating and cooling.
- High efficiency of heating achieved through dielectric polarisation and conduction (while conduction is the only mechanism in conventional heating).
- Desirable physical and chemical effects.
- Increased efficiency and decreased operating costs.
- Increased reaction rates in some cases.
- Reduction in unwanted side effects (reaction quenching).
- Increased purity of final product.
- Improved reproducibility.
- Lower energy usage.
- Increased environmental safety.

These potential beneficial effects have led to the widespread use of microwaves in various fields such as compound synthesis in chemistry, drug extraction, microwave assisted drying, sterilisation and pharmaceutical dosage form development (Solanki et al., 2011). However, controlling the temperature throughout an experimental run is a major challenge, since constant power does not ensure a constant temperature and changes in dielectric properties are likely to happen with phase changes during the process. Furthermore, the variable coupling capability of materials with microwaves causes thermal runaway as the temperature increases, which can produce detrimental effects in the final formulation (Waters et al., 2011). Therefore, temperature control is vital to make microwaves a potential alternative technique for the development of successful formulations.

1.5. Drug-excipient interactions

Orally administered drugs undergo rapid disintegration; therefore, systemic absorption of a dosage form containing a hydrophobic drug is controlled by the dissolution rate while permeation is the rate limiting step for hydrophilic drugs. Drug instability, such as degradation of drug into an inactive form and drug-excipient interactions, can affect its bioavailability during absorption (Panakanti and Narang, 2012). Therefore, careful consideration must be taken in selecting a suitable excipient because stability, efficacy and toxicity of the final active moiety are entirely dependent upon the drug-excipient interactions (Panakanti and Narang, 2012). Drug-excipient incompatibilities can produce serious biopharmaceutical implications such as modification in the release mechanism, reduced bioavailability and potency loss, thus implicating adverse effects. Modification in the physicochemical properties of drugs, produced as a result of drug-excipient interactions, can be divided into the following three categories:

a. Specific drug-excipient binding

Cyclodextrin complexation has been shown to enhance the dissolution rate of several drugs including ibuprofen (Nambu et al., 1978), nifedipine (Emara et al., 2002b), griseofulvin (Dhanaraju et al., 1998) and theophylline (Ammar et al., 1996). However, absorption and bioavailability of certain drugs has been decreased as a result of strong drug-excipient interactions. For example, complexation of tetracycline with divalent cations such as calcium (Shargel et al., 2005) and phenobarbital with PEG 4000 (Benet et al., 1966), decreased their bioavailability. Similarly, increased phenytoin toxicity was observed in patients receiving a phenytoin formulation containing lactose as the excipient compared with the initial formulations containing calcium sulphate. The decreased drug absorption with calcium sulphate was found to be a result of the development of an insoluble complex with the drug while no such complex formed with lactose, resulting in increased side effects (Cacek, 1986). Surfactants can also develop insoluble complexes, which are micellar in nature. For example, the complex formation of polysorbate 80 and sodium lauryl sulphate with chlorpromazine reduced its permeability through a polydimethylsiloxane membrane (Nakano, 1971).

b. Non-specific drug-excipient binding

Non-specific drug-excipient interactions are commonly encountered in immediate drug delivery systems. These are also known as ionic drug-excipient interactions (Panakanti and Narang, 2012). For example, interactions between croscarmellose sodium, a weakly acidic anionic excipient, and phenylpropanolamine HCl, a weakly basic cationic drug, resulted in a 40 % decrease in drug release in water, compared with the formulation containing starch as an excipient. The author proposed that a nonspecific ion-exchange mechanism could be the reason for these interactions (Hollenbeck, 1988). In addition to ionic binding, the entropic gain

produced by aggregation of surface active drugs accelerated strong interactions of amphiphilic drug with the excipient (Panakanti and Narang, 2012).

c. Drug adsorption on an excipient surface

The results of ketoprofen and griseofulvin adsorbed onto silica using supercritical carbon dioxide demonstrated an improved dissolution rate (Smirnova et al., 2004). Similarly, excipients such as magnesium aluminium trisilicate promoted wetting, which subsequently resulted in an increased dissolution rate of griseofulvin, indomethacin and prednisone. These drug-excipient bindings could be the result of weak van der Waals forces (McGinity and Harris, 1980). It was observed that the release of drug from an adsorption based formulation was reduced on exposure to a solution phase owing to strong drug binding to the insoluble excipient. For example, the antimicrobial activity of cetylpyridinium chloride decreased when prepared with magnesium stearate anions because of the ionic binding between drug and excipient (Richards et al., 1996). Another example is the reduced oral bioavailability of chlordiazepoxide, formulated with talc (Panakanti and Narang, 2012).

These studies indicate how drug-excipient interactions can affect the physicochemical and pharmacokinetic properties of drugs. The effective drug loading achieved through either covalent bonding or non-covalent bonding i.e. electrostatics, hydrophobic, or hydrogen-bonding, hinders the ultimate drug release from the dosage form. These strong drug-excipient bindings often reduce the optimum drug dose delivered to target site in humans or animals (da Silva et al., 2010). Therefore, a thorough understanding of drug-excipient interactions is the leading requirement to design an effective drug therapy. Over the years, drug-excipient interactions have been studied extensively from simple techniques, such as conductivity and

fluorescence spectroscopy to complex techniques, such as NMR. More recently, isothermal titration calorimetry (ITC) has gained importance when evaluating drug-excipient interactions (Freire, 2004; Falconer and Collins, 2011).

1.6. Isothermal titration calorimetry (ITC)

Almost any chemical reaction or physical change is accompanied by a change in heat or enthalpy. A measure of heat taken up from the surroundings (for an endothermic process) or given up to the surroundings (for an exothermic process) is simply equal to the amount of the reaction that has occurred, and the enthalpy changes for the reaction (Núñez et al., 2012). A calorimeter is therefore, an ideal instrument to measure the rate of reaction. In contrast to optical methods, calorimetric measurements are applicable for spectroscopically silent reactants (a chromophore or fluorophore tag is not required), opaque, turbid, or heterogeneous solutions (for example, cell suspensions), and a range of biologically relevant conditions (such as temperature, salt or pH.) (Núñez et al., 2012).

ITC has been used for the determination of binding affinities (K_a) (O'Neill and Gaisford, 2011) for several reasons including;

1. It does not require optical clarity of the solution.
2. It is rapid.
3. There is no need to develop a specific assay for each interaction.
4. It can be used for the direct measurement of binding enthalpy (Δ_aH)

Indeed, it is the only technique which can measure a thermodynamic profile directly and obviates the need for indirect determinations via van't Hoff analyses. Additionally, careful experimental design can provide information for parameters such as changes in the Gibbs free energy (Δ_aG), entropy (Δ_aS), heat capacity (ΔCp) and the stoichiometry (n), of binding in a single experiment (Freire et al., 1990, Gaisford and O'Neill, 2007).

1.6.1. ITC instrumentation

A schematic diagram of an ITC instrument is shown in Figure 1.8. It consists of two identical cells, sample and reference, shielded in an adiabatic jacket. These cells are kept at thermal equilibrium throughout the experiment to determine heat energy per unit time. When one component is injected from the syringe into the sample cell, an enthalpic change is produced in the form of raw ITC signals. If the interaction is exothermic less heat per unit time will be required by the sample cell to keep the two cells in thermal equilibrium; if the interaction is endothermic, the inverse will be observed (Núñez et al., 2012, Blandamer et al., 1998).

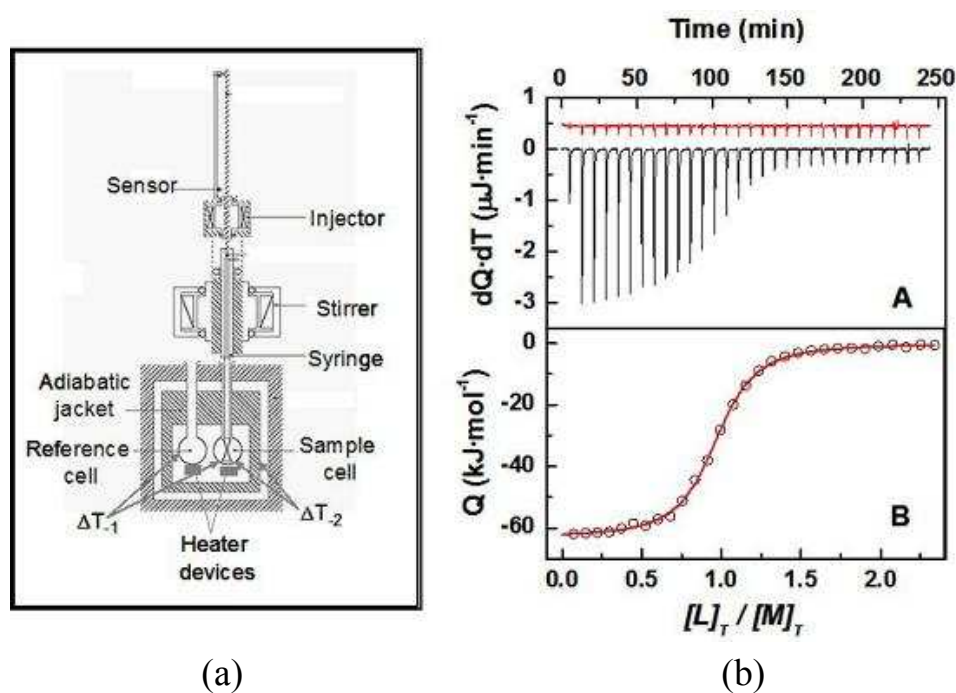


Figure 1.8: Isothermal titration calorimetry instrumentation: (a) a schematic diagram of the main components of a titration calorimeter, (b) a general representation of titration calorimetry experiment of a substrate with ligand. In panel A) the titration thermogram is represented as heat per unit of time released after each injection of the ligand into the substrate (black), as well as the dilution of ligand into buffer (red). In panel B) the dependence of released heat in each injection versus the ratio between total ligand concentration and total protein concentration is represented. Circles represent experimental data and the line corresponds to the best fitting model (Martinez et al., 2013).

1.6.2. General operation of ITC

The heat signals produced in ITC experiments may contain heat effects from several sources such as the heat of binding, the heat of dilution of the macromolecule, the heat of dilution of ligand and the heat of mixing. Therefore, control experiments are required to remove these artifacts which usually involve a further three blank experiments (O'Neill and Gaisford, 2011, Grolier and Del Río, 2012).

- I. Dilution of the ligand by the solvent.
- II. Dilution of the substrate by the solvent.
- III. Solvent mixing

These unwanted heat effects can be removed by subtracting these from the main ligand substrate experiment (O'Neill and Gaisford, 2011).

The raw data from an ITC experiment is a plot of power versus time displaying a series of peaks corresponding to successive injections of ligand solution into substrate solution (Figure 1.8. b. top). Integration of binding isotherms, using an appropriate fitting model, can generate a bonding constant (K_a) (Figure 1.8. b. bottom) along with a complete thermodynamic picture of binding (Grolier and Del Río, 2012, Velazquez-Campoy et al., 2004).

To derive meaningful binding constant values it is vital to choose suitable concentrations of reacting species, which passes through its saturation point during the binding process. This can be easily confirmed when the titration peaks settle to a constant and minimum value, representing just the dilution of ligand substrate. The strength of binding affinity dictates the generation of the binding isotherms which can be characterised through the use of a *c*-value where *c* is a unit-less parameter and equals the product of binding affinity (K_a), the

concentration of binding sites (S_{tot}) and the binding stoichiometry (n) (Eq. 1.3) (Velazquez-Campoy et al., 2004):

$$c = K_a [S_{\text{tot}}]^n \quad (\text{Eq. 1.3})$$

The c value lies between 1 and 1000 and can provide confidence in this type of analysis. The value of c is near to 1000 for those binding partners having a high concentration. In such cases, all the ligand molecules added in any injection will bind to its binding partner until saturation occurs and a steep increase in the shape of the ITC curve will result. In contrast, if the c value lies near to the concentration of the binding partner an exponential type of curve will result, in which saturation is barely reached. The optimum concentration of binding partners, with a c value around 500, can be used to produce a sigmoidal curve (Wiseman et al., 1989, Turnbull and Daranas, 2003).

1.6.3. ITC experiment analysis

A typical ITC experiment is carried out by the stepwise addition of ligand in the syringe to the macromolecule in the calorimetric cell. A certain amount of heat (q_i) will be released or absorbed, which is proportional to the amount of ligand that binds to the macromolecule in a particular injection ($V \times \Delta L_i$) and the characteristic binding enthalpy (ΔH) for the reaction as can be seen in Eq. (1.4).

$$q_i = V \times \Delta H \times \Delta L_i \quad (\text{Eq. 1.4})$$

where V is the volume of the reaction cell and ΔL_i is the increase in the concentration of bound ligand after i_{th} injections

The enthalpy change after each injection is obtained by calculating the area under each peak. The uncomplexed macromolecule available decreases after each successive injection as

shown by the magnitude of the peaks becoming progressively smaller. Once saturation has been achieved, subsequent injections produce similar peaks corresponding to dilution or mechanical effects that need to be subtracted before analysis. For one binding site the equation becomes that seen in Eq. (1.5) (Leavitt and Freire, 2001);

$$q = V \times \Delta H \times (P) \times \left[\frac{K_a[L]_i}{1+K_a[L]_i} - \frac{K_a[L]_{i-1}}{1+K_a[L]_{i-1}} \right] \quad (\text{Eq. 1.5})$$

where K_a is the binding constant, P is the product of a single binding event and $[L]$ is the concentration of free ligand, (as the known experimental quantity is the total ligand concentration, rather than the free ligand concentration). Analysis of the data yields ΔH and $\Delta G = -RT \ln k_a$. Heat capacity (C_p) associated with the binding reaction is determined by taking the derivative of enthalpy (ΔH) with respect to temperature (T), using Eq. (1.6) (Leavitt and Freire, 2001);

$$C_p = \frac{\partial \Delta H}{\partial T} \quad (\text{Eq. 1.6})$$

ITC has been used in several studies to evaluate drug-polymer interactions and characterise the thermodynamic profile of these systems (Yousefpour et al., 2011, Tian et al., 2007, Li et al., 2006b). Yousefpour and co-workers (2011) used ITC to characterise the thermodynamic profile of doxorubicin-dextran interactions. Thermal analysis of DOX-dextran complexation revealed that each DOX molecule bound with 3 dextran glycosyl monomers. Isothermal titration calorimetry clearly showed the pH effects on the DOX-polymer binding. The electrostatic interactions were found to be predominant for the DOX/ pluronic-PAA complex formation while a shielding effect of NaCl on the positively charged amino group and negatively charged COOH decreased the strength of interactions (Tian et al., 2007). The interaction of several other drugs such as verapamil HCl (Li et al., 2006b), imipramine HCl

(He et al., 2010), benzophenone and tamoxifen (Daoud-Mahammed et al., 2009) with their polymeric carriers have been studied using ITC. The objective of all these studies was to understand the basic mechanism of drug-polymer binding and thermodynamic profile to modify drug-delivery systems.

The enthalpy of sertaconazole/hydroxypropyl- β -cyclodextrin complexation was recorded by ITC which confirmed the potential use of cyclodextrins as solubilisers (Rodriguez-Perez et al., 2006). The association of anionic surfactants with β -cyclodextrin was also studied by means of ITC. The results demonstrated that the association phenomenon was characterised by favourable enthalpy and entropy changes (Eli et al., 1999).

Furthermore, isothermal titration calorimetry has been employed to obtain thermodynamic information for surfactant based systems to understand the underlying mechanism of drug-surfactant interactions.

Isothermal titration calorimetry (ITC) has become the method of choice to determine thermodynamic information for a variety of chemical and biological systems. It has also been used to evaluate the energetics of surfactant based systems, especially with respect to their ability to self-aggregate to form micelles (Chatterjee et al., 2001). The monitoring of micellisation phenomena of surfactants is possible through ITC as it can determine critical micellar concentration (CMC), changes in enthalpy (ΔH_{mic}), entropy (ΔS_{mic}) and free energy (ΔG_{mic}) of micellisation from a simple series of surfactant injections (Bouchemal et al., 2010).

For example, the effect of temperature on micelle formation for four surfactants has been investigated. The results indicated that a change in temperature produced a large change

in ΔH_{mic} and ΔS_{mic} but not in ΔG_{mic} (Paula et al., 1995). Several other studies have identified factors capable of modifying the physicochemical properties of the surfactant, including the CMC, such as the presence of NaCl (Volpe, 1995), aqueous buffers (Taheri-Kafrani and Bordbar, 2009) and polymers (Wang and Olofsson, 1998). For example, a study based on the interactions between polyethylene glycol and sodium dodecyl sulfate (SDS) revealed relationships between the molecular weight of polymer and binding behavior (Dai and Tam, 2001). Studies such as surfactant-membrane partitioning and membrane solubilisation, have only been possible through the development of high-sensitivity ITC (Heerklotz and Seelig, 2000) which has been shown to surpass more traditional techniques to determine CMC, such as conductivity, measurement of dielectric constants and quantitative model systems (Pérez-Rodríguez et al., 1998, Gezae Daful et al., 2011).

Furthermore, drug surfactant binding has been investigated to monitor a model for the hydrophobic contribution to the free energy of DNA intercalation reactions (Dignam et al., 2007). To obtain a thorough understanding of drug-micelle interactions, studies were expanded to other surfactants systems, particularly those with a differently charged head group, including cationic surfactant based systems (Akhtar et al., 2008).

In summary, even though only limited drug-micelle interaction based studies have utilised ITC (Bouchemal, 2008), it is already identified as a sensitive analytical tool for characterising drug-excipient interactions, such as those observed between pharmaceutical compounds and cyclodextrins (Waters et al., 2010).

1.7. Aims and objectives

The overall aim of the research presented in this thesis is to establish a novel formulation method for the development of solid dispersions and investigate thermodynamic parameters associated with these drug-excipient interactions.

The objectives of this work are as follows:

1. To develop bespoke mesoporous silica based solid dispersions using a novel microwave system.
2. To develop Syloid[®] silica based solid dispersions using a novel microwave system.
3. To develop a hydrophilic carrier based solid dispersion using a novel microwave system.
4. To investigate drug-excipient interactions based on surfactant saturation limits and micellisation studies.

In summary, this project seeks to develop novel formulations with enhanced physicochemical properties and use thermodynamic analysis to fully characterise such drug-excipient interactions.

References

- AKHTAR, F., HOQUE, M. A. & KHAN, M. A. 2008. Interaction of cefadroxyl monohydrate with hexadecyltrimethyl ammonium bromide and sodium dodecyl sulfate. *The Journal of Chemical Thermodynamics*, 40, 1082-1086.
- ALAM, M. A., AL-JENOABI, F. I. & AL-MOHIZEA, A. M. 2013. Commercially bioavailable proprietary technologies and their marketed products. *Drug discovery today*.
- ALBERT, A. 1958. Chemical aspects of selective toxicity. *Nature*, 182, 421-423.
- ALI, W., WILLIAMS, A. C. & RAWLINSON, C. F. 2010. Stoichiometrically governed molecular interactions in drug: poloxamer solid dispersions. *International Journal of Pharmaceutics*, 391, 162-168.
- AMIDON, G. L., LENNERNAS, H., SHAH, V. P. & CRISON, J. R. 1995. A theoretical basis for a biopharmaceutic drug classification: The correlation of in vitro drug product dissolution and in vivo bioavailability. *Pharmaceutical Research*, 12, 413-420.
- AMMAR, H. O., GHORAB, M., EL-NAHHAS, S. A., OMAR, S. M. & GHORAB, M. M. 1996. Improvement of some pharmaceutical properties of drugs by cyclodextrin complexation. 5. Theophylline. *Pharmazie*, 51, 42-46.
- ATKINSON, R., BEDFORD, C., CHILD, K. & TOMICH, E. 1962. Effect of particle size on blood griseofulvin-levels in man. *Nature*, 193, 588-589.
- AVDEEF, A. 2007. Solubility of sparingly-soluble ionizable drugs. *Advanced drug delivery reviews*, 59, 568-590.
- AYENEW, Z., PAUDEL, A. & VAN DEN MOOTER, G. 2012. Can compression induce demixing in amorphous solid dispersions? A case study of naproxen-PVP K25. *European Journal of Pharmaceutics and Biopharmaceutics*, 81, 207-213.
- BABOOTA, S., DHALIWAL, M. & KOHLI, K. 2005. Physicochemical characterization, in vitro dissolution behavior, and pharmacodynamic studies of rofecoxib-cyclodextrin inclusion compounds. Preparation and properties of rofecoxib hydroxypropyl β -cyclodextrin inclusion complex: A technical note. *AAPS PharmSciTech*, 6, E83-E90.
- BAIRD, J. A. & TAYLOR, L. S. 2012. Evaluation of amorphous solid dispersion properties using thermal analysis techniques. *Advanced drug delivery reviews*, 64, 396-421.
- BAK, A., GORE, A., YANEZ, E., STANTON, M., TUFEKCIC, S., SYED, R., AKRAMI, A., ROSE, M., SURAPANENI, S. & BOSTICK, T. 2008. The co-crystal approach to improve the exposure of a water-insoluble compound: AMG 517 sorbic acid co-crystal characterization and pharmacokinetics. *Journal of pharmaceutical sciences*, 97, 3942-3956.
- BENET, L. Z., BHATIA, V., SINGH, P., GUILLORY, J. K. & SOKOLOSKI, T. D. 1966. Effect of inert tablet ingredients on drug absorption I. Effect of polyethylene glycol 4000 on the intestinal absorption of four barbiturates. *Journal of pharmaceutical sciences*, 55, 63-68.
- BERGESE, P., COLOMBO, I., GERVASONI, D. & DEPERO, L. 2003. Microwave generated nanocomposites for making insoluble drugs soluble. *Materials Science and Engineering: C*, 23, 791-795.
- BIALLECK, S. & REIN, H. 2011. Preparation of starch-based pellets by hot-melt extrusion. *European Journal of Pharmaceutics and Biopharmaceutics*, 79, 440-448.
- BLAGDEN, N., DE MATAS, M., GAVAN, P. & YORK, P. 2007. Crystal engineering of active pharmaceutical ingredients to improve solubility and dissolution rates. *Advanced drug delivery reviews*, 59, 617-630.
- BLANDAMER, M. J., CULLIS, P. M. & ENGBERTS, J. B. 1998. Titration microcalorimetry. *J. Chem. Soc., Faraday Trans.*, 94, 2261-2267.

- BLEY, H., FUSSNEGGER, B. & BODMEIER, R. 2010. Characterization and stability of solid dispersions based on PEG/polymer blends. *International Journal of Pharmaceutics*, 390, 165-173.
- BOUCHEMAL, K. 2008. New challenges for pharmaceutical formulations and drug delivery systems characterization using isothermal titration calorimetry. *Drug discovery today*, 13, 960-972.
- BOUCHEMAL, K., AGNELY, F., KOFFI, A., DJABOUROV, M. & PONCHEL, G. 2010. What can isothermal titration microcalorimetry experiments tell us about the self-organization of surfactants into micelles? *Journal of Molecular Recognition*, 23, 335-342.
- BOWKER, M. J. 2002. A procedure for salt selection and optimization, Wiley-VCH, Weinheim, Germany.
- BRITAIN, H. G. 1999. Polymorphism in pharmaceutical solids, M. Dekker New York.
- BROUWERS, J., BREWSTER, M. E. & AUGUSTIJNS, P. 2009. Supersaturating drug delivery systems: The answer to solubility-limited oral bioavailability? *Journal of pharmaceutical sciences*, 98, 2549-2572.
- BRUCE, C., FEGELY, K. A., RAJABI-SIAHBOOMI, A. R. & MCGINITY, J. W. 2007. Crystal growth formation in melt extrudates. *International journal of pharmaceutics*, 341, 162-172.
- CACEK, A. T. 1986. Review of alterations in oral phenytoin bioavailability associated with formulation, antacids, and food. *Therapeutic drug monitoring*, 8, 166-171.
- CEBALLOS, A., CIRRI, M., MAESTRELLI, F., CORTI, G. & MURA, P. 2005. Influence of formulation and process variables on in vitro release of theophylline from directly-compressed Eudragit matrix tablets. *Il Farmaco*, 60, 913-918.
- CHARMAN, W. N. 2000. Lipids, lipophilic drugs, and oral drug delivery—some emerging concepts. *Journal of pharmaceutical sciences*, 89, 967-978.
- CHATTERJEE, A., MOULIK, S., SANYAL, S., MISHRA, B. & PURI, P. 2001. Thermodynamics of micelle formation of ionic surfactants: a critical assessment for sodium dodecyl sulfate, cetyl pyridinium chloride and dioctyl sulfosuccinate (Na salt) by microcalorimetric, conductometric, and tensiometric measurements. *The Journal of Physical Chemistry B*, 105, 12823-12831.
- CHAUHAN, H., HUI-GU, C. & ATEF, E. 2013. Correlating the behavior of polymers in solution as precipitation inhibitor to its amorphous stabilization ability in solid dispersions. *Journal of pharmaceutical sciences*.
- CHILDS, S. L., STAHLY, G. P. & PARK, A. 2007. The salt-cocystal continuum: the influence of crystal structure on ionization state. *Molecular Pharmaceutics*, 4, 323-338.
- CHIOU, W. L. & RIEGELMAN, S. 1969. Preparation and dissolution characteristics of several fast-release solid dispersions of griseofulvin. *Journal of pharmaceutical sciences*, 58, 1505-1510.
- CHIOU, W. L. & RIEGELMAN, S. 1971. Pharmaceutical applications of solid dispersion systems. *Journal of pharmaceutical sciences*, 60, 1281-1302.
- CHOI, S.-J., SHIN, S.-C. & CHOI, J.-S. 2011. Effects of myricetin on the bioavailability of doxorubicin for oral drug delivery in Rats: Possible role of CYP3A4 and P-glycoprotein inhibition by myricetin. *Archives of Pharmacal Research*, 34, 309-315.
- CROWLEY, M. M., ZHANG, F., REPKA, M. A., THUMMA, S., UPADHYE, S. B., KUMAR BATTU, S., MCGINITY, J. W. & MARTIN, C. 2007. Pharmaceutical applications of hot-melt extrusion: part I. Drug development and industrial pharmacy, 33, 909-926.
- ČUDINA, O., KARLJKOVIĆ-RAJIĆ, K., RUVARAC-BUGARČIĆ, I. & JANKOVIĆ, I. 2005. Interaction of hydrochlorothiazide with cationic surfactant micelles of

- cetyltrimethylammonium bromide. *Colloids and Surfaces A: Physicochemical and Engineering Aspects*, 256, 225-232.
- CUI, F., YANG, M., JIANG, Y., CUN, D., LIN, W., FAN, Y. & KAWASHIMA, Y. 2003. Design of sustained-release nitrendipine microspheres having solid dispersion structure by quasi-emulsion solvent diffusion method. *Journal of controlled release*, 91, 375-384.
- DA SILVA, A. R., ZANIQUELLI, M. E. D., BARATTI, M. O. & JORGE, R. A. 2010. Drug Release from Microspheres and Nanospheres of Poly (lactide-co-glycolide) without Sphere Separation from the Release Medium. *J. Braz. Chem. Soc*, 21, 214-225.
- DAI, S. & TAM, K. 2001. Isothermal titration calorimetry studies of binding interactions between polyethylene glycol and ionic surfactants. *The Journal of Physical Chemistry B*, 105, 10759-10763.
- DANNENFELSER, R. M., HE, H., JOSHI, Y., BATEMAN, S. & SERAJUDDIN, A. 2004. Development of clinical dosage forms for a poorly water soluble drug I: Application of polyethylene glycol-polysorbate 80 solid dispersion carrier system. *Journal of pharmaceutical sciences*, 93, 1165-1175.
- DAOUD-MAHAMMED, S., COUVREUR, P., BOUCHEMAL, K., CHÉRON, M., LEBAS, G., AMIEL, C. & GREF, R. 2009. Cyclodextrin and polysaccharide-based nanogels: entrapment of two hydrophobic molecules, benzophenone and tamoxifen. *Biomacromolecules*, 10, 547-554.
- DESAI, J., ALEXANDER, K. & RIGA, A. 2006. Characterization of polymeric dispersions of dimenhydrinate in ethyl cellulose for controlled release. *International Journal of Pharmaceutics*, 308, 115-123.
- DESAI, P. P., DATE, A. A. & PATRAVALE, V. B. 2012. Overcoming poor oral bioavailability using nanoparticle formulations—opportunities and limitations. *Drug Discovery Today: Technologies*, 9, e87-e95.
- DHANARAJU, M. D., SENTHIL KUMARAN, K., BASKARAN, T. & SREE RAMA MOORTHY, M. 1998. Enhancement of bioavailability of Griseofulvin by its complexation with β -cyclodextrin. *Drug Development and Industrial Pharmacy*, 24, 583-587.
- DIGNAM, J. D., QU, X., REN, J. & CHAIRES, J. B. 2007. Daunomycin binding to detergent micelles: a model system for evaluating the hydrophobic contribution to drug-DNA interactions. *The Journal of Physical Chemistry B*, 111, 11576-11584.
- DUDDU, S. P. & SOKOLOSKI, T. D. 1995. Dielectric analysis in the characterization of amorphous pharmaceutical solids. 1. Molecular mobility in poly (vinylpyrrolidone)–water systems in the glassy state. *Journal of pharmaceutical sciences*, 84, 773-776.
- ELI, W., CHEN, W. & XUE, Q. 1999. The association of anionic surfactants with β - cyclodextrin. An isothermal titration calorimeter study. *The Journal of Chemical Thermodynamics*, 31, 1283-1296.
- EMARA, L., BADR, R. & ABD ELBARY, A. 2002a. Improving the dissolution and bioavailability of nifedipine using solid dispersions and solubilizers. *Drug development and industrial pharmacy*, 28, 795-807.
- EMARA, L. H., BADR, R. M. & ELBARY, A. A. 2002b. Improving the dissolution and bioavailability of nifedipine using solid dispersions and solubilizers. *Drug Development and Industrial Pharmacy*, 28, 795-807.
- FAKES, M. G., VAKKALAGADDA, B. J., QIAN, F., DESIKAN, S., GANDHI, R. B., LAI, C., HSIEH, A., FRANCHINI, M. K., TOALE, H. & BROWN, J. 2009. Enhancement of oral bioavailability of an HIV-attachment inhibitor by nanosizing and amorphous formulation approaches. *International Journal of Pharmaceutics*, 370, 167-174.

- FALCONER, R. J. & COLLINS, B. M. 2011. Survey of the year 2009: applications of isothermal titration calorimetry. *Journal of Molecular Recognition*, 24, 1-16.
- FASINU, P., PILLAY, V., NDESENDO, V. M., DU TOIT, L. C. & CHOONARA, Y. E. 2011. Diverse approaches for the enhancement of oral drug bioavailability. *Biopharmaceutics & drug disposition*, 32, 185-209.
- FLEISHER, D., BONG, R. & STEWART, B. H. 1996. Improved oral drug delivery: solubility limitations overcome by the use of prodrugs. *Advanced drug delivery reviews*, 19, 115-130.
- FREIRE, E. 2004. Isothermal titration calorimetry: Controlling binding forces in lead optimization. *Drug Discovery Today: Technologies*, 1, 295-299.
- FREIRE, E., MAYORGA, O. L. & STRAUME, M. 1990. Isothermal titration calorimetry. *Analytical Chemistry*, 62, 950A-959A.
- GAISFORD, S. & O'NEILL, M. A. 2007. *Pharmaceutical isothermal calorimetry*, Informa Healthcare New York.
- GARCÍA-RODRIGUEZ, J. J., DE LA TORRE-IGLESIAS, P. M., VEGAS-SÁNCHEZ, M. C., TORRADO-DURÁN, S., BOLÁS-FERNÁNDEZ, F. & TORRADO-SANTIAGO, S. 2011. Changed crystallinity of mebendazole solid dispersion: improved anthelmintic activity. *International Journal of Pharmaceutics*, 403, 23-28.
- GEZAE DAFUL, A., BAULIN, V. A., BONET AVALOS, J. & MACKIE, A. D. 2011. Accurate Critical Micelle Concentrations from a Microscopic Surfactant Model. *The Journal of Physical Chemistry B*, 115, 3434-3443.
- GHARAEI-FATHABAD, E. 2011. Biosurfactants in pharmaceutical industry: A mini-review. *Am. J. Drug Discovery Dev*, 1, 58-69.
- GRANERO, G. E. & AMIDON, G. L. 2006. Stability of valacyclovir: implications for its oral bioavailability. *International journal of pharmaceutics*, 317, 14-18.
- GROLIER, J.-P. E. & DEL RÍO, J. M. 2012. Isothermal titration calorimetry: A thermodynamic interpretation of measurements. *The Journal of Chemical Thermodynamics*, 55, 193-202.
- GUZMAN, H. R., TAWA, M., ZHANG, Z., RATANABANANGKON, P., SHAW, P., GARDNER, C. R., CHEN, H., MOREAU, J. P., ALMARSSON, Ö. & REMENAR, J. F. 2007. Combined use of crystalline salt forms and precipitation inhibitors to improve oral absorption of celecoxib from solid oral formulations. *Journal of pharmaceutical sciences*, 96, 2686-2702.
- HE, E., YUE, C. & TAM, K. 2010. Binding and release studies of a cationic drug from a star-shaped four-arm poly (ethylene oxide)-b-poly (methacrylic acid). *Journal of pharmaceutical sciences*, 99, 782-793.
- HEERKLOTZ, H. & SEELIG, J. 2000. Titration calorimetry of surfactant-membrane partitioning and membrane solubilization. *Biochimica et Biophysica Acta (BBA)-Biomembranes*, 1508, 69-85.
- HENCHOZ, Y., BARD, B., GUILLARME, D., CARRUPT, P.-A., VEUTHEY, J.-L. & MARTEL, S. 2009. Analytical tools for the physicochemical profiling of drug candidates to predict absorption/distribution. *Analytical and bioanalytical chemistry*, 394, 707-729.
- HOLLENBECK, R. G. 1988. Bioavailability of phenylpropanolamine HCl from tablet dosage forms containing croscarmellose sodium. *International journal of pharmaceutics*, 47, 89-93.
- HÖRTER, D. & DRESSMAN, J. 2001. Influence of physicochemical properties on dissolution of drugs in the gastrointestinal tract. *Advanced drug delivery reviews*, 46, 75-87.
- HOSHINO, T., KUSAKI, F. & FUKUI, I. 2007. Solid dispersion preparation. EP Patent 1,847,260.

- HOSSEINZADEH, R., GHESHLAGI, M., TAHMASEBI, R. & HOJJATI, F. 2009. Spectrophotometric study of interaction and solubilization of procaine hydrochloride in micellar systems. *Central European Journal of Chemistry*, 7, 90-95.
- HUANG, J., WIGENT, R. J., BENTZLEY, C. M. & SCHWARTZ, J. B. 2006. Nifedipine solid dispersion in microparticles of ammonio methacrylate copolymer and ethylcellulose binary blend for controlled drug delivery: Effect of drug loading on release kinetics. *International Journal of Pharmaceutics*, 319, 44-54.
- JACHOWICZ, R. 1987. Dissolution rates of partially water-soluble drugs from solid dispersion systems. I. Prednisolone. *International Journal of Pharmaceutics*, 35, 1-5.
- JAIN, A., RAN, Y. & YALKOWSKY, S. H. 2004. Effect of pH-sodium lauryl sulfate combination on solubilization of PG-300995 (an anti-HIV agent): a technical note. *AAPS PharmSciTech*, 5, 65-67.
- JANSSENS, S. & VAN DEN MOOTER, G. 2009. Review: physical chemistry of solid dispersions. *Journal of Pharmacy and Pharmacology*, 61, 1571-1586.
- JINNO, J.-I., KAMADA, N., MIYAKE, M., YAMADA, K., MUKAI, T., ODOMI, M., TOGUCHI, H., LIVERSIDGE, G. G., HIGAKI, K. & KIMURA, T. 2006. Effect of particle size reduction on dissolution and oral absorption of a poorly water-soluble drug, cilostazol, in beagle dogs. *Journal of Controlled Release*, 111, 56-64.
- JOSHI, H. N., TEJWANI, R. W., DAVIDOVICH, M., SAHASRABUDHE, V. P., JEMAL, M., BATHALA, M. S., VARIA, S. A. & SERAJUDDIN, A. 2004. Bioavailability enhancement of a poorly water-soluble drug by solid dispersion in polyethylene glycol-polysorbate 80 mixture. *International Journal of Pharmaceutics*, 269, 251-258.
- JOUNELA, A., PENTIKÄINEN, P. & SOTHMANN, A. 1975. Effect of particle size on the bioavailability of digoxin. *European journal of clinical pharmacology*, 8, 365-370.
- JUNG, M. S., KIM, J. S., KIM, M. S., ALHALAWEH, A., CHO, W., HWANG, S. J. & VELAGA, S. P. 2010. Bioavailability of indomethacin-saccharin cocrystals. *Journal of Pharmacy and Pharmacology*, 62, 1560-1568.
- KALIVODA, A., FISCHBACH, M. & KLEINEBUDDE, P. 2012. Application of mixtures of polymeric carriers for dissolution enhancement of oxeglitazar using hot-melt extrusion. *International Journal of Pharmaceutics*.
- KARATAŞ, A., YÜKSEL, N. & BAYKARA, T. 2005. Improved solubility and dissolution rate of piroxicam using gelucire 44/14 and labrasol. *Il Farmaco*, 60, 777-782.
- KARAVAS, E., KTISTIS, G., XENAKIS, A. & GEORGARAKIS, E. 2006. Effect of hydrogen bonding interactions on the release mechanism of felodipine from nanodispersions with polyvinylpyrrolidone. *European journal of pharmaceutics and biopharmaceutics*, 63, 103-114.
- KAWABATA, Y., WADA, K., NAKATANI, M., YAMADA, S. & ONOUE, S. 2011. Formulation design for poorly water-soluble drugs based on biopharmaceutics classification system: Basic approaches and practical applications. *International Journal of Pharmaceutics*, 420, 1-10.
- KAWABATA, Y., YAMAMOTO, K., DEBARI, K., ONOUE, S. & YAMADA, S. 2010. Novel crystalline solid dispersion of tranilast with high photostability and improved oral bioavailability. *European Journal of Pharmaceutical Sciences*, 39, 256-262.
- KERC, J., SRCIC, S. & KOFLER, B. 1998. Alternative solvent-free preparation methods for felodipine surface solid dispersions. *Drug development and industrial pharmacy*, 24, 359-363.
- KERNS, E. H. 2001. High throughput physicochemical profiling for drug discovery. *Journal of pharmaceutical sciences*, 90, 1838-1858.

- KOHLI, K., CHOPRA, S., DHAR, D., ARORA, S. & KHAR, R. K. 2010. Self-emulsifying drug delivery systems: an approach to enhance oral bioavailability. *Drug discovery today*, 15, 958-965.
- KOSTEWICZ, E. S., WUNDERLICH, M., BRAUNS, U., BECKER, R., BOCK, T. & DRESSMAN, J. B. 2004. Predicting the precipitation of poorly soluble weak bases upon entry in the small intestine. *Journal of pharmacy and pharmacology*, 56, 43-51.
- KU, H. S., SIORES, E., TAUBE, A. & BALL, J. A. 2002. Productivity improvement through the use of industrial microwave technologies. *Computers & Industrial Engineering*, 42, 281-290.
- LACHMAN, L., LIEBERMAN, H. A. & KANIG, J. L. 1986. *The theory and practice of industrial pharmacy*.
- LANGHAM, Z. A. 2011. *Design and performance of felodipine-based solid dispersions*. University of Nottingham.
- LEAVITT, S. & FREIRE, E. 2001. Direct measurement of protein binding energetics by isothermal titration calorimetry. *Current opinion in structural biology*, 11, 560-566.
- LEUNER, C. & DRESSMAN, J. 2000. Improving drug solubility for oral delivery using solid dispersions. *European Journal of Pharmaceutics and Biopharmaceutics*, 50, 47-60.
- LI, C., LI, C., LE, Y. & CHEN, J.-F. 2011. Formation of bicalutamide nanodispersion for dissolution rate enhancement. *International journal of pharmaceutics*, 404, 257-263.
- LI, F.-Q., HU, J.-H., DENG, J.-X., SU, H., XU, S. & LIU, J.-Y. 2006a. In vitro controlled release of sodium ferulate from Compritol 888 ATO-based matrix tablets. *International Journal of Pharmaceutics*, 324, 152-157.
- LI, S., WONG, S., SETHIA, S., ALMOAZEN, H., JOSHI, Y. M. & SERAJUDDIN, A. T. 2005. Investigation of solubility and dissolution of a free base and two different salt forms as a function of pH. *Pharmaceutical Research*, 22, 628-635.
- LI, Y., TAULIER, N., RAUTH, A. M. & WU, X. Y. 2006b. Screening of lipid carriers and characterization of drug-polymer-lipid interactions for the rational design of polymer-lipid hybrid nanoparticles (PLN). *Pharmaceutical research*, 23, 1877-1887.
- LIM, H.-T., BALAKRISHNAN, P., OH, D. H., JOE, K. H., KIM, Y. R., HWANG, D. H., LEE, Y.-B., YONG, C. S. & CHOI, H.-G. 2010. Development of novel sibutramine base-loaded solid dispersion with gelatin and HPMC: Physicochemical characterization and pharmacokinetics in beagle dogs. *International journal of pharmaceutics*, 397, 225-230.
- LIVERSIDGE, G. G. & CUNDY, K. C. 1995. Particle size reduction for improvement of oral bioavailability of hydrophobic drugs: I. Absolute oral bioavailability of nanocrystalline danazol in beagle dogs. *International Journal of Pharmaceutics*, 125, 91-97.
- LOFTSSON, T. & BREWSTER, M. E. 1996. Pharmaceutical applications of cyclodextrins. 1. Drug solubilization and stabilization. *Journal of pharmaceutical sciences*, 85, 1017-1025.
- LOWN, K. S., BAILEY, D. G., FONTANA, R. J., JANARDAN, S. K., ADAIR, C. H., FORTLAGE, L. A., BROWN, M. B., GUO, W. & WATKINS, P. B. 1997. Grapefruit juice increases felodipine oral availability in humans by decreasing intestinal CYP3A protein expression. *Journal of Clinical Investigation*, 99, 2545.
- MANIRUZZAMAN, M., BOATENG, J. S., SNOWDEN, M. J. & DOUROUMIS, D. 2012. A review of hot-melt extrusion: process technology to pharmaceutical products. *ISRN pharmaceutics*, 2012.
- MARTINEZ, J. C., MURCIANO-CALLES, J., COBOS, E. S., IGLESIAS-BEXIGA, M., LUQUE, I. & RUIZ-SANZ, J. 2013. Isothermal Titration Calorimetry: Thermodynamic Analysis of the Binding Thermograms of Molecular Recognition Events by Using Equilibrium Models.

- MCGINITY, J. W. & HARRIS, W. R. 1980. Increasing dissolution rates of poorly soluble drugs by adsorption to montmorillonite. *Drug Development and Industrial Pharmacy*, 6, 35-48.
- MCMORLAND, G. H., DOUGLAS, M. J., JEFFERY, W. K., ROSS, P. L., AXELSON, J. E., KIM, J. H., GAMBLING, D. R. & ROBERTSON, K. 1986. Effect of pH-adjustment of bupivacaine on onset and duration of epidural analgesia in parturients. *Canadian Anaesthetists' Society Journal*, 33, 537-541.
- MCNAMARA, D. P., CHILDS, S. L., GIORDANO, J., IARRICCIO, A., CASSIDY, J., SHET, M. S., MANNION, R., O'DONNELL, E. & PARK, A. 2006. Use of a glutaric acid cocrystal to improve oral bioavailability of a low solubility API. *Pharmaceutical Research*, 23, 1888-1897.
- MEHANNA, M. M., MOTAWAA, A. M. & SAMAHA, M. W. 2010. In sight into tadalafil-block copolymer binary solid dispersion: Mechanistic investigation of dissolution enhancement. *International journal of pharmaceutics*, 402, 78-88.
- MIYAZAKI, T., ASO, Y., YOSHIOKA, S. & KAWANISHI, T. 2011. Differences in crystallization rate of nitrendipine enantiomers in amorphous solid dispersions with HPMC and HPMCP. *International Journal of Pharmaceutics*, 407, 111-118.
- MOES, J., KOOLEN, S., HUITEMA, A., SCHELLENS, J., BEIJNEN, J. & NUIJEN, B. 2011. Pharmaceutical development and preliminary clinical testing of an oral solid dispersion formulation of docetaxel (ModraDoc001). *International Journal of Pharmaceutics*, 420, 244-250.
- MONEGHINI, M., BELLICH, B., BAXA, P. & PRINCIVALLE, F. 2008. Microwave generated solid dispersions containing ibuprofen. *International journal of pharmaceutics*, 361, 125-130.
- MOSHARRAF, M. & NYSTRÖM, C. 1995. The effect of particle size and shape on the surface specific dissolution rate of micro-sized practically insoluble drugs. *International Journal of Pharmaceutics*, 122, 35-47.
- MUELLER, E. A., KOVARIK, J. M., VAN BREE, J. B., TETZLOFF, W., GREVEL, J. & KUTZ, K. 1994. Improved dose linearity of cyclosporine pharmacokinetics from a microemulsion formulation. *Pharmaceutical Research*, 11, 301-304.
- MÜLLER, R. H. & PETERS, K. 1998. Nanosuspensions for the formulation of poorly soluble drugs: I. Preparation by a size-reduction technique. *International Journal of Pharmaceutics*, 160, 229-237.
- MURPHY, C., PILLAY, V., CHOONARA, Y. E., DU TOIT, L. C., NDESENDO, V. M., CHIRWA, N. & KUMAR, P. 2012. Optimization of a dual mechanism gastrofloatable and gastroadhesive delivery system for narrow absorption window drugs. *AAPS PharmSciTech*, 13, 1-15.
- NAKANO, M. 1971. Effects of interaction with surfactants, adsorbents, and other substances on the permeation of chlorpromazine through a dimethyl polysiloxane membrane. *Journal of pharmaceutical sciences*, 60, 571-575.
- NAMBU, N., SHIMODA, M., TAKAHASHI, Y., UEDA, H. & NAGAI, T. 1978. Bioavailability of powdered inclusion compounds of nonsteroidal antiinflammatory drugs with β -cyclodextrin in rabbits and dogs. *Chemical and Pharmaceutical Bulletin*, 26, 2952-2956.
- NELSON, E. 1957. Solution rate of theophylline salts and effects from oral administration. *Journal of the American Pharmaceutical Association*, 46, 607-614.
- NELSON, E. 1958. Comparative dissolution rates of weak acids and their sodium salts. *Journal of the American Pharmaceutical Association*, 47, 297-299.

- NESLIHAN GURSOY, R. & BENITA, S. 2004. Self-emulsifying drug delivery systems (SEDDS) for improved oral delivery of lipophilic drugs. *Biomedicine & Pharmacotherapy*, 58, 173-182.
- NOLLENBERGER, K., GRYCZKE, A., MEIER, C., DRESSMAN, J., SCHMIDT, M. & BRÜHNE, S. 2009. Pair distribution function X-ray analysis explains dissolution characteristics of felodipine melt extrusion products. *Journal of pharmaceutical sciences*, 98, 1476-1486.
- NOYES, A. A. & WHITNEY, W. R. 1897. The rate of solution of solid substances in their own solutions. *Journal of the American Chemical Society*, 19, 930-934.
- NÚÑEZ, S., VENHORST, J. & KRUSE, C. G. 2012. Target–drug interactions: first principles and their application to drug discovery. *Drug discovery today*, 17, 10-22.
- NURJAYA, S. & WONG, T. 2005. Effects of microwave on drug release properties of matrices of pectin. *Carbohydrate polymers*, 62, 245-257.
- O'NEILL, M. A. & GAISFORD, S. 2011. Application and use of isothermal calorimetry in pharmaceutical development. *International journal of pharmaceutics*, 417, 83-93.
- OKONOJI, S., OGUCHI, T., YONEMOCHI, E., PUTTIPIATKHACHORN, S. & YAMAMOTO, K. 1997. Improved dissolution of ofloxacin via solid dispersion. *International Journal of Pharmaceutics*, 156, 175-180.
- ONOUE, S., TAKAHASHI, H., KAWABATA, Y., SETO, Y., HATANAKA, J., TIMMERMANN, B. & YAMADA, S. 2010. Formulation design and photochemical studies on nanocrystal solid dispersion of curcumin with improved oral bioavailability. *Journal of pharmaceutical sciences*, 99, 1871-1881.
- OVERHOFF, K. A., ENGSTROM, J. D., CHEN, B., SCHERZER, B. D., MILNER, T. E., JOHNSTON, K. P. & WILLIAMS III, R. O. 2007. Novel ultra-rapid freezing particle engineering process for enhancement of dissolution rates of poorly water-soluble drugs. *European journal of pharmaceutics and biopharmaceutics*, 65, 57-67.
- OWUSU-ABABIO, G., EBUBE, N. K., REAMS, R. & HABIB, M. 1998. Comparative dissolution studies for mefenamic acid-polyethylene glycol solid dispersion systems and tablets. *Pharmaceutical development and technology*, 3, 405-412.
- OZEKI, T., YUASA, H. & KANAYA, Y. 2000. Controlled release from solid dispersion composed of poly (ethylene oxide)–Carbopol® interpolymer complex with various cross-linking degrees of Carbopol®. *Journal of controlled release*, 63, 287-295.
- PANAKANTI, R. & NARANG, A. S. 2012. Impact of excipient interactions on drug bioavailability from solid dosage forms. *Pharmaceutical research*, 29, 2639-2659.
- PAPADIMITRIOU, S. A., BIKIARIS, D. & AVGOUSTAKIS, K. 2008. Microwave-induced enhancement of the dissolution rate of poorly water-soluble tibolone from poly (ethylene glycol) solid dispersions. *Journal of Applied Polymer Science*, 108, 1249-1258.
- PARIKH, R., MANSURI, N., GOHEL, M. & SONLWALA, M. 2005. Dissolution enhancement of nimesulide using complexation and salt formation techniques. *Indian drugs*, 42, 149-154.
- PASSERINI, N., ALBERTINI, B., GONZÁLEZ-RODRÍGUEZ, M. L., CAVALLARI, C. & RODRIGUEZ, L. 2002. Preparation and characterisation of ibuprofen–poloxamer 188 granules obtained by melt granulation. *European journal of pharmaceutical sciences*, 15, 71-78.
- PASSERINI, N., ALBERTINI, B., PERISSUTTI, B. & RODRIGUEZ, L. 2006. Evaluation of melt granulation and ultrasonic spray congealing as techniques to enhance the dissolution of praziquantel. *International journal of pharmaceutics*, 318, 92-102.

- PAULA, S., SUES, W., TUCHTENHAGEN, J. & BLUME, A. 1995. Thermodynamics of micelle formation as a function of temperature: a high sensitivity titration calorimetry study. *The Journal of Physical Chemistry*, 99, 11742-11751.
- PÉREZ-RODRÍGUEZ, M., PRIETO, G., REGA, C., VARELA, L. M., SARMIENTO, F. & MOSQUERA, V. 1998. A comparative study of the determination of the critical micelle concentration by conductivity and dielectric constant measurements. *Langmuir*, 14, 4422-4426.
- POUTON, C. W. 2006. Formulation of poorly water-soluble drugs for oral administration: physicochemical and physiological issues and the lipid formulation classification system. *European Journal of Pharmaceutical Sciences*, 29, 278-287.
- PUDIPEDDI, M. & SERAJUDDIN, A. 2005. Trends in solubility of polymorphs. *Journal of pharmaceutical sciences*, 94, 929-939.
- RANGEL-YAGUI, C. O., PESSOA JR, A. & TAVARES, L. C. 2005. Micellar solubilization of drugs. *J Pharm Pharm Sci*, 8, 147-163.
- RAUTIO, J., KUMPULAINEN, H., HEIMBACH, T., OLIYAI, R., OH, D., JÄRVINEN, T. & SAVOLAINEN, J. 2008. Prodrugs: design and clinical applications. *Nature Reviews Drug Discovery*, 7, 255-270.
- RICHARDS, R. M. E., XING, J. Z. & MACKAY, K. M. 1996. Excipient interaction with cetylpyridinium chloride activity in tablet based lozenges. *Pharmaceutical research*, 13, 1258-1264.
- RODRÍGUEZ-SPONG, B., PRICE, C. P., JAYASANKAR, A., MATZGER, A. J. & RODRÍGUEZ-HORNEDO, N. R. 2004. General principles of pharmaceutical solid polymorphism: a supramolecular perspective. *Advanced drug delivery reviews*, 56, 241-274.
- RODRIGUEZ-PEREZ, A. I., RODRIGUEZ-TENREIRO, C., ALVAREZ-LORENZO, C., TABOADA, P., CONCHEIRO, A. & TORRES-LABANDEIRA, J. J. 2006. Sertaconazole/hydroxypropyl- β -cyclodextrin complexation: Isothermal titration calorimetry and solubility approaches. *Journal of pharmaceutical sciences*, 95, 1751-1762.
- S DARWICH, A., NEUHOFF, S., JAMEI, M. & ROSTAMI-HODJEGAN, A. 2010. Interplay of metabolism and transport in determining oral drug absorption and gut wall metabolism: a simulation assessment using the Advanced Dissolution, Absorption, Metabolism (ADAM) model. *Current drug metabolism*, 11, 716-729.
- SAVJANI KETAN, T., GAJJAR ANURADHA, K. & SAVJANI JIGNASA, K. 2012. Drug Solubility: Importance and enhancement techniques. *ISRN pharmaceuticals*, 2012.
- SCHOLZ, A., ABRAHAMSSON, B., DIEBOLD, S. M., KOSTEWICZ, E., POLENTARUTTI, B. I., UGELL, A.-L. & DRESSMAN, J. B. 2002. Influence of hydrodynamics and particle size on the absorption of felodipine in labradors. *Pharmaceutical Research*, 19, 42-46.
- SCHULTHEISS, N. & NEWMAN, A. 2009. Pharmaceutical cocrystals and their physicochemical properties. *Crystal Growth and Design*, 9, 2950-2967.
- SEKIGUCHI, K. & OBI, N. 1961. Studies on Absorption of Eutectic Mixture. I. A Comparison of the Behavior of Eutectic Mixture of Sulfathiazole and that of Ordinary Sulfathiazole in Man. *Chemical & pharmaceutical bulletin*, 9, 866-872.
- SERAJUDDIN, A. 1999. Solid dispersion of poorly water-soluble drugs: early promises, subsequent problems, and recent breakthroughs. *Journal of pharmaceutical sciences*, 88, 1058-1066.
- SHARGEL, L., ANDREW, B. & WU-PONG, S. 2005. Applied biopharmaceutics and pharmacokinetics, Appleton & Lange Reviews/McGraw-Hill, Medical Pub. Division.

- SHEGOKAR, R. & MÜLLER, R. H. 2010. Nanocrystals: industrially feasible multifunctional formulation technology for poorly soluble actives. *International Journal of Pharmaceutics*, 399, 129-139.
- SHIN, S.-C., OH, I.-J., LEE, Y.-B., CHOI, H.-K. & CHOI, J.-S. 1998. Enhanced dissolution of furosemide by coprecipitating or cogrinding with croscopovidone. *International Journal of Pharmaceutics*, 175, 17-24.
- SIMONELLI, A., MEHTA, S. & HIGUCHI, W. 1969. Dissolution Rates of High Energy Polyvinylpyrrolidone (PVP)-Sulfathiazole Coprecipitates. *Journal of pharmaceutical sciences*, 58, 538-549.
- SMIRNOVA, I., SUTTIRUENGWONG, S., SEILER, M. & ARLT, W. 2004. Dissolution rate enhancement by adsorption of poorly soluble drugs on hydrophilic silica aerogels. *Pharmaceutical development and technology*, 9, 443-452.
- SOLANKI, H. K., PRAJAPATI, V. D. & JANI, G. K. 2011. Microwave Technology—A Potential Tool in Pharmaceutical Science. *International Journal of PharmTech Research*, 2, 1754-1761.
- STELLA, V. J. & NTI-ADDAE, K. W. 2007. Prodrug strategies to overcome poor water solubility. *Advanced drug delivery reviews*, 59, 677-694.
- SWARBIRCK, J. & BOYLAN, J. C. 2001. *Encyclopedia of Pharmaceutical Technology: Supplement 3*, CRC Press.
- SYLVESTRE, J.-P., TANG, M.-C., FURTOS, A., LECLAIR, G., MEUNIER, M. & LEROUX, J.-C. 2011. Nanonization of megestrol acetate by laser fragmentation in aqueous milieu. *Journal of Controlled Release*, 149, 273-280.
- SZÚTS, A., LANG, P., AMBRUS, R., KISS, L., DELI, M. A. & SZABÓ-RÉVÉSZ, P. 2011. Applicability of sucrose laurate as surfactant in solid dispersions prepared by melt technology. *International Journal of Pharmaceutics*, 410, 107-110.
- TACHIBANA, T. & NAKAMURA, A. 1965. A method for preparing an aqueous colloidal dispersion of organic materials by using water-soluble polymers: Dispersion of β -carotene by polyvinylpyrrolidone. *Kolloid-Zeitschrift und Zeitschrift für Polymere*, 203, 130-133.
- TAHERI-KAFRANI, A. & BORDBAR, A.-K. 2009. Energetics of micellization of sodium n-dodecyl sulfate at physiological conditions using isothermal titration calorimetry. *Journal of thermal analysis and calorimetry*, 98, 567-575.
- TANAKA, N., IMAI, K., OKIMOTO, K., UEDA, S., TOKUNAGA, Y., IBUKI, R., HIGAKI, K. & KIMURA, T. 2006. Development of novel sustained-release system, disintegration-controlled matrix tablet (DCMT) with solid dispersion granules of nilvadipine (II): in vivo evaluation. *Journal of controlled release*, 112, 51-56.
- TAYLOR, L. S. & ZOGRAFI, G. 1997. Spectroscopic characterization of interactions between PVP and indomethacin in amorphous molecular dispersions. *Pharmaceutical research*, 14, 1691-1698.
- TIAN, Y., RAVI, P., BROMBERG, L., HATTON, T. A. & TAM, K. C. 2007. Synthesis and aggregation behavior of Pluronic F87/poly (acrylic acid) block copolymer in the presence of doxorubicin. *Langmuir*, 23, 2638-2646.
- TORCHILIN, V. 2007. Micellar nanocarriers: pharmaceutical perspectives. *Pharmaceutical research*, 24, 1-16.
- TURNBULL, W. B. & DARANAS, A. H. 2003. On the value of c: can low affinity systems be studied by isothermal titration calorimetry? *Journal of the American Chemical Society*, 125, 14859-14866.
- VAN DEN MOOTER, G. 2012. The use of amorphous solid dispersions: A formulation strategy to overcome poor solubility and dissolution rate. *Drug Discovery Today: Technologies*, 9, e79-e85.

- VAN DEN MOOTER, G., WEUTS, I., DE RIDDER, T. & BLATON, N. 2006. Evaluation of Inutec SP1 as a new carrier in the formulation of solid dispersions for poorly soluble drugs. *International Journal of Pharmaceutics*, 316, 1-6.
- VAN DROOGE, D., HINRICHS, W. & FRIJLINK, H. 2004. Anomalous dissolution behaviour of tablets prepared from sugar glass-based solid dispersions. *Journal of controlled release*, 97, 441-452.
- VAN DROOGE, D., HINRICHS, W., VISSER, M. & FRIJLINK, H. 2006. Characterization of the molecular distribution of drugs in glassy solid dispersions at the nano-meter scale, using differential scanning calorimetry and gravimetric water vapour sorption techniques. *International Journal of Pharmaceutics*, 310, 220-229.
- VASANTHAVADA, M., TONG, W.-Q., JOSHI, Y. & KISLALIOGLU, M. S. 2004. Phase behavior of amorphous molecular dispersions I: Determination of the degree and mechanism of solid solubility. *Pharmaceutical research*, 21, 1598-1606.
- VASANTHAVADA, M., TONG, W.-Q. T., JOSHI, Y. & KISLALIOGLU, M. S. 2005. Phase behavior of amorphous molecular dispersions II: Role of hydrogen bonding in solid solubility and phase separation kinetics. *Pharmaceutical research*, 22, 440-448.
- VASCONCELOS, T., SARMENTO, B. & COSTA, P. 2007. Solid dispersions as strategy to improve oral bioavailability of poor water soluble drugs. *Drug discovery today*, 12, 1068-1075.
- VELAZQUEZ-CAMPOY, A., LEAVITT, S. A. & FREIRE, E. 2004. Characterization of protein-protein interactions by isothermal titration calorimetry. *Protein-Protein Interactions*. Springer.
- VEMULA, V. R., LAGISHETTY, V. & LINGALA, S. 2010. Solubility enhancement techniques. *International journal of pharmaceutical sciences review and research*, 5, 41-51.
- VENKATESH, S., LI, J., XU, Y., VISHNUVAJALA, R. & ANDERSON, B. D. 1996. Intrinsic solubility estimation and pH-solubility behavior of cosalane (NSC 658586), an extremely hydrophobic diprotic acid. *Pharmaceutical research*, 13, 1453-1459.
- VERHOEVEN, E., DE BEER, T., SCHACHT, E., VAN DEN MOOTER, G., REMON, J. P. & VERVAET, C. 2009. Influence of polyethylene glycol/polyethylene oxide on the release characteristics of sustained-release ethylcellulose mini-matrices produced by hot-melt extrusion: in vitro and in vivo evaluations. *European Journal of Pharmaceutics and Biopharmaceutics*, 72, 463-470.
- VIPPAGUNTA, S. R., WANG, Z., HORNING, S. & KRILL, S. L. 2007. Factors affecting the formation of eutectic solid dispersions and their dissolution behavior. *Journal of pharmaceutical sciences*, 96, 294-304.
- VISSER, M. R., BAERT, L., KLOOSTER, G. V. T., SCHUELLER, L., GELDOF, M., VANWELKENHUYSEN, I., DE KOCK, H., DE MEYER, S., FRIJLINK, H. W. & ROSIER, J. 2010. Inulin solid dispersion technology to improve the absorption of the BCS Class IV drug TMC240. *European Journal of Pharmaceutics and Biopharmaceutics*, 74, 233-238.
- VO, C. L.-N., PARK, C. & LEE, B.-J. 2013. Current trends and future perspectives of solid dispersions containing poorly water-soluble drugs. *European Journal of Pharmaceutics and Biopharmaceutics*.
- VOLPE, P. L. 1995. Calorimetric study of SDS micelle formation in water and in NaCl solution at 298 K. *Thermochimica acta*, 257, 59-66.
- WANG, G. & OLOFSSON, G. 1998. Titration calorimetric study of the interaction between ionic surfactants and uncharged polymers in aqueous solution. *The Journal of Physical Chemistry B*, 102, 9276-9283.

- WATERS, L. J., BEDFORD, S., PARKES, G. & MITCHELL, J. 2010. Influence of lipophilicity on drug–cyclodextrin interactions: A calorimetric study. *Thermochimica Acta*, 511, 102-106.
- WATERS, L. J., BEDFORD, S. & PARKES, G. M. 2011. Controlled microwave processing applied to the pharmaceutical formulation of ibuprofen. *AAPS PharmSciTech*, 12, 1038-1043.
- WILLIAMS, M., TIAN, Y., JONES, D. S. & ANDREWS, G. P. 2010. Hot-melt extrusion technology: optimizing drug delivery. *European Journal of Parenteral Sciences and Pharmaceutical Sciences*, 15, 61.
- WISEMAN, T., WILLISTON, S., BRANDTS, J. F. & LIN, L.-N. 1989. Rapid measurement of binding constants and heats of binding using a new titration calorimeter. *Analytical biochemistry*, 179, 131-137.
- WON, D.-H., KIM, M.-S., LEE, S., PARK, J.-S. & HWANG, S.-J. 2005. Improved physicochemical characteristics of felodipine solid dispersion particles by supercritical anti-solvent precipitation process. *International Journal of Pharmaceutics*, 301, 199-208.
- WONG, T., WAHAB, S. & ANTHONY, Y. 2008. Drug release responses of zinc ion crosslinked poly (methyl vinyl ether-*co*-maleic acid) matrix towards microwave. *International journal of pharmaceutics*, 357, 154-163.
- WONG, T. W., CHAN, L. W., KHO, S. B. & HENG, P. W. S. 2005. Aging and microwave effects on alginate/chitosan matrices. *Journal of controlled release*, 104, 461-475.
- WONG, T. W., CHAN, L. W., KHO, S. B. & SIA HENG, P. W. 2002. Design of controlled-release solid dosage forms of alginate and chitosan using microwave. *Journal of Controlled release*, 84, 99-114.
- WU, Y., LOPER, A., LANDIS, E., HETTRICK, L., NOVAK, L., LYNN, K., CHEN, C., THOMPSON, K., HIGGINS, R. & BATRA, U. 2004. The role of biopharmaceutics in the development of a clinical nanoparticle formulation of MK-0869: a Beagle dog model predicts improved bioavailability and diminished food effect on absorption in human. *International Journal of Pharmaceutics*, 285, 135-146.
- XIA, D., CUI, F., PIAO, H., CUN, D., PIAO, H., JIANG, Y., OUYANG, M. & QUAN, P. 2010. Effect of crystal size on the in vitro dissolution and oral absorption of nitrendipine in rats. *Pharmaceutical Research*, 27, 1965-1976.
- YAN, Y.-D., SUNG, J. H., KIM, K. K., KIM, D. W., KIM, J. O., LEE, B.-J., YONG, C. S. & CHOI, H.-G. 2012. Novel valsartan-loaded solid dispersion with enhanced bioavailability and no crystalline changes. *International journal of pharmaceutics*, 422, 202-210.
- YOSHIOKA, M., HANCOCK, B. C. & ZOGRAFI, G. 1994. Crystallization of indomethacin from the amorphous state below and above its glass transition temperature. *Journal of pharmaceutical sciences*, 83, 1700-1705.
- YOUSEFPOUR, P., ATYABI, F., FARAHANI, E. V., SAKHTIANCHI, R. & DINARVAND, R. 2011. Polyanionic carbohydrate doxorubicin–dextran nanocomplex as a delivery system for anticancer drugs: in vitro analysis and evaluations. *International journal of nanomedicine*, 6, 1487.
- YÜKSEL, N., KARATAŞ, A., ÖZKAN, Y., SAVAŞER, A., ÖZKAN, S. A. & BAYKARA, T. 2003. Enhanced bioavailability of piroxicam using Gelucire 44/14 and Labrasol: in vitro and in vivo evaluation. *European Journal of Pharmaceutics and Biopharmaceutics*, 56, 453-459.
- ZAJC, N., OBREZA, A., BELE, M. & SRČIČ, S. 2005. Physical properties and dissolution behaviour of nifedipine/mannitol solid dispersions prepared by hot melt method. *International Journal of Pharmaceutics*, 291, 51-58.

- ZHANG, M., LI, H., LANG, B., O'DONNELL, K., ZHANG, H., WANG, Z., DONG, Y., WU, C. & WILLIAMS III, R. O. 2012. Formulation and delivery of improved amorphous fenofibrate solid dispersions prepared by thin film freezing. *European Journal of Pharmaceutics and Biopharmaceutics*.
- ZHU, J., LEE, S., HO, M. K., HU, Y., PANG, H., IP, F. C., CHIN, A. C., HARLEY, C. B., IP, N. Y. & WONG, Y. H. 2010. In vitro intestinal absorption and first-pass intestinal and hepatic metabolism of cycloastragenol, a potent small molecule telomerase activator. *Drug metabolism and pharmacokinetics*, 1009210035.

Chapter 2: Materials and methods

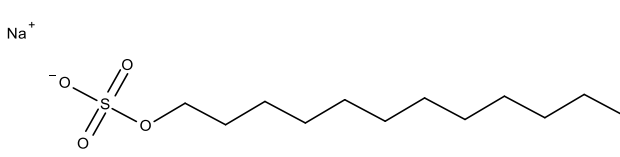
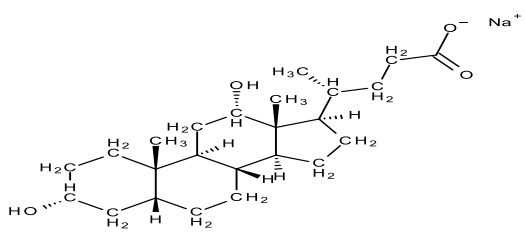
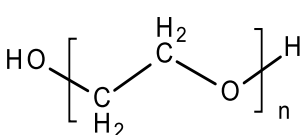
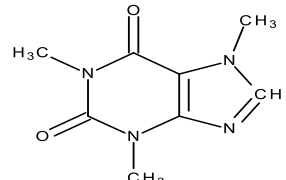
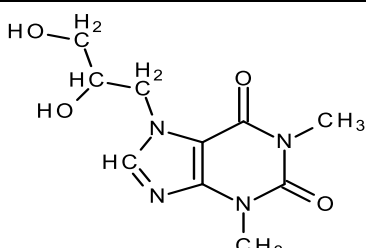
This chapter provides information about the materials, i.e. the drugs and excipients, for the development of formulations using different approaches. The methods for solid state characterisation of formulations, as well as techniques used to evaluate drug-excipient interactions in solution, are also discussed.

2.1. Chemicals

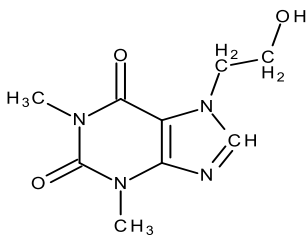
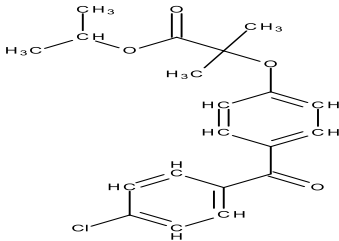
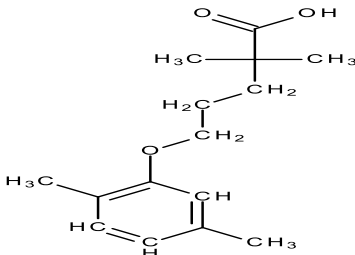
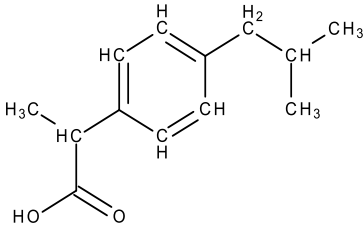
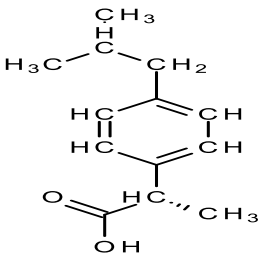
All samples of mesoporous silica, namely Core Shell (CS), Core Shell rehydrox (CSR), SBA-15 (SBA) and the non-porous Stober (ST), were supplied by Glantreo Ltd., Ireland. Silica gel (SG) was supplied from Alfa Aesar (UK). Syloid[®] (SYL) was supplied from WR Grace (USA). Polyethylene glycol 6000 (PEG) (Sigma-Aldrich, Dorset, UK), sodium dodecyl sulphate (SDS) (Sigma-Aldrich, Dorset, UK) and sodium deoxycholate (NaDC) (Fisher Scientific, UK) were used as purchased with a minimum purity of 99 %. Caffeine (Fisher Scientific, UK), diprophylline (Acros Organics, UK), etofylline (TCI, UK), fenofibrate (Sigma-Aldrich, Dorset, UK), gemfibrozil (Sigma-Aldrich, Dorset, UK), ibuprofen (BASF, Cheshire, UK), ibuprofen S (Shahsun pharmaceuticals limited, India), paracetamol (Sigma-Aldrich, Dorset, UK), phenylbutazone (Sigma-Aldrich, Dorset, UK) and theophylline (TCI, UK) were used as purchased with a minimum purity of 99 %. Disodium hydrogen orthophosphate dodecahydrate and sodium dihydrogen orthophosphate anhydrous were purchased from Fisher Scientific, UK with a minimum purity of 99 %. De-ionised water was used throughout the experiments.

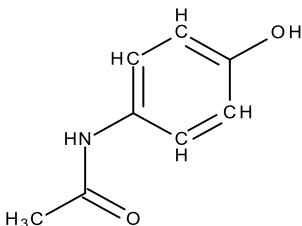
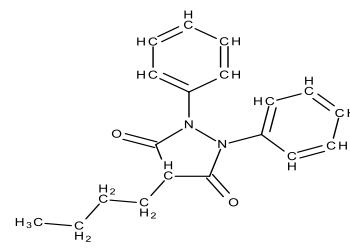
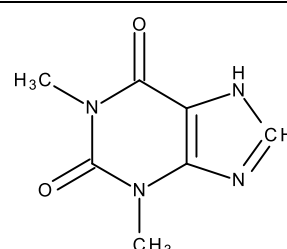
The structures of chemicals, along with their physicochemical properties, are presented in Table 2.1.

Table 2.1: Physicochemical properties of chemicals¹

Sodium Dodecyl Sulphate		Structure
Molecular weight	288.4 g/mol	
Melting point	204-207 °C	
Charge	Anionic	
CMC	8.1 mM	
CAS no.	151-21-3	
Sodium Deoxycholate		
Molecular weight	414.55 g/mol	
Melting point	357-365 °C	
Charge	Anionic	
CMC	5 mM	
CAS no.	302-95-4	
Polyethylene glycol 6000		
Molecular weight	6000	
Melting point	45-65 °C	
Charge	Neutral	
CAS no.	25322-68-3	
Caffeine		
Molecular weight	194.2 g/mol	
Melting point	238 °C	
LogP	-0.13	
Charge	Neutral	
CAS no.	58-08-2	
Diprophylline		
Molecular weight	254.2 g/mol	
Melting point	158 °C	
LogP	-1.10	
Charge	Neutral	
CAS no.	479-18-5	

¹ Molecular weight, melting point, CMC and LogP were generated from ACD/Labs, RSC

Etofylline		Structure
Molecular weight	224.2 g/mol	
Melting point	161-166 °C	
LogP	-0.55	
Charge	Neutral	
CAS no.	519-37-9	
Fenofibrate		
Molecular weight	360.8 g/mol	
Melting point	80-81 °C	
LogP	4.80	
Charge	Neutral	
CAS no.	49562-28-9	
Gemfibrozil		
Molecular weight	250.33 g/mol	
Melting point	59-63 °C	
LogP	4.39	
Charge	Anionic	
CAS no.	25812-30-0	
Ibuprofen		
Molecular weight	206.3 g/mol	
Melting point	75-77 °C	
LogP	3.72	
Charge	Anionic	
CAS no.	15687-27-1	
Ibuprofen S (+)		
Molecular weight	206.3 g/mol	
Melting point	52-55 °C	
LogP	3.72	
Charge	Anionic	
CAS no.	51146-56-6	

Paracetamol		
Molecular weight	151.2 g/mol	
Melting point	169-170 °C	
LogP	1.08	
Charge	Neutral	
CAS no.	103-90-2	
Phenylbutazone		
Molecular weight	308.4 g/mol	
Melting point	105 °C	
LogP	3.16	
Charge	Neutral	
CAS no.	50-33-9	
Theophylline		
Molecular weight	180.2 g/mol	
Melting point	270-274 °C	
LogP	-0.17	
Charge	Neutral	
CAS no.	58-55-9	

The physicochemical properties of the bespoke forms of mesoporous silica are depicted in Table 2.2.

Table 2.2: Physicochemical properties of mesoporous silica

Silica grade	Description	Surface area (m ² g ⁻¹)	Particle size (µm)	Manufacturer
SBA-15 (SBA)	Hexagonally ordered high surface area silica	660	10	Glantreo
Core Shell (CS)	Core Shell silica material (solid core with porous outer shell)	91	5.0	Glantreo
Core Shell rehydrox (CSR)	Core Shell silica material (solid core with porous outer shell) rehydroxylated in acid	91	5.0	Glantreo

Silica Gel (SG)	Standard silica gel	462	70	Alfa Aesar
Stober (ST)	Non-porous silica particles	3.0	0.4	Glantreo
Syloid® (SYL)	Syloid AL 1 FP (SYL 1) A pharmaceutical grade excipient	676	7.0	WR Grace
	Syloid 72 FP (SYL 72) A pharmaceutical grade excipient	405	6.0	WR Grace
	Syloid 244 FP EU (SYL 244) A pharmaceutical grade excipient	379	5.5	WR Grace

2.2. Methods

The main novelty in the formulation aspects of this project is the application of microwave heating. Two specialised systems were used. The first is based around a modified domestic microwave oven (multi-mode cavity) and used for the formulations prepared in an aqueous medium (Waters et al., 2011). The system uses pulse-width modulation to control the power (0 to 800 W) and accurate temperature measurement is provided using a fibre optic temperature probe (Luxtron) located directly in the formulation suspension.

The second microwave system utilises a single-mode cavity with a variable power supply (0 to 1000 W) and was used for the solid-phase formulations. Originally designed for microwave thermogravimetry (Williams and Parkes, 2008), the system incorporates a 5-figure balance and utilises a IR pyrometer (Omega) for temperature measurement (Figure 2.1). The balance means that the mass of the sample can be monitored in real-time which can be useful in detecting if any thermal decomposition of the formulation occurs during processing.

Both microwave systems have computerised control and data acquisition where the microwave power can be continuously altered so that the temperature of the mixture being processed follows a pre-defined programme (e.g. 5 °C min⁻¹ to 100 °C, hold isothermally for 20 minutes, etc.). Experiments using manual control of the microwave power are also possible.

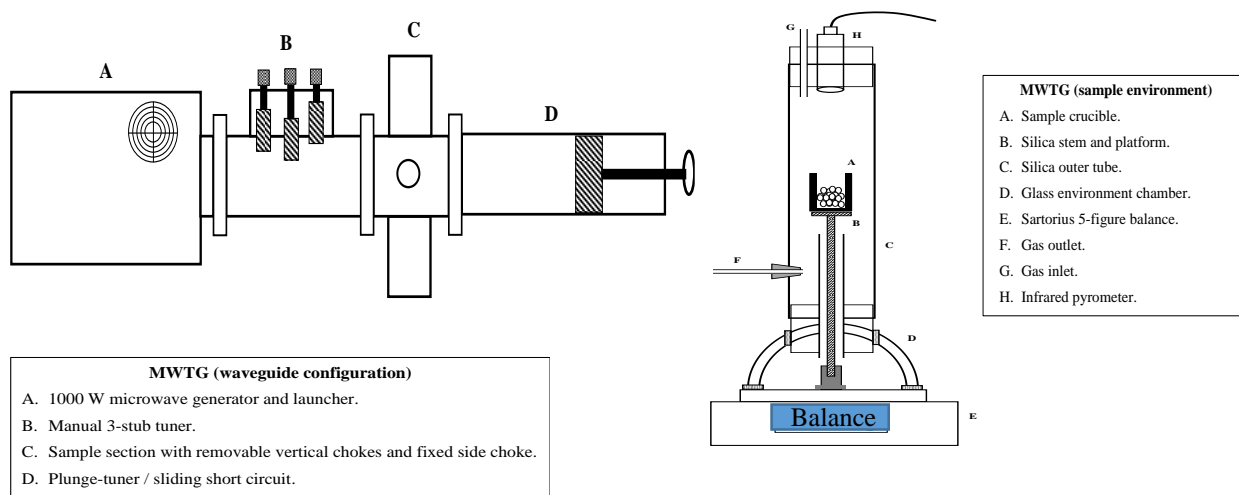


Figure 2.1: Schematic view of the single-mode microwave system used to heat solid materials under controlled conditions.

2.2.1. Mesoporous silica based formulations

Prior to formulation using microwave based methods, a more conventional method was adopted for comparative purposes

2.2.1.1. Conventional melt formulation

Physical mixtures of all six silica samples (CS, CSR, SBA, SG, SYL 1 and ST) were each prepared with fenofibrate at 1:1, 3:1 and 5:1 excipient drug to mass ratios using tumble mixing for 5 minutes to achieve a homogenous mixture. A sample mass (0.5 g) of each

formulation was added to 35 mL of deionised water (DI), placed on a hot plate stirrer with the temperature gradually increased from 25 °C to 90 °C, monitored using the fibre optic temperature probe. This temperature was maintained for 10 minutes, removed from the hot plate and allowed to cool to 25 °C with the resultant product collected by vacuum filtration and dried overnight at 45 °C in a standard oven.

2.2.1.2. Multi-mode microwave processed formulation

Silica samples together with fenofibrate were tumble mixed as described for the conventionally prepared samples. 0.5 g of each formulation was added to 35 mL of deionised water (DI) and placed in a 100 mL beaker in the microwave oven. The fibre optic probe was placed in the liquid which was slowly stirred with the aid of a magnetic stirrer. The software was set to heat the water-suspended mixture to 90 °C and hold isothermally for 10 minutes before the microwave power was reduced to zero to allow the sample to cool. Stirring was maintained throughout. Samples were then collected by vacuum filtration and dried overnight at 45 °C. A typical example of core shell (CS): fenofibrate (1:1) is illustrated in Figure 2.2.

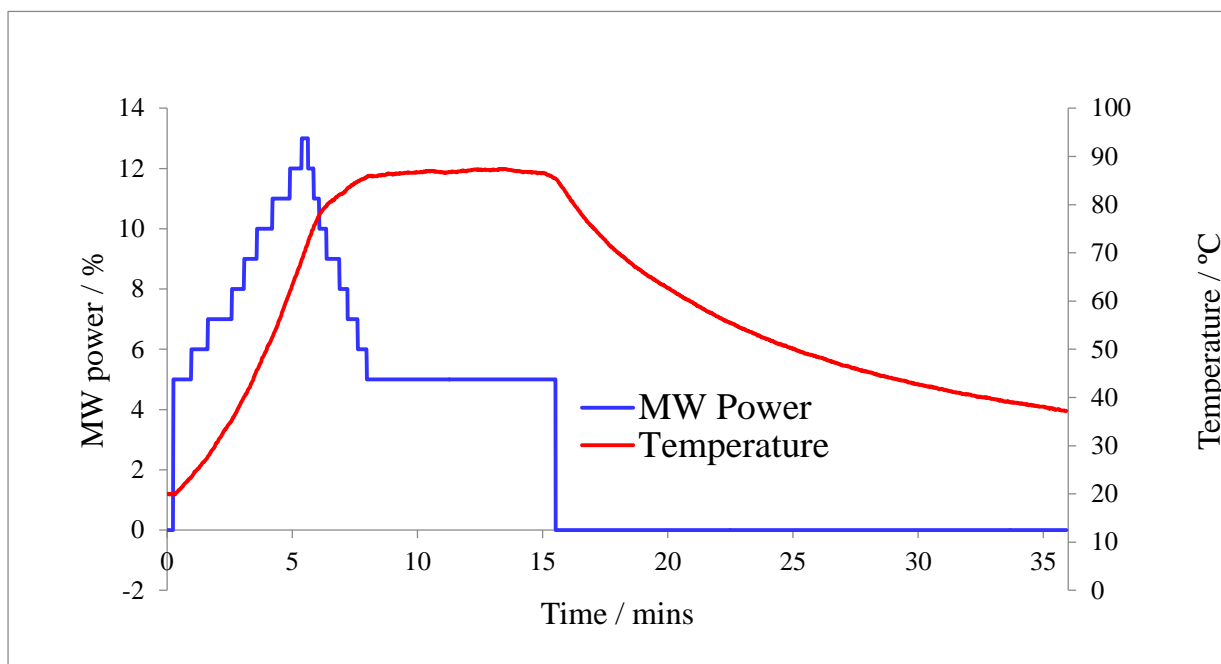


Figure 2.2: Example of processing of fenofibrate and Core Shell (1:1) using the multi-mode microwave system.

2.2.1.3. Single-mode microwave processed formulation

0.5 g of a physically mixed sample of fenofibrate with silica (CS, CSR, SBA, SG, SYL 1 and ST) at silica/drug ratios of 1:1, 3:1, 5:1 and gemfibrozil with silica (Syloid AL-1, Syloid 72 and Syloid 244) at silica/drug ratios of 1:1 and 3:1, was placed in an alumina crucible in the microwave oven with the fibre optic probe positioned directly in the sample. The software was set to continuously modify the microwave power such that the sample was heated slightly above the melting temperature of the respective drug, maintained isothermally (10 minutes for fenofibrate and 20 minutes for gemfibrozil) and then cooled to room temperature, after which the sample was removed and cooled. An example of dry microwave heating is illustrated in Figure 2.3.

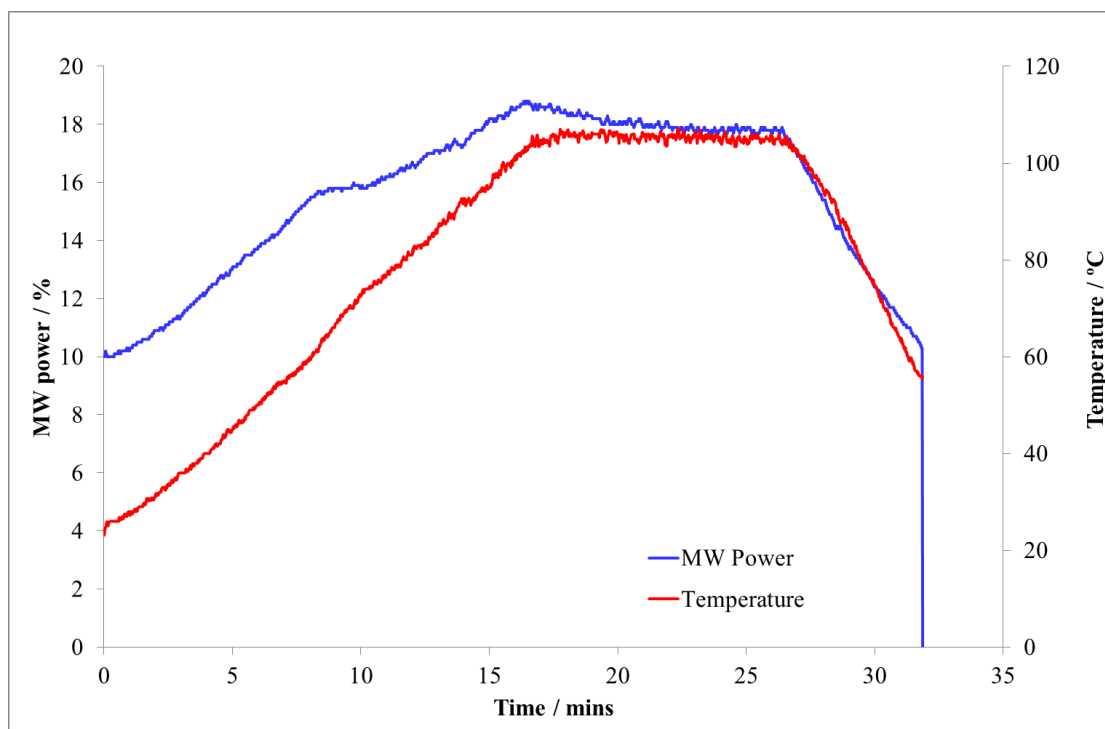


Figure 2.3: Example of processing of fenofibrate and Core Shell (1:5) using the single mode microwave system.

All the formulations were subjected to drug content analysis. Three random samples of 10 mg drug equivalent from each formulation were dissolved in methanol and appropriately diluted and the drug content was evaluated by UV-analysis. The drug content was found to be in the range of 90-98 %.

2.2.2. Polyethylene glycol 6000 (PEG) based formulations

Solid dispersions of fenofibrate (FF), ibuprofen (IBU), ibuprofen S (IBU S) and phenylbutazone (PB) were formulated with polyethylene glycol (PEG) firstly using conventional heating, followed by microwave heating for comparison.

2.2.2.1. Conventional formulation method

For conventional heating, PEG together with FF, IBU or IBU S were tumble mixed in ratios of 1:1, 3:1, 5:1 while 1:1 and 1:5 ratios were prepared for PB. A sample mass (0.5 g) of

each formulation was heated to the respective melting temperature of each drug in a conventional oven for 20 minutes, removed from the oven and then cooled to room temperature.

2.2.2.2.Microwave formulation method

PEG, together with FF, IBU, IBU S and PB were tumble mixed as described for the conventionally prepared samples. 0.5 g of each formulation was placed in an alumina crucible and heated in the single mode microwave system. At this point two distinct methods were employed. Firstly, the software was set to continuously modify the microwave power such that the sample was heated to the melting temperature of the excipient, maintained isothermally for 20 minutes and then cooled to room temperature, after which time the sample was removed and cooled. For identification, these formulations were denoted with a symbol MW*. For the second method the temperature of the samples was increased continuously up to the melting temperature of the drugs, maintained isothermally for 20 minutes and then cooled to room temperature, after which time the sample was removed and cooled. These formulations were identified with a symbol MW.

All the formulations were pulverised in a mortar and pestle, sieved through a 150-mesh screen, and stored in screwed-cap vials at room temperature until further use.

Drug content was determined spectrophotometrically (in methanol) and found to be in the range of 95-97 %.

2.3. Characterisation techniques

In summary, a total of 117 formulations were prepared using both mesoporous silica and polyethylene glycol based excipients (with a total of five drugs) to investigate the suitability of microwave heating as a formulation technique. Little can be determined from the

physical appearance of the resultant products, the true suitability of microwave formulation can only be determined based on their physicochemical properties, which in turn dictates the bioavailability and stability of the products. Therefore, following on from formulation it was essential to undertake a thorough analytical review of all products.

2.3.1. Dissolution testing

To assess the drug release of developed formulations, dissolution analysis was performed using the type II (paddle method). This was a fully automated assembly, comprising a dissolution bath (Pharmatest DT 70), peristaltic pump and UV visible spectrophotometer (Cecil 3021, series 3000) (Figure 2.4).



Figure 2.4: Dissolution apparatus used for analysing formulations.

2.3.1.1. In vitro dissolution of mesoporous silica based formulations

Formulated samples of fenofibrate (equivalent to 10 mg of drug in each) were placed in 900 mL of freshly prepared 0.1 M HCl solution ($\text{pH } 1.2 \pm 0.1$) containing 1 % (w/v) sodium

dodecyl sulphate. Samples of gemfibrozil (equivalent to 20 mg of drug in each) were placed in 500 mL of freshly prepared 0.1 M HCl solution (pH 1.2 ± 0.1) containing 0.5 % (w/v) sodium dodecyl sulphate. The temperature of the dissolution bath was set at 37 °C and a paddle stirring speed of 50 rpm. Samples were taken by an auto sampling system equipped with filters at intervals of 5 minutes over a time period of 30 minutes and returned to the original solution. UV measurements were carried out at 290 nm and 277 nm for fenofibrate and gemfibrozil respectively. All experiments were repeated in triplicate with percentages of drug release calculated based on a series of standard solutions at known concentrations.

2.3.1.2. In vitro dissolution of PEG based formulations

Formulated samples (equivalent to 10 mg of fenofibrate in each or equivalent to 10 mg of phenylbutazone in each) were placed in 900 mL of freshly prepared 0.1 M HCl solution (pH 1.2 ± 0.1) containing 1 % (w/v) sodium dodecyl sulphate or 0.5 % (w/v) sodium dodecyl sulphate respectively. Samples (equivalent to 25 mg of ibuprofen or ibuprofen S in each) were placed in 500 mL of freshly prepared 0.1 M phosphate buffer solution (pH 6.8 ± 0.1). The temperature of the dissolution bath was set at 37 °C and a paddle stirring speed of 50 rpm. Samples were taken by an auto sampling system equipped with filters at intervals of 5 minutes over a time period of 30 minutes and returned to the original solution. UV analysis was carried out at wavelengths of 290 nm, 238 nm, 222 nm and 222 nm for fenofibrate, phenylbutazone, ibuprofen and ibuprofen S respectively. All experiments were repeated in triplicate with percentages of drug release calculated based on a series of standard solutions at known concentrations.

2.3.2. Solid state characterisation

The elucidation of a drug's physical state within a solid dispersion is a vital step to investigate the mechanism by which an enhanced dissolution profile occurs. The particular techniques used in this work are discussed in the following section.

2.3.2.1. X-ray diffraction (XRD)

XRD is an established tool to evaluate the crystalline or amorphous content of solid dispersions and forms the basis of most solid-state testing regimens in the pharmaceutical industry. For this study, powder X-ray diffraction experiments utilised a D2-Phaser (Bruker) X-ray diffractometer, equipped with a Cu K α radiation source at 30 kV voltage and 10 mA current. Diffraction patterns were obtained in the 2 θ range of 5–50° using a 0.02 step size.

2.3.2.2. Differential scanning calorimetry (DSC)

Differential scanning calorimetry (DSC) is the most frequently used thermal analysis technique, mainly because of its promptness, simplicity and wide range of applications. DSC is routinely used to investigate the miscibility of solid dispersion components and to identify the crystalline or amorphous nature of materials. DSC may involve heating or cooling a sample at a constant temperature rate, holding at a specific temperature, or any sequence of these in an inert atmosphere under the flow of a suitable gas. Detailed information based on phase transitions of substances can be obtained (for example, melting points, recrystallisation and glass transitions).

In this study differential scanning (Mettler Toledo DSC 821) analysis for all formulations was performed using 5–10 mg samples, an atmosphere of flowing nitrogen at 50 mL per minute and a temperature program of 10 °C/min from 25 °C to 120 °C.

2.3.2.3. Fourier-transform infrared spectroscopy (FTIR)

Fourier-transform infrared spectroscopy (FTIR) is routinely used to identify functional groups of compounds, whereas, in the field of solid dispersions, it can provide information about drug-drug and drug-excipient intermolecular bonding. In this study, the infrared spectrum for all formulations was recorded using a Nicolet-380 Fourier Transform Infrared spectrometer (FT-IR) with an ATR crystal. Powder samples were placed directly onto the diamond crystal and the anvil lowered to ensure that sample was in full contact with the diamond. Each spectrum was obtained in the range of 400 – 4000 cm^{-1} with 2 cm^{-1} resolution.

2.3.2.4. Scanning electron microscopy (SEM)

Scanning electron microscopy (SEM) is a technique in which the sample is scanned using a high-energy beam of electrons, to produce images at much higher levels of magnification than is possible with optical microscopy. Sample preparation involves mounting the material to a specimen stub, and coating the surface of the material in an ultrathin layer of gold to inhibit accumulation of electrostatic charges, making the surface of the sample electrically conductive. In this study, the morphology of the prepared samples was characterised using scanning electron microscopy (SEM), (JEOL JSM-6060LV, Japan) with gold-plating prior to imaging using a sputter coater (SC7620).

2.3.3. Isothermal titration calorimetry (ITC)

Thermodynamic interactions were investigated using a Microcal calorimetric unit (ITC) linked to a Microcal MCS observer with data analysed using Origin software (Figure 2.5). A thorough review of the theory of ITC can be found in Chapter 1.



Figure 2.5: A MicroCal VP-ITC used in this study to investigate the thermodynamics of drug-excipient interactions.

In this study a chemical test reaction, namely, the complex formation between barium (Ba^{+2}) and 18-crown-6 (1, 4, 7, 10, 13, 26-hexaoxacyclooctadecane) was conducted to avoid systemic instrumental errors. It was chosen as it is reliable test reaction involving inexpensive and stable compounds that are easily available in sufficiently pure form (Wadsö and Goldberg, 2001).

In this study, the values obtained for the binding stoichiometry (N) 1.0 ± 0.01 , binding constant (K_a), $6.0 \pm 0.1 \times 10^3 \text{ mol.dm}^{-3}$ and binding enthalpy (ΔH_b), $-31.0 \pm 0.1 \text{ KJ.mol}^{-1}$ were in good agreement with values reported previously (Wadsö and Goldberg, 2001, Sgarlata et al., 2013) (Figure 2.6).

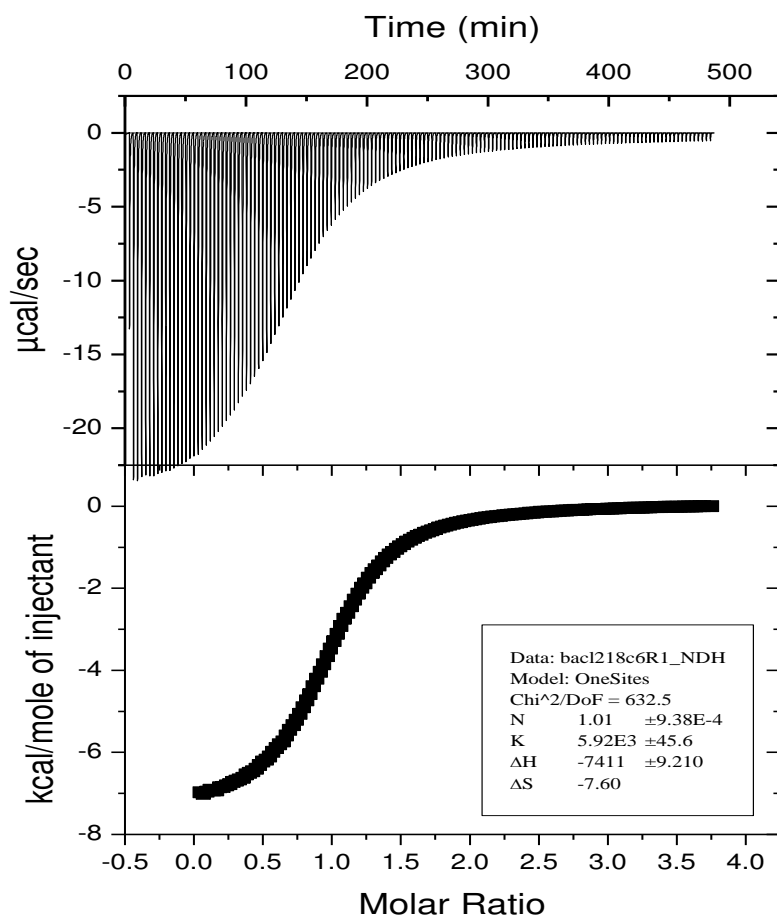


Figure 2.6: ITC calibration of barium (Ba^{+2}) and 18-crown-6.

ITC studies focused on saturation limit measurements and CMC determinations. Firstly, saturation studies were conducted by injecting aqueous drug solution into a micellar solution in which micelles were in excess over the course of titration such that all drug added at each step partitioned (Waters et al., 2005), i.e. moved from the aqueous solvent phase to within the micellar core. The sample cell (1.413 cm^3) was filled with an aqueous micellar solution of SDS (20 mM) and the syringe (0.290 cm^3) was filled with aqueous drug solution. The drug concentration chosen for each set of experiments was based on initial findings where each experiment was optimised to give a signal of appropriate amplitude to suit the calorimetric output, i.e. 30 mM for theophylline, 80 mM for etofylline and diprophylline, 90 mM for

paracetamol and 100 mM for caffeine. The volume per injection was 0.010 cm³ with a time between each injection of 200 s and duration for each injection of 20 s. Experiments were conducted at T = 298 K and 310 K with the change in cell feedback measured as a function of time with each experiment repeated in triplicate with freshly prepared solutions. Heats of dilution were determined by titrating an equivalent concentration of drug solution into deionised water alongside deionised water titrated into micellar solutions. The area under each peak was obtained by integration (following subtraction of the heats of dilution); the resultant values were combined together and divided by the total number of moles of drug added to calculate the enthalpy change. This enthalpy change corresponded to the process related to the saturation of a micelle with drug and is therefore referred to as $\Delta H_{\text{saturation}}$ / (kJ · mol⁻¹) of drug.

From these data, it was possible to calculate the drug: surfactant ratio based on the knowledge of the concentrations of both solutions along with the syringe and cell volumes. Through calculating the number of drug molecules added during the experiment and based on an average surfactant aggregation number of $n = 62$ (Mutelet et al., 2003), the saturation limit for the micellar solutions in the presence of drugs was determined, i.e. the number of drug molecules per micelle, given by Equations (2.1) and (2.2).



where N_1 is the average number of SDS molecules in a micelle and N_2 is the average number of ligands L bound to the micelle.

It should be noted that this work assumed the aggregation number does not vary during the course of the study or in the presence of drugs. Furthermore, a small change in the aggregation number would not dramatically alter the drug to micelle ratios presented in this work and changes in the associated enthalpy are independent of this factor. Using luminescent probes, it is possible to measure the aggregation number for a surfactant (da Graça Miguel, 2001) although data are not available for the surfactant used in this work in the presence of these particular drugs and therefore assumed to be unaffected by this potential variable.

Following on from saturation studies, ITC was secondly used to determine the CMC of surfactants alone or in the presence of drugs. This was achieved by titrating micelles (concentration of SDS surfactant solution $[SDS_1] = 200$ mM or NaDC surfactant solution $[NaDC_1] = 50$ mM) from the 290 μ L syringe into deionised water (DI) or an aqueous drug solution in the sample cell (1.4 mL) at $T = 298, 304$ and 310 K. When time $t = 0$, the concentration of SDS $[SDS_2]$ or NaDC $[NaDC_2]$ in the cell was zero and then upon injections, increased through the respective CMC points. At all times, $[SDS_1 \text{ or } NaDC_1] > [SDS_2 \text{ or } NaDC_2]$. Initially, there were no micelles present until the point of micellisation was reached which is identified as a break in the thermogram. The enthalpy (ΔH_{mic}) of micellisation was calculated by integrating the area under each peak and summing the values obtained. Data was also analysed to determine the change in Gibbs free energy (ΔG_{mic}) and entropy (ΔS_{mic}). The concentration of drugs used was 20 mM in all cases (with the exception of paracetamol at 60 mM) with a pH range from 6.4 to 8.0 as detailed earlier in the experimental section. All experiments were comprised of 48 ten second 2.5 μ L injections with a time interval between each injection of 240 s. The stirring speed was set at 307 rpm. Each experiment was repeated in triplicate with freshly prepared solutions.

To investigate the possible excipient-excipient or drug-excipient interactions, the same study was repeated with PEG 6000 as an excipient. The sample cell comprised of either PEG solution (0.2 mM) or drug-PEG solution where the concentration of drugs used was the same as in the previous experiments. This was titrated with 200 mM SDS or 50 mM NaDC solution in the 290 μ L syringe and stirred at 307 rpm. Experiments were conducted at three temperatures (298, 304 and 310 K), all in triplicate to ensure reproducibility. The effect of PEG and drugs on the critical micelle concentration of both surfactants was evaluated through data analysis. A full thermodynamic profile including changes in enthalpy (ΔH_{mic}), Gibbs free energy (ΔG_{mic}) and entropy (ΔS_{mic}) of micellisation were also obtained.

In summary, six analytical techniques were utilised to investigate the range of products formulated in this work. Each technique provides valuable information concerning specific properties, which, when combined, can help to evaluate the potential suitability of each formulated product as a medicinal product.

References

- DA GRAÇA MIGUEL, M. 2001. Association of surfactants and polymers studied by luminescence techniques. *Advances in Colloid and Interface Science*, 89–90, 1-23.
- MUTELET, F., ROGALSKI, M. & GUERMOUCHE, M. H. 2003. Micellar liquid chromatography of polyaromatic hydrocarbons using anionic, cationic, and nonionic surfactants: Armstrong model, LSER interpretation. *Chromatographia*, 57, 605-610.
- SGARLATA, C., ZITO, V. & ARENA, G. 2013. Conditions for calibration of an isothermal titration calorimeter using chemical reactions. *Analytical and Bioanalytical Chemistry*, 405, 1085-1094.
- WADSÖ, I. & GOLDBERG, R. N. 2001. Standards in isothermal microcalorimetry: (IUPAC Technical Report). *Pure and Applied Chemistry*, 73, 1625-1639.
- WATERS, L. J., LEHARNE, S. A. & MITCHELL, J. C. 2005. Saturation determination of micellar systems using isothermal titration calorimetry. *Journal of Thermal Analysis and Calorimetry*, 80, 43-47.
- WATERS, L. J., BEDFORD, S. & PARKES, P. M. 2011. Controlled microwave processing applied to the pharmaceutical formulation of ibuprofen. *AAPS PharmSciTech*, 12, 1038-1043
- WILLIAMS, H. M. & PARKES, G. 2008. Activation of a phenolic resin-derived carbon in air using microwave thermogravimetry. *Carbon*, 46, 1169-1172.

Chapter 3: Mesoporous silica based formulations

3.1. Introduction

Many drugs exhibit poor water solubility, leading to limitations in potential formulation options and in some cases, resulting in drug candidates being rejected during the development process. Limited solubility results in low levels of bioavailability, often overcome using a variety of methods including alterations to the physical properties of the drug, for example, by forming solid dispersions (Torrado et al., 1996). In the last 10 years, mesoporous silica based drug delivery systems have been investigated to enhance solubility and thus improve bioavailability (Vallet-Regí et al., 2007). These systems offer the ability to maintain therapeutic levels of a drug over a specified period of time through the controlled design of ordered pore networks, high pore volumes, high surface areas and functionalised surfaces. Furthermore, silica based formulations offer a biocompatible and stable product that has become a suitable method for the sustained release of drugs to specific organs within the body (Barbé et al., 2004).

Many ordered and non-ordered forms of mesoporous silica have been proposed as carriers for drugs that exhibit poor water solubility. This is because the increase in surface area, along with the potential of the drug to exist in pores in the amorphous form (rather than crystalline), can aid dissolution. Kinnari et al. have shown that the anti-fungal drug itraconazole exists in the amorphous form when formulated with silica (Kinnari et al., 2011), while Mellaerts et al. working with the same drug combined with SBA-15 found it to reside both in the micro- and mesopores (Mellaerts et al., 2008). Through modifying the pore size, connectivity and geometry, it is known that drug release can be controlled for model drugs such as ibuprofen (Andersson et al., 2004; Zhu et al., 2005) and many other compounds (Van Speybroeck et al., 2009, Zhang et al., 2010).

Modifying the structure of the silica is not the only approach researchers have taken to enhance drug release from silica based systems. An alternative route to achieving enhanced bioavailability is to modify the formulation method employed to encourage drug particles to enter the ordered silica structure. Examples of such methods include spray-drying (Takeuchi et al., 2004), wet granulation (Vialpando et al., 2012), the freeze-thaw method (Tozuka et al., 2010) and, more recently, supercritical carbon dioxide processing (Ahern et al., 2012). Loading methods, such as those discussed here, have also been compared with several functionalised ordered and non-ordered mesoporous silicas to establish which overall system provides optimal release conditions (Limnell et al., 2011).

This study involves the application of a unique formulation method with a model drug known to exhibit poor water solubility, namely fenofibrate which is used to treat high cholesterol levels. One area of research that has only received limited interest to date is the preparation of drug-silica materials using microwave irradiation despite the possibility that it could provide an ideal formulation method to create materials with a highly predictable and potentially enhanced drug release profile. A limited number of studies have attempted to use microwave-based methods to incorporate materials with poorly water soluble drugs, such as loratidine with cyclodextrin derivatives and found that an enhanced product results from this method (Nacsa et al., 2008). Usually such methods involve irradiation of a sample with no power control, i.e. the sample is heated for a specified period of time regardless of sample temperature during the experiment. This is known to be problematic as samples may heat uncontrollably with significant consequences for the stability of the drug concerned. However, more recently a novel method of heating samples with a feedback system has been adapted to ensure the temperature of the sample can be controlled throughout the duration of the experiment (Waters et al., 2011). This method ensures that a sample does not exceed a specified

temperature, helping avoid unwanted drug degradation reactions. A similar heating approach is used in this study with its first application for producing mesoporous silica based drug delivery materials.

3.2. Results and discussion

3.2.1. In-vitro dissolution of fenofibrate

The in vitro release profiles of drug from drug-silica samples, along with pure and processed fenofibrate measured using standard dissolution analysis over a period of 30 minutes are presented in Figures 3.1-3.6.

3.2.1.1. Dissolution studies of Core Shell silica based formulations

Figure 3.1 highlights results for formulations based on Core Shell silica as the excipient using microwaves and traditional heating along with physically mixed products over a period of 30 minutes. Formulating fenofibrate with Core Shell silica increased the extent of dissolution compared with the percentage release of pure fenofibrate, i.e. 41.9 (\pm 0.6) % after 30 minutes (Figure 3.1c). For the Core Shell dry microwave (DM) formulations, the 5:1 (Figure 3.1c) and 3:1 (Figure 3.1b) products provided the greatest drug release, i.e. 84.1 (\pm 4.9) % and 73.4 (\pm 0.4) %, respectively, whereas percentage releases of 46.6 (\pm 0.3) % and 45.2 (\pm 0.9) %, respectively, were achieved from the physical mixtures (PM) of the same products, after 30 minutes. Diverse dissolution profiles were observed from formulations prepared using wet microwave (WM) and traditional heating (TH) techniques (Figure 3.1a, b & c). From some formulations, a slightly increased extent of drug release was observed compared with pure fenofibrate, however, a marked reduction in the extent of dissolution was observed for the remaining formulations.

Upon melting using the dry microwave method it is plausible that fenofibrate molecules could be transported into the pores under capillary action and interact with the free silanol groups. However, surface adsorption would also be anticipated. The effective pore volume accommodates drug molecules and on cooling, the surface adsorbed and pore confined drug can exist in an amorphous or a semi-crystalline state depending on the silica content of formulation. When this formulation comes into contact with the dissolution media, a rapid release of fenofibrate in the form of fine particles occurs, possibly because of desorption of fenofibrate by the influx of the dissolution media inside the pores. However, less drug dissolved over a period of 30 minutes from the 1:1 dry microwave formulation. The available drug/pore ratio for the loading of drug is less, hence, the drug left after pore filling is deposited between the pore walls and on the free surface of silica. Such loaded drug can easily attain a crystalline state on cooling as confirmed from the SEM images (See Section 3.2.2.2). Consequently, an influx of dissolution media in the pores is hindered by the bulk crystalline drug accumulated on the surface which results in a slow release in comparison with samples containing higher silica content. The significantly slower release of fenofibrate was also observed using water as a vehicle which might be displaced into the pores of silica causing partial pore blockage, thus the drug crystallises on top of the pores. This co-adsorbed water significantly affects the interactions of drug molecules with pore walls and thereby alters the adsorption, and diffusion behaviour of drug molecules.

In summary, it would appear that the presence of Core Shell silica can influence the dissolution of fenofibrate. This is especially true if combined with the application of the dry microwave based technique, doubling the percentage of release after 30 minutes.

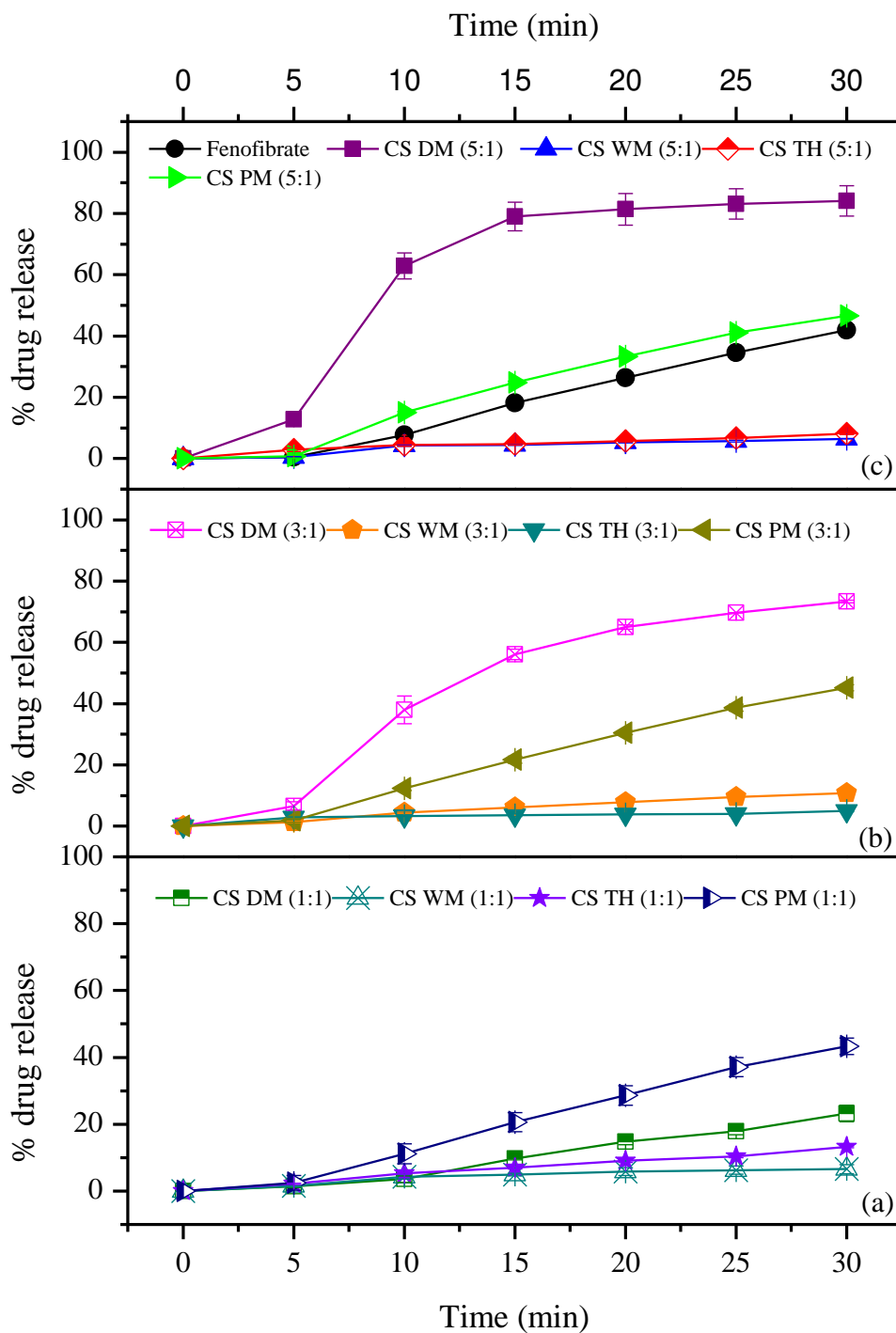


Figure 3.1: Fenofibrate release profiles for pure fenofibrate along with Core Shell (CS) based formulations using traditional heating methods (TH), physical mixing (PM), microwave irradiation wet (WM) and dry (DM), all at silica/drug ratios of 1:1 (a), 3:1 (b) and 5:1 (c). Each data point represents the mean of 3 results with SD error bars.

3.2.1.2. Dissolution studies of Core Shell rehydrox based formulations

The release behaviour of fenofibrate from Core Shell rehydrox (CSR) is presented in Figure 3.2. For the CSR dry microwave based formulations, the 5:1 (Figure 3.2c) and 3:1 (Figure 3.2b) products provided the greatest drug release, i.e. $86.6 (\pm 2.8) \%$ and $81.2 (\pm 9) \%$, respectively after 30 minutes. The physical properties of CSR resemble those of CS except its surface was treated to increase the hydrophobicity of the silica which might justify the slightly higher dissolution rate compared with Core Shell (CS). As fenofibrate is hydrophobic in nature, the drug could be entrapped through hydrophobic interactions (along with van der Waals interactions) with the pore walls which aids the movement of drug molecules into the pores during the melting process. For the remaining formulations with Core Shell rehydrox a wide range of dissolution profiles was observed. In some cases, formulation made little difference to the dissolution behaviour, compared with pure fenofibrate yet for others a marked reduction in the extent of dissolution was observed.

In summary, Core Shell rehydrox had a similar enhancement on dissolution compared with core shell silica using the dry microwave formulation method for both the 3:1 and 5:1 ratios.

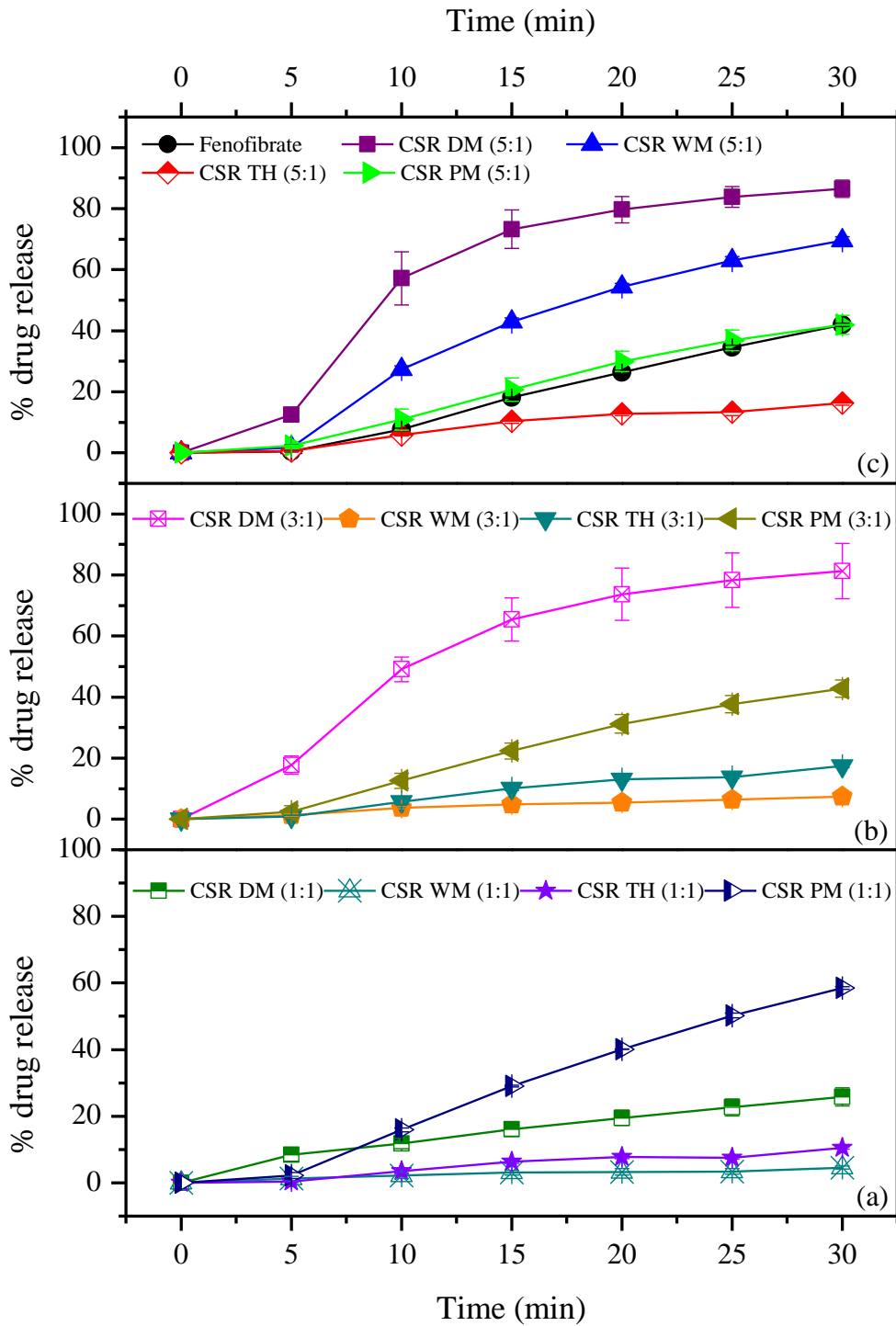


Figure 3.2: Fenofibrate release profiles for pure fenofibrate (FF) along with Core Shell rehdiox (CSR) based formulations using traditional heating methods (TH), physical mixing (PM), microwave irradiation wet (WM) and dry (DM), all at silica/drug ratios of 1:1 (a), 3:1 (b) and 5:1 (c). Each data point represents the mean of 3 results with SD error bars.

3.2.1.3. Dissolution studies of SBA-15 based formulations

Dissolution profiles for fenofibrate from SBA silica based formulations over a period of 30 minutes are presented in Figure 3.3. An improved dissolution rate was observed at different drug to silica ratios but there was no particular trend between the extent of drug release and ratio of drug to silica in the SBA samples. From analysis of the dissolution profiles, it appears that a significant amount of drug was released from the dry microwave formulation at a silica/drug ratio of 3:1, i.e. $78.8 (\pm 6.5) \%$ after 30 minutes (Figure 3.3b). A percentage release of $65.5 (\pm 4.1) \%$ from the physically mixed product at a silica/drug ratio of 3:1 after 30 minutes confirmed the influence of the silica surface on the transformation of a crystalline to a non-crystalline drug state which resulted in enhanced release compared with pure fenofibrate (Figure 3.3b). A delayed release behaviour was observed from the traditionally heated and wet microwave processed formulations (Figure 3.3a, b & c).

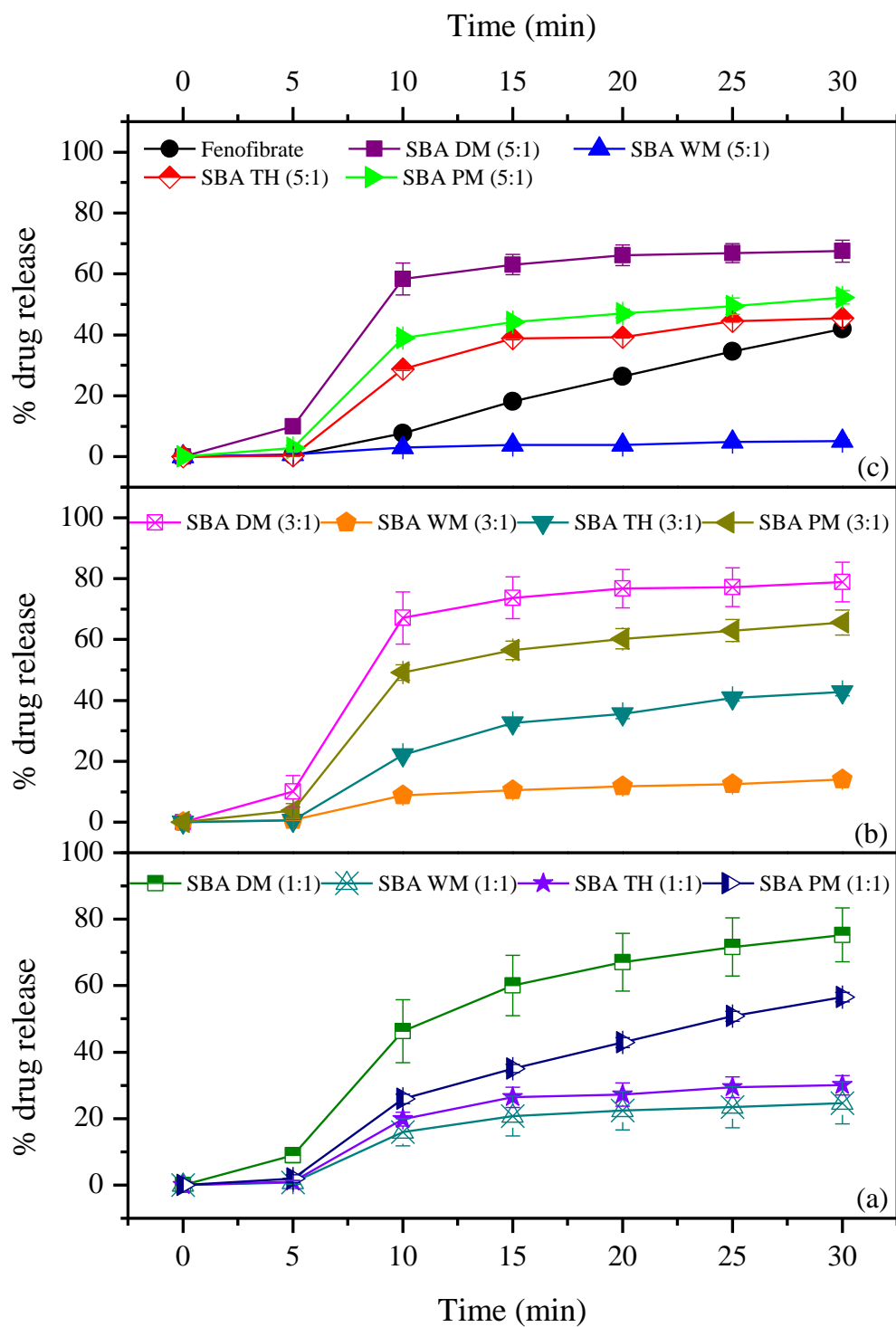


Figure 3.3: Fenofibrate release profiles for pure fenofibrate (FF) along with SBA-15 (SBA) based formulations using traditional heating methods (TH), physical mixing (PM), microwave irradiation wet (WM) and dry (DM), all at silica/drug ratios of 1:1 (a), 3:1 (b) and 5:1 (c). Each data point represents the mean of 3 results with SD error bars.

3.2.1.4. Dissolution studies of Syloid AL-1 based formulations

The release behaviour of fenofibrate from Syloid AL-1 (SYL 1) silica is depicted in Figure 3.4. For the SYL 1 dry microwave based formulations, the 3:1 product provided the greatest drug release, i.e. 87.3 (\pm 0.7) %, after 30 minutes as seen in Figure 3.4b. At the same silica/drug ratio, the physically mixed formulation released 63.6 (\pm 3.1) %, after 30 minutes (Figure 3.4b). The large surface area presented by SYL 1 can be considered as a potential reason for the enhanced release of fenofibrate. For the remaining formulations, a markedly reduced extent of dissolution was observed compared with pure fenofibrate (Figure 3.4a, b & c).

In summary, the dissolution results confirmed that the 3:1 dry microwave product is an ideal formulation for both SBA-15 and Syloid AL-1 silica.

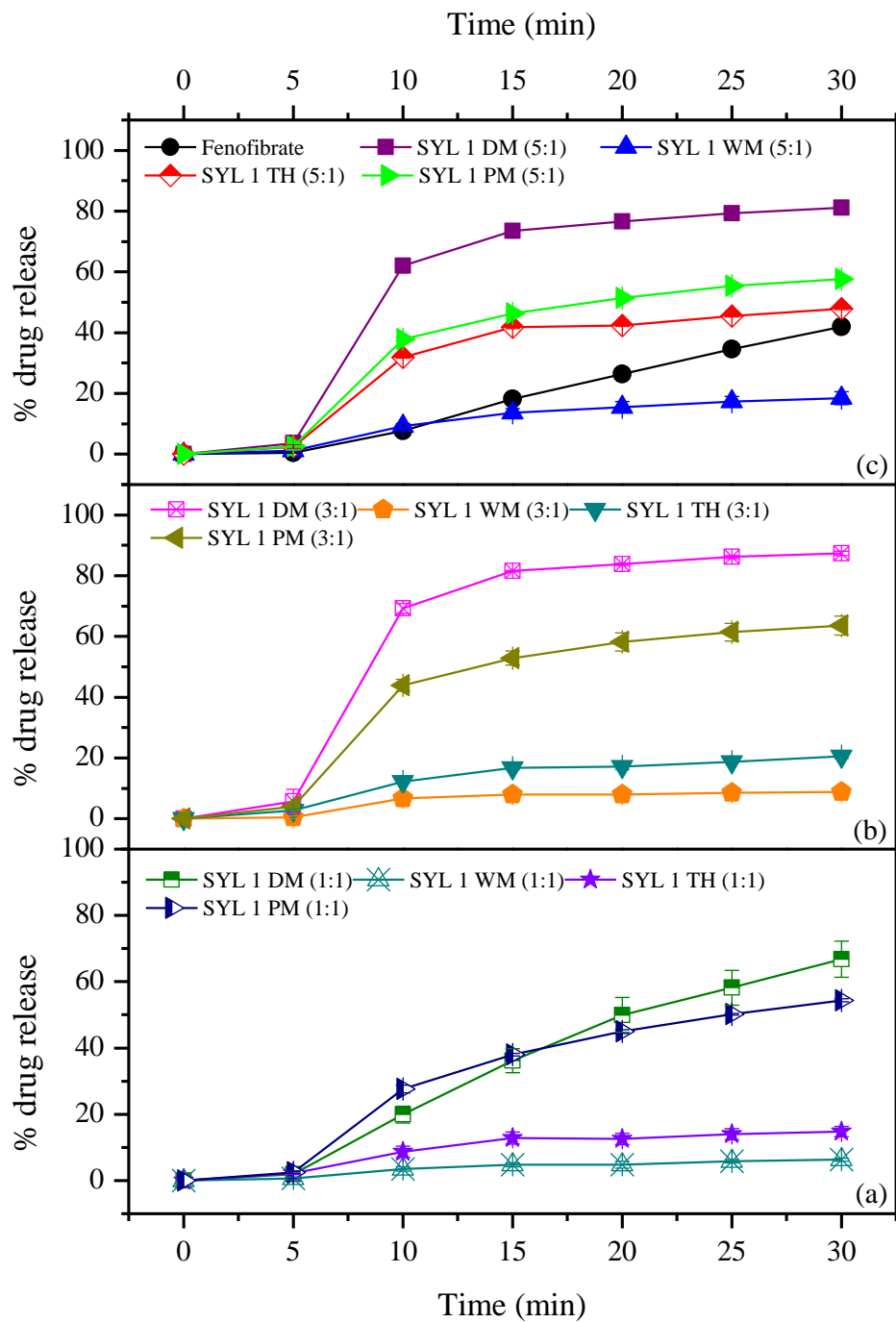


Figure 3.4: Fenofibrate release profiles for pure fenofibrate (FF) along with Syloid AL-1 (SYL 1) based formulations using traditional heating methods (TH), physical mixing (PM), microwave irradiation wet (WM) and dry (DM), all at silica/drug ratios of 1:1 (a), 3:1 (b) and 5:1 (c). Each data point represents the mean of 3 results with SD error bars.

3.2.1.5. Dissolution studies of silica gel based formulations

Figure 3.5 highlights fenofibrate release from silica gel (SG) based formulations. For the silica gel (SG) dry microwave formulations, the 1:1 product provided the greatest extent of drug release, i.e. $85.8 (\pm 1.3) \%$ whereas a percentage release of $64.5 (\pm 3.8) \%$ was achieved from the physical mixture of the same product after 30 minutes (Figure 3.5a). This can be explained on the basis of the physical properties of silica as the particle size was $70 \mu\text{m}$ along with a pore diameter of 4.7 nm and a pore volume of $0.71 \text{ cm}^3\text{g}^{-1}$. The viscous molten drug has therefore possibly diffused deep into the pores. Consequently, rapid release was observed from the 1:1 product as a result of the free direct contact between the dissolution media and dispersed drug particles. The reduced release at the high SG ratio can be ascribed to the larger silica particle size as drug molecules were entrapped deep inside the large silica particles and media influx into the silica faced strong steric hindrance. For the traditionally heated and wet microwave processed formulations a significant reduction in the extent of dissolution was observed (Figure 3.5a, b & c).

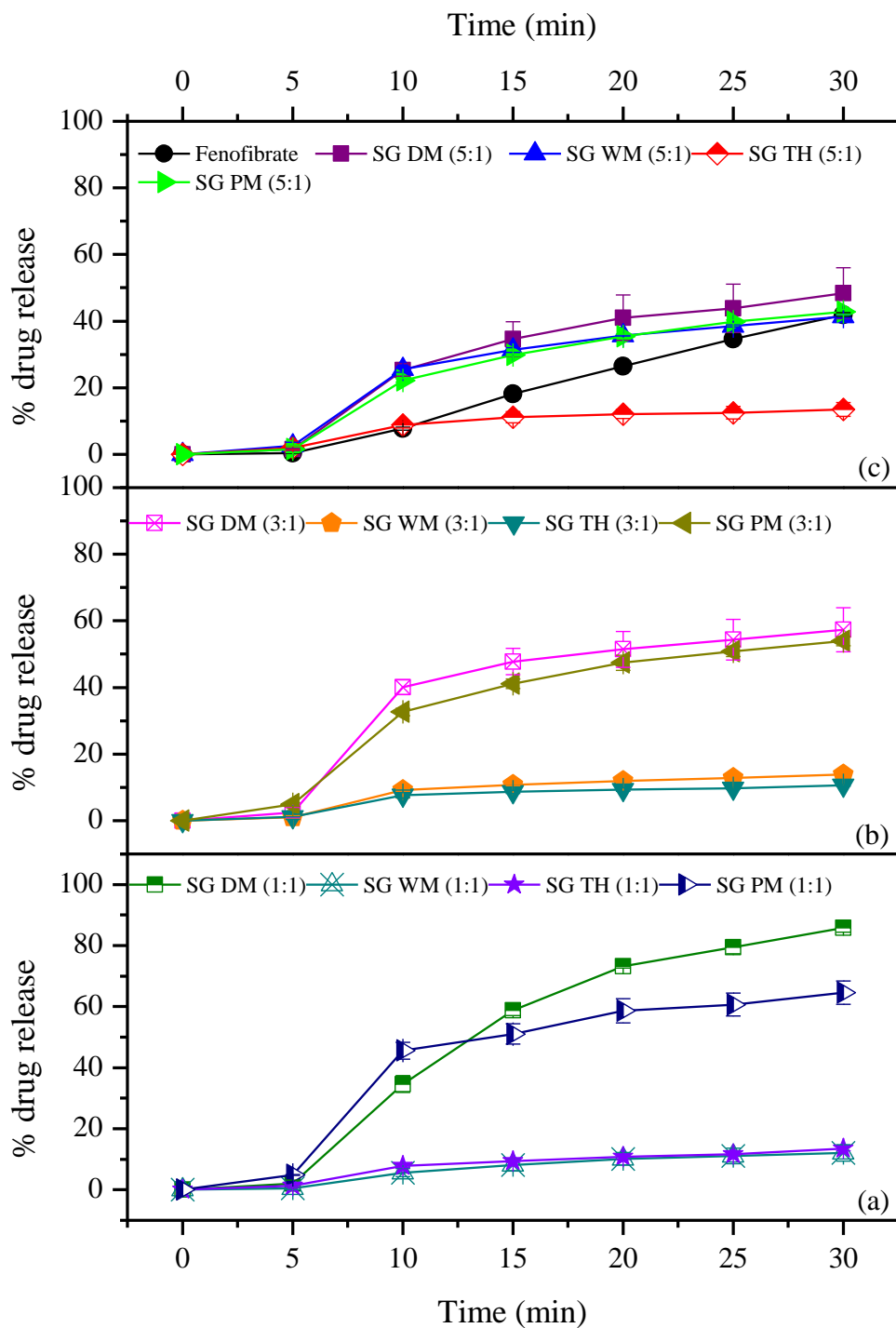


Figure 3.5: Fenofibrate release profiles for pure fenofibrate (FF) along with silica gel (SG) based formulations using traditional heating methods (TH), physical mixing (PM), microwave irradiation wet (WM) and dry (DM), all at silica/drug ratios of 1:1 (a), 3:1 (b) and 5:1 (c). Each data point represents the mean of 3 results with SD error bars.

To this end, it appeared that silica/drug products formulated through dry microwave irradiation generally increased drug release. Furthermore, the physical properties of the silica particles such as pore size, volume and surface area seem to influence the dissolution rate.

3.2.1.6. Dissolution studies of Stober based formulations

To further confirm the role of silica physical properties on the drug release, a non-porous silica, namely Stober was used to compare with porous silica materials. As expected, Stober did not show any enhancement in drug release after formulation with the maximum achievable drug release only 14.3 (± 0.8) % (Figure 3.6a, b & c). This anomaly can be attributed to the dramatically different properties of the silica, compared with the other five in the series. Stober has a far smaller pore volume, particle size and surface area compared with the other forms of silica; furthermore, this silica is the only non-porous silica tested, which could result in far less drug entering the pores during the formulation process and not creating the same type of product as seen for the remaining silicas.

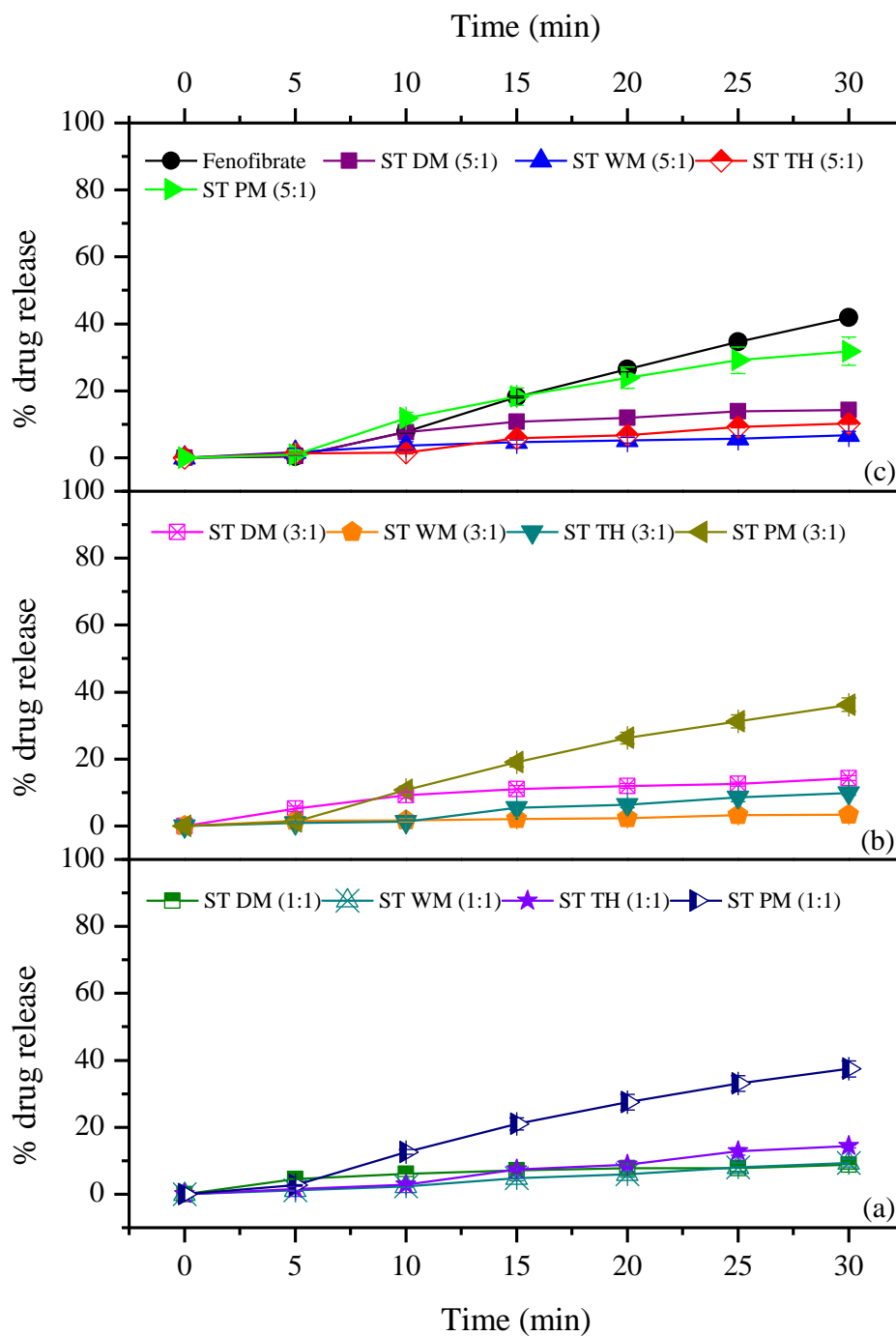


Figure 3.6: Fenofibrate release profiles for pure fenofibrate (FF) along with Stober (ST) based formulations using traditional heating methods (TH), physical mixing (PM), microwave irradiation wet (WM) and dry (DM), all at silica/drug ratios of 1:1 (a), 3:1 (b) and 5:1 (c). Each data point represents the mean of 3 results with SD error bars.

3.2.1.7. Summary

For all six forms of silica in the series, it was very clear that using traditional heating methods did not positively influence, and in some cases even retarded, the extent of drug release compared with pure fenofibrate over a 30 minutes period. For example, using traditional heating methods at a 1:1 ratio, SYL 1 silica only achieved a percentage drug release of 14.8 (\pm 1.5) % (Figure 3.4a) compared with drug alone 41.9 (\pm 0.6) % after 30 minutes (Figure 3.4c). More surprisingly, using microwave irradiation in the presence of water also retarded drug release with a percentage drug release of only 5.1 (\pm 0.4) % for a 5:1 formulation for SBA over 30 minutes (Figure 3.3c). This phenomenon can be explained as water may interact with silanol groups inside the pores of silica, reduce drug loading and therefore, the drug may retain its crystalline state which may result in a decreased rate of dissolution.

Such a dramatic increase in drug release can be explained by considering the physicochemical properties of the drug under investigation, i.e. fenofibrate is a hydrophobic compound with poor aqueous solubility. Therefore, it is plausible that during the microwave formulation process, the drug melts into the pores of the silica where it is stored in the partially crystalline or amorphous form, thus helping encourage a more rapid and extensive, subsequent drug release. In the majority of cases for the five forms of silica in the series where this phenomenon is observed, products formulated using a physical mixing method proved to be the next most efficient method to maximise the extent of drug release for fenofibrate. This also supports the theory that drug enters the silica pores as a partial enhancement was observed, yet the amorphous transformation is not so dramatic without the direct input of energy supplied by the microwave source thus only creating a partial increase in drug release. This could be a result of simple particle size reduction as a consequence of the physical mixing process.

3.2.2. Solid state characterisation

3.2.2.1. Differential scanning calorimetry (DSC) and X-ray diffraction (XRD)

DSC and XRD were employed to investigate the crystal lattice of pure and processed fenofibrate with various mesoporous silica. Figures 3.7 and 3.8 depict the DSC thermograms for SBA-15 and Syloid AL-1 based physical mixtures and dry microwave formulations along with pure fenofibrate. Fenofibrate was characterised by a single sharp melting endothermic peak at 82.43 °C. The peak onset temperature and heat of fusion (ΔH_f) were 80.51 °C and -72.94 Jg⁻¹, respectively. This characteristic peak appeared in the physical mix formulations at all silica/drug ratios with slight variations in terms of melting peak depression and broadening, indicating the transition from a crystalline to a semi-crystalline state. When the fenofibrate was formulated with SBA and SYL at a silica/drug ratio of 1:1 using dry microwave formulations, a melting peak with less intensity was detected. At this ratio, the pore volume of silica was insufficient for hosting the extra fenofibrate molecules, and the residual fenofibrate would instead reside on the external surface of silica. However, the melting peak was completely absent in SBA and SYL 1 based dry microwave assisted formulations at silica/drug ratios of 3:1 and 5:1, confirming the amorphous state of fenofibrate within formulations.

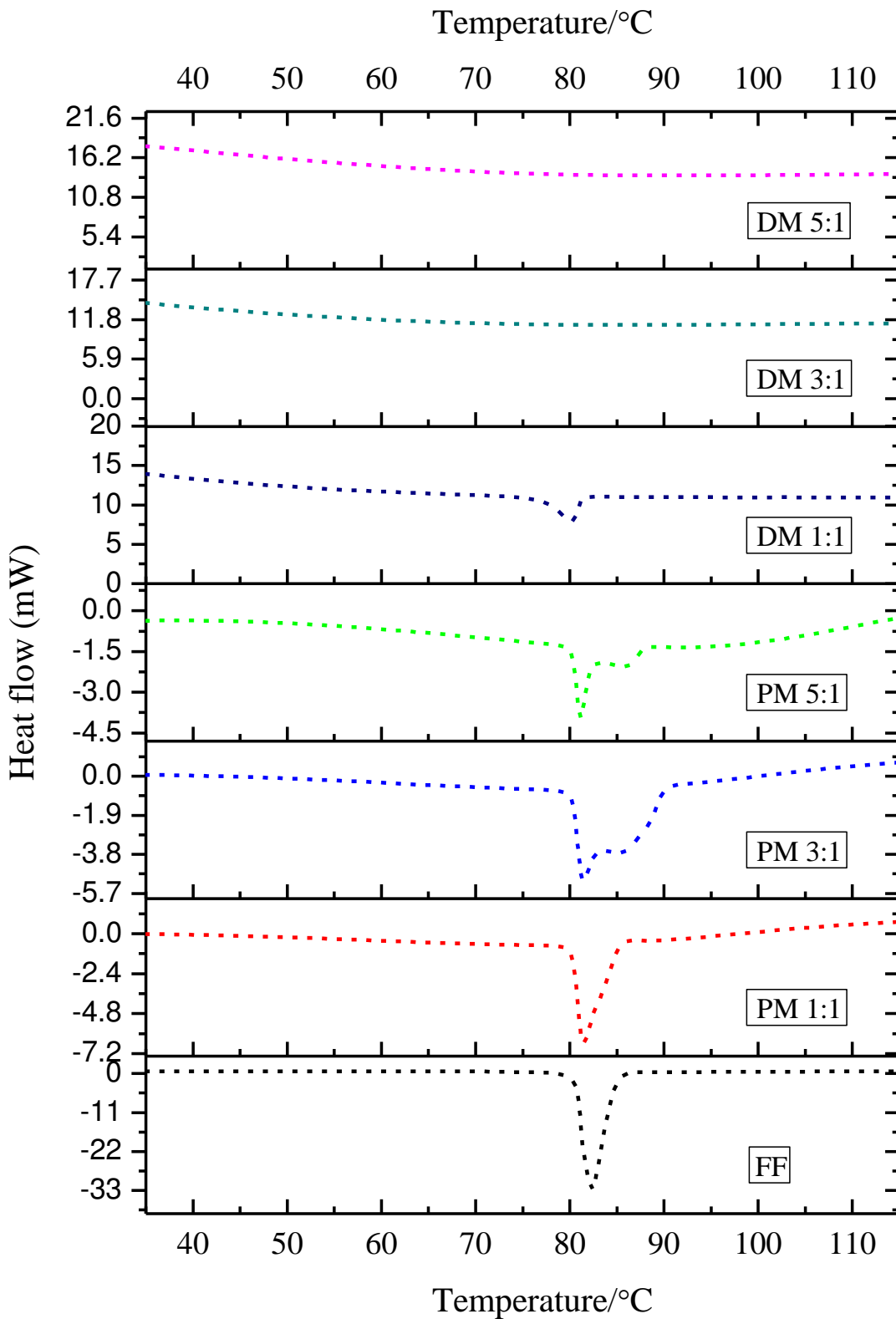


Figure 3.7: DSC curves for fenofibrate (FF) along with SBA-15 (SBA) based physical mixture (PM) and dry microwave (DM) formulations all at silica / drug ratios of 1:1, 3:1 and 5:1.

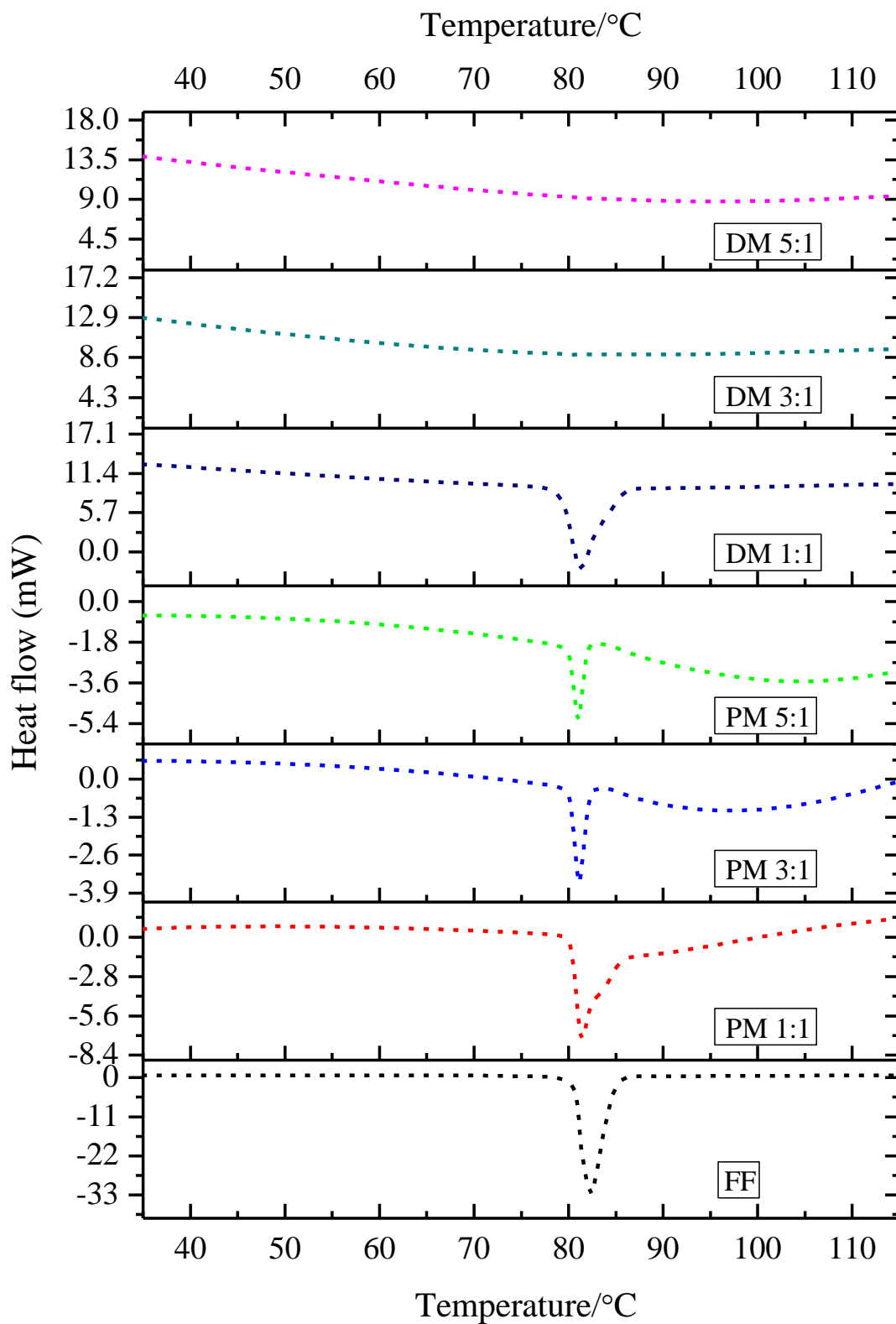


Figure 3.8: DSC curves for fenofibrate (FF) along with Syloid AL-1 (SYL 1) based physical mixture (PM) and dry microwave (DM) formulations all at silica / drug ratios of 1:1, 3:1 and 5:1.

Figures 3.9 and 3.10 display the XRD patterns of SBA and SYL 1 based physical mixes and dry microwave formulations at ratios of 1:1 and 3:1. The characteristic diffraction peaks observed at 11.99°, 14.3°, 16.2°, 16.8° and 22.4°, correspond to the powder diffraction pattern for pure fenofibrate while the absence of diffraction peaks in SBA and SYL 1 silica confirm their amorphous structure. The fenofibrate crystalline state in the physical mix of SBA and SYL 1 is evident with the existence of characteristic diffraction peaks. The less intense diffraction peak at a ratio of 1:1 using dry microwave formulation, indicates the partial crystalline state of fenofibrate, deposited between the pore walls as a result of the blockage of pores with viscous molten drug. However, the XRD pattern at a ratio of 3:1 using a dry microwave formulation technique suggests the amorphous structure of fenofibrate within the formulation. It also confirms that the fenofibrate was confined inside the pores of silica. The XRD results agree with the DSC observations previously discussed. For the crystallisation process to occur in confined spaces, it is reported that the diameter of pores must be twenty times larger than the molecular size of drug (Sliwiska-Bartkowiak et al., 2001). The pore diameters for silicas used in this work were usually in the range of 3-5 nm which is about 3-5 times of the dimension of the fenofibrate molecule (estimated to be 0.98-1.27 nm) (Cha et al., 2012). Therefore, the restricted pore size of mesoporous silica may have inhibited the crystallisation of fenofibrate inside the pores.

The melting peak depression and decreased intensities of XRD peaks were also observed with the Core Shell, Core Shell rehydrox and silica gel based dry microwave formulations (See Appendix 1 & 2, respectively), revealing the transition from a crystalline to semi-crystalline or amorphous state of fenofibrate. The findings based on DSC and XRD results are in good agreement with the exemplified SBA and SYL silica. However, the formulations developed with Stober silica exhibit a characteristic melting endothermic peak

and X-ray diffraction peaks which corresponds to fenofibrate, confirming the crystalline state of fenofibrate, even after processing with microwaves as a result of its non-porous nature. (See Appendix 3 & 4). In summary, the transformation of fenofibrate from crystalline to amorphous (or partially crystalline state) is highly dependent on the selection of an optimum silica/drug ratio and the input provided by the formulation method.

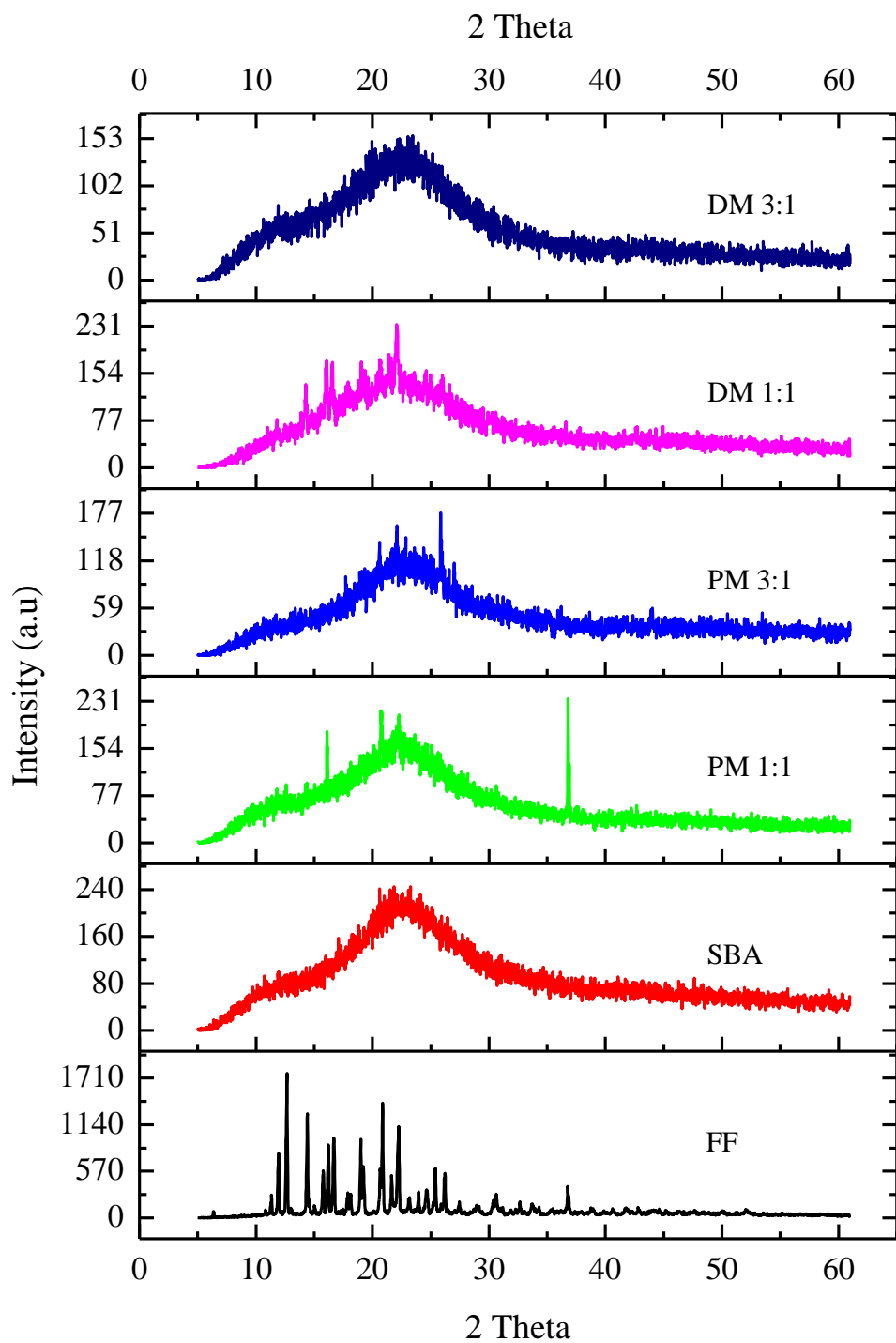


Figure 3.9: XRD patterns for fenofibrate (FF) and SBA-15 (SBA) along with physical mix (PM) and dry microwave (DM) formulations at silica / drug ratios of 1:1 and 3:1.

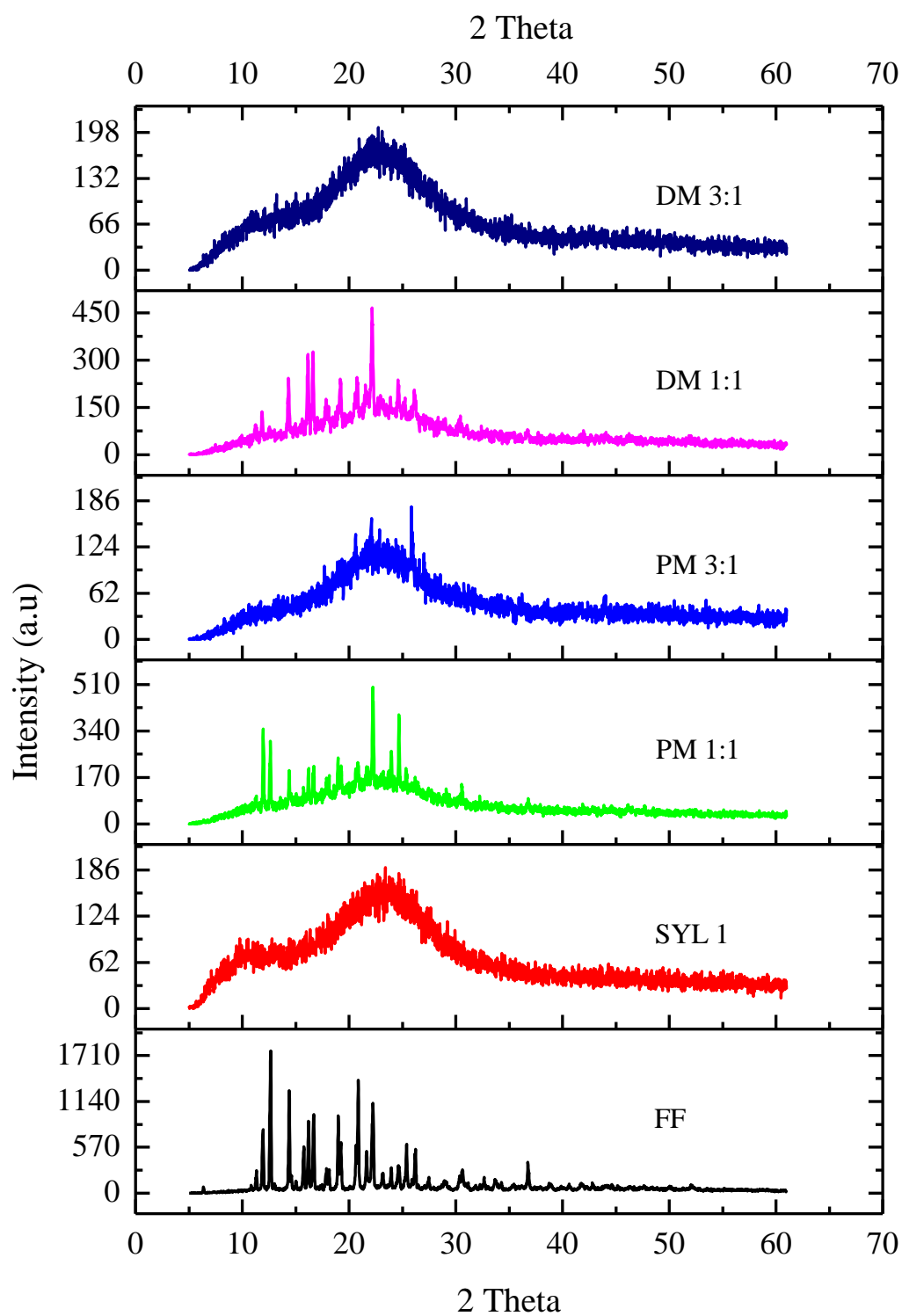


Figure 3.10: XRD pattern of fenofibrate (FF) and Syloid AL-1 (SYL 1) along with physical mix and dry microwave (DM) formulations at silica/drug ratios of 1:1 and 3:1.

3.2.2.2. Scanning electron microscopy (SEM)

Figure 3.11 demonstrates the SEM images of Core Shell, Core Shell rehydrox, SBA-15, silica gel, Syloid AL-1 and Stober silica material used in this work. The CS and CSR silica particles are smooth and globular in shape with an estimated particle diameter of 5 μm . Such particle surfaces provide a uniform distribution of drugs. SBA formulations were composed of agglomerated sub-micron particles, presenting a large surface area and pore volume. The silica gel and Syloid AL-1 consisted of irregular, non-ordered silica particles, having rough surfaces for drug adsorption. The images also revealed the non-porous nature of Stober.

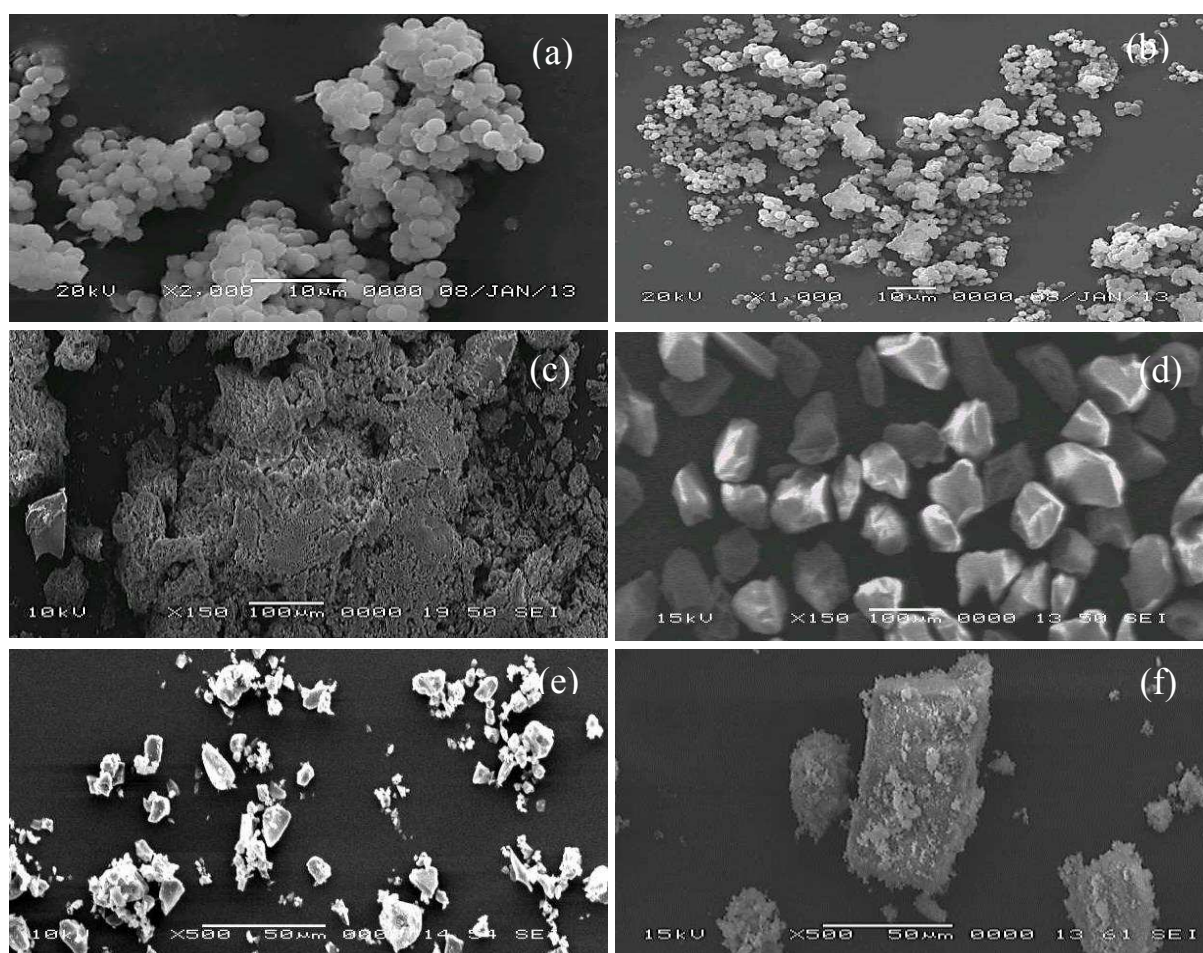


Figure 3.11: SEM images of (a) Core Shell, (b) Core Shell rehydrox, (c) SBA-15, (d) silica gel, (e) Syloid AL-1, (f) Stober.

Scanning electron microscopy (SEM) images were used to indicate any observable differences in the physical characteristics of the formulated products compared with the pure drug or a simple physical mixture of drug and silica. Figure 3.12 illustrates six SEM images to exemplify the general findings of this work. It can be clearly seen that the drug has distinct crystalline particles and on physical mixing with core shell silica, did not mix well and retained their crystalline structure. SEM images also confirmed the insignificant effect of the traditional and wet microwave formulation methods as recrystallised drug was present in the samples. However, there was an appropriate distribution of drug observed in the dry microwave formulations especially as the ratio of silica to drug increased, i.e. there was a more uniform appearance to the resultant formulation as the drug and excipient combined to a greater extent.

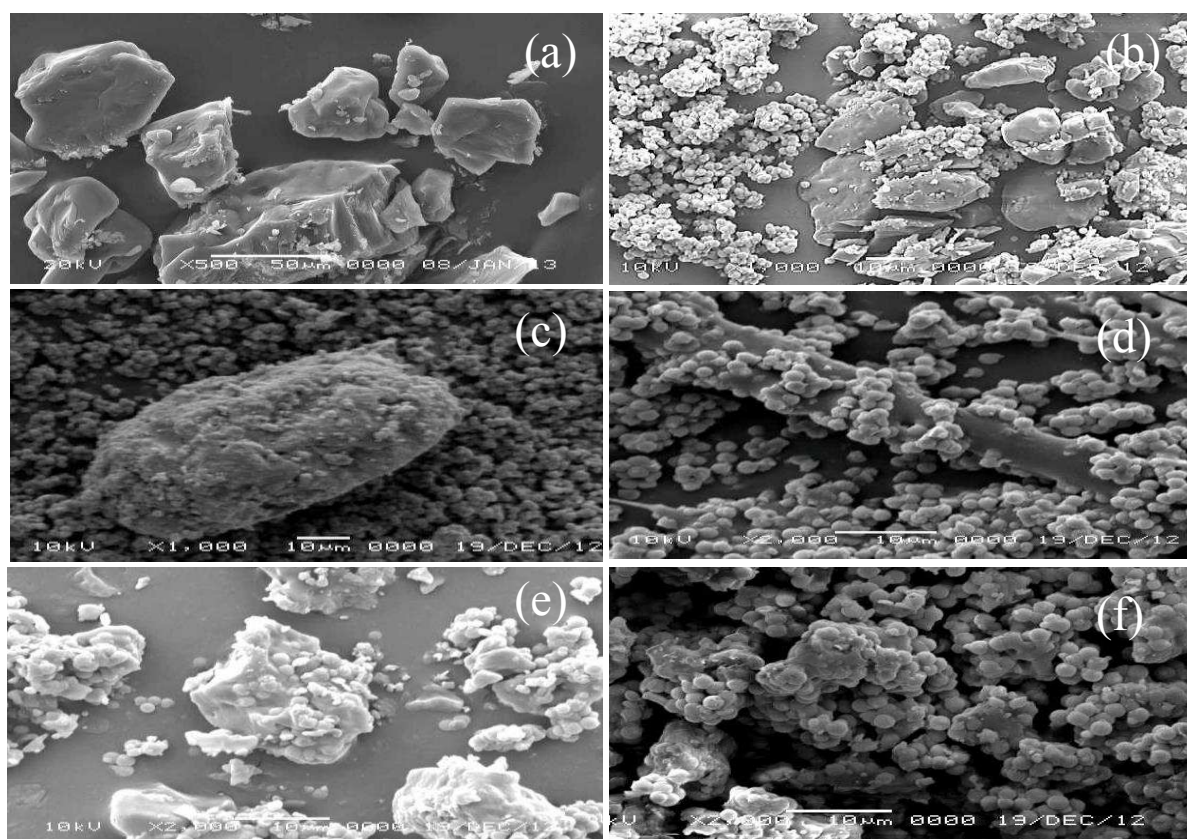


Figure 3.12: SEM images of (a) fenofibrate, (b) a physical mix of CS and FF (1:1), (c) TH formulation of CS and FF (5:1), (d) WM formulation of CS and FF (5:1) and DM formulation CS/FF at ratios of (e) 1:1 and (f) 5:1.

Figure 3.13 presents the SBA-15 and silica gel materials along with their dry microwave formulations (5:1). As both the silicas have a large surface area, molten drug possibly adsorbed in monolayers and evenly distributed in pores, hence cannot be identified as segregated drug particles. These images confirmed the DSC and XRD results where complete amorphous materials were detected at a high silica content, indicating a homogenised system. A similar relationship was observed for the remaining silicas investigated in this study. Overall, it would seem that subjecting the drug to a dry microwave formulation process can modify the extent of crystallinity in the sample and create a product that contains a uniform dispersion of drug within the silica matrix.

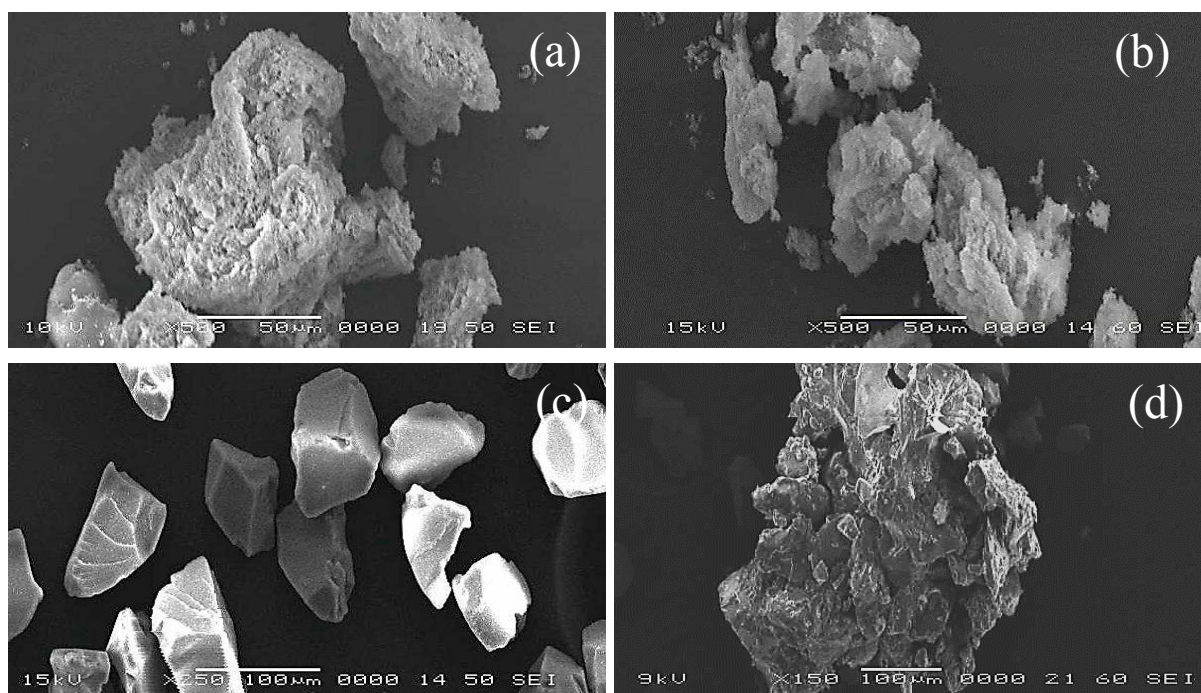


Figure 3.13: SEM images of (a) SBA-15, (b) DM SBA-15/FF (5:1), (c) Silica gel, (d) DM Silica gel/FF (5:1).

3.2.2.3. Fourier transform infrared spectroscopy (FTIR)

FTIR was used to investigate potential interactions between fenofibrate and different silica materials. Figure 3.14 displays the IR analysis of pure fenofibrate along with core shell and SBA-15 silica. Specific fenofibrate peaks were observed at 2983, 1722, 1650 and 1598 cm^{-1} corresponding to an O-H stretching vibration, C-H vibration, ester stretching vibration and lactone carbonyl functional group respectively. The signal at 1243 cm^{-1} is assigned to CH_2Cl stretching vibrations. The SBA-15 and Core Shell spectra show the typical silica bands associated with the main inorganic backbone. The strong and broad signals observed at 1070 cm^{-1} (Core Shell) and 1054 cm^{-1} (SBA-15), correspond to the asymmetric stretching vibrations, ν_{as} (Si-O-Si), of the siliceous framework. The symmetric stretch, ν_{s} (Si-O-Si), and the bending vibration, δ (Si-O-Si), of the siliceous framework were observed at 798, 445 cm^{-1} (Core Shell) and 800, 439 cm^{-1} (SBA-15), respectively. The band at 954 cm^{-1} for core shell and 944 cm^{-1} for SBA-15, was attributed to Si-OH bending. The broad signal that appeared at about 3400 cm^{-1} in some silica materials can be assigned to the O-H stretching frequency of Si-O-H groups and / or water from the atmosphere and within the porous sample (Guo et al., 2013). The characteristic siliceous framework peaks as exemplified in Core Shell and SBA-15, were observed in the spectra of all mesoporous silica samples used in this work.

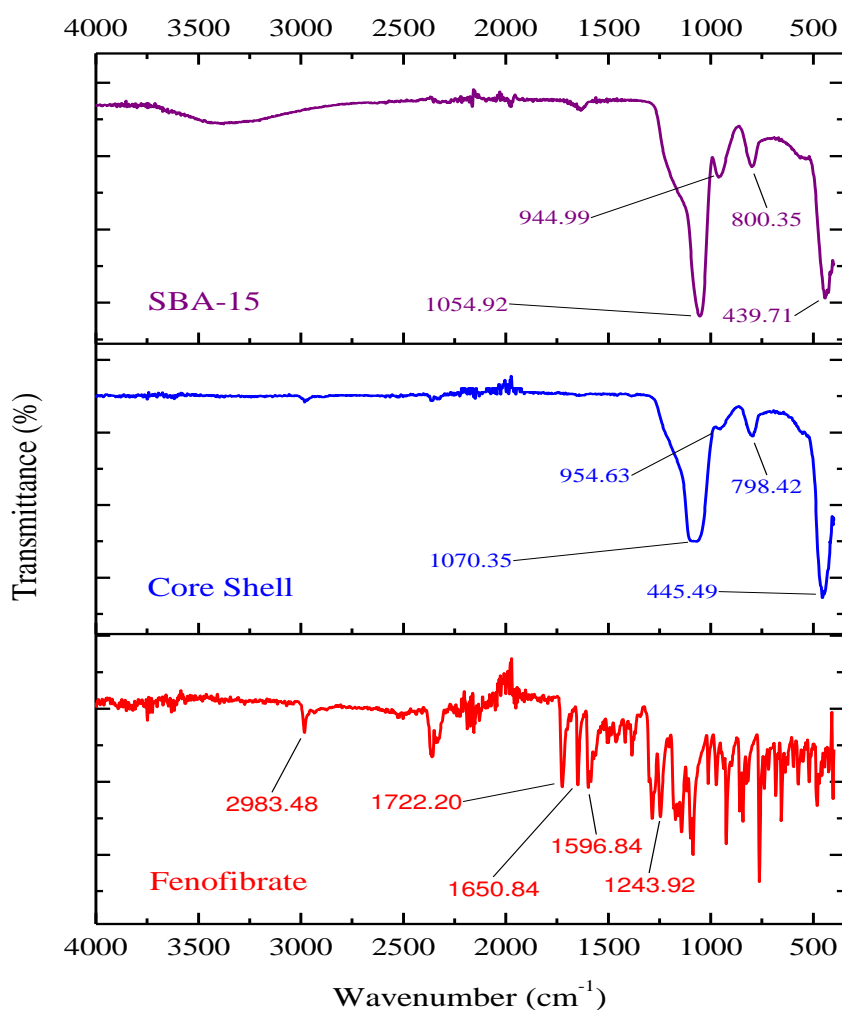


Figure 3.14: FTIR spectra of pure fenofibrate, Core Shell and SBA-15 silica.

Figure 3.15 demonstrates the IR spectrum of dry microwave (DM) formulations of fenofibrate (FF) with various mesoporous silica materials. The IR spectrum of Core Shell, Core Shell rehydrox, SBA-15, Syloid AL-1, silica gel and Stober based formulations exhibit characteristic fenofibrate peaks. These typical signals give a direct demonstration of the loading of fenofibrate molecules into the mesoporous silica framework. A similar pattern was observed for the physically mixed, wet microwave processed and traditionally heated formulations. The absorption bands of fenofibrate were, however, weaker in formulations having a higher silica content. In addition, no extra signals in the FTIR spectra of silica formulations were observed

which indicates that the surface of the particle remained unchanged after loading and the drug retained its chemical structure. In summary, it is confirmed that formulating fenofibrate using this novel microwave method does not detrimentally alter the physicochemical properties of the drug under investigation, according to the IR data presented.

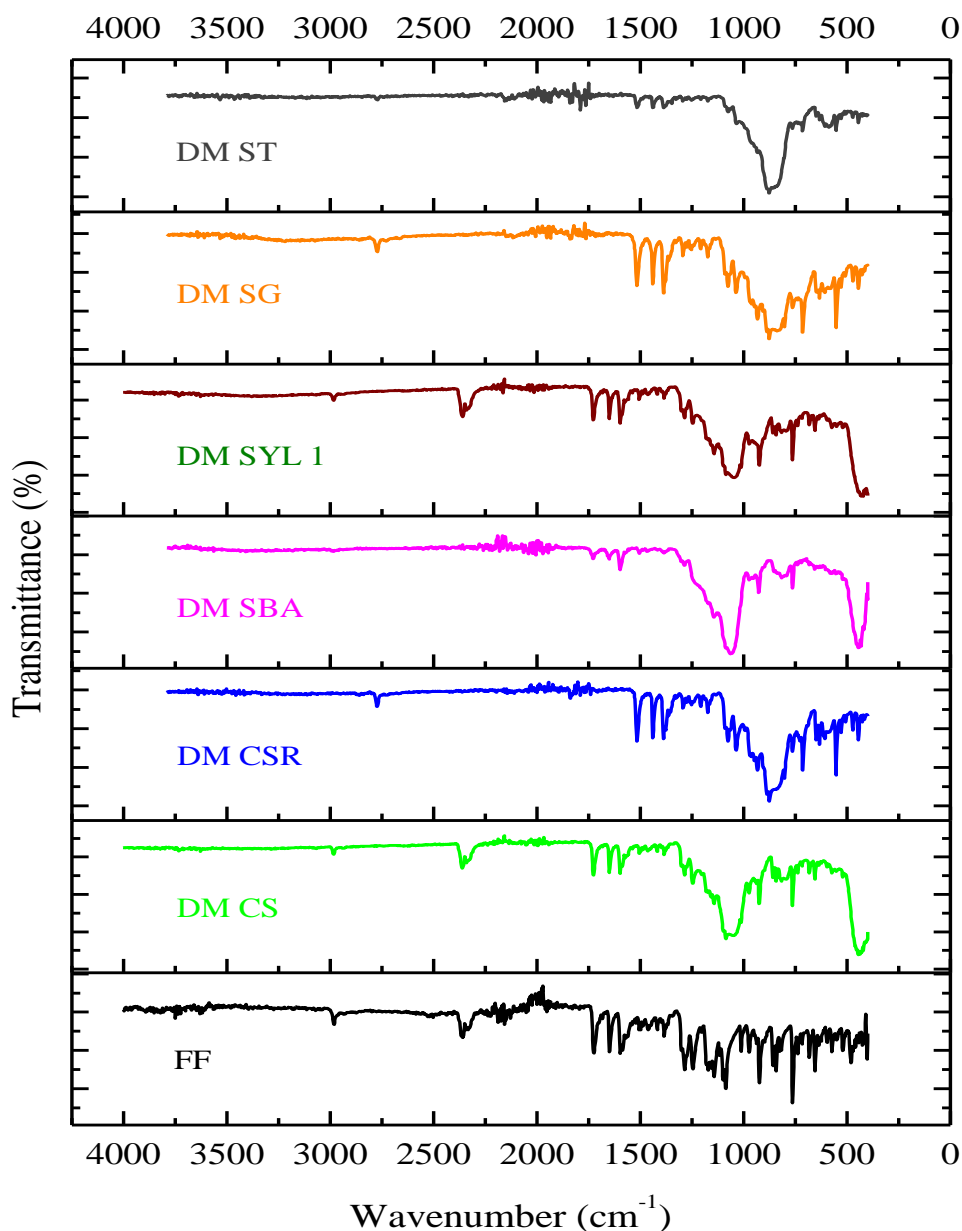


Figure 3.15: FTIR spectra of fenofibrate (FF) along with Core Shell (CS), Core Shell Rehydrox (CSR), SBA-15 (SBA), Syloid AL-1 (SYL 1), Silica gel (SG) and Stober (ST) based dry microwave (DM) formulations all at silica/drug ratio of 1:1.

3.3. Conclusions

In summary, it has been confirmed that it is possible to formulate silica based products containing a model drug using microwave irradiation. Furthermore, the resultant product exhibits enhanced drug release compared with the non-formulated versions. Characterisation of the samples using DSC and XRD implies that there is a transformation of the drug from a crystalline to a semi-crystalline or amorphous form as a result of the formulation process. SEM images indicated that at the highest drug/silica ratio investigated, it is possible to achieve a uniformly mixed product. FTIR spectra demonstrated the drug chemical stability after loading. Furthermore, drug release data have confirmed that for five of the six silicas investigated, it is possible to dramatically enhance the extent of fenofibrate release over a 30 minute period. These findings could be applied to a far wider range of compounds that exhibit poor aqueous solubility, thus helping improve bioavailability through the use of bespoke mesoporous silicas.

References

- AHERN, R. J., CREAN, A. M. & RYAN, K. B. 2012. The influence of supercritical carbon dioxide (SC-CO₂) processing conditions on drug loading and physicochemical properties. *International Journal of Pharmaceutics*, 439, 92-99.
- ANDERSSON, J., ROSENHOLM, J., AREVA, S. & LINDÉN, M. 2004. Influences of Material Characteristics on Ibuprofen Drug Loading and Release Profiles from Ordered Micro- and Mesoporous Silica Matrices. *Chemistry of Materials*, 16, 4160-4167.
- BARBÉ, C., BARTLETT, J., KONG, L., FINNIE, K., LIN, H. Q., LARKIN, M., CALLEJA, S., BUSH, A. & CALLEJA, G. 2004. Silica Particles: A Novel Drug-Delivery System. *Advanced Materials*, 16, 1959-1966.
- CHA, K. H., CHO, K. J., KIM, M. S., KIM, J. S., PARK, H. J., PARK, J., CHO, W., PARK, J. S. & HWANG, S. J. 2012. Enhancement of the dissolution rate and bioavailability of fenofibrate by a melt-adsorption method using supercritical carbon dioxide. *International Journal of Nanomedicine*, 7, 5565-5575.
- GUO, Z., LIU, X. M., MA, L., LI, J., ZHANG, H., GAO, Y. P. & YUAN, Y. 2013. Effects of particle morphology, pore size and surface coating of mesoporous silica on Naproxen dissolution rate enhancement. *Colloids and Surfaces B: Biointerfaces*, 101, 228-235.
- KINNARI, P., MÄKILÄ, E., HEIKKILÄ, T., SALONEN, J., HIRVONEN, J. & SANTOS, H. A. 2011. Comparison of mesoporous silicon and non-ordered mesoporous silica materials as drug carriers for itraconazole. *International Journal of Pharmaceutics*, 414, 148-156.
- LIMNELL, T., SANTOS, H. A., MÄKILÄ, E., HEIKKILÄ, T., SALONEN, J., MURZIN, D. Y., KUMAR, N., LAAKSONEN, T., PELTONEN, L. & HIRVONEN, J. 2011. Drug delivery formulations of ordered and nonordered mesoporous silica: Comparison of three drug loading methods. *Journal of Pharmaceutical Sciences*, 100, 3294-3306.
- MELLAERTS, R., JAMMAER, J. A. G., VAN SPEYBROECK, M., CHEN, H., HUMBEECK, J. V., AUGUSTIJNS, P., VAN DEN MOOTER, G. & MARTENS, J. A. 2008. Physical State of Poorly Water Soluble Therapeutic Molecules Loaded into SBA-15 Ordered Mesoporous Silica Carriers: A Case Study with Itraconazole and Ibuprofen. *Langmuir*, 24, 8651-8659.
- NACSA, Á., AMBRUS, R., BERKESI, O., SZABÓ-RÉVÉSZ, P. & AIGNER, Z. 2008. Water-soluble loratadine inclusion complex: Analytical control of the preparation by microwave irradiation. *Journal of Pharmaceutical and Biomedical Analysis*, 48, 1020-1023.
- SLIWINSKA-BARTKOWIAK, M., DUDZIAK, G., GRAS, R., SIKORSKI, R., RADHAKRISHNAN, R. & GUBBINS, K. E. 2001. Freezing behavior in porous glasses and MCM-41. *Colloids and Surfaces A: Physicochemical and Engineering Aspects*, 187-188, 523-529.
- TAKEUCHI, H., NAGIRA, S., YAMAMOTO, H. & KAWASHIMA, Y. 2004. Solid dispersion particles of tolbutamide prepared with fine silica particles by the spray-drying method. *Powder Technology*, 141, 187-195.
- TORRADO, S., TORRADO, S., TORRADO, J. J. & CADÓRNIGA, R. 1996. Preparation, dissolution and characterization of albendazole solid dispersions. *International Journal of Pharmaceutics*, 140, 247-250.
- TOZUKA, Y., SUGIYAMA, E. & TAKEUCHI, H. 2010. Release profile of insulin entrapped on mesoporous materials by freeze-thaw method. *International Journal of Pharmaceutics*, 386, 172-177.

- VALLET-REGÍ, M., BALAS, F. & ARCOS, D. 2007. Mesoporous Materials for Drug Delivery. *Angewandte Chemie International Edition*, 46, 7548-7558.
- VAN SPEYBROECK, M., BARILLARO, V., THI, T. D., MELLAERTS, R., MARTENS, J., VAN HUMBEECK, J., VERMANT, J., ANNAERT, P., VAN DEN MOOTER, G. & AUGUSTIJNS, P. 2009. Ordered mesoporous silica material SBA-15: A broad-spectrum formulation platform for poorly soluble drugs. *Journal of Pharmaceutical Sciences*, 98, 2648-2658.
- VIALPANDO, M., BACKHUIJS, F., MARTENS, J. A. & VAN DEN MOOTER, G. 2012. Risk assessment of premature drug release during wet granulation of ordered mesoporous silica loaded with poorly soluble compounds itraconazole, fenofibrate, naproxen, and ibuprofen. *European Journal of Pharmaceutics and Biopharmaceutics*, 81, 190-198.
- WATERS, L., BEDFORD, S. & PARKES, G. B. 2011. Controlled Microwave Processing Applied to the Pharmaceutical Formulation of Ibuprofen. *AAPS PharmSciTech*, 12, 1038-1043.
- ZHANG, Y., ZHI, Z., JIANG, T., ZHANG, J., WANG, Z. & WANG, S. 2010. Spherical mesoporous silica nanoparticles for loading and release of the poorly water-soluble drug telmisartan. *Journal of Controlled Release*, 145, 257-263.
- ZHU, Y.-F., SHI, J.-L., LI, Y.-S., CHEN, H.-R., SHEN, W.-H. & DONG, X.-P. 2005. Storage and release of ibuprofen drug molecules in hollow mesoporous silica spheres with modified pore surface. *Microporous and Mesoporous Materials*, 85, 75-81.

Chapter 4: Microwave processed formulations of gemfibrozil using non-ordered mesoporous silica

4.1. Introduction

The critical element in enhancing the dissolution profile of a poorly soluble compound is a reduction of the lattice energy of well-defined crystals by generating amorphous or disordered structures. Various ordered and non-ordered forms of mesoporous silica are used as potential carriers for therapeutic molecules. The surface chemistry of ordered and non-ordered silica is similar, consisting of siloxane groups (-Si-O-Si-), with the oxygen on the surface, and three forms of silanol groups (-Si-OH) (Kinnari et al., 2011). The major difference is in the pore structure as ordered silica materials contain very uni-directional and uniform pore structures compared with the disordered pore structures of non-ordered silica materials (Kinnari et al., 2011).

In previous work using a variety of mesoporous silicas (Chapter 3), successful inclusion of fenofibrate was made through the application of novel microwave heating methods. The results confirmed the remarkable enhancement in the extent of dissolution of silica incorporated fenofibrate. This approach worked well for fenofibrate but further investigation is required to make full use of the microwave technique to develop mesoporous silica based formulations. It is an established fact that various properties of mesoporous materials affect the loading and release rate of incorporated drugs, such as the particle size, surface area, pore size, pore volume and surface chemistry (Xu et al., 2013). Therefore, the aim of the present study was to evaluate the effect of the silicas properties along with the microwave method of formulation on the release rate of a poorly water soluble drug “gemfibrozil”. Gemfibrozil, 5-(2, 5-dimethylphenoxy)-2, 2- dimethyl pentanoic acid, is a benzene derivative of valeric acid with lipophilic character and poor water solubility. It is a lipid regulating agent which is

effective in reducing serum cholesterol and triglyceride levels. It is beneficial in decreasing the incidence of coronary heart disease (Mart nez-Oh rriz et al., 2008, Molinari et al., 2009). Gemfibrozil was loaded in three non-ordered mesoporous silica materials, namely, Syloid AL-1, Syloid 72 and Syloid 244 with different physical properties (Table 4.1). The release behaviour of the formulations was measured in a dissolution medium composed of 0.1 M HCl and 0.5 % w/v SDS (pH 1.2) under sink conditions at 37 °C.

Table 4.1: Physical characteristics of mesoporous silica

Mesoporous silica	Particle size (µm)	Surface area (m ² /g)	Pore volume (cm ³ /g)	Pore diameter (nm)
Syloid AL-1	6.5-8.1	605	0.3	2.9
Syloid 72	4.6-5.8	405	1.2	10
Syloid 244	2.5-3.7	379	1.6	16

4.2. Results and discussion

4.2.1. In vitro dissolution

Dissolution analysis was carried out to investigate the influence of the physical properties of Syloid silica along with the microwave loading method on the dissolution behaviour of gemfibrozil. The in vitro release profiles of gemfibrozil from three different Syloid grades (based on physical properties presented in Table 4.1) along with pure gemfibrozil in an acidic medium of pH 1.2 over a period of 30 minutes are presented in Figures 4.1- 4.3.

4.2.1.1. Dissolution studies of Syloid AL-1 based formulations

Figure 4.1 displays the dissolution profile of gemfibrozil (GF) along with Syloid AL-1 formulations over a period of thirty minutes. Formulating gemfibrozil with Syloid AL-1

increased the extent of dissolution compared with the observed percentage release of pure gemfibrozil, i.e. 15.4 (\pm 8.7) % after 30 minutes (Figure 4.1). The microwave formulations of gemfibrozil at silica/drug ratios of 1:1 and 3:1 provided the greatest drug releases, i.e. 31.6 (\pm 3.0), and 40.9 (\pm 1.8) % respectively, after 30 minutes (Figure 4.1). The physically mixed formulations of gemfibrozil with Syloid AL-1/drug ratios of 1:1 and 3:1 released only 17.7 (\pm 2.9) % and 26.9 (\pm 1.2) %, respectively after 30 minutes (Figure 4.1). In this typical dissolution profile, only the physically mixed product (3:1) displayed a burst release of 20.1 (\pm 1.6) % in the first five minutes and then slowed while the drug release profiles for the remaining formulations achieved a greater percentage release after 30 minutes.

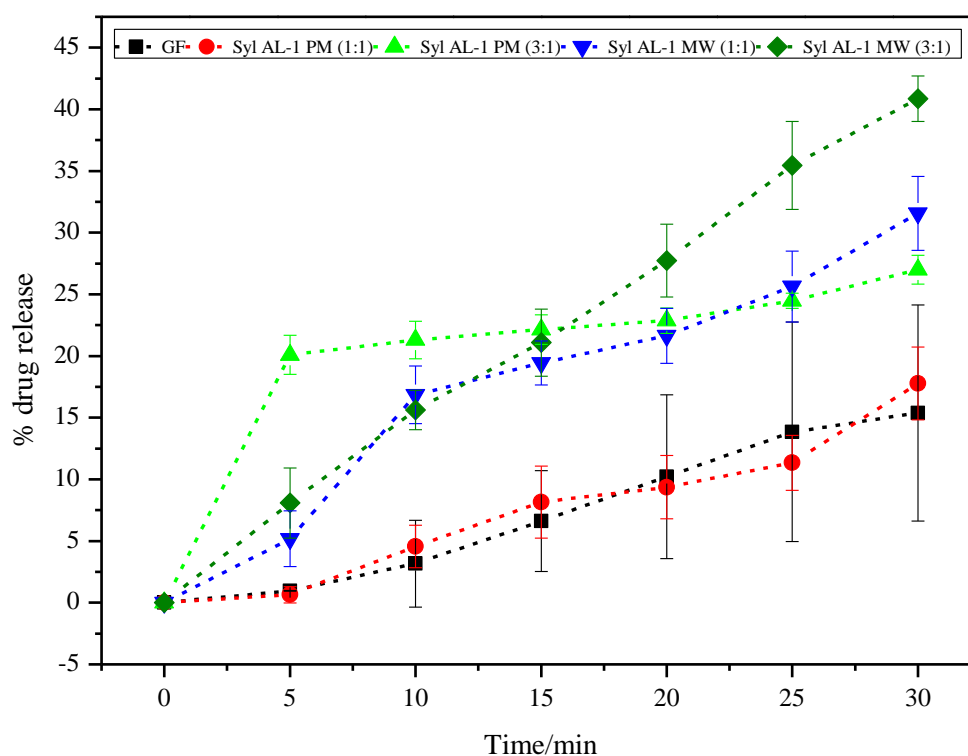


Figure 4.1: Gemfibrozil release profiles for pure gemfibrozil (GF) along with Syloid AL-1 based formulations using microwave irradiation (MW) and physical mixing (PM), at silica/drug ratios of 1:1 and 3:1. Each data point represents the mean of 3 results with SD error bars.

4.2.1.2. Dissolution studies of Syloid 72 based formulations

The release behaviour of gemfibrozil from Syloid 72 is presented in Figure 4.2. For the Syloid 72, the microwave formulated products at silica/drug ratios of 1:1 and 3:1 provided the greatest drug release, i.e. 62.1 (\pm 1.9) % and 55.9 (\pm 1.3) %, respectively, after 30 minutes (Figure 4.2). The physically mixed formulations made little difference to the dissolution behaviour but were still significant compared with the pure gemfibrozil (Figure 4.2). Based on these findings, the physicochemical properties of Syloid 72 are best suited to load drug using the microwave technique as drug is then transported into the pores and distributed uniformly inside the pores. This process accelerates the transition of drug molecules from a crystalline to an amorphous state, confirmed by the results of XRD (See Section 4.2.2.1). This change in state of drug molecules facilitates the enhanced dissolution of drug (Figure 4.2).

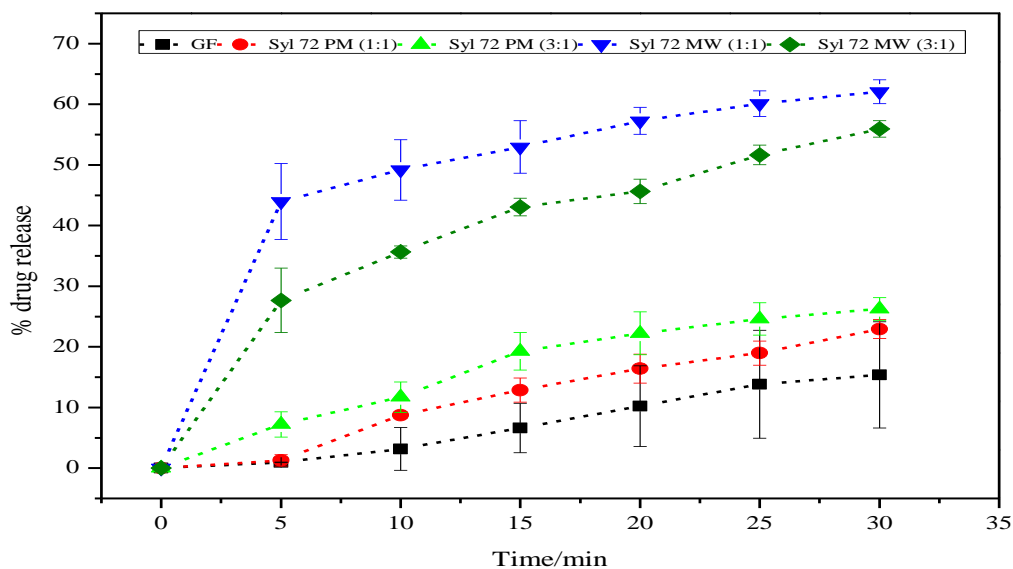


Figure 4.2: Gemfibrozil release profiles for pure gemfibrozil (GF) along with Syloid 72 based formulations using microwave irradiation (MW) and physical mixing (PM), at silica/drug ratios of 1:1 and 3:1. Each data point represents the mean of 3 results with SD error bars.

4.2.1.3. Dissolution studies of Syloid 244 based formulations

Figure 4.3 highlights results for physically mixed and microwave processed formulations of Syloid 244 at silica/drug ratios of 1:1 and 3:1. The greatest drug release, i.e. 49.7 (\pm 6.9) % was achieved with a physically mixed formulation at a silica/drug ratio of 1:1 (Figure 4.3). This was far greater than the release from the microwave product, i.e. 20 (\pm 2.9) %, after 30 minutes. However, comparable release profiles for gemfibrozil from microwave and physically mixed formulations at a silica/drug ratio of 3:1 were achieved, i.e. 42.8 (\pm 1.2) % and 36.9 (\pm 3.3) %, respectively, after 30 minutes (Figure 4.3). The small particle size of Syloid 244 could be the reason for rapid drug release from the physical mixture compared with the microwave processed formulations. However, the microwave loading method increased the release to some extent even after recrystallisation (during cooling) of drug.

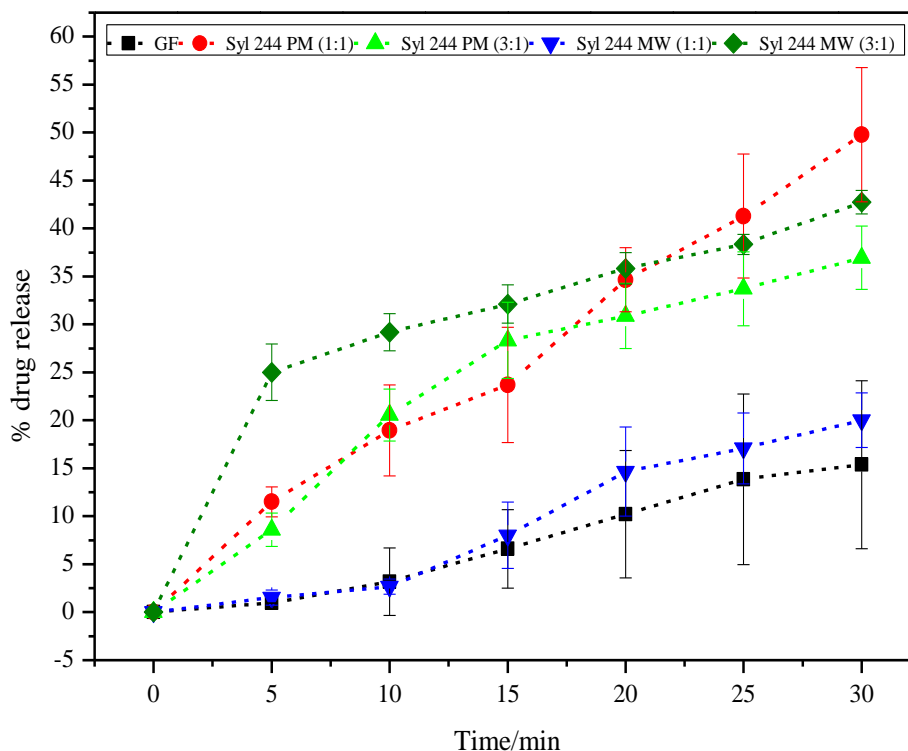


Figure 4.3: Gemfibrozil release profiles for pure gemfibrozil (GF) along with Syloid 244 based formulations using microwave irradiation (MW) and physical mixing (PM), at silica/drug ratios of 1:1 and 3:1. Each data point represents the mean of 3 results with SD error bars.

4.2.1.4. Summary

The dissolution profile of gemfibrozil from all mesoporous silica formulations was significantly higher than from pure gemfibrozil. Based on previous research several factors enhance dissolution, such as the lack of a crystalline form, increased surface area of the drug, as well as the hydrophilic surface of the silica carriers (Wang et al., 2013). It is an established fact that nanosized drug crystals can increase the effective surface area available for dissolution according to the Noyes-Whitney equation (Merisko-Liversidge et al., 2003, Müller et al.,

2001). The formation of a less ordered or semi-crystalline form could be the reason for the dramatically enhanced dissolution of gemfibrozil (Wang et al., 2013).

Comparing the dissolution profile of microwave based formulations of gemfibrozil from Syloid AL-1, Syloid 72 and Syloid 244, the dissolution extent of gemfibrozil was greater from Syloid 72 compared with Syloid AL-1 and Syloid 244. The difference in the matrix architecture, including the pore size, pore volume and surface area may be mainly responsible for the difference in the drug dissolution profiles. Drug release from a carrier requires two main processes: dissolving of entrapped drug and diffusion of the dissolved drug through the pore channel into the dissolution media (Wang et al., 2013). These results indicate the use of mesoporous silica having optimal physical properties. Syloid silica 244 having a large pore diameter along with high pore volume can accommodate a large amount of drug. However, wider pores can furnish enough space for molten drug molecules to recrystallise on cooling which could subsequently limit release of drug from pores. Similarly, for a silica material such as Syloid AL-1 having a small pore diameter and lower pore volume, non-uniform pore filling can be encountered. In such silica materials drug can reside in the pore walls and on the external large surface which are likely to be recrystallised. Therefore, the dissolution media faces steric hindrance to accessing drug molecules confined inside the pores, resulting in less drug release. However, these results indicate that Syloid 72 (having optimum physical characteristics) makes it a suitable carrier for loading of poorly soluble drugs using the microwave approach, which results in enhanced release profiles.

In summary, an enhanced release profile of gemfibrozil was achieved with all mesoporous silica materials. Along with the selection of drug loading method, the difference in the extent of release from different silica materials was attributed to their diverse architectural properties. These results highlight the judicious selection of silica materials for the loading of model drug to achieve optimum release profiles.

4.2.2. Solid state characterisation

Solid state characterisation was undertaken using DSC, XRD and SEM to investigate the melting transition, crystalline state and crystal morphology of pure and processed drug.

4.2.2.1. Differential scanning calorimetry (DSC) and X-ray diffraction (XRD)

Figures 4.4-4.6 depict the DSC thermograms for Syloid AL-1, Syloid 72 and Syloid 244 based physical mixtures and microwave formulations along with pure gemfibrozil, respectively. Gemfibrozil was characterised by a sharp melting endothermic peak at 64.36 °C. The peak onset temperature and heat of fusion (ΔH_f) were 61.3 °C and -77.5 Jg^{-1} , respectively (Figure 4.4). The melting peak appeared in the physical mix formulations as well as in the microwave processed formulations at all silica/drug ratios under investigation with some variation in melting peak depression and broadening, indicating the transition from a crystalline to a semi-crystalline state. This depression became more apparent as the silica content was increased in the formulations.

For gemfibrozil formulated with Syloid AL-1 at a silica/drug ratio of 1:1 using the microwave method or physical mixing, peak intensity was less affected compared with those formulations prepared at a silica/drug ratio of 3:1 (Figure 4.4). The small pore volume could be the reason why the host accepts drug molecules beyond its capacity and therefore, the drug molecule is likely to be deposited on the external silica surface. These drug molecules were scanned using DSC, providing peak intensities. At a 3:1 silica/drug ratio, the large surface area of Syloid AL-1 accommodated a major portion of loaded drug inside the pores while residual drug resided on the external surface as a consequence of the low pore volume, i.e. $0.3 \text{ cm}^3/\text{g}$.

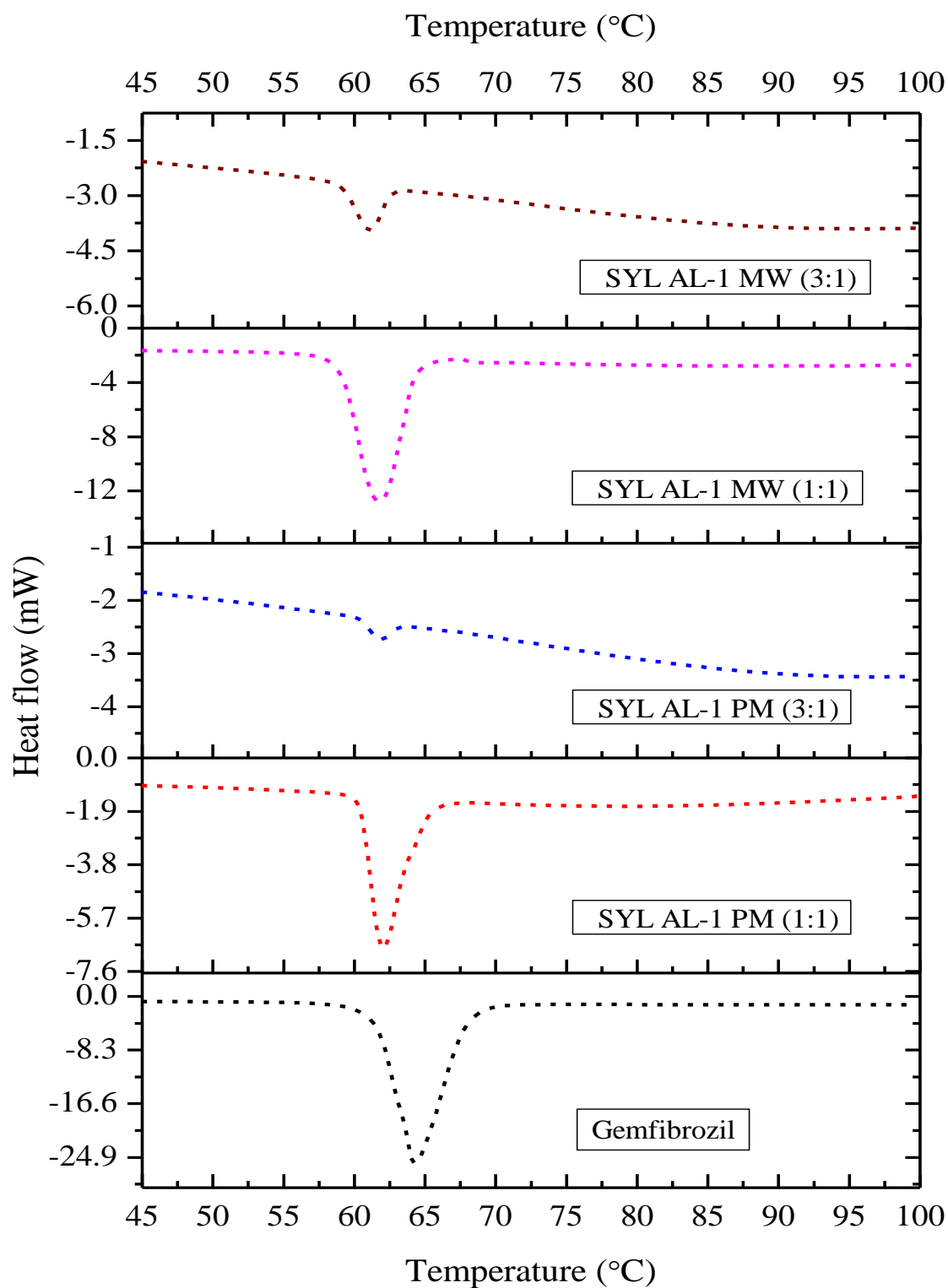


Figure 4.4: DSC profiles for gemfibrozil (GF) along with Syloid AL-1 based physical mixture (PM) and microwave (MW) formulations at silica / drug ratios of 1:1 and 3:1.

For Syloid 72, a marked melting peak shift was seen in the microwave formulations compared with the physically mixed product, confirming that drug was loaded inside the pores to full capacity. In addition, some residual drug was deposited on the external surface as Syloid 72 has a medium pore volume, i.e. $1.2 \text{ cm}^3/\text{g}$ (Figure 4.5). However, the melting peak was absent in the Syloid 244 based microwave formulation at a silica/drug ratio of 3:1, confirming the amorphous state of gemfibrozil within the formulation (Figure 4.6). For Syloid 244 based physically mixed and microwave assisted formulations, the peak intensity was prominently decreased and even disappeared in the microwave formulation at a silica/drug ratio of 3:1, attributed to the large pore diameter and pore volume, i.e. 16 nm and $1.5 \text{ cm}^3/\text{g}$, respectively. Syloid 244 can easily accommodate drug molecules deep inside its pores and the drug might even deposit in multilayers, hence during scanning, the drug cannot be detected, indicating the change in the physical state of the drug.

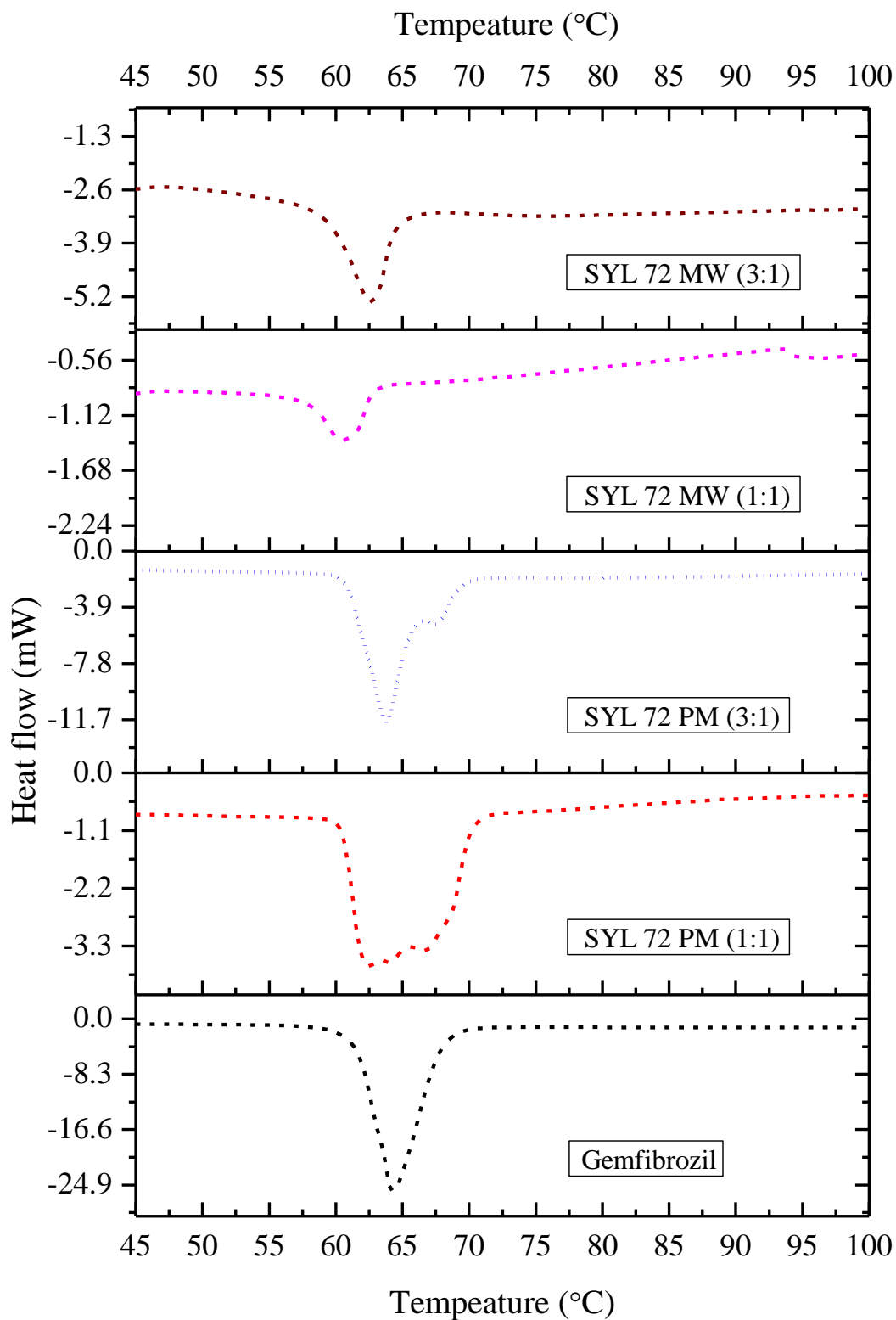


Figure 4.5: DSC profiles for gemfibrozil (GF) along with Syloid 72 based physical mixture (PM) and microwave (MW) formulations at silica / drug ratios of 1:1 and 3:1.

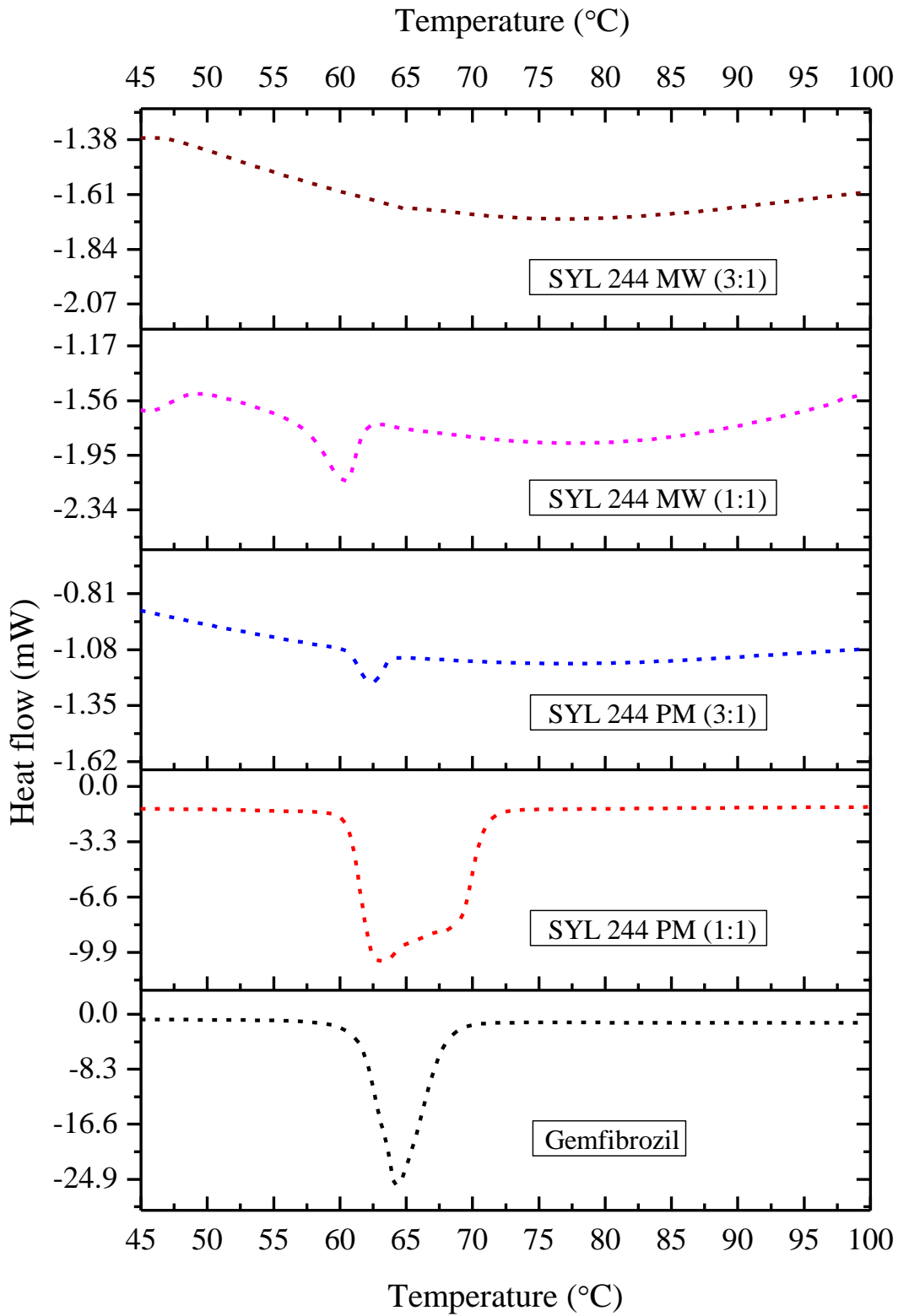


Figure 4.6: DSC profiles for gemfibrozil (GF) along with Syloid 244 based physical mixture (PM) and microwave (MW) formulations at silica / drug ratios of 1:1 and 3:1.

Figures 4.7-4.9 demonstrate the XRD patterns of Syloid AL-1, Syloid 72 and Syloid 244 based physically mixed and microwave treated formulations at ratios of 1:1 and 3:1. The characteristic diffraction peaks observed at 11.57°, 12.74°, 13.88°, 17.98° and 24.07°, correspond to the powder diffraction pattern for pure gemfibrozil while the absence of diffraction peaks in Syloid AL-1, Syloid 72 and Syloid 244 silica confirm their amorphous structure. The gemfibrozil diffraction peaks with decreased intensities were present in physically mixed formulations along with the microwave product at a 1:1 ratio of Syloid AL-1, demonstrating the partially crystalline state of drug (Figure 4.7). The diffraction peak absence in the microwave assisted formulation at a 3:1 ratio indicates the amorphous state of pore confined drug.

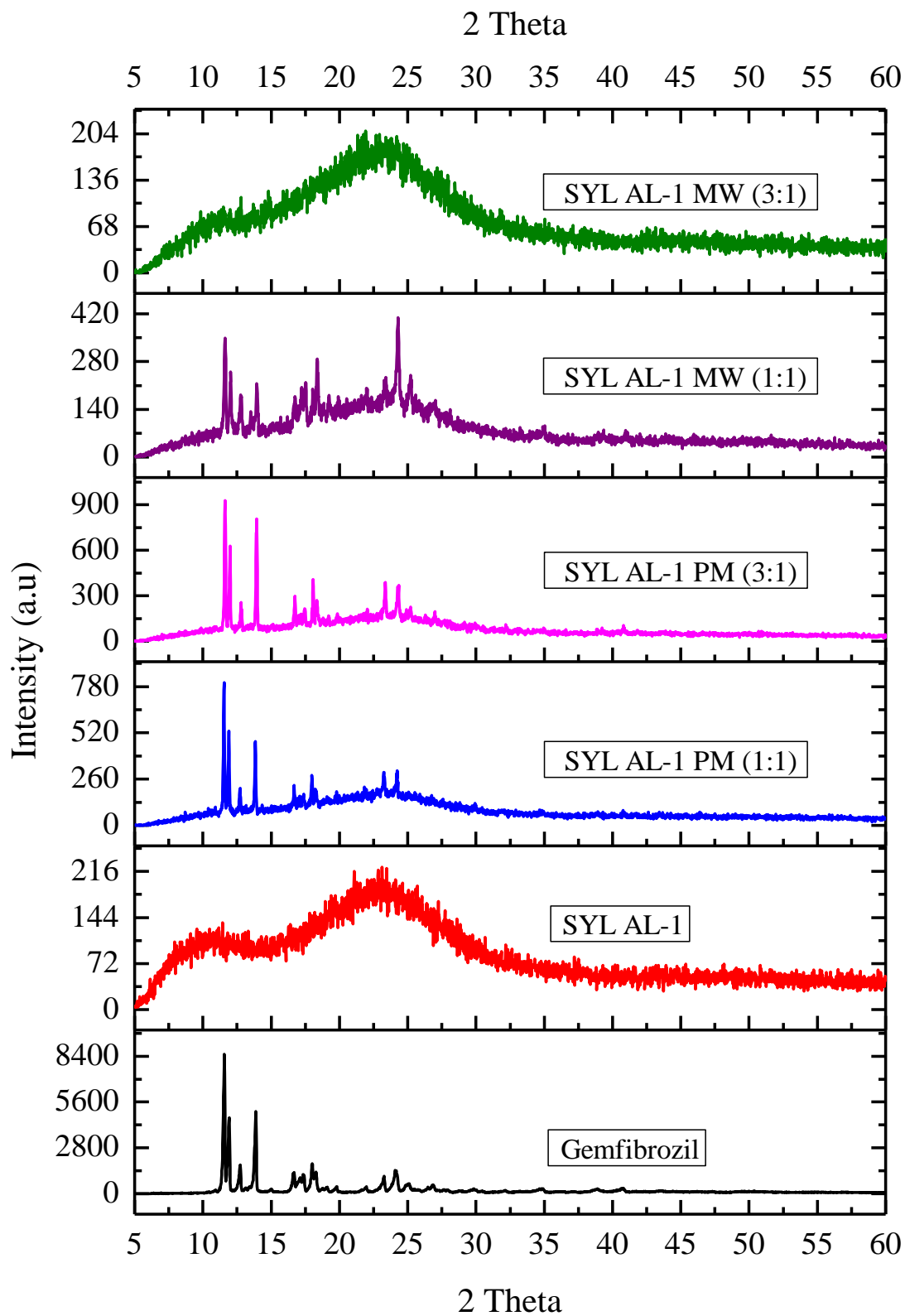


Figure 4.7: XRD pattern of gemfibrozil (GF) and Syloid AL-1 along with physical mix (PM) and microwave (MW) formulations at silica/drug ratios of 1:1 and 3:1.

The peaks corresponding to the crystalline state of gemfibrozil were observed in Syloid 72 based physical mixtures while the amorphous state of drug after microwave treatment was confirmed (Figure 4.8). These findings confirm the appropriate pore diameter of Syloid 72 to entrap drug molecules inside its pores (estimated diameter of gemfibrozil is 1.5 nm) as the restricted pore space inhibited the recrystallisation process of drug molecules.

Gemfibrozil, physically mixed with Syloid 244 at ratios of 1:1 and 3:1 displayed characteristic peaks with decreased intensities, confirming the semi-crystalline state of the drug. However, only a peak at 11.57° can be identified in the microwave assisted formulations, indicating that some of the drug molecules retained a crystalline structure i.e. there was enough pore space to facilitate the recrystallisation of molten drug.

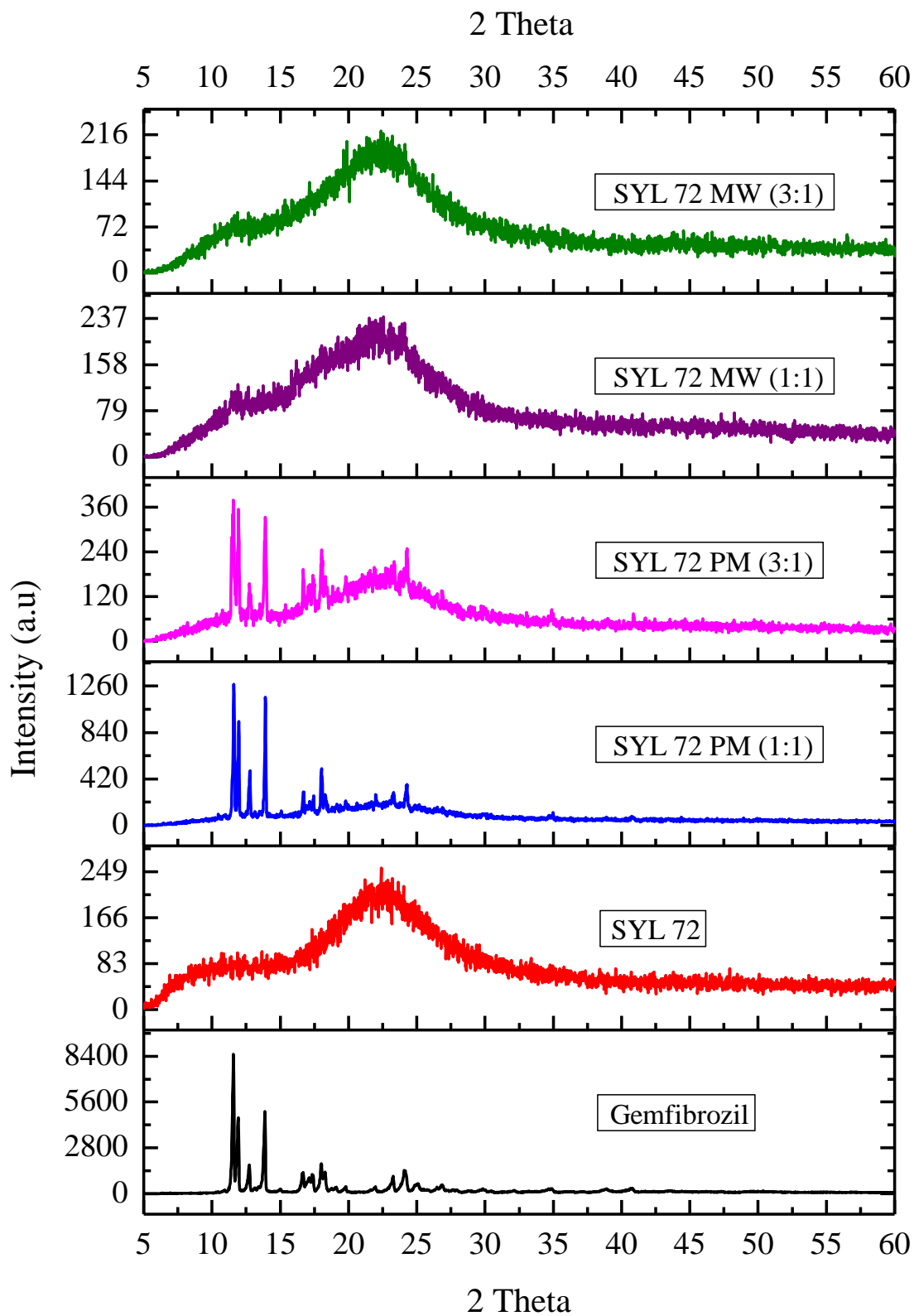


Figure 4.8: XRD pattern of gemfibrozil (GF) and Syloid 72 along with physical mix (PM) and microwave (MW) formulations at silica/drug ratios of 1:1 and 3:1.

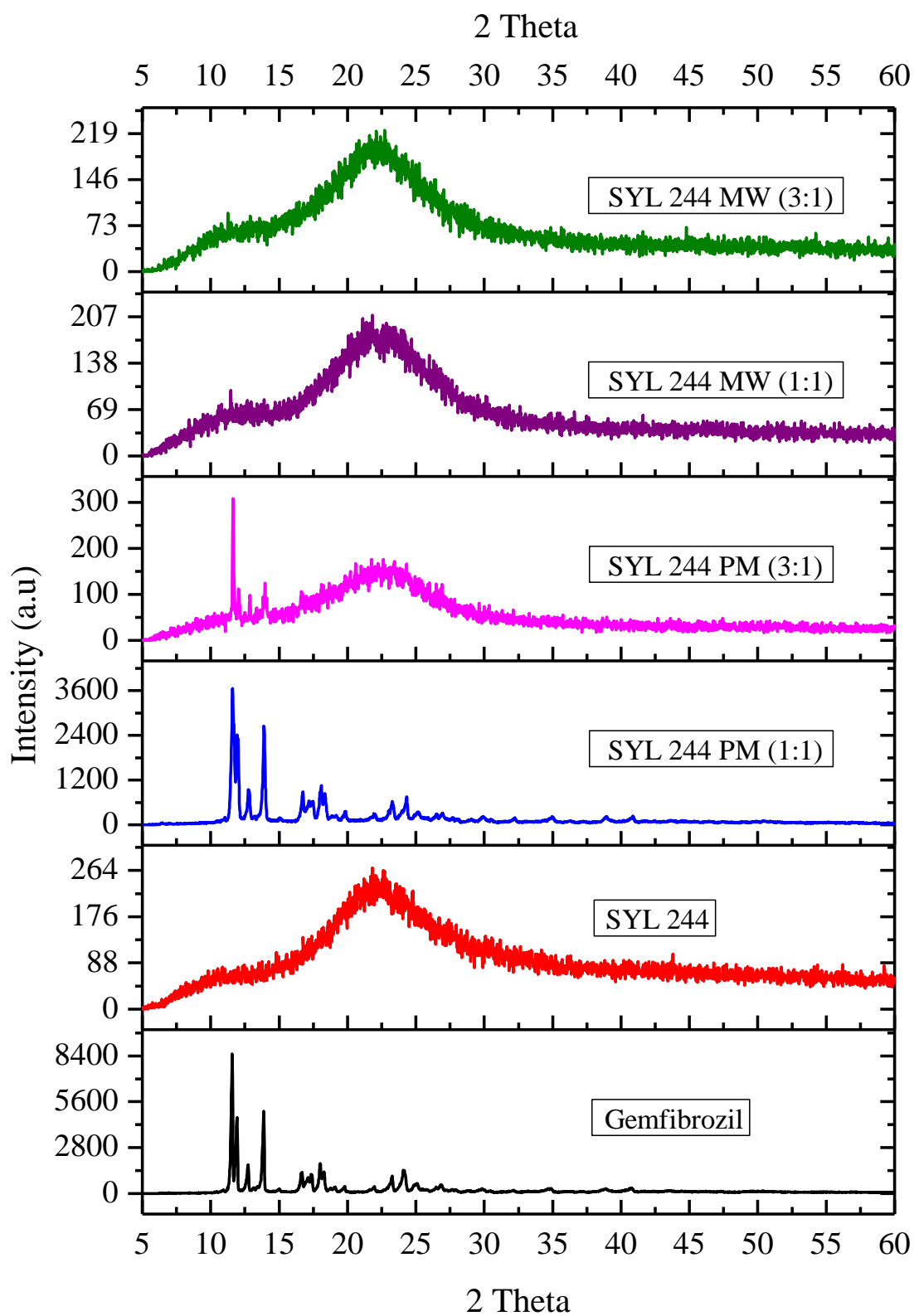


Figure 4.9: XRD pattern of gemfibrozil (GF) and Syloid 244 along with physical mix (PM) and microwave (MW) formulations at silica/drug ratios of 1:1 and 3:1.

4.2.2.2. Scanning electron microscopy (SEM)

Scanning electron microscopy (SEM) images were used to identify any apparent changes in the physical characteristics of the formulated products compared with the pure drug or a simple physical mixture of drug and silica. The general findings of this work are exemplified in Figure 4.10. The drug crystalline state, along with the disordered irregular shape of Syloid AL-1 silica, was evident by SEM (Figure 4.10). SEM images also confirmed the insignificant effect of physical mixing as the drug retained a crystalline structure. However, there is a uniform distribution of gemfibrozil observed in microwave formulations.

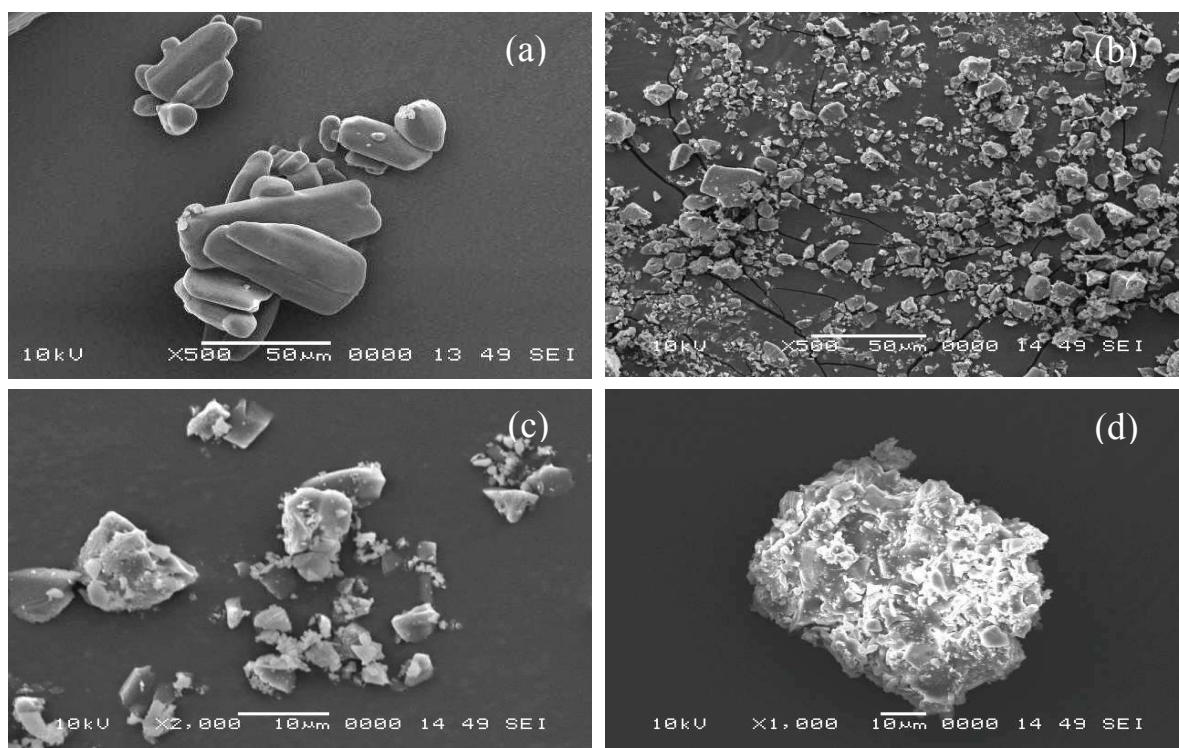


Figure 4.10: SEM images of (a) gemfibrozil, (b) Syloid AL-1, (c) a physical mix of Syloid AL-1 and gemfibrozil (1:1), (d) microwave formulation of Syloid AL-1 and gemfibrozil (1:1).

Figure 4.11 presents the SEM images for Syloid 72 and Syloid 244 along with their microwave formulation at a silica/drug ratio of 1:1. The molten drug molecules are adsorbed and evenly distributed in both silica pores while some portion of drug recrystallised in Syloid

244 as it has a larger pore width, providing enough space for recrystallisation. Overall, it appears that the microwave formulation process can modify the crystallinity in the sample and create a product that contains a uniform dispersion of drug within the silica matrix.

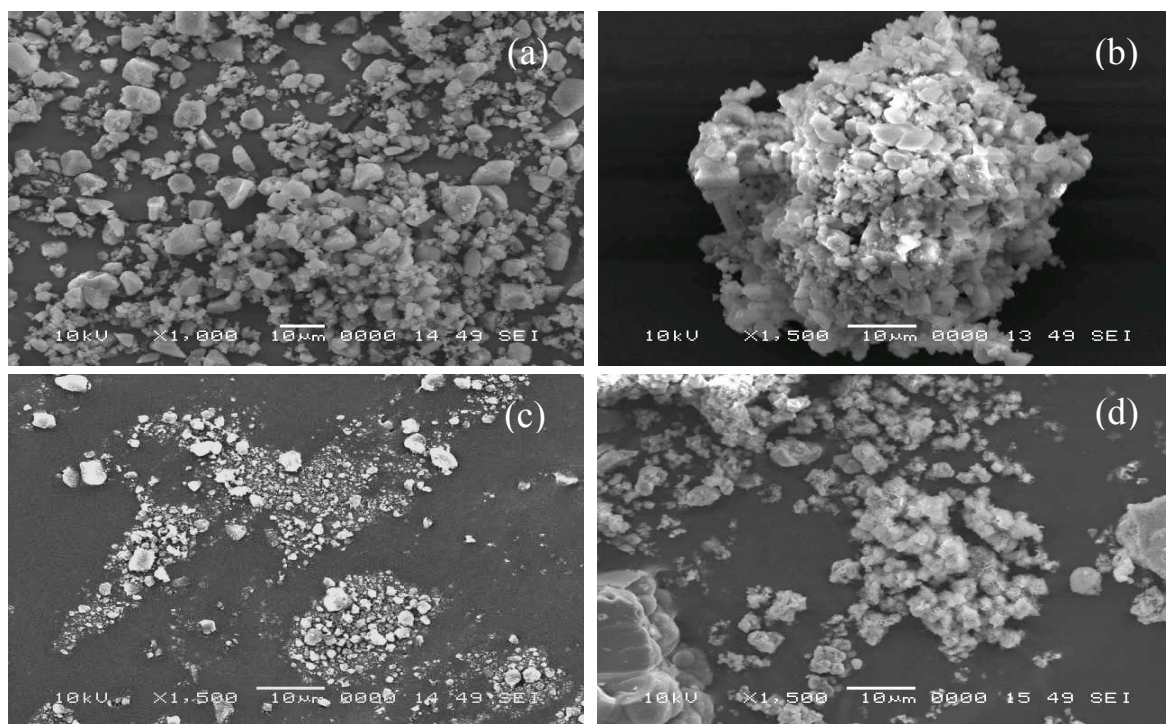


Figure 4.11: SEM images of (a) Syloid 72, (b) microwave formulation of Syloid 72 and gemfibrozil (1:1), (c) Syloid 244, (d) microwave formulation of Syloid 244 and gemfibrozil (1:1).

4.2.2.3. Fourier transform infrared spectroscopy (FTIR)

FTIR was used to investigate the possible interaction between gemfibrozil and silica materials. Figure 4.12 illustrates IR spectra of pure gemfibrozil and Syloid 244 silica. Characteristic gemfibrozil peaks were observed at 2919.83, 1704.84, 1587.21, 1265.13 and 931.49 cm^{-1} corresponding to an O-H stretching vibration, C=O stretching vibration, C-C ring stretching, O-H deformation and C-H deformation, respectively. The Syloid 244 spectrum displays the typical silica band associated with the main inorganic backbone. The sharp IR

signal observed at 1070 cm^{-1} corresponds to the asymmetric stretching vibration, ν_{as} (Si-O-Si), of the siliceous framework. The symmetric stretch, ν_{s} (Si-O-Si), and the bending vibration, δ (Si-O-Si), of the siliceous framework were observed at 794 and 447 cm^{-1} , respectively. The band at 966.20 cm^{-1} corresponds to Si-OH bending. The characteristic siliceous peaks (as exemplified in Syloid 244) were observed in the spectra of Syloid 72 and Syloid AL-1 silica samples.

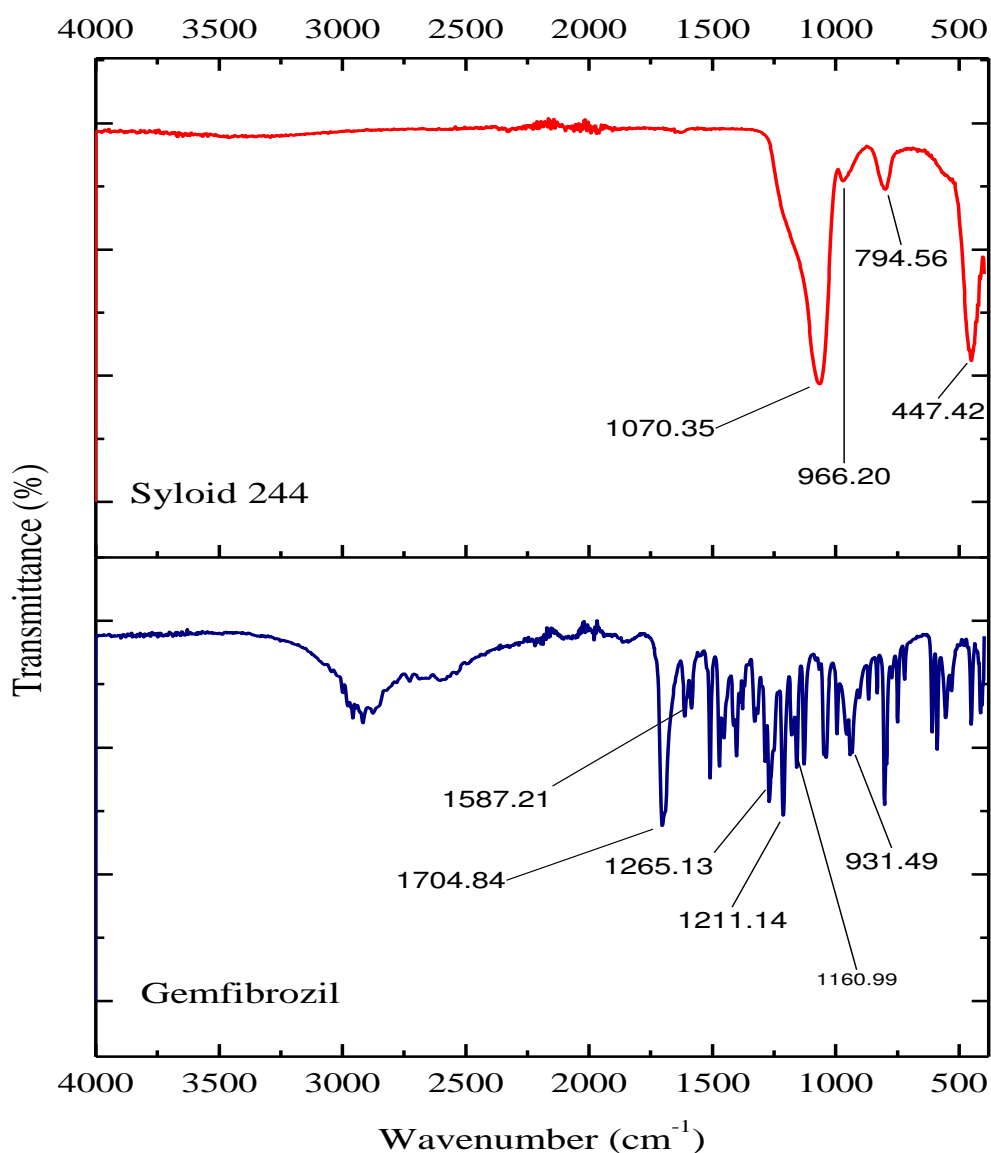


Figure 4.12: FTIR spectra of pure gemfibrozil and Syloid 244 silica.

Figure 4.13 displays the IR spectra of physically mixed and microwave processed formulations of gemfibrozil with Syloid AL-1, Syloid 244 and Syloid 72 at a ratio of 1:1. The loading of gemfibrozil was reflected by the appearance of characteristic bands in the IR spectra. The presence of specific peaks corresponds to silica and drug, suggesting the lack of interaction between drug and silica material. In summary, IR data highlights the successful loading of gemfibrozil within silica formulations.

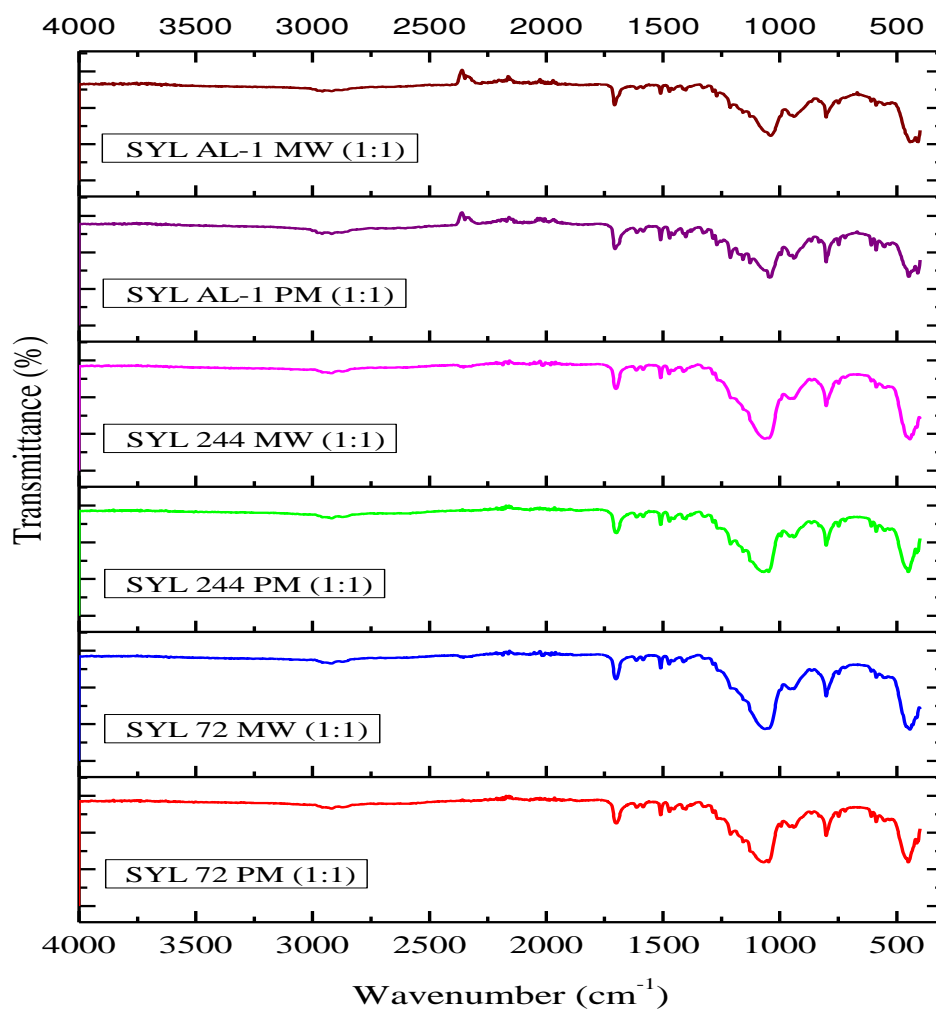


Figure 4.13: FTIR spectra of Syloid 72, Syloid 244 and Syloid AL-1 based physical mix (PM) and microwave (MW) formulation, at a silica/drug ratio of 1:1.

4.3. Conclusions

In the present study, three non-ordered mesoporous silica materials with different physical properties were formulated with gemfibrozil and subsequently analysed. The most significant output in terms of dissolution enhancement was displayed by Syloid 72 microwave formulations, attributed to the optimal physical architecture (such as pore diameter and volume). However, an appreciable amount of drug was released from the other two silica materials, hence, non-ordered silica materials are promising for dissolution enhancement of drug formulations, which renders them a viable alternative for carriers of hydrophobic drugs.

Characterisation tools such as DSC and XRD confirmed the transformation of the drug from a crystalline to a semi-crystalline or amorphous form as a result of the formulation process. SEM images indicate a uniformly mixed product of drug/silica sample after microwave processing. FTIR spectra demonstrated the drug stability after loading. Furthermore, these findings confirm the application of non-ordered silica along with microwave potential to resolve dissolution related issues for a wide range of compounds exhibiting poor aqueous solubility.

References

- KINNARI, P., MÄKILÄ, E., HEIKKILÄ, T., SALONEN, J., HIRVONEN, J. & SANTOS, H. A. 2011. Comparison of mesoporous silicon and non-ordered mesoporous silica materials as drug carriers for itraconazole. *International journal of pharmaceutics*, 414, 148-156.
- MARTINEZ-OHERRIZ, M., MARTIN, C., VILLAZ, I., SANCHEZ, M. & ZORNOZA, A. 2008. Analysis of the complexation of gemfibrozil with β - and hydroxypropyl- β -cyclodextrins. *Journal of Pharmaceutical and Biomedical Analysis*, 47, 943-948.
- MERISKO-LIVERSIDGE, E., LIVERSIDGE, G. G. & COOPER, E. R. 2003. Nanosizing: a formulation approach for poorly-water-soluble compounds. *European Journal of Pharmaceutical Sciences*, 18, 113-120.
- MOLINARI, R., ARGURIO, P. & POERIO, T. 2009. Flux enhancement of stagnant sandwich compared to supported liquid membrane systems in the removal of Gemfibrozil from waters. *Journal of Membrane Science*, 340, 26-34.
- MÜLLER, R., JACOBS, C. & KAYSER, O. 2001. Nanosuspensions as particulate drug formulations in therapy: rationale for development and what we can expect for the future. *Advanced drug delivery reviews*, 47, 3-19.
- WANG, Y., ZHAO, Q., HU, Y., SUN, L., BAI, L., JIANG, T. & WANG, S. 2013. Ordered nanoporous silica as carriers for improved delivery of water insoluble drugs: a comparative study between three dimensional and two dimensional macroporous silica. *International Journal of Nanomedicine*, 8, 4015.
- XU, W., RIIKONEN, J. & LEHTO, V.-P. 2013. Mesoporous systems for poorly soluble drugs. *International Journal of Pharmaceutics*, 453, 181-197.

Chapter 5: Microwave assisted formulation in the presence of a hydrophilic carrier

5.1. Introduction

Drugs with a limited dissolution and absorption rate might benefit from a reduction in particle size, as well as from an increase in saturation solubility. Thereby, solid dispersions, having both these features, can be considered as a potential strategy that can result in increased solubility and dissolution (Moneghini et al., 2009, Six et al., 2004). The judicious choice of a carrier system along with the method of preparation presents a significant influence on the properties of the resultant solid dispersion. In previous work (Chapters 3 and 4), enhanced dissolution profiles of poorly soluble drugs were achieved using mesoporous silica as a carrier material and formulations were prepared using microwave processing.

The successful utilisation of microwave energy in formulating silica based products encourages extension of this work from mesoporous silica to polymers for a thorough investigation regarding microwave potential in formulation development. Among hydrophilic polymers, polyethylene glycol (PEG) is extensively used for the preparation of solid dispersions. PEG is a semi-crystalline polymer with a low melting point and is also water-soluble (Henning, 2001, Knop et al., 2010, Zhu et al., 2012). The relatively low melting point of PEG is advantageous to formulate solid dispersions as the molecular size favours the formation of interstitial solid solutions with APIs and the highly viscous nature of the melt tends to entrap drug in a molecular state (Ginés et al., 1996). However, there is only limited literature concerning the production of microwave-induced solid dispersions, particularly regarding formulations with PEG as the carrier material. For example, Papadimitriou (Papadimitriou et al., 2008) and Maurya (Maurya et al., 2010) used PEG to formulate solid

dispersions of tibolone and atorvastatin, respectively through microwave processing. The resultant enhancement in dissolution through microwave processing justified their claim that this technique is a better alternative than traditional heating. Microwave assisted formulation of glipizide (Biswal et al., 2008) with PEG 4000 displayed a significant enhancement in solubility and bioavailability in comparison with formulations prepared by conventional heating. Microwave energy has also been used to develop a formulation of the poorly water soluble drug repaglinide with PEG 6000 (Zawar and Bari, 2013). The resultant microwave fused solid dispersion demonstrated an increased in vitro dissolution rate, possibly as a consequence of the crystalline drug being converted to an amorphous state. Microwaves have also been used to formulate solid dispersions of poorly water soluble drugs with other excipients, for example, an inclusion complex of carvedilol (Wen et al., 2004), aceclofenac (Ranpise et al., 2010) and loratidine (Nacsá et al., 2008) with cyclodextrins.

The aforementioned microwave method involved irradiation of a sample with no power control, i.e. the sample was heated for a specified period of time regardless of the sample temperature during the experiment. This is known to be problematic as samples may heat uncontrollably with significant consequences for the stability of the drug concerned. Two recent publications highlight a novel method of heating samples with a feedback system to ensure the temperature of the sample can be controlled throughout the duration of the experiment (Waters et al., 2011, Waters et al., 2013). This method ensures that a sample does not exceed a specified temperature, helping avoid unwanted drug degradation reactions. A similar heating approach is used in this study with its first application for producing PEG based drug delivery with poorly water soluble drugs, namely, fenofibrate (FF), ibuprofen (IBU), ibuprofen (+) S (IBU S) and phenylbutazone (PB). The formulation development method was previously discussed in Section 2.2.2.

5.2. Results and discussion

5.2.1. In vitro dissolution

In vitro release of microwave assisted formulations was assessed by comparing the dissolution profiles for all formulations prepared using conventional heating or a physical mixture, alongside the pure drugs.

5.2.1.1. Dissolution studies of ibuprofen

Figure 5.1 displays the dissolution profile of ibuprofen (IBU) along with the PEG based formulations over a period of thirty minutes. Formulating ibuprofen with PEG increased the extent of dissolution compared with the observed percentage release of pure ibuprofen (Figure 5.1). The microwave formulated products (MW* and MW represent excipient melted and excipient alongside drug melted formulations, previously discussed in Section 2.2.2.) of ibuprofen with PEG/drug at a 1:1 ratio provided the greatest drug release, i.e. $98 (\pm 0.9) \%$ and $94.6 (\pm 0.8) \%$, respectively, after 30 minutes (Figure 5.1a). At the same PEG/drug ratio, the physically mixed and conventionally heated formulations released $51.3 (\pm 3.0) \%$ and $71.1 (\pm 0.9) \%$, respectively, after 30 minutes (Figure 5.1a).

5.2.1.2. Dissolution studies of ibuprofen (+) S

The release behaviour of ibuprofen (+) S (enantiomer of ibuprofen) from PEG based formulations is presented in Figure 5.2. The microwave formulation (MW) of PEG/IBU S at a 1:1 ratio demonstrated the greatest release, i.e. $90.5 (\pm 1.2) \%$ compared with the pure ibuprofen (+) S release, i.e. $46.7 (\pm 1.2) \%$ after 30 minutes (Figure 5.2a). Drug release from the physically mixed and conventionally heated formulations was slow and only $48.5 (\pm 0.6) \%$ (Figure 5.2a) and $67.6 (\pm 0.7) \%$ (Figure 5.2a), respectively, after 30 minutes.

For both IBU and IBU S, these results show an enhanced extent of dissolution after microwave processing compared with pure drugs. Along with this increase, the release profile for ibuprofen and ibuprofen (+) S formulated using microwave heating appeared to improve the dissolution of the drug to a greater extent than conventional heating and physical mixtures. However, there was no marked difference in the dissolution observed using various proportions of PEG/IBU or PEG/IBU S, indicating that the ibuprofen and ibuprofen (+) S release behaviour is independent of PEG fraction (Figures 5.1 and 5.2a, b & c).

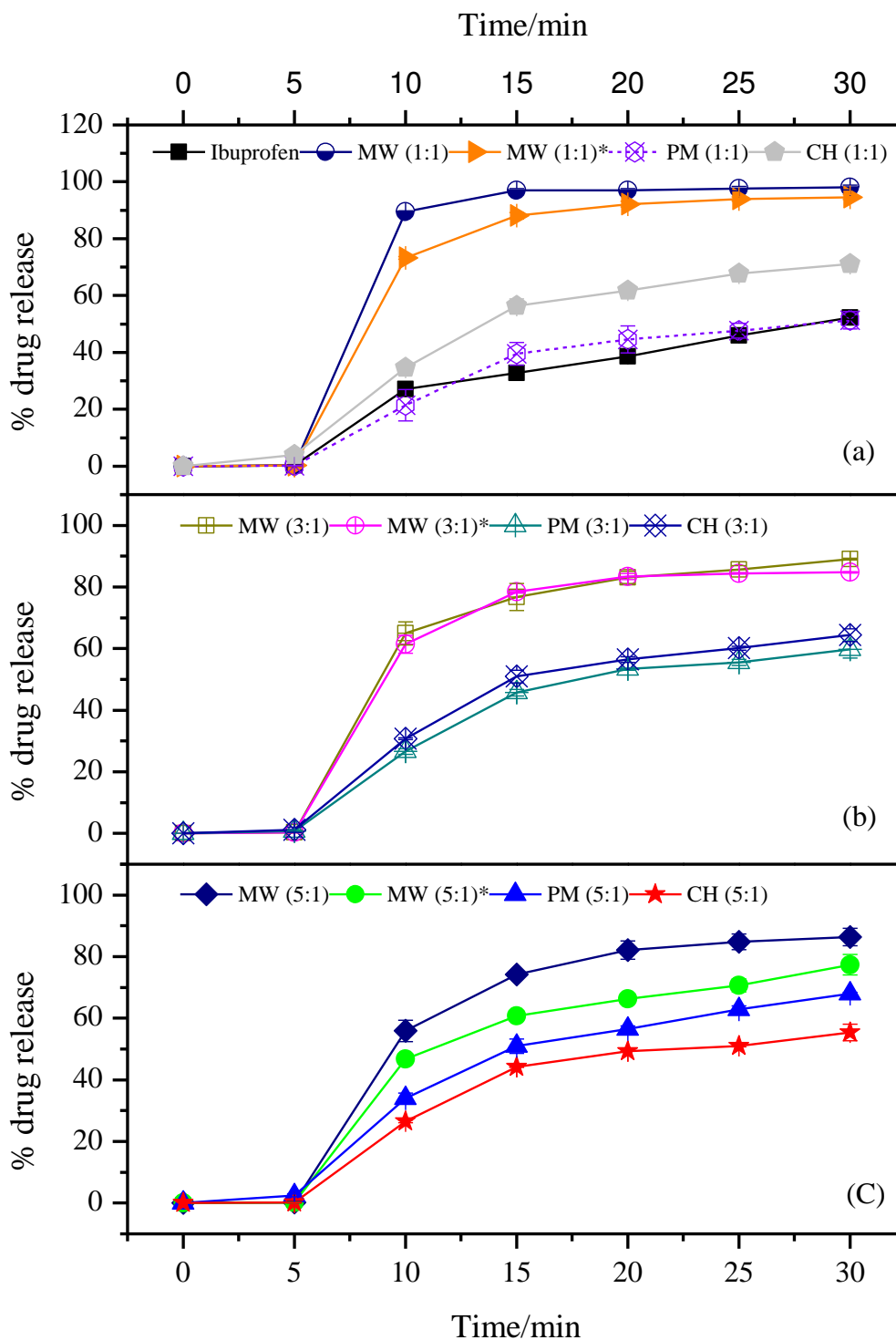


Figure 5.1: Ibuprofen release profiles for pure ibuprofen (IBU) along with PEG based formulations using microwave irradiation (MW* and MW), conventional heating methods (CH) and physical mixing (PM), all at PEG/drug ratios of 1:1 (a), 3:1 (b) and 5:1 (c). Each data point represents the mean of 3 results with SD error bars.

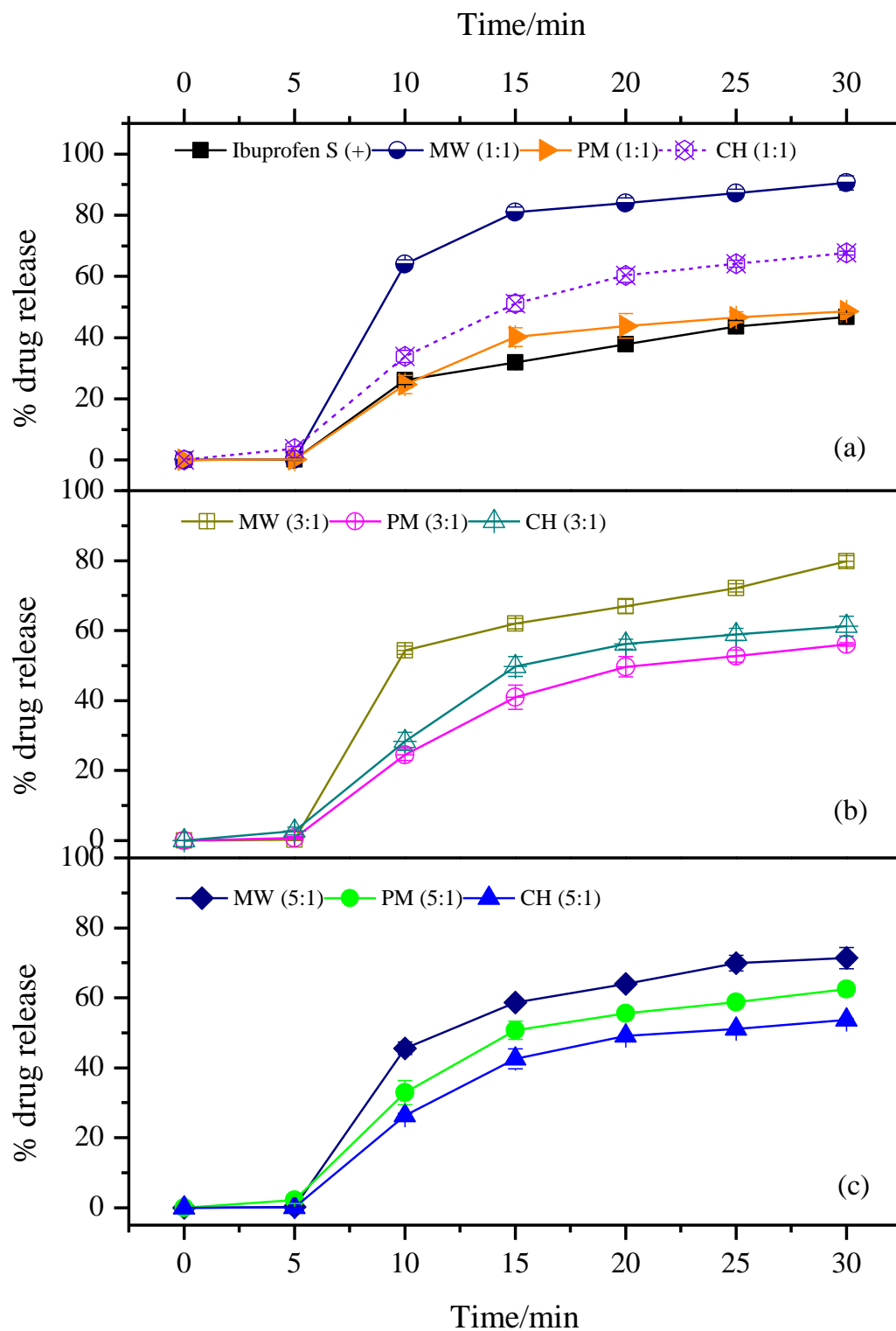


Figure 5.2: Ibuprofen (+) S release profiles for pure ibuprofen (+) S (IBU S) along with PEG based formulations using microwave irradiation (MW), conventional heating methods (CH) and physical mixing (PM), all at PEG/drug ratios of 1:1 (a), 3:1 (b) and 5:1 (c). Each data point represents the mean of 3 results with SD error bars.

5.2.1.3. Dissolution studies of fenofibrate

Figure 5.3 displays fenofibrate release from physically mixed, conventionally heated and microwave based formulations. The greatest drug releases, i.e. 91.0 (\pm 1.9) % and 86.7 (\pm 1.2) % were achieved with microwave formulation (MW* and MW, respectively) at PEG/drug ratios of 5:1 (Figure 5.3c). This was far greater than drug release from the physically mixed product, i.e. 52.6 (\pm 4.2) % and that conventionally heated, i.e. 46.6 (\pm 3.2) %, respectively, after 30 minutes (Figure 5.3c). The influence of polymer content on the extent of drug release was evident from the dissolution of PEG/drug ratio of 1:1 microwave formulations (MW* and MW), i.e. 45.0 (\pm 4.5) % and 25.7 (\pm 4.0) %, respectively (Figure 5.3a). There also appears to be little or no difference in the extent of dissolution of fenofibrate using conventional heating or standard physical mixing. However, the significantly enhanced dissolution for fenofibrate from formulations prepared using microwaves, can be explained on the basis of the uniformly distributed drug in the excipient under the influence of microwave energy. These results emphasise the importance of determining an optimum carrier to drug ratio and formulation approach on the effectiveness of the resultant product.

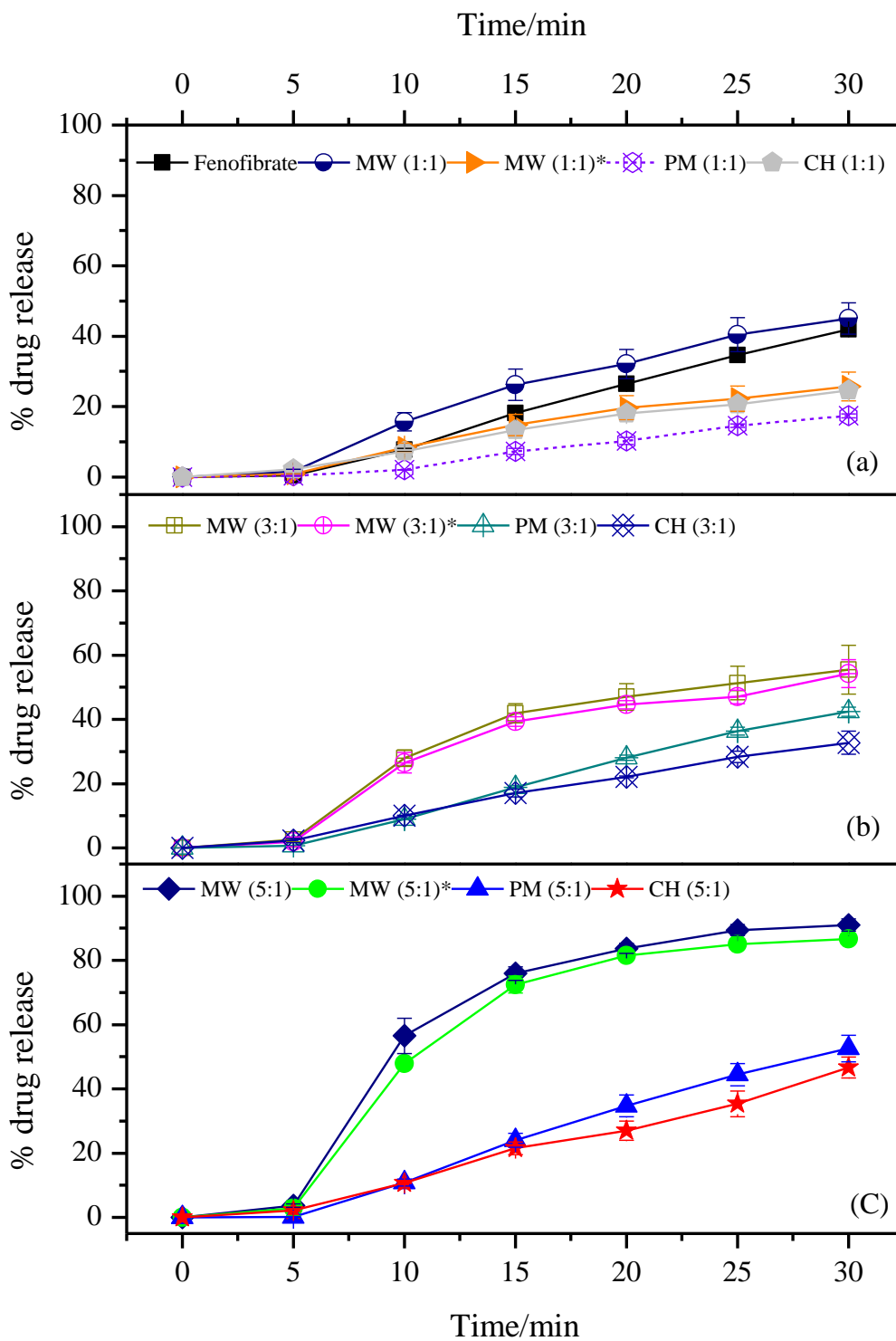


Figure 5.3: Fenofibrate release profiles for pure fenofibrate (FF) along with PEG based formulations using microwave irradiation (MW* and MW), conventional heating methods (CH) and physical mixing (PM), all at PEG/drug ratios of 1:1 (a), 3:1 (b) and 5:1 (c). Each data point represents the mean of 3 results with SD error bars.

5.2.1.4. Dissolution studies of phenylbutazone

The dissolution profile of phenylbutazone (PB) along with PEG based formulations is shown in Figure 5.4. Phenylbutazone alone provided the most limited release, i.e. only 44.6 (\pm 2.1) % after 30 minutes (Figure 5.4b). Percentage releases of 47.0 (\pm 0.7) % and 52.2 (\pm 1.6) % from the physically mixed and conventionally heated formulations, respectively, after 30 minutes, indicate their insignificant effect on the extent of dissolution of phenylbutazone (Figure 5.4b). However, the percentage drug release from PEG/PB ratio of 5:1 was 80.6 (\pm 2.8) % and 70.7 (\pm 3.3) % for microwave formulations (MW* and MW, respectively), after 30 minutes (Figure 5.4b). An increase in phenylbutazone concentration (i.e. 1:1 PEG/PB formulations) decreased the extent of dissolution to 54.1 (\pm 2.8) % and 36.5 (\pm 2.9) % for MW* and MW formulations, respectively, after 30 minutes (Figure 5.4a). These results suggest that an enhanced dissolution of hydrophobic drugs such as phenylbutazone, can be achieved using a higher carrier to drug content.

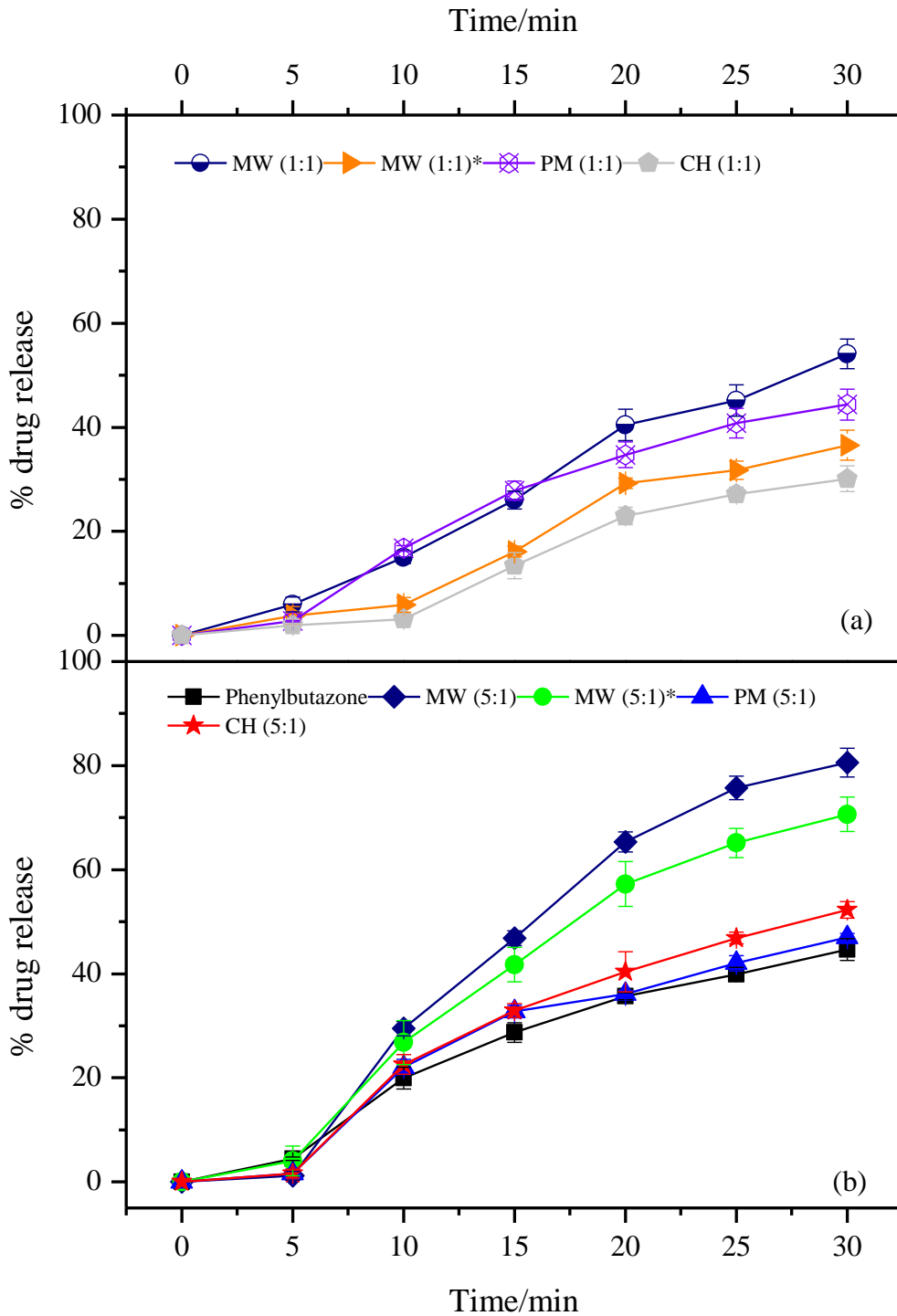


Figure 5.4: Phenylbutazone release profiles for pure phenylbutazone (PB) along with PEG based formulations using microwave irradiation (MW* and MW), conventional heating methods (CH) and physical mixing (PM), all at PEG/drug ratios of 1:1 (a) and 5:1 (b). Each data point represents the mean of 3 results with SD error bars.

5.2.1.5. Summary

In summary, the preparation of solid dispersions using microwave formulation modified the dissolution of all drugs under investigation. The dissolution results of microwave formulations revealed that drug released rapidly at a 1:1 PEG/drug ratio for ibuprofen and ibuprofen (+) S whereas a 5:1 PEG/drug ratio provided the greatest dissolution for fenofibrate and phenylbutazone, depicted in Figures 5.1 - 5.4. It is well established that materials such as PEG may increase the solubility of a range of drugs, particularly at high concentrations (Al-Angary et al., 1996, Lin and Cham, 1996). This could possibly be attributed to the wettability offered by the polymer and the conversion of crystalline drug into amorphous form. Possible mechanisms of increase in dissolution for solid dispersions have been proposed by Ford (1986), and include: reduction of particle size, a solubilisation property of the carrier, improved wettability and dispersibility of a drug in the solid dispersion and conversion of drug into an amorphous form.

In summary the extent of drug release was greatest from the microwave formulated products followed by the conventionally heated formulations and then physically mixed products for all four drugs under investigation as shown in Figures 5.1 - 5.4. The drug released rapidly from physical mixtures compared with drug alone for all drugs. This might be the result of an increased wetting ability of PEG for the hydrophobic crystalline drug surface. A similar result was obtained by Tantishaiyakul et al. (1999).

The modified dissolution profiles of ibuprofen, ibuprofen (+) S, fenofibrate and phenylbutazone formulated with PEG using both forms of microwave processing (either excipient melt or excipient/drug melt) confirmed its suitability. However, slight differences in

the dissolution profiles were observed between these two methods but overall the application of microwaves proved to be effective, rapid and devoid of detrimental effects.

5.2.2. Solid state characterisation

Solid state characterisation was undertaken to determine the melting transition, crystalline state and crystal morphology of pure and processed drug, using XRD, DSC and SEM.

5.2.2.1. X-ray diffraction (XRD)

Figure 5.5 displays the X-ray diffractogram for ibuprofen (IBU) and PEG based formulations, i.e. physically mixed, conventionally heated and microwave processed formulations at PEG/drug ratios of 1:1 and 5:1. The diffraction pattern of ibuprofen confirmed the drug to be crystalline as demonstrated by characteristic peaks observed at 2θ of 12.06° , 16.55° , 20.06° and 22.29° . PEG displayed two peaks with highest intensity at 2θ of 19.38° and 23.48° . The characteristic peaks for ibuprofen and PEG were clearly seen with decreased intensities at a PEG/IBU ratio of 1:1 for all formulations (Figure 5.5a). Further decreased intensities were observed for ibuprofen peaks in the physically mixed product along with the absence of certain peaks in the microwave and conventionally heated formulations at a PEG/drug ratio of 5:1 (Figure 5.5b). These observations indicate a transition from a crystalline to a semi-crystalline state, attributed to a reduction in particle size of ibuprofen. However, the PEG diffraction peaks retained their position indicating the dispersed state of ibuprofen in the molten polymer and confirmed the fine miscibility of PEG and ibuprofen.

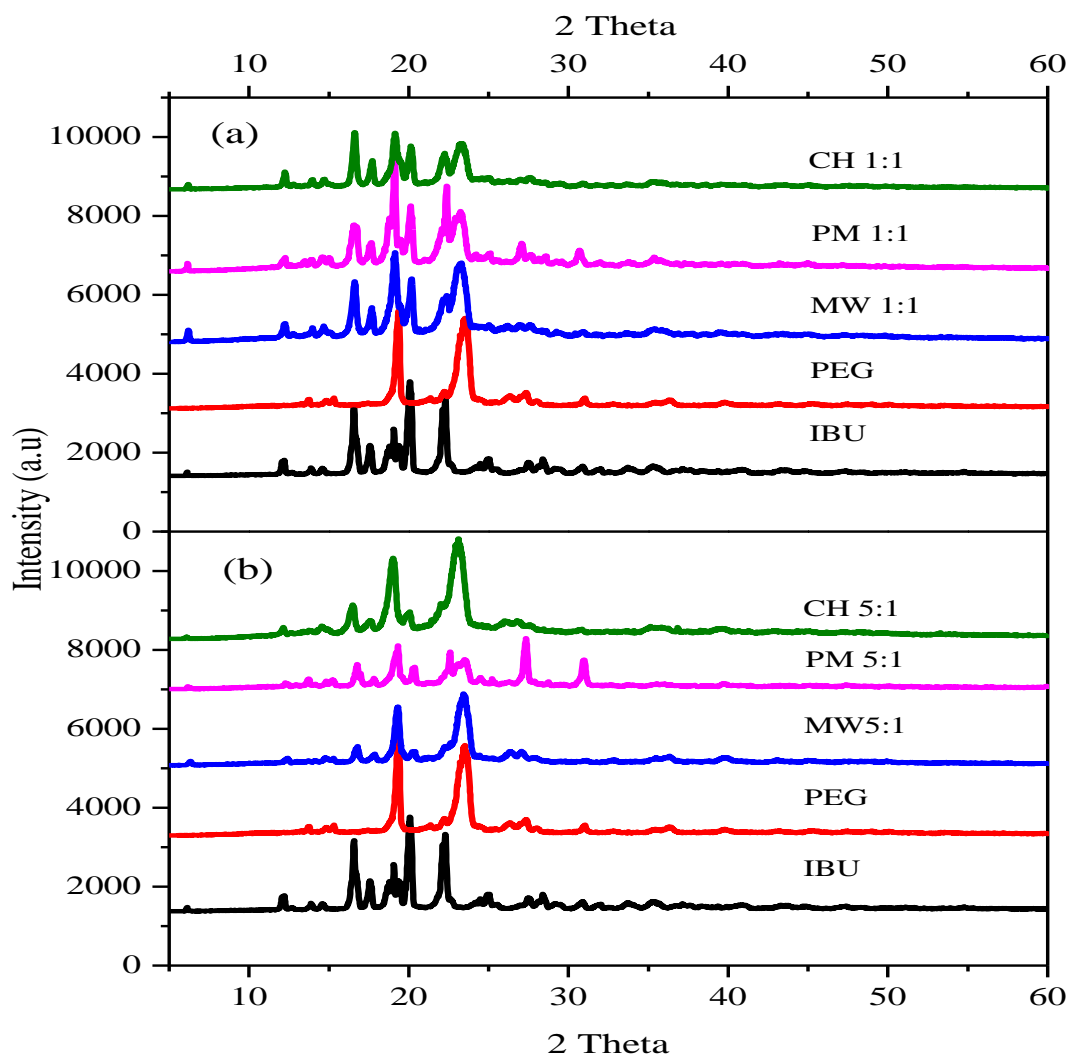


Figure 5.5: XRD patterns for ibuprofen (IBU) and physically mixed (PM), conventionally heated (CH) and dry microwave (MW) based formulations at PEG / drug ratios of 1:1 (a) and 5:1 (b).

The XRD patterns of microwave based formulations of PEG with ibuprofen (+) S, fenofibrate and phenylbutazone are presented in Figure 5.6 (a, b & c respectively). The characteristic diffraction peaks that correspond to ibuprofen (+) S were similar to ibuprofen as mentioned above (Figure 5.5a). The characteristic diffraction peaks observed at 11.99° , 14.3° , 16.2° , 16.8° and 22.4° , correspond to the powder diffraction pattern for pure fenofibrate (Figure 5.6b) while phenylbutazone is identified by characteristic peaks observed at 2θ of 7.28° ,

15.05°, 20.31° and 20.97° (Figure 5.6c). From XRD results, it is clear that all the principal diffraction peaks corresponding to PEG, ibuprofen (+) S, fenofibrate and phenylbutazone were present in the microwave based formulations, although with lower intensity. However, no new peaks were observed, suggesting the absence of a chemical interaction between drugs and the carrier. Upon increasing the concentration of PEG in the formulations, the diffraction intensity decreased to a level at which the main drug peaks became difficult to detect, i.e. at a ratio of 5:1 (Figure 5.6). These observations suggest the micro-crystalline state of drugs within PEG based formulations. The diffraction pattern for the physically mixed and conventionally heated formulations of ibuprofen (+) S, fenofibrate and phenylbutazone follow the same trend as observed for ibuprofen (See Appendix 5, 6 and 7, respectively).

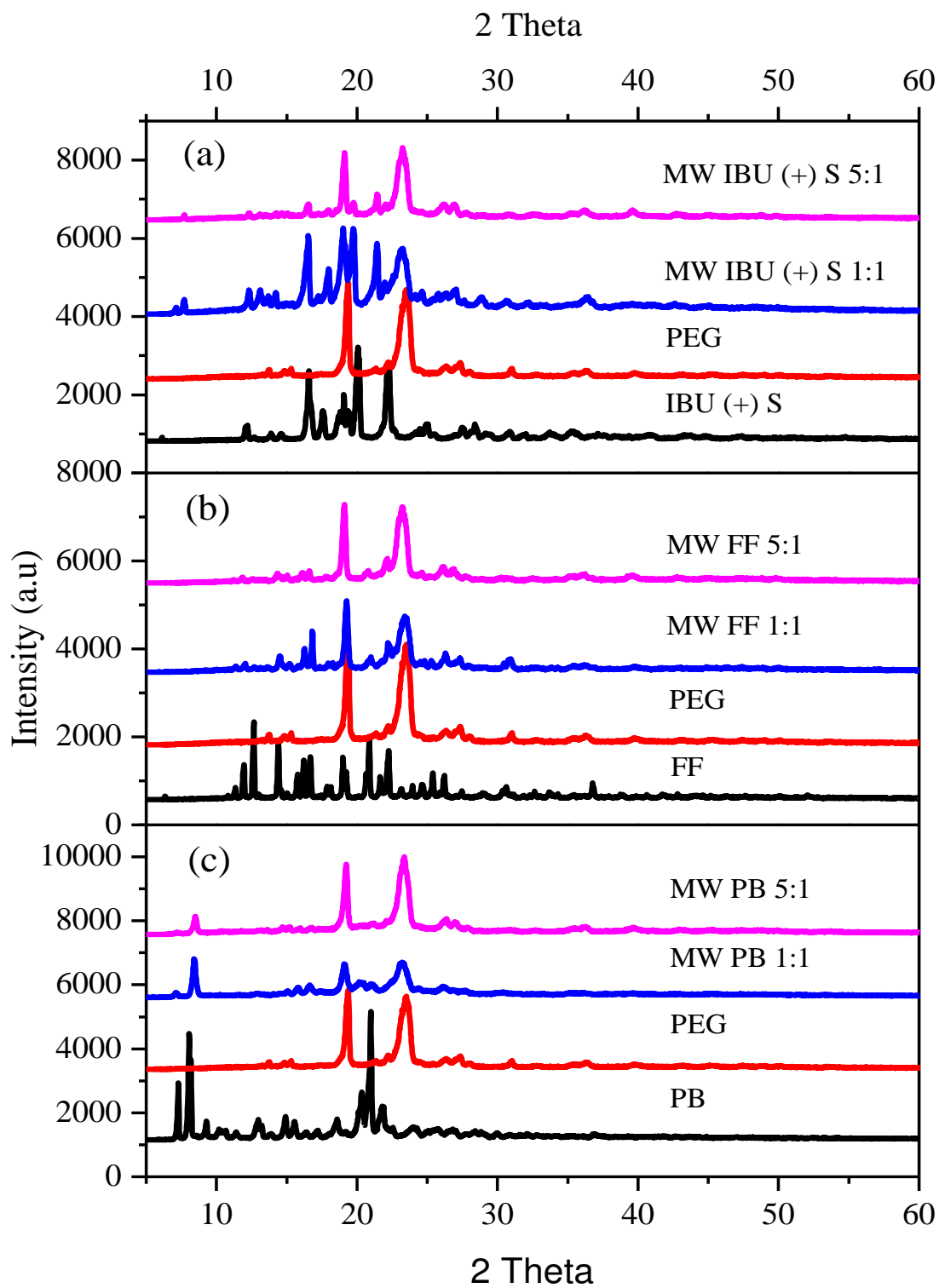


Figure 5.6: XRD patterns for PEG with microwave (MW) formulations of ibuprofen (+) S (a), fenofibrate (FF) (b) and phenylbutazone (PB) (c) at 5:1 and 1:1 ratios along with each pure drug.

5.2.2.2. Differential scanning calorimetry (DSC)

Figure 5.7 shows the DSC thermogram of PEG and ibuprofen, physically mixed and formulations prepared using microwave (MW* and MW) and conventional heating at PEG/drug ratios of 1:1 and 5:1. The DSC thermogram of ibuprofen and PEG showed an apparent endothermic peak at 78.9 °C and 65.3 °C with an enthalpy of fusion (ΔH_f) - 100.3 J/g and - 160.6 J/g, respectively (Figure 5.7). However, the physically mixed product along with the conventionally heated and microwave processed formulations demonstrated a single transition, corresponding to the melting of PEG (Figure 5.7). The absence of the drug melting peak has been attributed to the solubilisation of the drug within the molten carrier during the heating scan.

The DSC thermogram for PEG based formulations of ibuprofen (+) S at PEG/drug ratios of 1:1 and 5:1 is presented in Figure 5.8. The ibuprofen (+) S melting endothermic peak appeared at 55.1 °C with an enthalpy of fusion (ΔH_f) of - 77.8 J/g (Figure 5.8). The physical mixture of IBU (+) S indicated two transitions: the first corresponding to the melting of the drug and the second to the melting of PEG. DSC scans for the conventionally produced and microwave formulations revealed an interesting profile. Microwave based formulations at a PEG/drug ratio of 5:1 exhibited peaks corresponding to the melting of drug at 53.13 °C and the melting of PEG at 58.8 °C. However, formulations at a ratio of 1:1 displayed a single endothermic peak at 52.3 °C, corresponding to the melting of PEG with an enthalpy of fusion (ΔH_f) of - 176.2 J/g. These results indicate that a polymer/drug ratio of 1:1 is a prerequisite to form a eutectic system for formulations based on those drugs and polymers having a similar melting range. The DSC results for both IBU and IBU S at a PEG/drug ratio of 3:1 were similar to formulations developed at a PEG/drug ratio of 5:1.

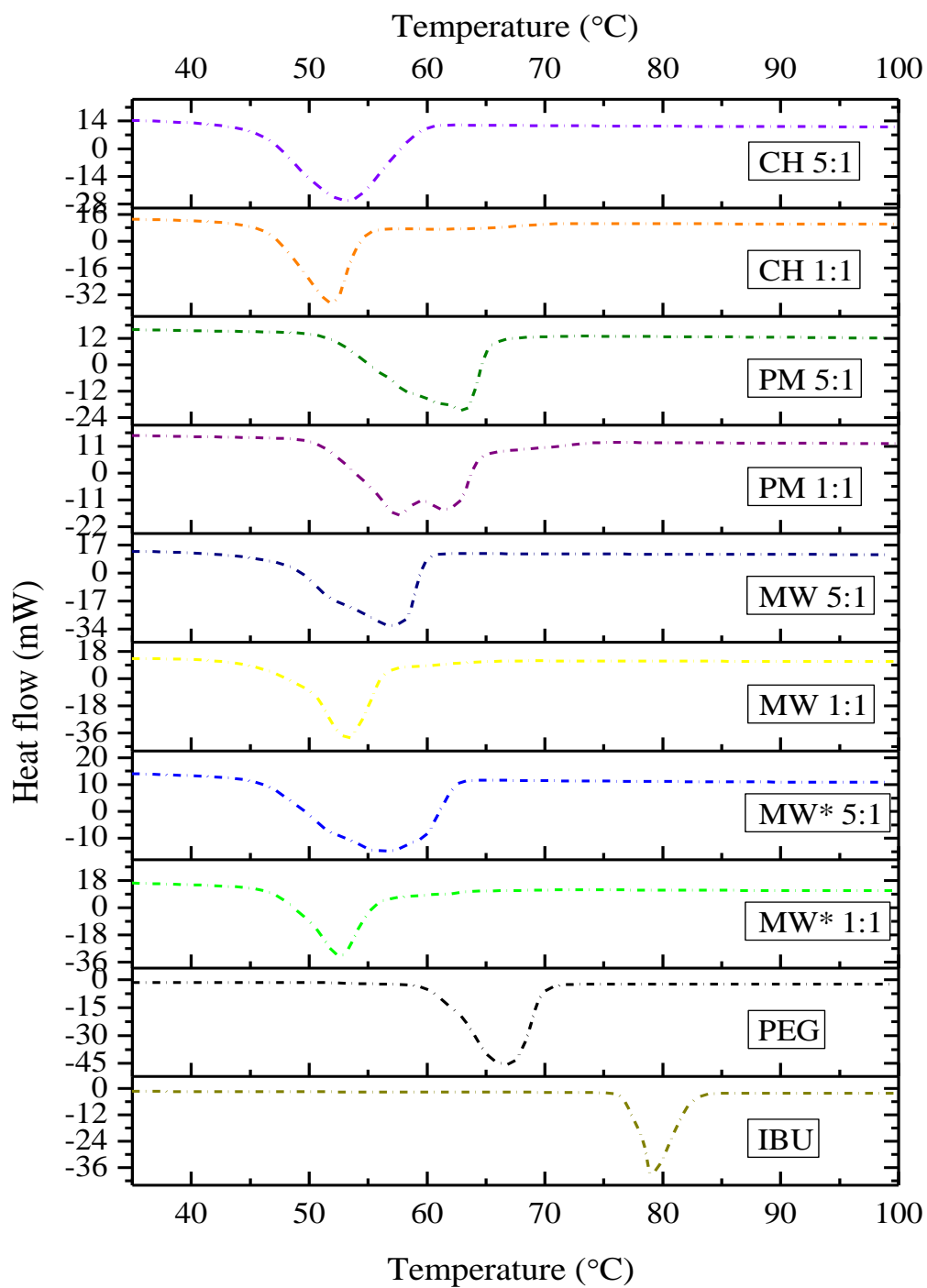


Figure 5.7: DSC profiles for ibuprofen (IBU) and PEG along with PEG based physical mixtures (PM), conventionally heated (CH) products and microwave (MW* and MW) formulations all at PEG / drug ratios of 1:1 and 5:1.

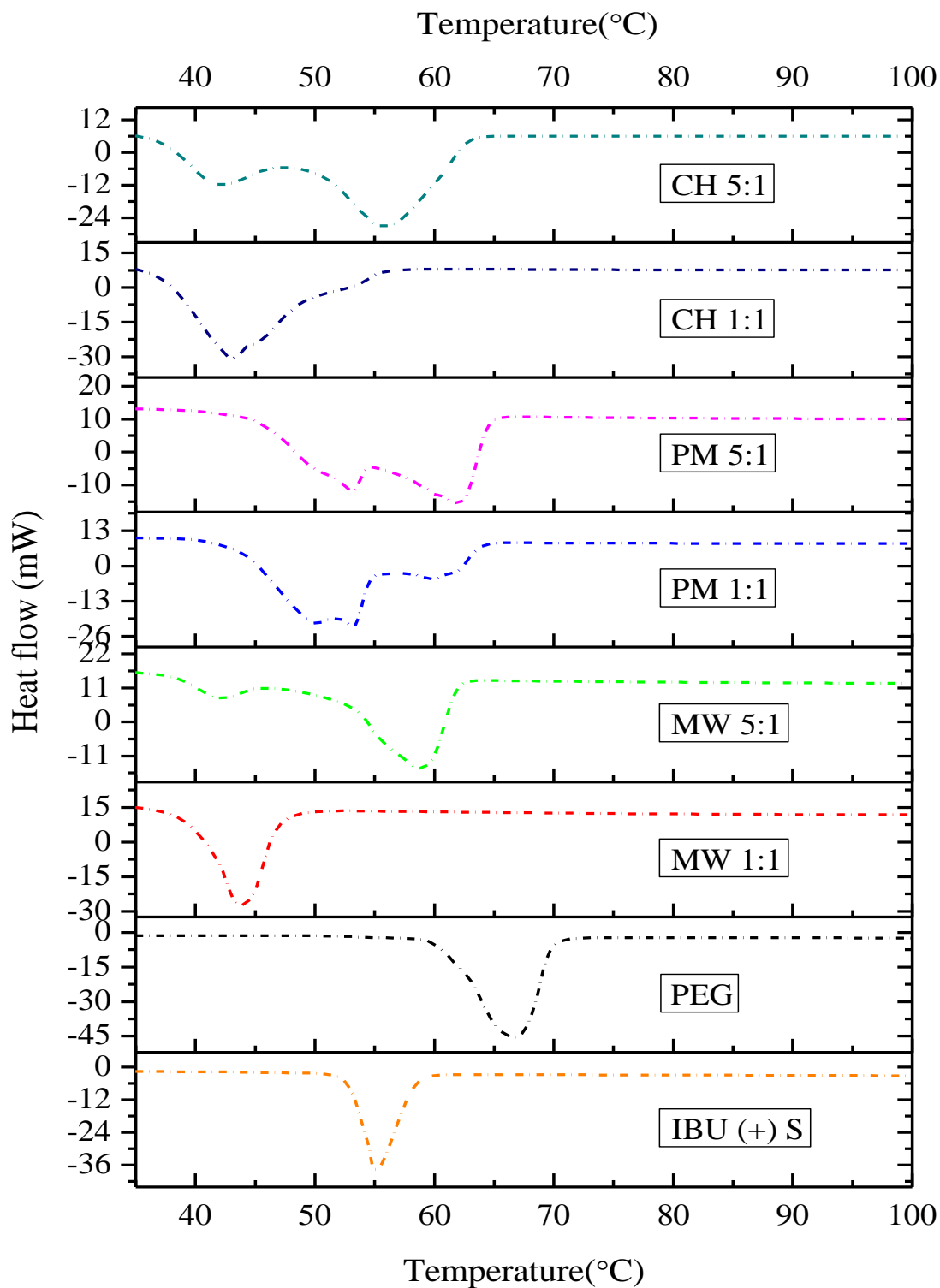


Figure 5.8: DSC profiles for ibuprofen (+) S (IBU S) and PEG along with PEG based physical mixtures (PM), conventionally heated (CH) products and microwave (MW) formulations all at PEG / drug ratios of 1:1 and 5:1.

Figure 5.9 exemplifies the thermogram of fenofibrate and phenylbutazone formulated together with PEG using microwave irradiation at a PEG/drug ratio of 1:1 and 5:1. The characteristic melting endothermic peak corresponded to those expected for fenofibrate and phenylbutazone, at 82.4 °C and 108.7 °C with an enthalpy of fusion (ΔH_f) of - 72.9 J/g and - 94.7 J/g, respectively. The melting peak broadened and shifted towards the lower temperature observed in microwave formulations for fenofibrate and phenylbutazone at a PEG/drug ratio of 1:1 (Figure 5.9). The DSC thermogram of fenofibrate and phenylbutazone demonstrated the appearance of two peaks, corresponding to the melting of PEG and respective drugs. The characteristic sharpness of drug melting peaks was lost, attributed to the dissolved crystals in the molten polymer (Figure 5.9). However, the endothermic peak corresponding to drug melting disappeared in the microwave formulations having a higher ratio of PEG to drug (as exemplified for fenofibrate and phenylbutazone at a ratio of 5:1). These results suggest that there is enhanced solubility of drugs in the molten polymer, forming a eutectic system. Further analysis of the thermograms also confirmed the slight shift in the melting temperature of the PEG endothermic peak but it still appeared indicating the inappreciable effect of fenofibrate and phenylbutazone on the crystalline state of PEG.

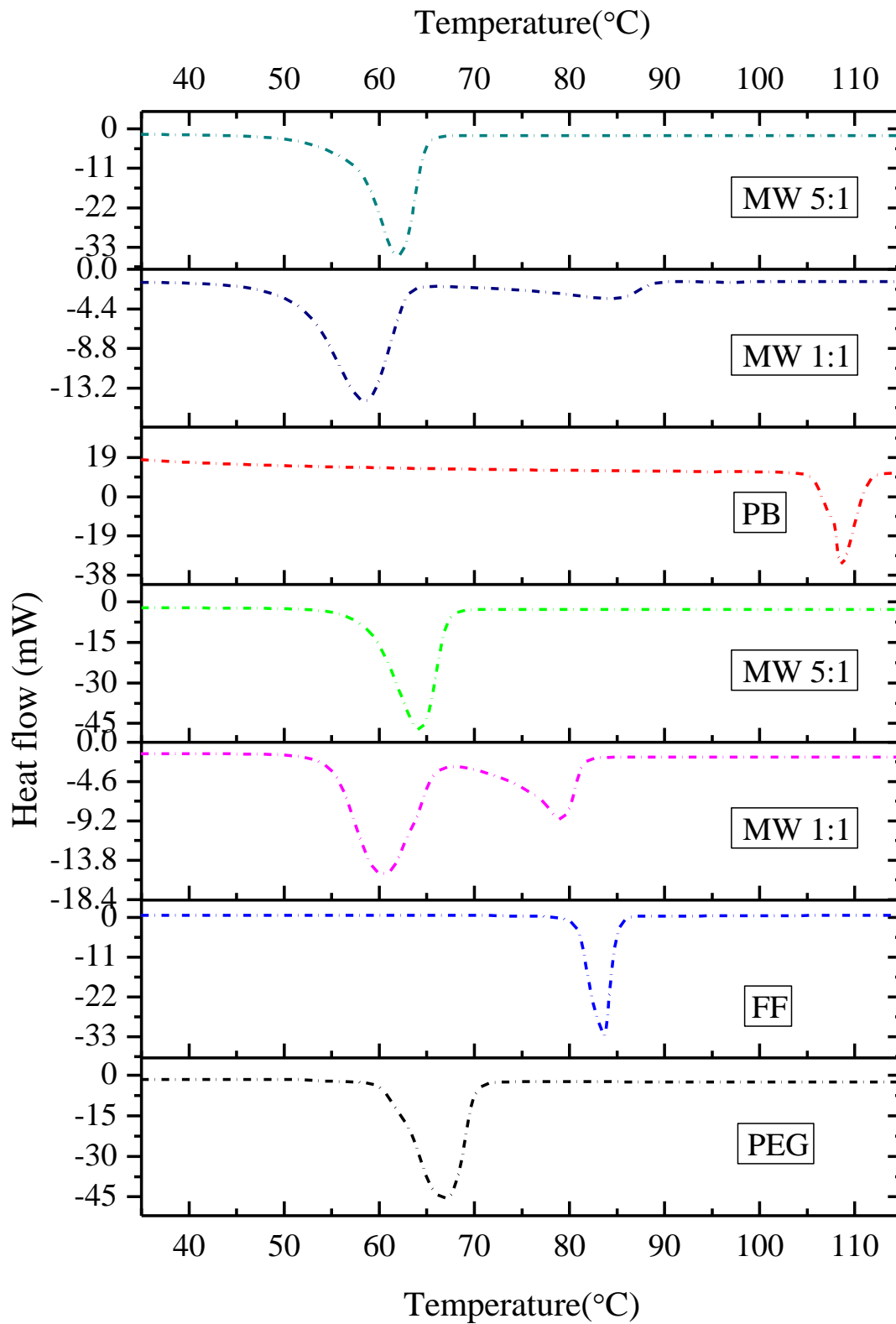


Figure 5.9: DSC profiles for PEG, fenofibrate (FF) and phenylbutazone (PB) along with PEG based microwave (MW) formulations all at PEG / drug ratios of 1:1 and 5:1.

5.2.2.3. Scanning electron microscopy (SEM)

Figure 5.10 illustrates six SEM images to exemplify the general findings of this work. PEG appeared to be large, irregular crystalline particles whereas pure ibuprofen has distinct crystalline structures. Figure 5.10 demonstrates the existence of ibuprofen in a crystalline state in the physical mix yet a non-uniform product from the conventionally heated ibuprofen in which it exists in a crystalline and dispersed state with PEG. The disappearance of the original crystalline form of drug and PEG confirmed a homogenised system was prepared using the microwave based technique (Figure 5.10).

Figure 5.11 depicts SEM images for ibuprofen (+) S (IBU S), fenofibrate (FF) and phenylbutazone (PB) along with their microwave processed (MW* and MW) formulations. In scanning electron micrographs, ibuprofen (+) S, fenofibrate and phenylbutazone appeared as smooth-surfaced rectangular crystalline structures, a distinct crystalline structure and the needle like crystalline structure, respectively (Figure 5.11.a, d and g respectively). SEM images suggest that surface properties of IBU S, FF and PB along with PEG were lost during the formation of solid dispersions from the microwave method, resulting in dispersion of the drug molecules within the carrier system. Moreover, these results also substantiate an enhancement in the dissolution profile of the drug candidates, possibly due to dispersion of the drug molecules and the absence of any crystalline particles.

In summary it appears that the microwave formulation process can modify the extent of crystallinity in the sample and create a product that contains a uniform dispersion of drug within the PEG matrix.

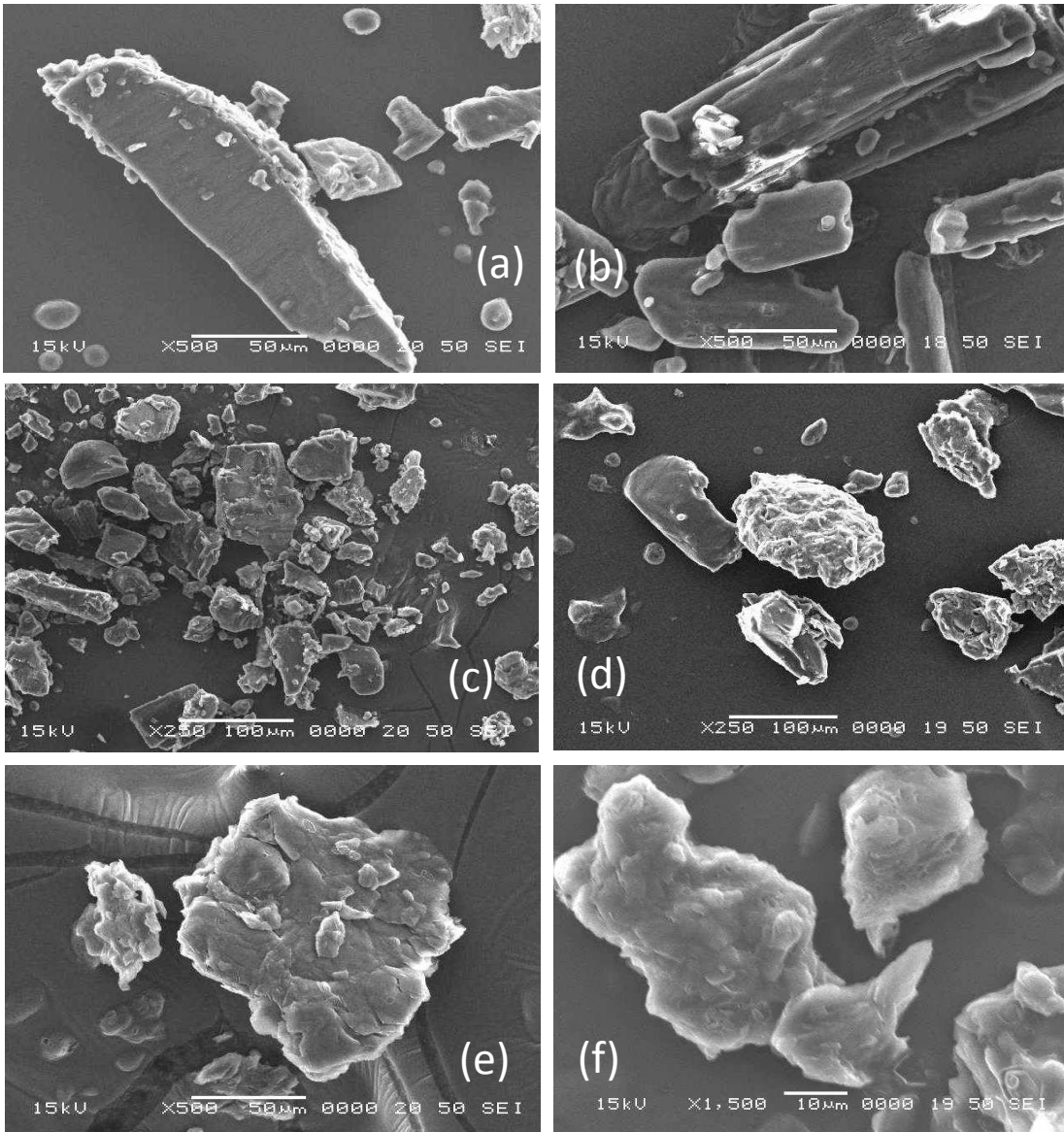


Figure 5.10: SEM images of (a) PEG, (b) pure ibuprofen (IBU), (c) a physical mix of PEG and IBU (5:1), (d) conventionally heated formulation of PEG and IBU (5:1), (e) microwave processed (MW*) product of PEG and IBU (5:1), (f) microwave processed (MW) product of PEG and IBU (5:1).

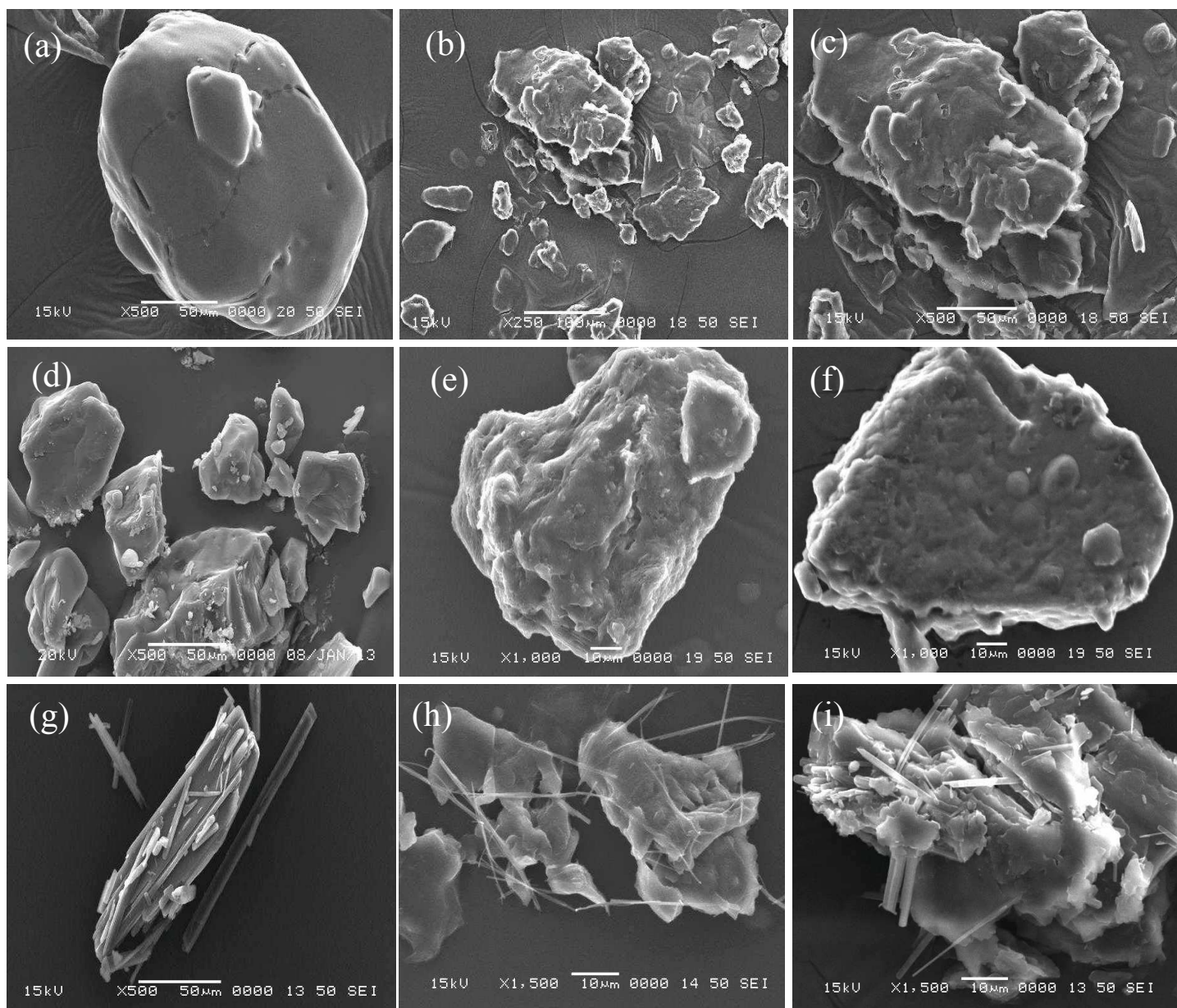


Figure 5.11: SEM images of (a) pure ibuprofen (+) S (IBU S), (b) microwave processed (MW*) formulation of PEG and IBU S (5:1), (c) microwave processed (MW) formulation of PEG and IBU S (5:1), (d) pure fenofibrate (FF), (e) microwave processed (MW*) formulation of PEG and FF, (f) microwave processed (MW) formulation of PEG and FF, (g) pure phenylbutazone (PB), (h) microwave processed (MW*) formulation of PEG and PB and (i) microwave processed (MW) formulation of PEG and PB.

5.2.2.4. Fourier transform infrared spectroscopy (FTIR)

The FTIR spectra of pure PEG, ibuprofen, ibuprofen (+) S, phenylbutazone and fenofibrate are shown in Figure 5.12. In the FTIR analysis, the spectrum of PEG showed the

C-H of OC₂H₅ and C-O stretching at 2871.62 and 1087.70 cm⁻¹, respectively. Ibuprofen and ibuprofen (+) S showed an intense, well defined infrared band at 1708.70 cm⁻¹ (carbonyl-stretching of isopropionic acid group) and another band at around 2952.62 cm⁻¹ (hydroxyl group of carboxylic acid). Analysis of spectra for phenylbutazone displayed absorption bands at wave numbers 2921.77, 1712.56 and 1292.13 cm⁻¹ corresponding to the presence of C-H, C=O and C- N aromatic amine, respectively. Specific fenofibrate peaks were observed at 2983, 1722, 1650 and 1598 cm⁻¹ corresponding to an O-H stretching vibration, C-H vibration, ester stretching vibration and lactone carbonyl functional group respectively. The signals appeared at 1243 cm⁻¹ were assigned to CH₂Cl stretching vibrations.

The FTIR spectrum of ibuprofen, ibuprofen (+) S, phenylbutazone and fenofibrate microwave formulations at a PEG/drug ratio of 1:1 are presented in Figure 5.13. IR analysis of the microwave formulations did not reveal any changes in the specific absorption bands for PEG as well as the respective drugs, suggesting a lack of interaction between the two moieties.

Moreover, the absorption bands of all drugs under investigation were weaker in formulations having a higher PEG content. Comparing FTIR spectra for all drugs and their solid dispersions, no extra signal was observed which confirmed the stable state of drug within the carrier after formulation. In summary, it is confirmed that formulation development using this novel microwave method does not detrimentally alter the physicochemical properties of the drugs under investigation.

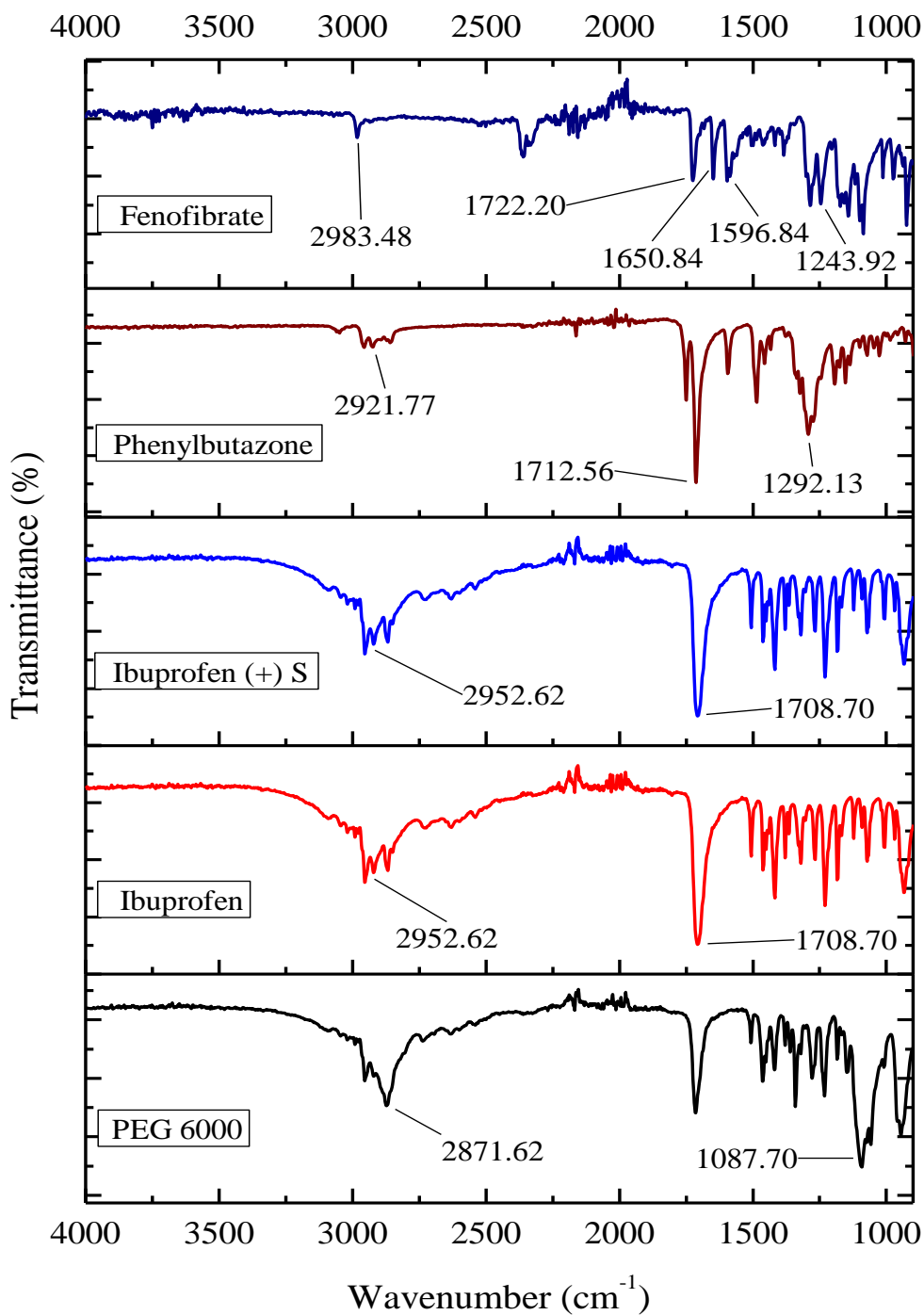


Figure 5.12: FTIR spectrum of pure PEG, ibuprofen (IBU), ibuprofen (+) S (IBU S), phenylbutazone (PB) and fenofibrate (FF).

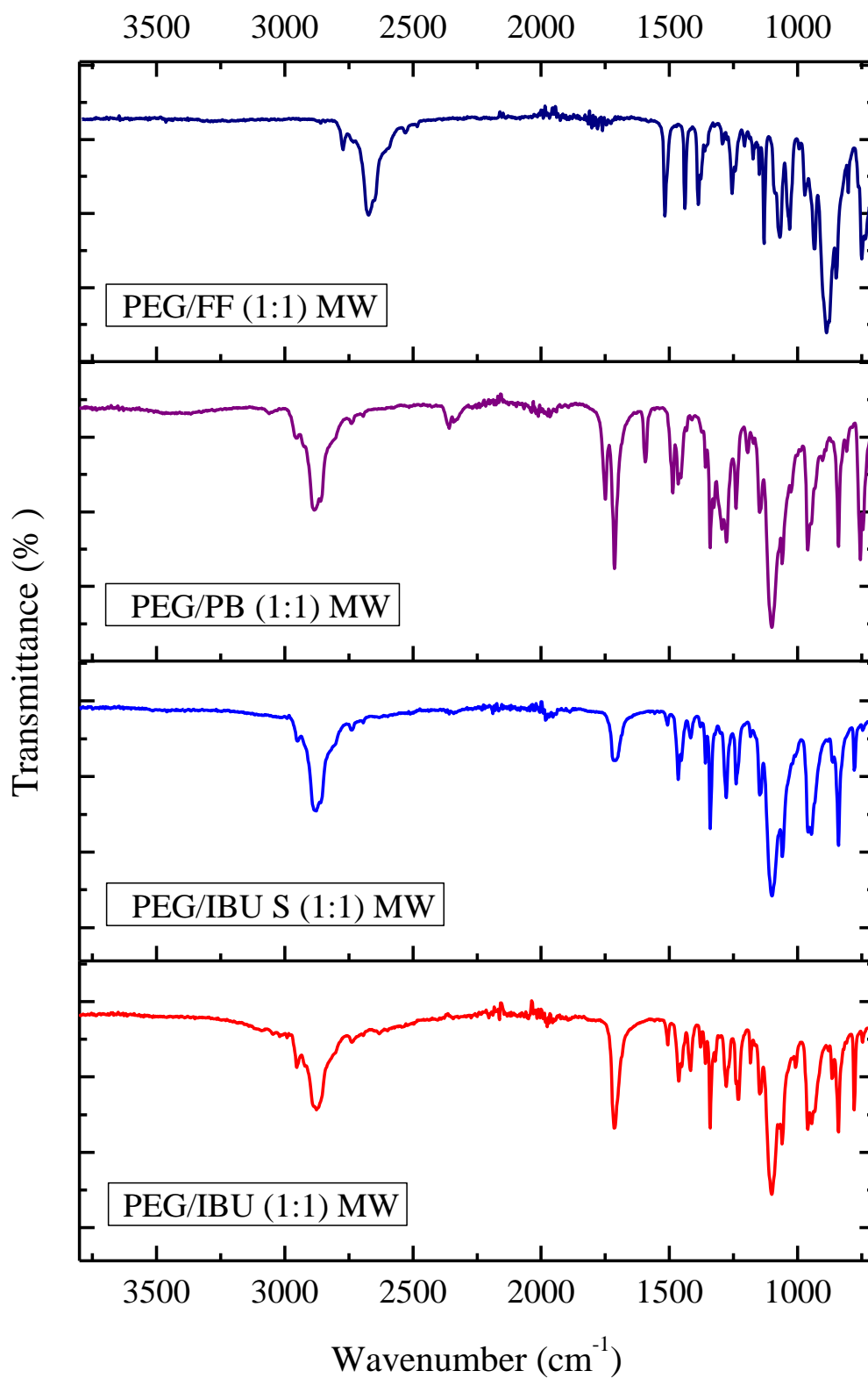


Figure 5.13: FTIR spectra of microwave formulations (MW) of ibuprofen (IBU), ibuprofen (+) S (IBU S), phenylbutazone (PB) and fenofibrate (FF) at PEG/drug ratio of 1:1.

5.3. Conclusions

In summary, it has been confirmed that it is possible to formulate PEG based solid dispersions with poorly soluble model drugs using microwave irradiation. Furthermore, microwave formulation successfully modified drug release compared with conventionally heated and the physically mixed products. PEG miscibility with drugs and transformation of the drug from crystalline to a semi-crystalline or amorphous state was confirmed by the DSC and XRD results. Surface morphology (using SEM) indicated the dispersed state of drugs with PEG after formulation. FTIR spectra revealed the chemical stability of drugs after microwave treatment. The dramatically enhanced release (yet maintained stability) for ibuprofen, ibuprofen (+) S, fenofibrate and phenylbutazone formulations with PEG confirmed the potential and effectiveness of microwave processing to develop a solid dispersion of compounds exhibiting poor aqueous solubility

References

- AL-ANGARY, A. A., AL-MESHAL, M. A., BAYOMI, M. A. & KHIDR, S. H. 1996. Evaluation of liposomal formulations containing the antimalarial agent, arteether. *International Journal of Pharmaceutics*, 128, 163-168.
- BISWAL, S., SAHOO, J., MURTHY, P. N., GIRADKAR, R. P. & AVARI, J. G. 2008. Enhancement of dissolution rate of gliclazide using solid dispersions with polyethylene glycol 6000. *AAPS PharmSciTech*, 9, 563-570.
- FORD, J. L., STEWART, A. F. & DUBOIS, J. L. 1986. The properties of solid dispersions of indomethacin or phenylbutazone in polyethylene glycol. *International Journal of Pharmaceutics*, 28, 11-22.
- GINÉS, J. M., ARIAS, M. J., MOYANO, J. R. & SÁNCHEZ-SOTO, P. J. 1996. Thermal investigation of crystallization of polyethylene glycols in solid dispersions containing oxazepam. *International Journal of Pharmaceutics*, 143, 247-253.
- HENNING, T. 2001. Polyethylene glycols (PEGs) and the pharmaceutical industry. *SÖFW-journal*, 127, 28-32.
- KNOP, K., HOOGENBOOM, R., FISCHER, D. & SCHUBERT, U. S. 2010. Poly (ethylene glycol) in drug delivery: pros and cons as well as potential alternatives. *Angewandte Chemie International Edition*, 49, 6288-6308.
- LIN, C. W. & CHAM, T. M. 1996. Effect of particle size on the available surface area of nifedipine from nifedipine-polyethylene glycol 6000 solid dispersions. *International Journal of Pharmaceutics*, 127, 261-272.
- MAURYA, D., BELGAMWAR, V. & TEKADE, A. 2010. Microwave induced solubility enhancement of poorly water soluble atorvastatin calcium. *Journal of Pharmacy and Pharmacology*, 62, 1599-1606.
- MONEGHINI, M., ZINGONE, G. & DE ZORDI, N. 2009. Influence of the microwave technology on the physical-chemical properties of solid dispersion with Nimesulide. *Powder Technology*, 195, 259-263.
- NACSA, A., AMBRUS, R., BERKESI, O., SZABÓ-RÉVÉSZ, P. & AIGNER, Z. 2008. Water-soluble loratadine inclusion complex: analytical control of the preparation by microwave irradiation. *Journal of pharmaceutical and biomedical analysis*, 48, 1020-1023.
- PAPADIMITRIOU, S. A., BIKIARIS, D. & AVGOUSTAKIS, K. 2008. Microwave-induced enhancement of the dissolution rate of poorly water-soluble tibolone from polyethylene glycol solid dispersions. *Journal of Applied Polymer Science*, 108, 1249-1258.
- RANPISE, N. S., KULKARNI, N. S., MAIR, P. D. & RANADE, A. N. 2010. Improvement of water solubility and in vitro dissolution rate of aceclofenac by complexation with β -cyclodextrin and hydroxypropyl- β -cyclodextrin. *Pharmaceutical development and technology*, 15, 64-70.
- SIX, K., VERRECK, G., PEETERS, J., BREWSTER, M. & VAN DEN MOOTER, G. 2004. Increased Physical Stability and Improved Dissolution Properties of Itraconazole, a Class II Drug, by Solid Dispersions that Combine Fast- and Slow-Dissolving Polymers. *Journal of Pharmaceutical Sciences*, 93, 124-131.
- TANTISHAIYAKUL, V., KAEWNOPPARAT, N. & INGKATAWORNWONG, S. 1999. Properties of solid dispersions of piroxicam in polyvinylpyrrolidone. *International Journal of Pharmaceutics*, 181, 143-151.
- WATERS, L. J., BEDFORD, S. & PARKES, G. M. B. 2011. Controlled microwave processing applied to the pharmaceutical formulation of ibuprofen. *AAPS PharmSciTech*, 12, 1038-1043.

- WATERS, L. J., HUSSAIN, T., PARKES, G., HANRAHAN, J. P. & TOBIN, J. M. 2013. Inclusion of fenofibrate in a series of mesoporous silicas using microwave irradiation. *European Journal of Pharmaceutics and Biopharmaceutics*, 85, 936-941.
- WEN, X., TAN, F., JING, Z. & LIU, Z. 2004. Preparation and study the 1:2 inclusion complex of carvedilol with β -cyclodextrin. *Journal of Pharmaceutical and Biomedical Analysis*, 34, 517-523.
- ZAWAR, L. & BARI, S. 2013. Microwave Induced Solid Dispersion as a Novel Technique for Enhancing Dissolution Rate of Repaglinide. *Advances in Pharmacology and Pharmacy*, 1, 95-101.
- ZHU, Q., HARRIS, M. T. & TAYLOR, L. S. 2012. Modification of crystallization behavior in drug/polyethylene glycol solid dispersions. *Molecular pharmaceutics*, 9, 546-553.

Chapter 6: Drug-excipient interactions: Saturation and micellisation studies of surfactant using isothermal titration calorimetry (ITC)

6.1. Introduction

The proportion of drug candidates with poor dissolution currently under development has grown significantly. To mitigate solubility challenges, “enabling formulations”, i.e. formulations which enhance bioavailability, have increasingly gained attention. Enabling formulation approaches include the use of co-solvents, complexing agents, surfactant systems, self-(micro- or nano-) emulsifying drug delivery systems, solid dispersions and mesoporous carriers (Buckley et al., 2013). Irrespective of the formulation approach employed, in vivo enhanced dissolution rarely matches that observed in in vitro dissolution testing of poorly soluble drugs. This can be a result of drug-excipient interactions through which drugs are loaded and released. Therefore, it is useful to investigate the underlying mechanism of enhancement and release of drugs from carrier systems (Buckley et al., 2013). To explore this, surfactants are ideal candidates as these are extensively used in formulation development along with being used as an integral part of many dissolution testing media, such as simulated fluids (gastric and intestinal).

Surfactants are amphiphilic molecules, that is, they contain a polar moiety and a hydrophobic moiety, typically an alkyl chain (Choudhary and Kishore, 2014). At high aqueous concentrations (i.e. above the critical micelle concentration, CMC), it becomes favourable for the surfactant molecules to associate via their hydrophobic chains to form micelles with a generally hydrophobic interior and a hydrophilic water-exposed exterior (Choudhary and Kishore, 2014, Otzen, 2011). Surfactants are generally classified by the charge of the hydrophobic head group i.e. anionic, cationic, nonionic, amphoteric or zwitterionic. Anionic

surfactants are most commonly used because of their low cost and commercial availability at high levels of purity. An anionic surfactant dissociates in aqueous solution to give a negatively charged surface and an inactive cation, commonly Na^+ or K^+ (Otzen, 2011).

Micelles exist in dynamic equilibrium with monomers in solution. The structure of a micelle is dependent on the concentration of monomers in the solution. At a concentration equal to, or above, the CMC, the monomers tend to aggregate to acquire a spherical shape. Generally, a certain number of monomers aggregate to form a micelle known as the aggregation number (AN). Different surfactants have different CMCs and ANs depending upon their physicochemical properties. Almost all surfactants will form spherical micelles at a concentration close to the CMC, however, ionic surfactants at higher concentrations will transform into elongated cylindrical, rod like, large lamellar and vesicular structures as shown in Figure 6.1. In the case of non-ionic surfactants, spherical micelles directly change into lamellar structures at higher concentrations (Moroi, 1992).

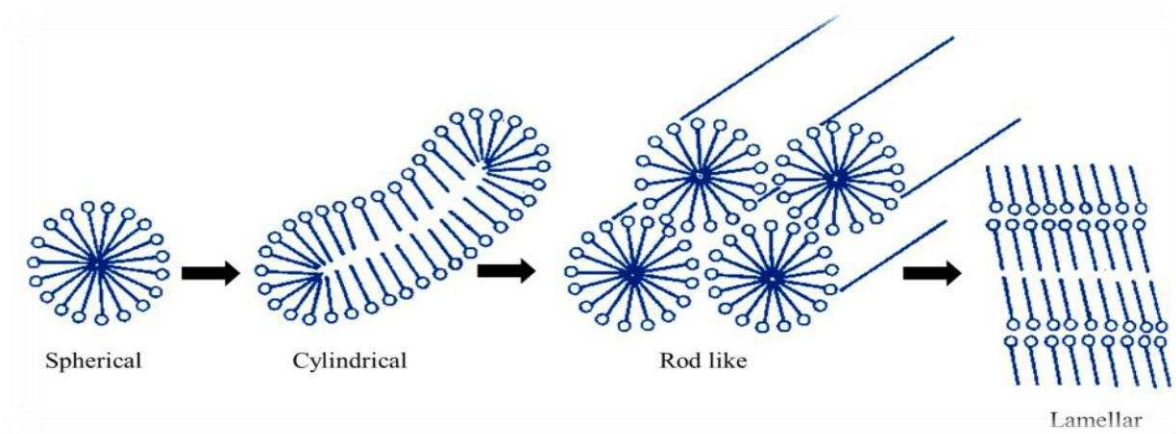


Figure 6.1: Transformation of micelles into different shapes on increasing surfactant (Moroi, 1992).

Commonly used techniques to measure the critical micelle concentration include, surface tension (Rosen et al., 1999), conductivity (Felippe et al., 2007), dynamic light scattering (Majhi and Blume, 2002) and fluorescence spectroscopy (Matsuoka and Moroi, 2002). In recent

years, more sophisticated techniques such as NMR (Pérez et al., 2007) and calorimetry (Paula et al., 1995) have been used to investigate the CMC of surfactants.

ITC was employed in this study to investigate drug-surfactant interactions, i.e. to determine the saturation of SDS by model drugs, namely, caffeine, diprophylline, etofylline, paracetamol and theophylline. This was undertaken along with the CMC determination of two surfactants, i.e. sodium dodecyl sulfate (SDS) and sodium deoxycholate (NaDC), both of which have reported values for their CMC and thermodynamic profiles (Paula et al., 1995). The chemical structure of NaDC is quite different from SDS which has a distinct hydrophilic head and hydrophobic tail (Garidel and Hildebrand, 2005). The convex side of the rigid steroid nucleus of NaDC has a hydrophobic surface and the concave side (making it a polar surface) consists of hydroxyl groups (Das et al., 2011) (Figure 6.2). The polarity of NaDC induces its amphiphilic character and molecules tend to self-assemble in aqueous media (Moroi, 1992). The micellisation of bile salts is a complex mechanism, therefore, various models for the micellar structure have been proposed over the last five decades. The widely accepted model is a stepwise formation of micelles, given by Small and Carey (1972). In this model, the primary micelles consist of two to nine monomers, held together by a hydrophobic interaction between the steroid nuclei. These primary micelles further aggregate to form large aggregates, held together by hydrogen bonding between the hydroxyl groups of the primary micelles.

Sodium deoxycholate is used in pharmaceutical formulations to solubilise poorly soluble molecules and is known to form micelles and mixed micelle systems such as with Tweens (Ćirin et al., 2012). The aggregation behaviour of NaDC has been reported with CMC values in the range 5.3 to 10.5 mM (Coello et al., 1996, Matsuoka and Moroi, 2002, Garidel et al., 2000, Hildebrand et al., 2004) with a clear temperature dependence. From a thermodynamic perspective, several values have been reported for the enthalpy of micellisation, for example,

from -0.5 kJ/mol at 298 K to -3.0 kJ/mol at 308 K (Bai et al., 2010). No such studies have been conducted prior to this work regarding the effect of additional compounds on the values obtained for these two particular micelles, with respect to their CMC values and thermodynamic profiles.

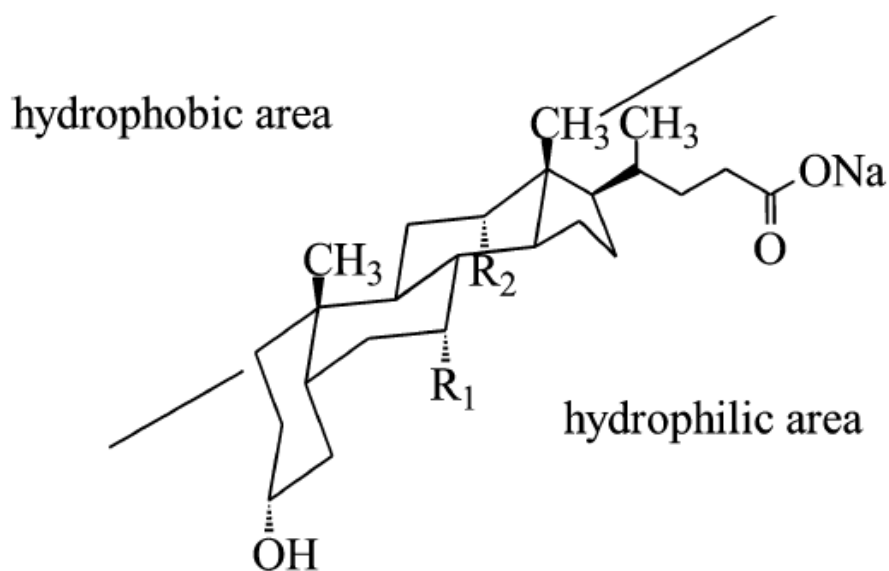


Figure 6.2: Chemical structure of NaDC, $R_1 = H$ and $R_2 = OH$ with hydrophobic and hydrophilic surfaces (Hildebrand et al., 2004).

Limited previous work has investigated isothermal titration calorimetric studies on the interaction between SDS and polyethylene glycols (PEGs) and the consequences on the micellar properties of such binding events. Unusual profiles have been attributed to the structural reorganisation of SDS/PEG aggregates with the effect observed at a critical PEG molecular weight observed through influences on the binding isotherms (Dai and Tam, 2006). This 'peculiar' behaviour includes endothermic and exothermic effects, including the binding of multiple micellar clusters on single polymeric chains (Bernazzani et al., 2004). Furthermore, increasing the polymeric concentrations can cause the polymer saturation concentration, C_2 , and CMC to increase although the concentration of those bound to polymer does not vary (Dai and Tam, 2001a).

In summary, little scientific data has been reported concerning the effects of the presence of both PEG and model drugs on the micellisation of either SDS or NaDC. This is of particular value if such systems are to be employed to help solubilise pharmaceutical compounds.

6.2. Results and discussion

6.2.1. Saturation limit of SDS

With an average aggregation number of 62 surfactant molecules per micelle of SDS (Mutelet et al., 2003), it was possible to calculate the concentration of drug required to saturate a micellar solution using ITC. This was witnessed as a sharp change in the measure of the power signal (cell feedback) upon reaching the saturation limit, as exemplified in Figure 6.3.

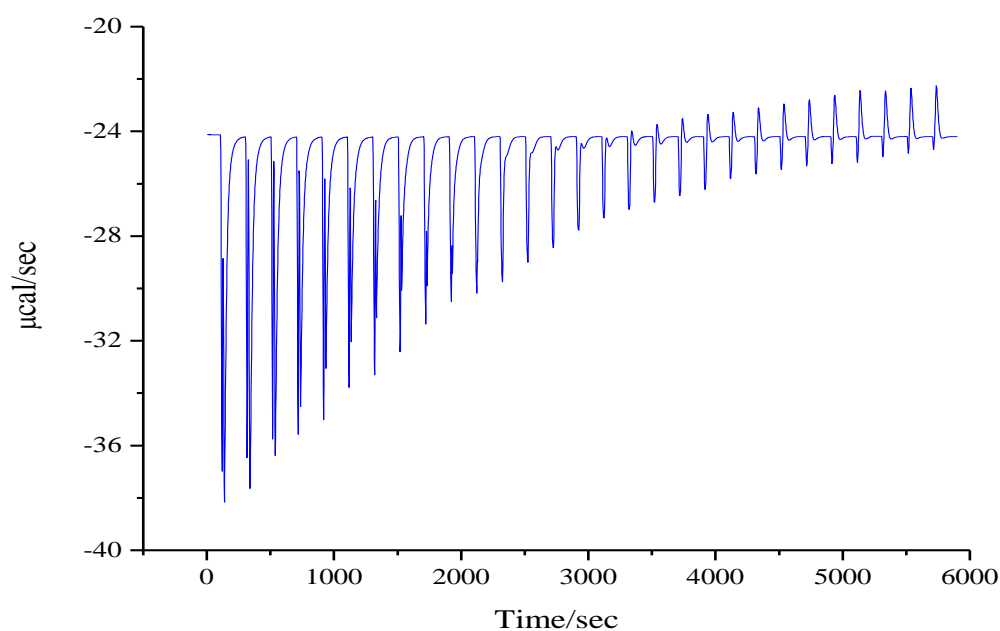


Figure 6.3: Raw ITC data for the saturation of 20 mM SDS micelles with 100 mM caffeine at $T = 298$ K.

A summary of thermodynamic data for the saturation of micelles with several model drugs can be seen in Table 6.1. Error limits represent standard deviation from the mean where $n = 3$. Five drugs were studied with the maximum number of molecules of drug per micelle, i.e. the occurrence of saturation, ranging from 17 molecules per micelle for theophylline at $T = 298$ K up to 63 molecules per micelle for caffeine at $T = 310$ K. At both temperatures, the five drugs followed the same general trend in the ratio of drug molecules to surfactant molecules with caffeine the greatest, followed by paracetamol, then diprophylline and etofylline equally favoured and theophylline with the lowest ratio of all. With respect to the changes in enthalpies of drug–micelle partitioning until the point at which saturation was attained, it is interesting to note that the values observed at $T = 298$ K ($\Delta H_{\text{saturation}}$) are significantly different from those at $T = 310$ K ($\Delta H_{\text{saturation}}$). Most notable is the dramatic shift in the change in enthalpy for paracetamol and theophylline ($\Delta\Delta H_{\text{saturation}}$) from $T = 298$ K to 310 K. As the change in enthalpy is closely linked to the driving force behind the partitioning process, it is significant that for paracetamol an exothermic partitioning phenomenon becomes

endothermic upon increasing the temperature. In addition to this, the enthalpy change associated with the partitioning and subsequent saturation of theophylline drops dramatically from $-68.3 \text{ kJ. mol}^{-1}$ to $-7.6 \text{ kJ. mol}^{-1}$ upon increasing the temperature to $T = 310 \text{ K}$. For all five drugs, the enthalpy change associated with the process is less exothermic at the higher temperature as partitioning into the micellar phase becomes less favourable.

Table 6.1: Molecular ratios and associated enthalpic values for the micellar saturation of SDS in the presence of five drugs at $T = 298 \text{ K}$ and 310 K

Temperature/ K	Drug	Molecules of drug per micelle	Drug: surfactant ratio	ΔH saturation/ (KJ.mol ⁻¹ of drug)
298	Caffeine	58 ± 2	0.93 : 1	-21.5 ± 0.9
	Diprophylline	42 ± 3	0.68 : 1	-26.0 ± 1.2
	Etofylline	42 ± 4	0.68 : 1	-15.6 ± 0.7
	Paracetamol	53 ± 3	0.85 : 1	-21.9 ± 0.5
	Theophylline	17 ± 1	0.27 : 1	-68.3 ± 2.4
310	Caffeine	63 ± 1	1.01 : 1	-2.6 ± 0.3
	Diprophylline	46 ± 2	0.73 : 1	-2.6 ± 0.6
	Etofylline	46 ± 3	0.73 : 1	-2.8 ± 0.1
	Paracetamol	55 ± 4	0.89 : 1	18.6 ± 1.4
	Theophylline	18 ± 2	0.28 : 1	-7.6 ± 0.8

With respect to variations in the behaviour amongst the five compounds, two can be considered to behave in a very similar manner, namely diprophylline and etofylline. This is because both compounds are substituted imidazole based structures with similar negative partition coefficient (LogP) values at the pH investigated (-1.2 and -0.9, respectively) and comparatively high aqueous solubilities. This results in similar affinities for migration into the micellar phase. Caffeine, also a substituted imidazole based structure, displays a similar energetic profile to diprophylline and etofylline although the concentration required to saturate the micelles is higher which can be explained by the greater lipophilicity, as reflected in the greater LogP value (-0.6). Paracetamol is structurally dissimilar to the other compounds and has an even greater LogP value at the pH under investigation (0.5), yet surprisingly, this shows a reduced ability to be incorporated in each micelle. Theophylline is an unsubstituted imidazole based structure and the least soluble of all the drugs with a calculated LogP of -0.2. At present, the mechanism of interaction between theophylline and SDS is not fully understood. However, ion pairing of the drug with surfactant would offer an alternative mechanism for incorporation which may explain this anomaly.

In summary, while the number of drug molecules per micelle is largely unchanged from 298 to 310 K for each drug, the change in the enthalpy of saturation is less favourable at the higher temperature in all cases. In particular, for paracetamol, the shift to a positive enthalpy change indicates the process must be entropically driven for the overall reaction to be a favourable one.

6.2.2. Micellisation protocol for surfactants using ITC

Each micellisation experiment was performed whereby the sample cell was filled with deionised water and the titration syringe filled with a concentrated micellar solution, i.e. (C_{sy}

> CMC), as illustrated in Figure 6.4. Each experiment involved injecting a series of injections of the micellar solution in small aliquots into the solution in the sample cell, each injection induces a heat flow as a function of time (Gregoriadis, 2006).

The first few injections represent dilution of the micellar solution in the cell as shown in Figure 6.4 (a) since the concentration of surfactant in the cell (C_{cell}) is less than the surfactant CMC. With further addition of surfactant solution, the monomer concentration in the sample cell increases to a concentration ($C_{\text{cell}} = \text{CMC}$), where micelles start developing (Figure 6.4.b). After the CMC, the surfactant concentration in micellar form increases to a stage ($C_{\text{cell}} > \text{CMC}$) where the heat of each injection represents simply the increase in quantity of micelles (Figure 6.4.c) (Garti, 2000).

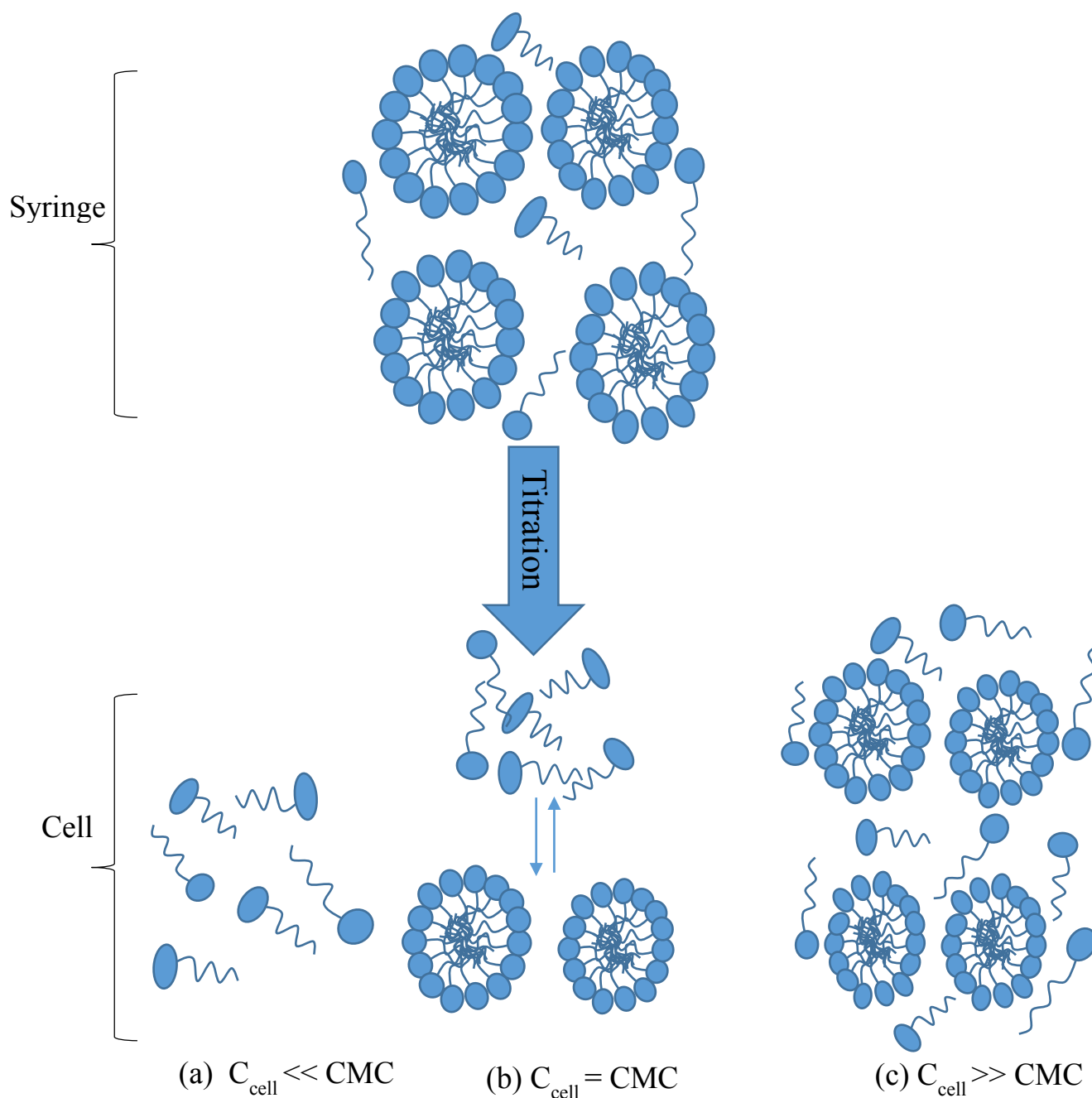


Figure 6.4: Schematic representation of a typical demicellisation experiment (Gregoriadis, 2006).

The heat of reaction was obtained by integration of each heat flow peak and plotted as a function of concentration from which the CMC and ΔH_{mic} were obtained. The standard free energy of micelle formation per mole of monomer (ΔG_{mic}) can be calculated using Equation 6.1 where m/n is a fraction of the charge of the surfactant ions, also known as the counter ion

binding constant and X_{cmc} the critical micelle concentration expressed in mole fraction (Volpe, 1995; Laidler, 1995).

$$\Delta G_{mic} = RT (1 + m/n) \ln X_{CMC} \quad (\text{Eq. 6.1})$$

From this, the change in entropy upon micellisation (ΔS_{mic}) can be calculated for any temperature under investigation using Equation 6.2.

$$\Delta G_{mic} = \Delta H_{mic} - T\Delta S_{mic} \quad (\text{Eq. 6.2})$$

Thus, a complete thermodynamic profile of the micellisation system can be determined using ITC.

6.2.3. Sodium dodecyl sulfate (SDS) micellisation in the presence of model drugs and PEG

The CMC of SDS was measured using ITC in the sequential presence of the same five model drugs at a concentration corresponding to that used in the saturation determination experiments. ITC experiments were carried out by titrating a concentrated solution of SDS in a micellar state into the sample cell containing deionised water and/or model drug in solution. The raw heat signals were recorded in $\mu\text{cal}/\text{sec}$. A clear end point corresponding to the CMC of SDS was calculated by plotting the differential of heat versus the concentration of surfactant solution in the sample cell after each injection, as exemplified in Figure 6.5. The endothermic process of initial demicellisation changed to an exothermic process above the CMC as exemplified in Figure 6.6. The enthalpy of micellisation was obtained by integrating the area of each raw ITC signal up to the point of micelle formation and normalised by the molar concentration of SDS added.

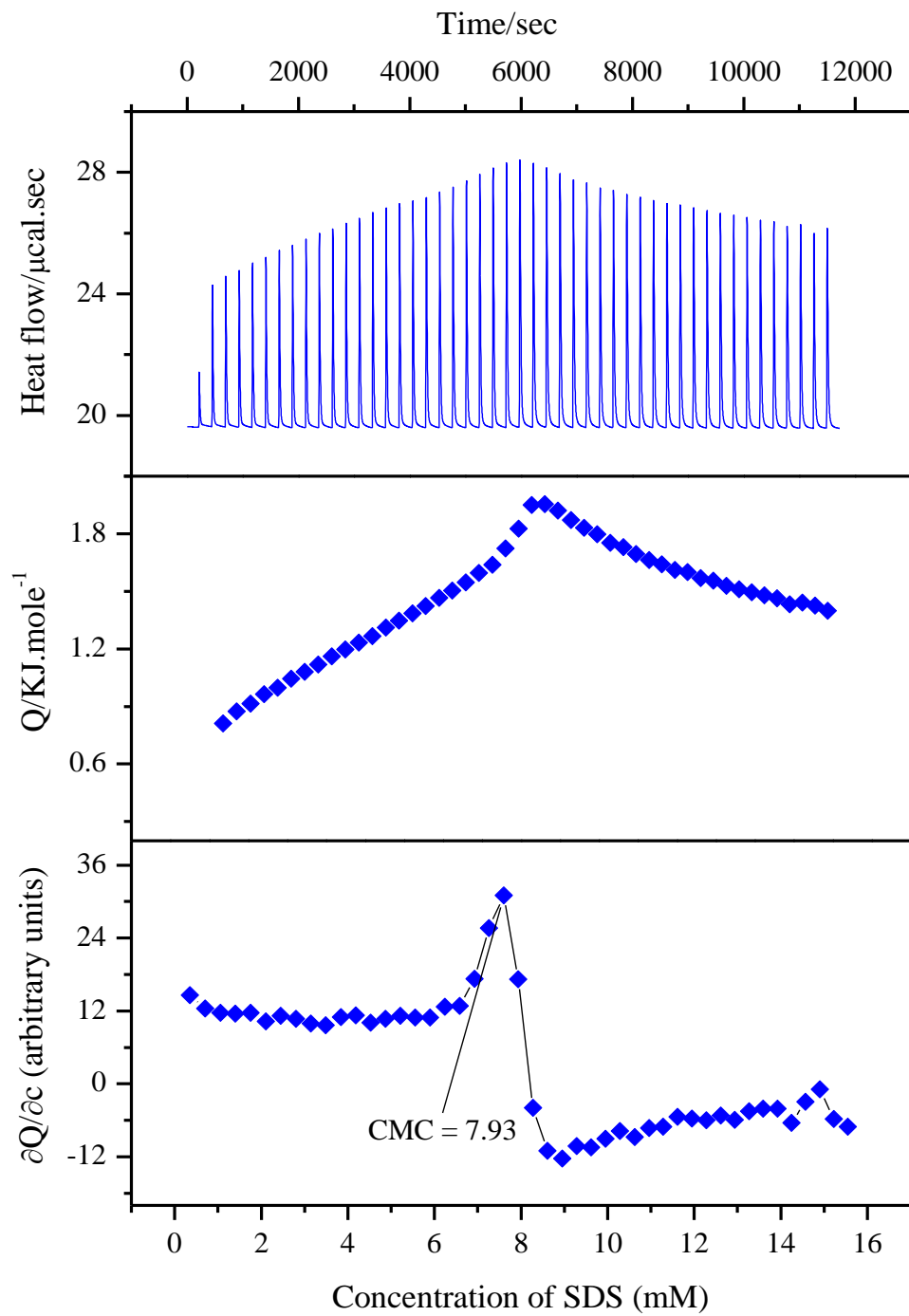


Figure 6.5: Raw ITC data and subsequent data analysis to determine the CMC of SDS in aqueous solution at $T = 298 \text{ K}$.

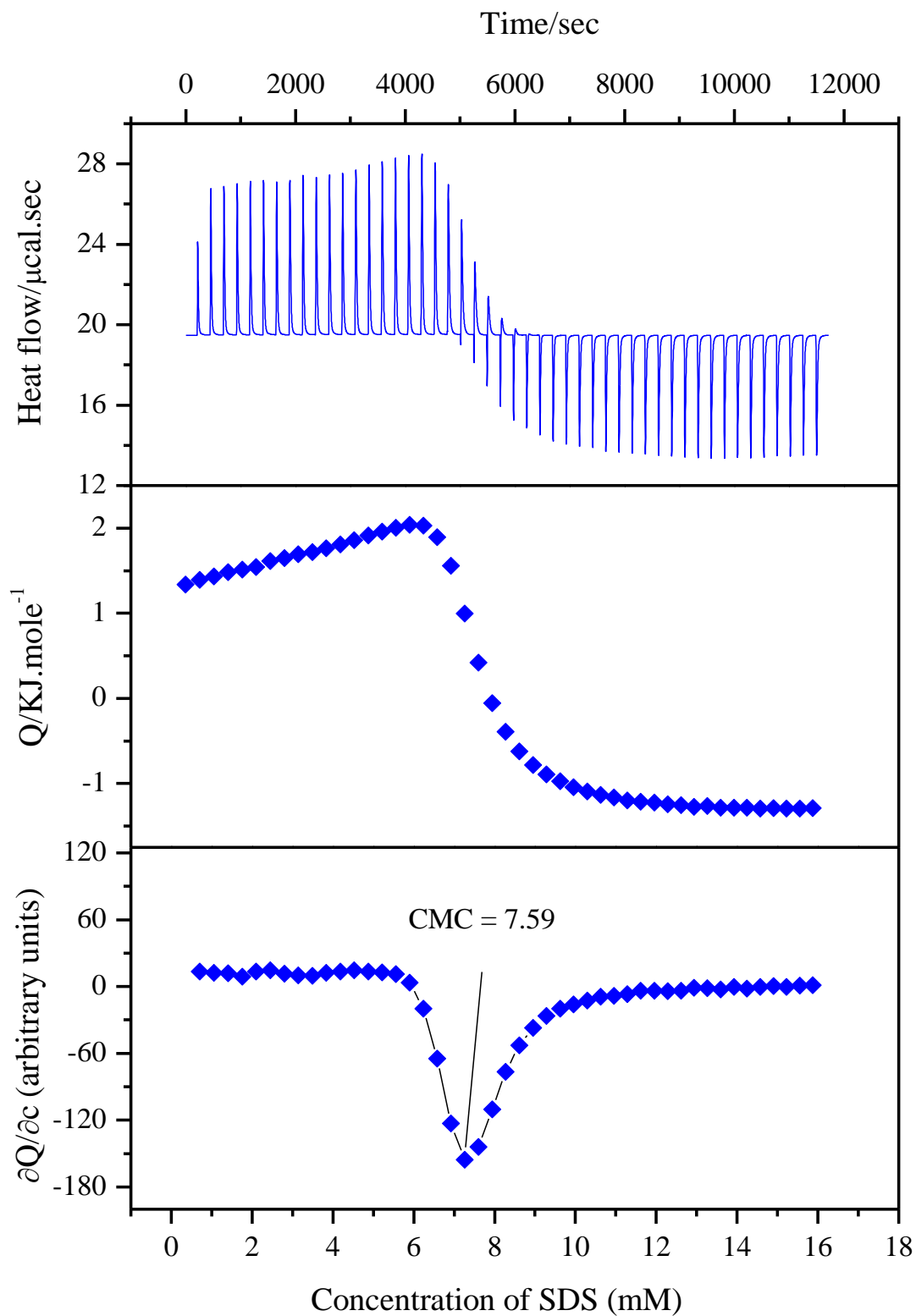


Figure 6.6: Raw ITC data and subsequent data analysis to determine the CMC of SDS in the presence of 60 mM Paracetamol at $T = 298 \text{ K}$.

Using ITC, it was possible to determine the CMC, and corresponding change in enthalpy, of SDS in the presence of five drugs as summarised in Table 6.2. Values presented in Table 6.2 for the CMC and change in enthalpy are quoted as the mean where the error limits represent standard deviation from the mean and $n = 3$.

Table 6.2: Critical micellar concentrations and thermodynamic values associated with the micellisation of SDS in the presence of five model compounds at 298, 304 and 310 K

Temp. / (K)		CMC/mM	ΔH°_{mic} / (KJ.mol ⁻¹)	ΔG°_{mic} / (KJ.mol ⁻¹)	$T\Delta S^{\circ}_{mic}$ / (KJ.mol ⁻¹)
298.2	water	7.9 (\pm 0.34)	-20.4 (\pm 1.30)	-38.0 (\pm 0.34)	17.6 (\pm 0.2)
	caffeine	7.9 (\pm 0.02)	-29.7 (\pm 1.80)	-38.0 (\pm 0.02)	8.3 (\pm 0.1)
	diprophylline	8.3 (\pm 0.01)	-12.1 (\pm 0.60)	-37.8 (\pm 0.01)	25.7 (\pm 0.4)
	etofylline	8.3 (\pm 0.02)	-11.9 (\pm 0.80)	-37.8 (\pm 0.02)	25.9 (\pm 0.1)
	paracetamol	7.6 (\pm 0.01)	-40.9 (\pm 0.50)	-42.2 (\pm 0.04)	1.3 (\pm 0.2)
	theophylline	7.9 (\pm 0.01)	-7.8 (\pm 0.20)	-38.0 (\pm 0.01)	30.2 (\pm 0.4)
304.2	water	8.3 (\pm 0.001)	-10.1 (\pm 0.01)	-38.6 (\pm 0.001)	28.5 (\pm 0.3)
	caffeine	7.3 (\pm 0.001)	-10.5 (\pm 0.24)	-39.1 (\pm 0.001)	28.6 (\pm 0.2)
	diprophylline	8.4 (\pm 0.24)	-11.1 (\pm 1.54)	-38.5 (\pm 0.24)	27.5 (\pm 0.3)
	etofylline	8.4 (\pm 0.24)	-10.3 (\pm 0.40)	-38.5 (\pm 0.24)	28.2 (\pm 0.2)
	paracetamol	6.9 (\pm 0.001)	-10.6 (\pm 0.30)	-39.3 (\pm 0.001)	28.7 (\pm 0.3)
	theophylline	7.6 (\pm 0.001)	-10.6 (\pm 0.20)	-38.9 (\pm 0.001)	28.4 (\pm 0.5)
310.2	water	8.9 (\pm 0.20)	-20.7 (\pm 1.10)	-39.0 (\pm 0.20)	18.3 (\pm 0.1)
	caffeine	7.9 (\pm 0.01)	-29.1 (\pm 1.60)	-39.5 (\pm 0.01)	10.4 (\pm 0.1)
	diprophylline	8.3 (\pm 0.20)	-12.3 (\pm 0.90)	-39.3 (\pm 0.20)	27.0 (\pm 0.1)
	etofylline	7.8 (\pm 0.20)	-12.6 (\pm 0.50)	-39.6 (\pm 0.20)	26.3 (\pm 0.6)
	paracetamol	8.2 (\pm 0.20)	-16.6 (\pm 1.40)	-39.4 (\pm 0.20)	22.7 (\pm 0.4)
	theophylline	8.3 (\pm 0.01)	-28.4 (\pm 0.70)	-39.3 (\pm 0.01)	10.9 (\pm 0.1)

As expected, for SDS alone, an increase in temperature from $T = 298$ K to 310 K resulted in a small increase in CMC from (7.9 to 8.9) mM (Majhi and Blume, 2001), while the change in enthalpy for the process was largely unchanged at $T = 298$ K and 310 K, yet a drop in enthalpy was observed at $T = 304$ K, as expected (Chatterjee et al., 2001). The presence of

all five drugs did not significantly modify the CMC compared with the value obtained when no drug was present at $T = 298$ K. However, the presence of caffeine, paracetamol and theophylline lowered the CMC at $T = 304$ K while at $T = 310$ K, all drugs lowered the CMC as the micelles formed more favourably (possibly as a result of complimentary drug–surfactant interactions). For the most structurally similar compounds, i.e. the substituted imidazole moieties, namely caffeine, diprophylline, and etofylline, there is little change in the CMC or enthalpy of micellisation with respect to temperature. For both paracetamol and theophylline, the CMC of SDS slightly decreased from $T = 298$ K to $T = 304$ K and then increased at $T = 310$ K yet the changes in enthalpy dramatically differed. In the case of paracetamol, micellisation is enthalpically less favourable at the higher temperature yet for theophylline the inverse is observed. From an entropic perspective, the relationship between temperature and enthalpy change is a reflection of the causation of micelle formation, i.e. demonstrating a shift in the driving force from an enthalpy controlled process to an entropy-driven process (or vice versa). In this study, as previously mentioned, only two of the drugs exhibited a noticeable (yet contrasting) change in enthalpy with increasing temperature implying the presence of an enthalpy–entropy compensation event and the importance of the hydrophobic effect in micelle formation (Chen et al., 1998).

If the process of micellisation is separated into the desolvation and aggregation stages, then hydrophobic effects are usually reduced with increasing temperature as a loss of solvent structure occurs (influencing desolvation), this would appear to be the case for paracetamol while the converse is true for theophylline (in agreement with the fact that paracetamol is a far more hydrophobic drug than theophylline based on calculated LogP values). The physicochemical properties of such drug–surfactant interactions can be explained by considering electrostatic effects with a strong interaction observed between charged surfactants and hydrophilic drugs. Conversely, drugs that exhibit an appreciable hydrophobic surface area

in the presence of surfactants will have an interaction dominated by the hydrophobic effect, with the electrostatic effect playing only a minor role (Khosravi, 1997). Paracetamol is more hydrophobic than theophylline, thus the former will have a drug–surfactant interaction more strongly dominated by the hydrophobic effect rather than electrostatic effects, compared with the latter which is dominated by electrostatic interactions. This is in agreement with similar studies, for example the existence of surfactant interactions has been reported between polymer aggregates and SDS as a result of favourable hydrophobic and electrostatic effects (Bai et al., 2004).

Table 6.2 shows aggregation data with the incorporation of thermodynamic data for SDS. At all three temperatures and in the absence, or presence of all five model drugs, there is little influence on the change in Gibbs free energy observed. The negative values for ΔG_{mic} indicates that the micelles along with the drug-micelles system has less free energy as compared with monomers or free drug molecules. These negative values of enthalpy and Gibbs free energy, consequently promote micellisation and drug micelle interaction. These findings imply that the overall energetics behind the aggregation phenomenon are not significantly altered by temperature or drugs, in agreement with the lack of change in the concentration at which it occurs. Interestingly, more substantial changes in the change in enthalpy and entropy for the micellisation event were observed implying an entropy-enthalpy compensation phenomenon. Micellisation is an entropically driven process and results of this study are in good agreement with the previous reported studies. The gain in entropy was observed at all temperatures under investigation, however, $T = 304\text{ K}$ favours a more entropically driven micellisation (Table 6.2). This gain in entropy is a result of the transfer of bound water into the bulk phase during the demicellisation phenomenon. The trend of micellisation entropy in the presence of all drugs (except theophylline) is similar to the entropy of SDS/H₂O micellisation. For theophylline, the change in entropy decreased from 298 K to 310 K while enthalpy

increased, indicating that enthalpy-entropy together facilitate micelle formation at $T = 310\text{ K}$ in the presence of theophylline, (Table 6.2).

To further investigate the effects additional compounds may have on the micellisation event, a second compound was added to the system in the presence of each model drug in turn, namely PEG. Previous work has implied that the interaction between SDS and PEG is dependent upon the molecular weight of the PEG and known to be thermodynamically ‘peculiar’ exhibiting both endothermic and exothermic effects (Dai and Tam, 2001b). Calorimetry results appeared to follow this expectation, as exemplified in Figure 6.7, for the micellisation of SDS in the presence of PEG. The first derivative peak of the titration curve corresponds to the CMC of SDS while the second broad inflection can be attributed to the PEG-SDS interaction (Figure 6.7).

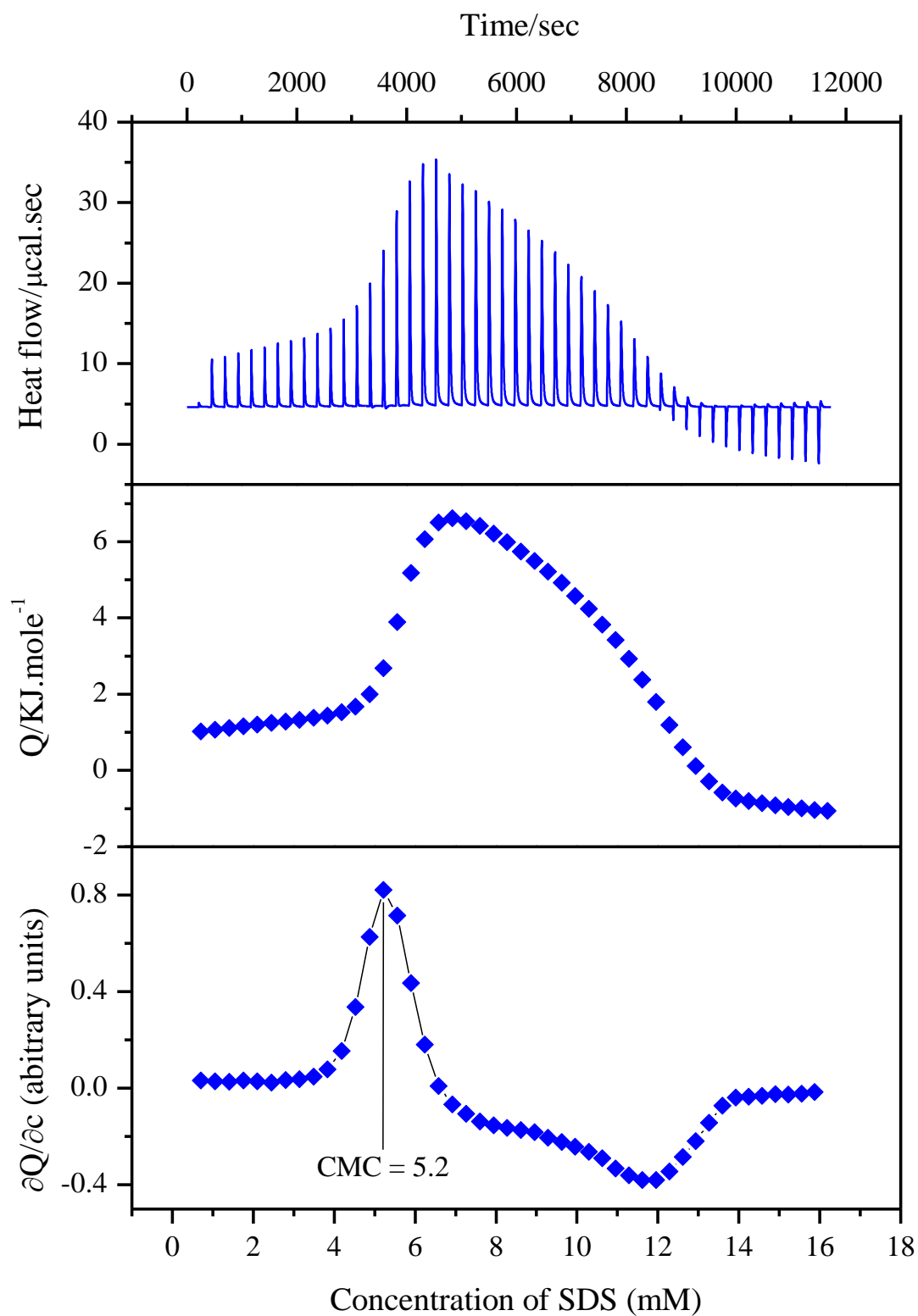


Figure 6.7: Raw ITC data and subsequent data analysis to determine the CMC of SDS in the presence of 0.2 mM PEG-6000 at $T = 298 \text{ K}$.

A summary of the CMC values and associated thermodynamic behaviour for SDS in the presence of PEG for all five systems studied at the three temperatures can be seen in Table 6.3.

Table 6.3: Critical micellar concentrations and thermodynamic values associated with the micellisation of SDS in the presence of PEG and five model compounds at 298, 304 and 310 K

Temp. / (K)		CMC/mM	$\Delta^\circ H_{mic}$ / (KJ.mol ⁻¹)	$\Delta^\circ G_{mic}$ / (KJ.mol ⁻¹)	$T\Delta^\circ S_{mic}$ / (KJ.mol ⁻¹)
298.2	water	5.2 (± 0.20)	-11.3 (± 0.20)	-39.6 (± 0.10)	28.4 (± 0.1)
	caffeine	5.5 (± 0.01)	-10.8 (± 0.40)	-39.5 (± 0.001)	28.7 (± 0.4)
	diprophylline	5.5 (± 0.01)	-10.0 (± 0.90)	-39.5 (± 0.08)	29.5 (± 0.9)
	etofylline	5.3 (± 0.40)	-11.0 (± 0.20)	-39.7 (± 0.42)	28.7 (± 0.6)
	paracetamol	4.5 (± 0.12)	-11.7 (± 0.04)	-40.5 (± 0.12)	28.7 (± 0.1)
	theophylline	5.4 (± 0.26)	-11.0 (± 0.10)	-39.6 (± 0.22)	28.6 (± 0.2)
304.2	water	4.7 (± 0.30)	-7.9 (± 0.20)	-41.0 (± 0.30)	33.1 (± 0.4)
	caffeine	4.9 (± 0.20)	-8.5 (± 0.10)	-40.8 (± 0.06)	32.3 (± 0.1)
	diprophylline	5.1 (± 0.17)	-8.1 (± 0.20)	-40.6 (± 0.15)	32.6 (± 0.2)
	etofylline	5.1 (± 0.20)	-8.3 (± 0.01)	-40.7 (± 0.20)	32.4 (± 0.2)
	paracetamol	4.0 (± 0.12)	-8.6 (± 0.04)	-41.8 (± 0.47)	32.3 (± 0.4)
	theophylline	4.7 (± 0.27)	-8.5 (± 0.10)	-40.7 (± 0.32)	32.1 (± 0.3)
310.2	water	4.3 (± 0.20)	-10.3 (± 0.20)	-42.2 (± 0.20)	31.9 (± 0.1)
	caffeine	4.4 (± 0.40)	-10.7 (± 0.10)	-42.1 (± 0.40)	31.4 (± 0.5)
	diprophylline	4.7 (± 0.27)	-10.7 (± 0.01)	-41.8 (± 0.27)	31.2 (± 0.3)
	etofylline	4.4 (± 0.24)	-10.7 (± 0.10)	-42.2 (± 0.25)	31.5 (± 0.3)
	paracetamol	3.1 (± 0.01)	-11.0 (± 0.01)	-43.6 (± 0.15)	32.6 (± 0.2)
	theophylline	4.4 (± 0.20)	-10.4 (± 0.30)	-42.1 (± 0.20)	31.8 (± 0.2)

For SDS and PEG based systems, the addition of PEG reduced the CMC in all cases with this phenomenon becoming more apparent as the temperature increased (highlighted in Figure 6.8).

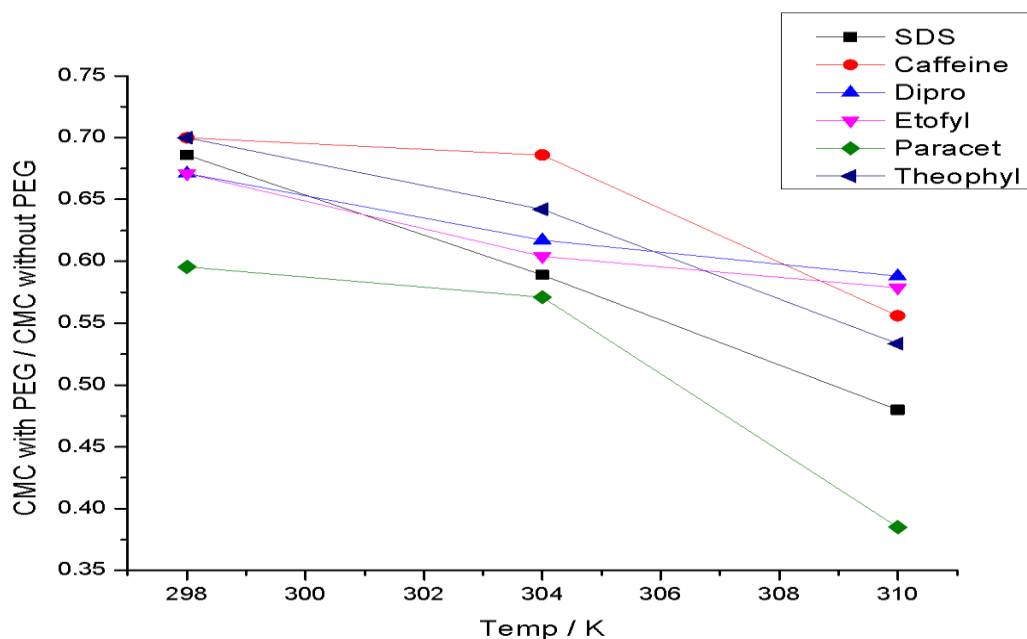


Figure 6.8: The effect upon micellisation of SDS in the presence of PEG and five model compounds.

Figure 6.8 exemplifies how the presence of PEG encourages the micellisation process at lower concentrations with values for the CMC with PEG/without PEG all below 1. Although PEG is known to self-aggregate under certain conditions (Azri et al., 2012), it is not believed to be the process being observed in these studies with the use of low concentrations (0.2mM) and a high molecular weight PEG. A more plausible explanation is the observance of hydrophobic interactions between SDS and PEG leading to the formation of a stable complex, similar to that previously reported in literature (Ballerat-Busserolles et al., 1997).

The decreasing trend in the enthalpy of micellisation was observed in the presence of PEG, for example, ΔH_{mic} (-20.4 ± 1.30 KJ/mol) of SDS into water (Table 6.2) decreased to $-11.3 (\pm 0.20)$ KJ/mol for SDS into PEG solution (Table 6.3). A similar trend was observed in the presence of model drugs with PEG whereby a negative enthalpy (along with a large negative free energy) promoted aggregation of SDS.

The demicellisation curve of SDS into water or PEG solution was divided into three regions (Figure 6.9). In region I, the enthalpy curves for SDS/PEG and that for the SDS/H₂O are parallel up to the point of the critical aggregation point (cac) (Yan et al., 2007), suggesting that there is no interaction between PEG and SDS. In region II, a large endothermic deviation was followed by an exothermic event which appeared in the SDS/PEG curve while only an endothermic event was apparent in the SDS/H₂O curve

The SDS-PEG interaction suggests that SDS monomers interact with the ethylene segment of PEG exothermically, presumably by polar - polar attraction after reaching the CMC point. This process completes at the intersection point (Figure 6.9). Hence polymer induced surfactant micellisation can be considered one explanation for the observed reduction in CMC of SDS. Region III is past the CMC for SDS/H₂O, indicating that SDS micelles have become the dominant species. From the concentrations of SDS and PEG used in this experiment, the ratio of SDS micelles to a PEG molecule obtained is 2:1, implying that each PEG molecule can wrap around two micelles (Figure 6.9).

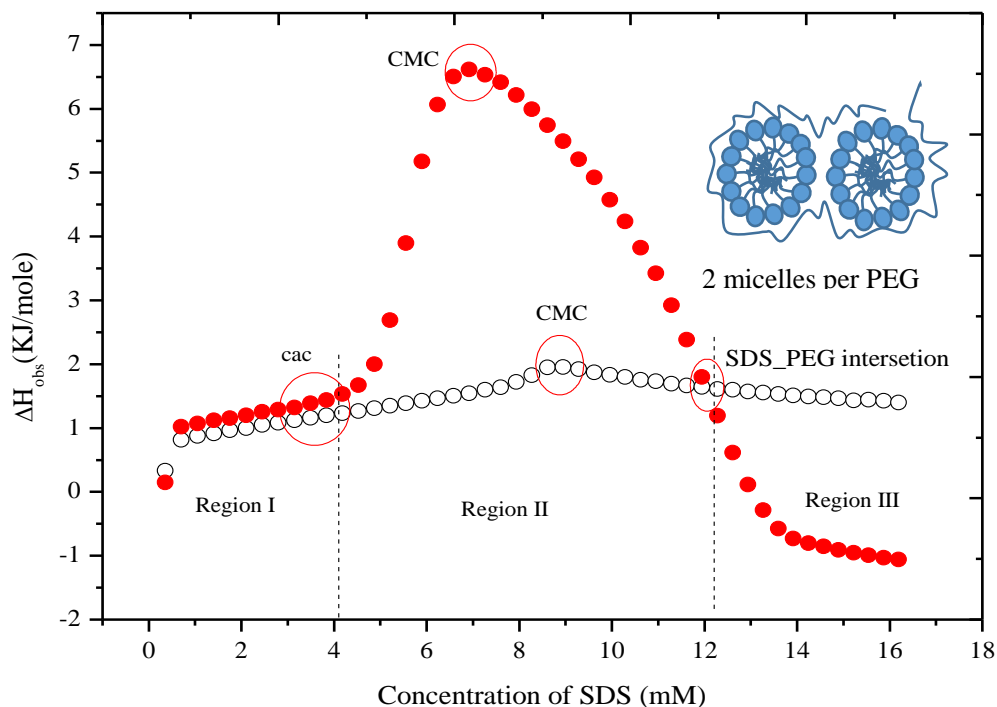


Figure 6.9: Enthalpy change for the titration of 200 mM SDS into deionised water (open circle) or 0.2 mM PEG (red circle) at 298 K.

Table 6.3 shows that ΔG_{mic} is large and negative yet ΔH_{mic} is small and negative, indicating that the process is marginally exothermic. In addition, $T^\circ \Delta S_{\text{mic}}$ is large and positive implying a net increase in entropy during the micellisation process. The experimental results have clearly shown that micelle formation involves only a small enthalpy change while the negative free energy is the result of a large positive entropy. This can lead to the possible conclusion that micelle formation is predominantly an entropy driven process. The change in entropy is partially related to the “hydrophobic effect” encountered in the transfer process and partially from the transfer of monomers to micelles. An additional entropy contribution is associated with the partial neutralisation of the ionic charge by the counter ions during the aggregation process which will add to the entropy increase resulting from the above effects (Laidler, 1995).

6.2.4. Sodium deoxycholate (NaDC) micellisation in the presence of model drugs and PEG

Sodium deoxycholate (NaDC) is a more complex surfactant than SDS, with published data often referring to a second micellisation event, similar in concentration to that for the main micellisation (Garidel et al., 2000). The ITC thermogram for NaDC, (especially in the presence of PEG or drugs) cannot be exploited directly as no clear break point in the heat (Q) versus concentration was observed. In such cases, curve analysis was used to determine the concentrations corresponding to the start (ST: start of transition) and to the end (ET: end of transition) of the micellisation process (Raju et al., 2001; Roques et al., 2009). This phenomenon is explained in Figure 6.10, the linear fitting of the data in the lower and the upper concentration domains provided the inflection point, corresponding to the CMC of NaDC alone and in the presence of PEG. The data points for the determination of the ST and the ET, remained approximate using this method. A systematic thermodynamic study was undertaken for NaDC with the same five compounds as SDS, presented in Table 6.4.

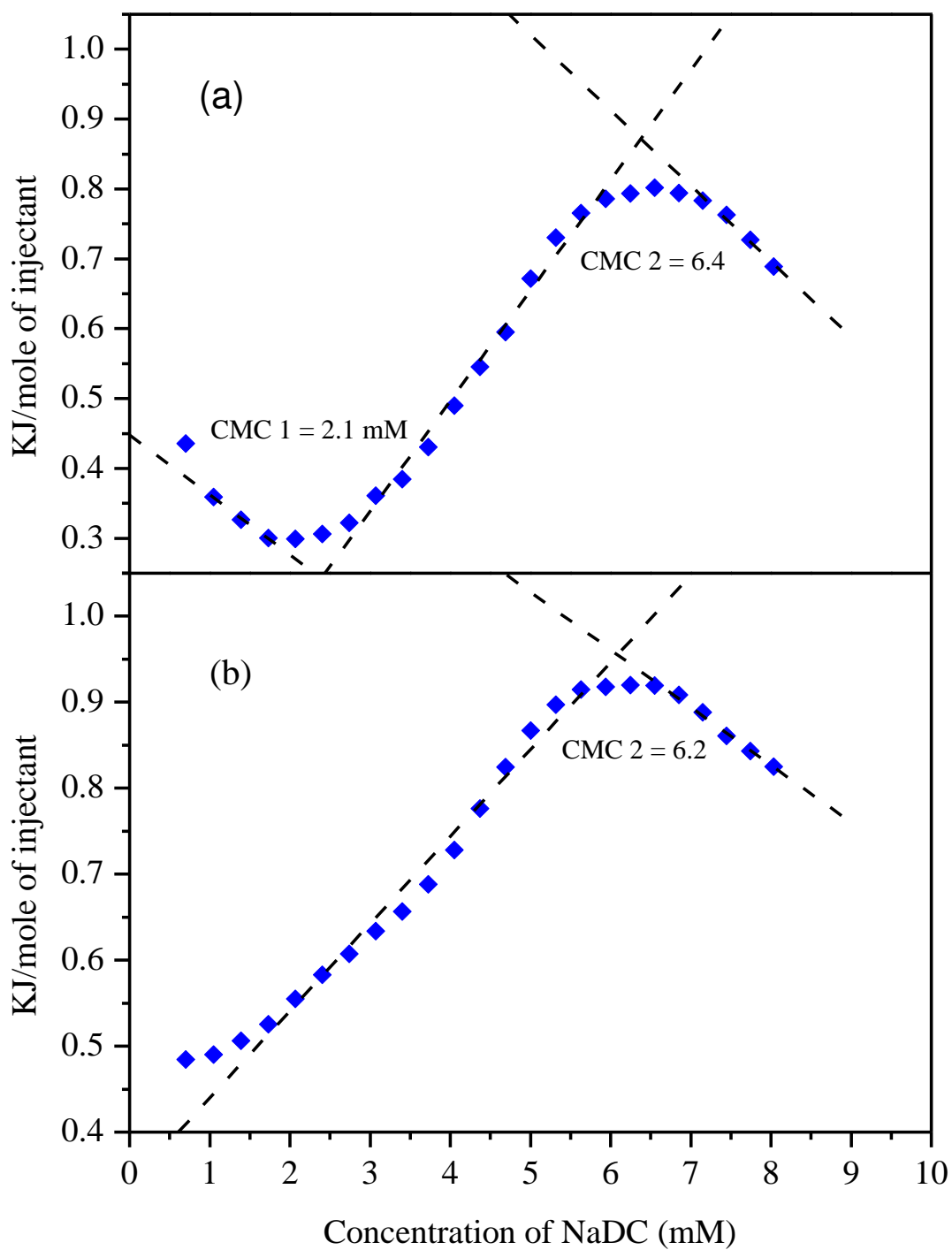


Figure 6.10: Integrated ITC heat data indicating the micellisation point of (a) NaDC alone (CMC 1 and 2) and (b) in the presence of PEG at 298 K.

Table 6.4: Critical micellar concentrations and thermodynamic values associated with the micellisation of NaDC in the presence of five model compounds at 298, 304 and 310 K

Temp. / (K)		CMC/mM	$\Delta^\circ H_{mic} / (KJ.mol^{-1})$	$\Delta^\circ G_{mic} / (KJ.mol^{-1})$	$T\Delta^\circ S_{mic} / (KJ.mol^{-1})$
298.2	water	2.1 (\pm 0.23), 6.4 (\pm 0.17)	-1.6 (\pm 0.05), 1.7 (\pm 0.01)	-33.0 (\pm 0.39), 29.2 (\pm 0.08)	31.5 (\pm 0.3), 27.5 (\pm 0.1)
	caffeine	5.4 (\pm 0.17)	-1.6 (\pm 0.04)	-30.1 (\pm 0.63)	28.1 (\pm 0.1)
	diprophylline	6.0 (\pm 0.17)	-1.6 (\pm 0.01)	-29.4 (\pm 0.08)	27.8 (\pm 0.1)
	etofylline	6.0 (\pm 0.18)	-1.5 (\pm 0.12)	-29.0 (\pm 0.09)	27.9 (\pm 0.1)
	paracetamol	3.9 (\pm 0.20)	1.8 (\pm 0.02)	-30.8 (\pm 0.14)	32.6 (\pm 0.2)
	theophylline	6.2 (\pm 0.52)	-1.7 (\pm 0.01)	-29.3 (\pm 0.26)	27.7 (\pm 0.3)
304.2	water	1.6 (\pm 0.17), 5.1 (\pm 0.17)	-1.1 (\pm 0.12), 1.4 (\pm 0.02)	-34.4 (\pm 0.37), -30.6 (\pm 0.11)	33.3 (\pm 0.2) 29.2 (\pm 0.1)
	caffeine	4.5 (\pm 0.40)	-1.3 (\pm 0.06)	-31.2 (\pm 0.33)	29.7 (\pm 0.4)
	diprophylline	4.6 (\pm 0.17)	-1.0 (\pm 0.05)	-30.9 (\pm 0.12)	29.9 (\pm 0.1)
	etofylline	4.4 (\pm 0.19)	-1.1 (\pm 0.25)	-30.8 (\pm 0.12)	30.0 (\pm 0.2)
	paracetamol	3.5 (\pm 0.35)	-1.3 (\pm 0.02)	-31.8 (\pm 0.32)	30.5 (\pm 0.3)
	theophylline	4.8 (\pm 0.35)	-1.4 (\pm 0.02)	-30.8 (\pm 0.24)	29.4 (\pm 0.2)
310.2	water	4.3 (\pm 0.23)	-1.3 (\pm 0.01)	-31.8 (\pm 0.17)	30.5 (\pm 0.2)
	caffeine	4.1 (\pm 0.51)	-1.1 (\pm 0.02)	-31.2 (\pm 1.22)	30.7 (\pm 0.4)
	diprophylline	4.2 (\pm 0.40)	-1.0 (\pm 0.05)	-31.9 (\pm 0.33)	30.8 (\pm 0.4)
	etofylline	4.0 (\pm 0.35)	-1.1 (\pm 0.17)	-32.0 (\pm 0.29)	30.9 (\pm 0.5)
	paracetamol	3.4 (\pm 0.57)	-1.2 (\pm 0.02)	-32.6 (\pm 0.60)	31.4 (\pm 0.6)
	theophylline	4.2 (\pm 0.51)	-1.2 (\pm 0.02)	-31.5 (\pm 0.38)	30.3 (\pm 0.4)

The CMC results of NaDC using ITC are in agreement with the reported studies as two inflection points indicating CMC 1 and CMC 2 were observed (Table 6.4). Micellisation of NaDC completely changed at $T = 310$ K where only one CMC point was identified, i.e. 4.3 ± 0.2 mM, indicating the temperature dependent behaviour of NaDC. The observed CMC for NaDC was affected by the presence of the drugs. Most notably, of the five drugs considered, paracetamol dramatically reduced the CMC to 3.4 mM at $T = 310$ K (Table 6.4). Micellisation of NaDC in the presence of paracetamol changed from a positive change in enthalpy at $T = 298$

K, to a more negative change in enthalpy at $T = 304$ and 310 K (Table 6.4) indicating an entropically driven process. This agrees with the raw ITC signals that are exothermic at 298 K and endothermic at 304 and 310 K (Figure 6.11). From these results, it is evident that paracetamol, being a slightly hydrophobic drug, induced rapid aggregation of monomers compared with the other drugs. The overall findings suggest that drugs encourage the formation of micelles as in all cases the CMC in the presence of drugs was less than that in water alone. This finding can be seen at all three temperatures studied. Unlike SDS, little variation in the change in enthalpy and entropy can be seen in Table 6.4 and a consistent value for the change in Gibbs free energy was also found. Such consistency implies that although the CMC may have decreased to varying extents the thermodynamics of the process has not altered. A comparison of Table 6.2 with Table 6.4 highlights the change in enthalpy change between the two surfactants, with a smaller modification to the remaining thermodynamic parameters.

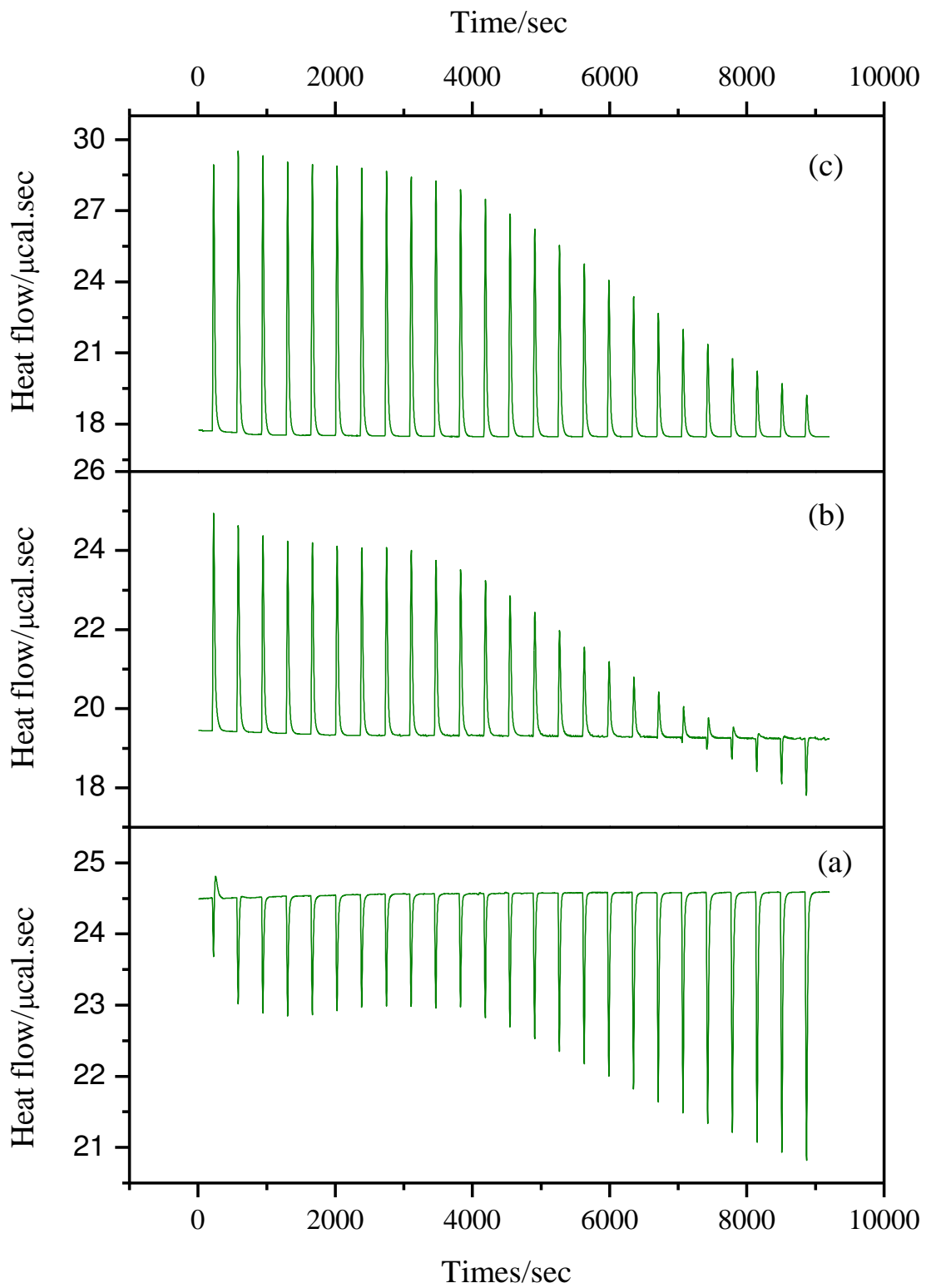


Figure 6.11: Raw ITC data for the titration of 50 mM NaDC into a 60 mM paracetamol solution at (a) 298 K, (b) 304 K and (c) 310 K.

As with SDS, the effect of the presence of PEG on the micellisation event was monitored for NaDC, as shown in Table 6.5. The complete disappearance of the first CMC along with the little variation in the second CMC of NaDC was observed with the additional presence of PEG and the five model compounds. Similarly, the thermodynamics of the micellisation process did not dramatically alter with the addition of PEG. This finding is in contrast to that for SDS where PEG was found to be influential in the micellisation concentration and change in enthalpy associated with the process. This finding implies there is little, or no, interaction between NaDC and PEG to encourage the formation of micelles as was previously seen for SDS. Non cooperative binding between PEG and NaDC was also revealed which could be the possible explanation of the unaffected CMC in the presence of PEG (Figure 6.12).

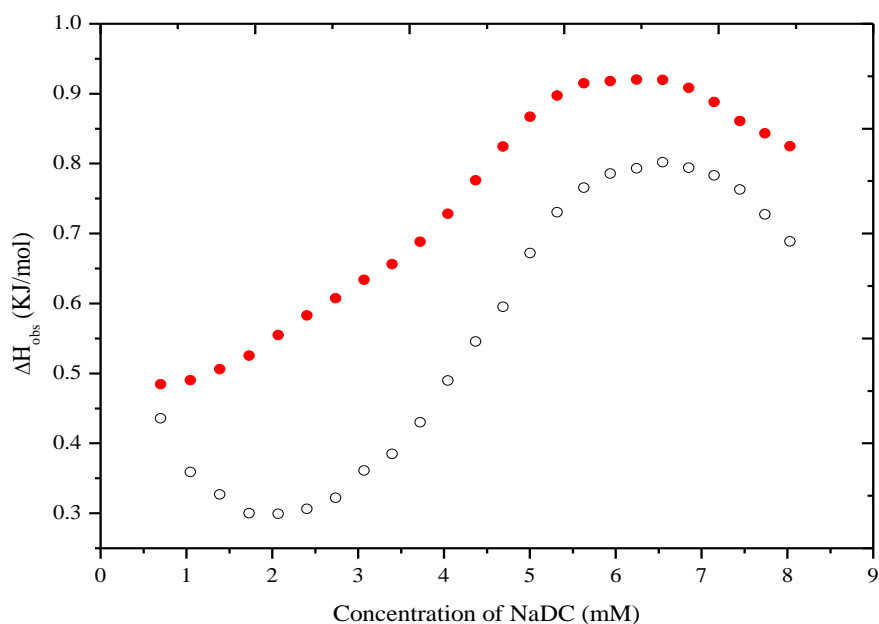


Figure 6.12: Enthalpy change for titration of 50 mM NaDC into deionised water (open circle) and 0.2 mM PEG (red circle) at 298 K.

Table 6.5: Critical micellar concentrations and thermodynamic values associated with the micellisation of NaDC in the presence of PEG and five model compounds at 298, 304 and 310 K

Temp. / (K)		CMC/mM	$\Delta^\circ H_{mic}$ / (KJ.mol ⁻¹)	$\Delta^\circ G_{mic}$ / (KJ.mol ⁻¹)	T $\Delta^\circ S_{mic}$ / (KJ.mol ⁻¹)
298.2	water	6.2 (± 0.30)	-1.8 (± 0.05)	-29.3 (± 0.15)	27.6 (± 0.2)
	caffeine	5.1 (± 0.17)	-1.6 (± 0.02)	-30.3 (± 0.46)	28.3 (± 0.1)
	diprophylline	5.8 (± 0.17)	-1.6 (± 0.02)	-29.5 (± 0.10)	27.9 (± 0.1)
	etofylline	5.8 (± 0.17)	-1.5 (± 0.11)	-29.5 (± 0.98)	28.0 (± 0.2)
	paracetamol	3.7 (± 0.30)	1.7 (± 0.55)	-31.0 (± 0.26)	32.8 (± 0.3)
	theophylline	6.1 (± 0.34)	-1.7 (± 0.02)	-29.4 (± 0.17)	27.7 (± 0.2)
304.2	water	4.9 (± 0.17)	-1.3 (± 0.02)	-30.7 (± 0.11)	29.4 (± 0.1)
	caffeine	4.4 (± 0.35)	-1.3 (± 0.04)	-31.4 (± 0.31)	29.8 (± 0.3)
	diprophylline	4.4 (± 0.35)	-1.0 (± 0.08)	-30.7 (± 0.34)	30.1 (± 0.3)
	etofylline	4.3 (± 0.23)	-1.1 (± 0.83)	-31.1 (± 0.18)	30.1 (± 0.1)
	paracetamol	3.4 (± 0.57)	-1.3 (± 0.01)	-32.0 (± 0.59)	30.6 (± 0.6)
	theophylline	4.7 (± 0.57)	-1.4 (± 0.10)	-30.5 (± 0.16)	29.5 (± 0.4)
310.2	water	4.2 (± 0.35)	-1.2 (± 0.04)	-31.3 (± 1.32)	30.8 (± 0.3)
	caffeine	3.8 (± 0.51)	-1.2 (± 0.08)	-31.4 (± 1.70)	31.0 (± 0.5)
	diprophylline	4.1 (± 0.57)	-0.9 (± 0.06)	-31.9 (± 0.49)	31.0 (± 0.5)
	etofylline	3.9 (± 0.50)	-1.0 (± 0.13)	-32.1 (± 0.43)	31.0 (± 0.6)
	paracetamol	3.3 (± 0.75)	-1.2 (± 0.02)	-32.7 (± 0.84)	31.5 (± 0.85)
	theophylline	4.1 (± 0.40)	-1.2 (± 0.40)	-31.6 (± 0.31)	30.4 (± 0.3)

The unchanged thermodynamic data of NaDC micellisation in the presence of PEG confirms the absence of PEG/NaDC interaction. Table 6.4 and 6.5 have clearly shown that micelle formation involves only a small enthalpy change while negative free energy is the result of a large positive entropy. Therefore, micelle formation involving hydrophobic interactions is predominantly an entropy driven process.

6.3. Conclusions

Isothermal titration calorimetry was successfully used to determine the drug-excipient interaction through saturation and micellisation studies. Table 6.1 shows a relationship between the behaviour of the five compounds and their ability to saturate micelles. A common interaction appeared to occur between the imidazole based compounds and SDS resulting in similar saturation limits and changes in enthalpy at the two temperatures studied. Paracetamol behaved in a slightly different manner, as expected, as it has a different chemical structure to the other compounds, where the significant change in enthalpy upon an increase in temperature implied a large entropic effect. Paracetamol, being a hydrophobic drug, favoured the entropically driven interaction.

The possible effect of drugs on excipients was evaluated by investigating micellisation of SDS and NaDC in the presence of drugs and PEG. In summary, the influence of five model drugs on the micellisation phenomenon indicates there is little interaction between the drugs and SDS yet there is a more favourable interaction between the drugs and NaDC. In contrast, the presence of PEG appeared to encourage micellisation for SDS yet not for NaDC. These differences can be attributed to their subtle differing functionality as they are generally similar in that they are both anionic surfactants containing hydrophobic and hydrophilic sections. This work highlights the impact such small differences can have on their behaviour in solution.

The findings of this work based on thermodynamic data confirmed the potential of ITC and provided an opportunity to use ITC for the evaluation of other complex systems involving drugs and excipients.

References

- AZRI, A., GIAMARCHI, P., GROHENS, Y., OLIER, R. & PRIVAT, M. 2012. Polyethylene glycol aggregates in water formed through hydrophobic helical structures. *Journal of colloid and interface science*, 379, 14-19.
- BAI, G., CASTRO, V., NICHIFOR, M. & BASTOS, M. 2010. Calorimetric study of the interactions between surfactants and dextran modified with deoxycholic acid. *Journal of thermal analysis and calorimetry*, 100, 413-422.
- BAI, G., SANTOS, L. M. N. B. F., NICHIFOR, M., LOPES, A. & BASTOS, M. 2004. Thermodynamics of the interaction between a hydrophobically modified polyelectrolyte and sodium dodecyl sulfate in aqueous solution. *Journal of Physical Chemistry B*, 108, 405-413.
- BALLERAT-BUSSEROLLES, K., ROUX-DESGRANGES, G. & ROUX, A. H. 1997. Thermodynamics in micellar solutions: confirmation of complex formation between sodium dodecyl sulfate and polyethylene glycol. *Langmuir*, 13, 1946-1951.
- BEEZER, A. E. & GAISFORD, S. 2013. Isothermal calorimetry in the pharmaceutical sciences. *European Pharmaceutical Review*, 18, 64-68.
- BERNAZZANI, L., BORSACCHI, S., CATALANO, D., GIANNI, P., MOLLICA, V., VITELLI, M., ASARO, F. & FERUGLIO, L. 2004. On the interaction of sodium dodecyl sulfate with oligomers of poly (ethylene glycol) in aqueous solution. *The Journal of Physical Chemistry B*, 108, 8960-8969.
- BUCKLEY, S. T., FRANK, K. J., FRICKER, G. & BRANDL, M. 2013. Biopharmaceutical classification of poorly soluble drugs with respect to “enabling formulations”. *European Journal of Pharmaceutical Sciences*, 50, 8-16.
- CAREY, M. C. & SMALL, D. M. 1972. Micelle formation by bile salts. Physical-chemical and thermodynamic considerations. *Archives of Internal Medicine*, 130, 506-527.
- CHATTERJEE, A., MOULIK, S. P., SANYAL, S. K., MISHRA, B. K. & PURI, P. M. 2001. Thermodynamics of micelle formation of ionic surfactants: A critical assessment for sodium dodecyl sulfate, cetyl pyridinium chloride and dioctyl sulfosuccinate (Na salt) by microcalorimetric, conductometric, and tensiometric measurements. *Journal of Physical Chemistry B*, 105, 12823-12831.
- CHEN, L. J., LIN, S. Y. & HUANG, C. C. 1998. Effect of hydrophobic chain length of surfactants on enthalpy-entropy compensation of micellization. *Journal of Physical Chemistry B*, 102, 4350-4356.
- CHOUDHARY, S. & KISHORE, N. 2014. Drug-protein interactions in micellar media: Thermodynamic aspects. *Journal of Colloid and Interface Science*, 413, 118-126.
- ĆIRIN, D. M., POŠA, M. M. & KRSTONOŠIĆ, V. S. 2012. Interactions between sodium cholate or sodium deoxycholate and nonionic surfactant (Tween 20 or Tween 60) in aqueous solution. *Industrial and Engineering Chemistry Research*, 51, 3670-3676.
- COELLO, A., MEIJIDE, F., RODRÍGUEZ NÚÑEZ, E. & VÁZQUEZ TATO, J. V. 1996. Aggregation behavior of bile salts in aqueous solution. *Journal of Pharmaceutical Sciences*, 85, 9-15.
- DAI, S. & TAM, K. 2001a. Isothermal titration calorimetry studies of binding interactions between polyethylene glycol and ionic surfactants. *The Journal of Physical Chemistry B*, 105, 10759-10763.
- DAI, S. & TAM, K. C. 2001b. Isothermal Titration Calorimetry Studies of Binding Interactions between Polyethylene Glycol and Ionic Surfactants. *The Journal of Physical Chemistry B*, 105, 10759-10763.

- DAI, S. & TAM, K. C. 2006. Isothermal titration calorimetric studies on the interaction between sodium dodecyl sulfate and polyethylene glycols of different molecular weights and chain architectures. *Colloids and Surfaces A: Physicochemical and Engineering Aspects*, 289, 200-206.
- DAS, S., DEY, J., MUKHIM, T. & ISMAIL, K. 2011. Effect of sodium salicylate, sodium oxalate, and sodium chloride on the micellization and adsorption of sodium deoxycholate in aqueous solutions. *Journal of Colloid and Interface Science*, 357, 434-439.
- FELIPPE, A. C., SCHWEITZER, B., DAL BÓ, A. G., EISING, R., MINATTI, E. & ZANETTE, D. 2007. Self-association of sodium cholate with poly (ethylene oxide) cooperatively induced by sodium dodecyl sulfate. *Colloids and Surfaces A: Physicochemical and Engineering Aspects*, 294, 247-253.
- GARIDEL, P. & HILDEBRAND, A. 2005. Thermodynamic properties of association colloids. *Journal of Thermal Analysis and Calorimetry*, 82, 483-489.
- GARIDEL, P., HILDEBRAND, A., NEUBERT, R. & BLUME, A. 2000. Thermodynamic characterization of bile salt aggregation as a function of temperature and ionic strength using isothermal titration calorimetry. *Langmuir*, 16, 5267-5275.
- GARTI, N. 2000. *Thermal behavior of dispersed systems*, CRC Press, New York.
- GREGORIADIS, G. 2006. *Liposome Technology: Interactions of liposomes with the biological milieu*, CRC press.
- HILDEBRAND, A., GARIDEL, P., NEUBERT, R. & BLUME, A. 2004. Thermodynamics of demicellization of mixed micelles composed of sodium oleate and bile salts. *Langmuir*, 20, 320-328.
- KHOSSRAVI, D. 1997. Drug-surfactant interactions: effect on transport properties. *International Journal of Pharmaceutics*, 155, 179-190.
- LAIDLER, K. J. 1995. *The world of physical chemistry*, Oxford University Press Oxford.
- MAJHI, P. R. & BLUME, A. 2001. Thermodynamic characterization of temperature-induced micellization and demicellization of detergents studied by differential scanning calorimetry. *Langmuir*, 17, 3844-3851.
- MAJHI, P. R. & BLUME, A. 2002. Temperature-induced micelle-vesicle transitions in DMPC-SDS and DMPC-DTAB mixtures studied by calorimetry and dynamic light scattering. *The Journal of Physical Chemistry B*, 106, 10753-10763.
- MATSUOKA, K. & MOROI, Y. 2002. Micelle formation of sodium deoxycholate and sodium ursodeoxycholate (Part 1). *Biochimica et Biophysica Acta (BBA)-Molecular and Cell Biology of Lipids*, 1580, 189-199.
- MOROI, Y. 1992. *Micelles: theoretical and applied aspects*, Springer.
- MUTELET, F., ROGALSKI, M. & GUERMOUCHE, M. H. 2003. Micellar liquid chromatography of polyaromatic hydrocarbons using anionic, cationic, and nonionic surfactants: Armstrong model, LSER interpretation. *Chromatographia*, 57, 605-610.
- O'NEILL, M. A. A. & GAISFORD, S. 2011. Application and use of isothermal calorimetry in pharmaceutical development. *International Journal of Pharmaceutics*, 417, 83-93.
- OTZEN, D. 2011. Protein-surfactant interactions: A tale of many states. *Biochimica et Biophysica Acta - Proteins and Proteomics*, 1814, 562-591.
- PAULA, S., SÜS, W., TUCHTENHAGEN, J. & BLUME, A. 1995. Thermodynamics of micelle formation as a function of temperature: A high sensitivity titration calorimetry study. *Journal of Physical Chemistry*, 99, 11742-11751.
- PÉREZ, L., PINAZO, A., INFANTE, M. R. & PONS, R. 2007. Investigation of the micellization process of single and gemini surfactants from arginine by SAXS, NMR self-diffusion, and light scattering. *The Journal of Physical Chemistry B*, 111, 11379-11387.

- RAJU, B. B., WINNIK, F. M. & MORISHIMA, Y. 2001. A look at the thermodynamics of the association of amphiphilic polyelectrolytes in aqueous solutions: strengths and limitations of isothermal titration calorimetry. *Langmuir*, 17, 4416-4421.
- ROQUES, C., BOUCHEMAL, K., PONCHEL, G., FROMES, Y. & FATTAL, E. 2009. Parameters affecting organization and transfection efficiency of amphiphilic copolymers/DNA carriers. *Journal of Controlled Release*, 138, 71-77.
- ROSEN, M. J., MATHIAS, J. H. & DAVENPORT, L. 1999. Aberrant aggregation behavior in cationic gemini surfactants investigated by surface tension, interfacial tension, and fluorescence methods. *Langmuir*, 15, 7340-7346.
- VOLPE, P. L. 1995. Calorimetric study of SDS micelle formation in water and in NaCl solution at 298 K. *Thermochimica acta*, 257, 59-66.
- YAN, H., KAWAMITSU, H., KUSHI, Y., KUWAJIMA, T., ISHII, K. & TOSHIMA, N. 2007. Calorimetric study on interaction of water-soluble copolymers with ionic surfactant. *Journal of colloid and interface science*, 315, 94-98.

Chapter 7: Conclusions and future work

Recent drug discovery has led to an increasing number of poorly water soluble drug candidates, especially those administered orally. Such drug candidates tend to pass through the gastrointestinal tract, producing insufficient bioavailability because of their decreased dissolution. Therefore, it is a great challenge to develop effective techniques which can enhance dissolution and bioavailability of pharmaceutical formulations containing water insoluble APIs. Various approaches have been used to circumvent such issues utilising excipients that can enhance the solubility of an API, such as the successful formulations developed in this study. This thesis proposed a potential alternative novel microwave technique to replace conventional heating for the formulation of poorly soluble drugs.

The objectives of the thesis, as stated in Chapter 1, were successfully achieved and are summarised as follows:

1. To develop bespoke mesoporous silica based solid dispersions using a novel microwave system.

Chapter 3 discussed the inclusion of fenofibrate using mesoporous silica as a carrier material through traditional and novel microwave methods. The resultant enhanced drug release of dry microwave formulations compared with the non-formulated (alongside traditionally heated formulations) confirmed the possibility of successful formulation development using a microwave irradiation method. The characterising tools such as DSC and XRD suggest the transformation of a crystalline to a semi-crystalline or amorphous form as a result of the formulation process. The uniform distribution of drug within formulations and drug stability was confirmed by SEM and FTIR. Furthermore, the dramatically enhanced release profiles of fenofibrate from five out of six silicas used in the study, confirmed the

suitability of silica as a carrier material and their compatibility with the microwave formulation method.

2. To develop Syloid[®] silica based solid dispersions using a novel microwave system.

Chapter 4 discussed the Syloid[®] silica based formulation development of gemfibrozil using a novel microwave technique. Three Syloid[®] silica grades, namely, Syloid AL -1, Syloid 72 and Syloid 244 (different physical properties) were used to investigate their influence along with the microwave processing method on the performance of the resultant products. The in vitro dissolution results confirmed the effect of physical properties of silica such as surface area, pore diameter and pore volume on the release behaviour of drug. The greatest extent of gemfibrozil release from Syloid 72, confirmed that its properties are well suited to formulate the product using the microwave method. Overall, an appreciable extent of dissolution resulted from all Syloid silica used in this study. The results of characterisation techniques are in agreement with the findings of dissolution.

3. To develop a hydrophilic carrier based solid dispersion using a novel microwave system.

In Chapter 5, the potential of microwave formulation was further investigated by extending that work from mesoporous silica to a hydrophilic polymer, namely, polyethylene glycol (PEG). PEG based formulations of four poorly soluble drugs, namely ibuprofen, ibuprofen (+) S, fenofibrate and phenylbutazone, were prepared through a novel microwave method and compared with physically mixed and traditionally heated formulations. Results confirmed the successful application of the microwave technique in PEG based formulation development. Furthermore, microwave formulations displayed enhanced drug release compared with conventional heating and the physically mixed products. DSC and XRD confirmed the miscibility and transition from a crystalline to amorphous state of drugs. The

molecularly dispersed state of drugs within formulations was indicated by SEM images. FTIR spectra suggested the chemical stability of drugs after microwave treatment.

4. To investigate drug-excipient interactions based on surfactant saturation limits and micellisation studies.

In Chapter 6, the potential of isothermal titration calorimetry (ITC) was evaluated to determine drug-excipient interactions through saturation and micellisation studies. These particular studies were conducted using five model drugs, namely, caffeine, diprophylline, etofylline, paracetamol and paracetamol along with three excipients. The interaction between the imidazole based compounds and SDS resulted in similar saturation limits and changes in enthalpy at the two temperatures studied. Paracetamol, being a hydrophobic drug, behaved slightly differently. It favoured the entropically driven interactions. From the micellisation results of SDS and NaDC in the presence of drugs and PEG, it was confirmed that there is little interaction between the drugs and SDS yet there was a more favourable interaction between the drugs and NaDC. In contrast the presence of PEG appeared to encourage micellisation for SDS yet not for NaDC. These findings suggest that drug excipient interactions can be evaluated using thermodynamic data obtained from ITC.

In summary, it can be concluded that the results based on drug-excipient interactions confirmed the potential of ITC to determine interactions involving complex systems.

Future work

This work can be expanded further in many areas of potential opportunity including:

- (i) Optimisation of the microwave technique

The temperature controlled novel microwave method to produce pharmaceutical formulations can be applied by varying certain parameters such as processing temperature and

time, which may help to investigate further the optimum conditions for the microwave method. Drugs with a variable melting range could be processed to evaluate possible heating effects on the resultant formulations. Rather than using mesoporous silica or PEG, the research could be expanded further using other synthetic and natural polymers such as soluplus, gelucire, chitosan or pectin. This could ultimately lead to a large range of tailored formulation possibilities.

(ii) Expansion of analytical techniques

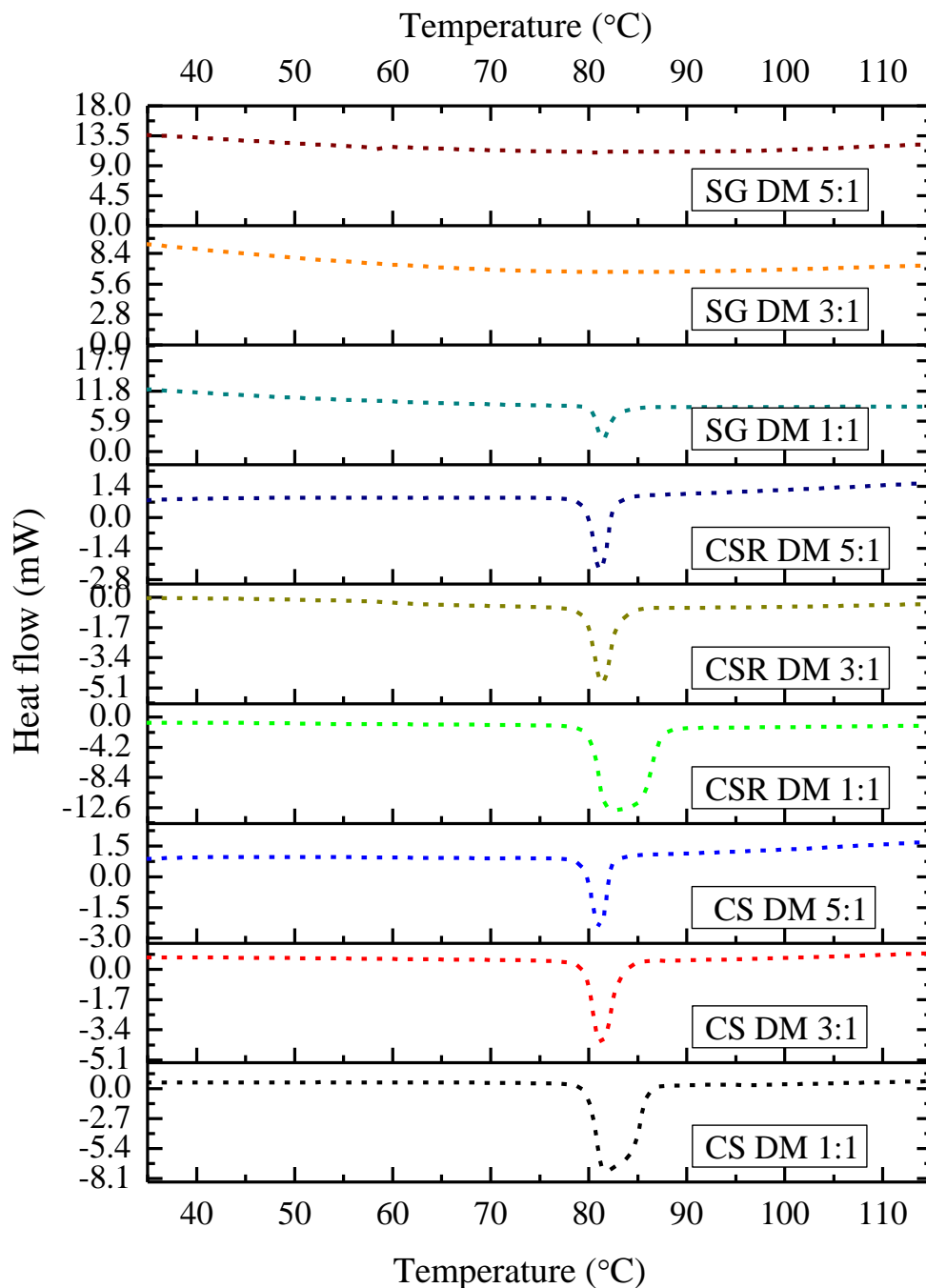
Analytical techniques such as DSC, XRD, SEM and FTIR were used to evaluate crystallinity, surface morphology and the stability of resultant products. However, other analytical techniques such as hot stage microscopy and transmission electron microscopy (TEM) may help to demonstrate the physical state of a drug within a formulation. Furthermore, X-ray photoelectron spectroscopy (XPS), along with standard BET nitrogen adsorption-desorption apparatus, may help to illustrate the degree of drug loading.

ITC work could be extended further to investigate drug-excipient interactions using a variety of drugs having different physicochemical properties, for example those that have a different ionisation state in aqueous solution, along with diverse Log P values. In addition, detailed thermodynamic data can be generated for comparison. It may also be possible to use a wider range of excipients, hence reliable data regarding drug-excipient interactions could be obtained. Anionic surfactants were used throughout this study, therefore, cationic and zwitterionic surfactants could also be used for comparison.

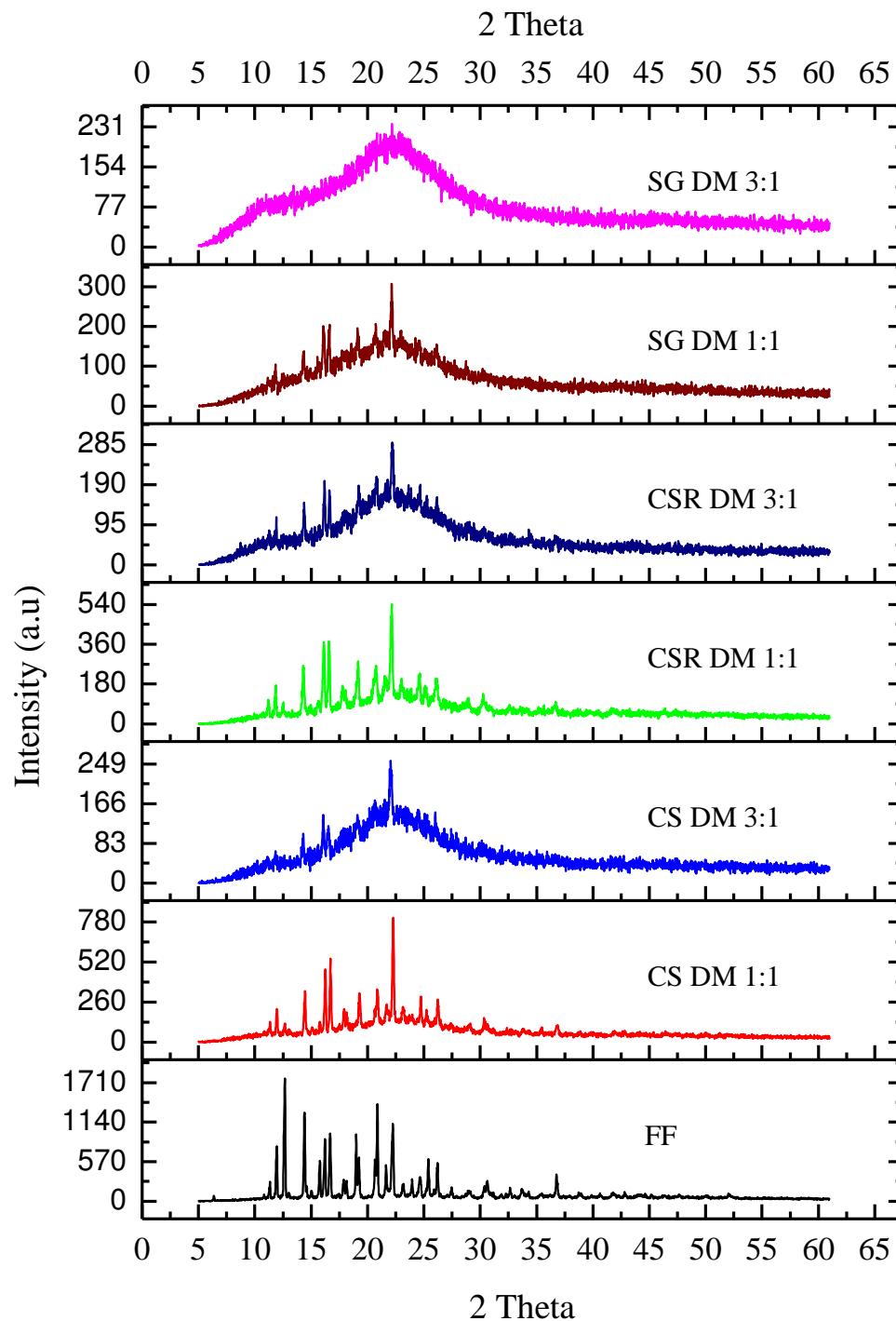
In summary, the research work of this thesis has confirmed the potential of the novel microwave method for formulation enhancement and ITC for an investigation of drug-excipient interactions. However, there is far more that could be conducted to fully explore the

potential application of the microwave formulation method alongside ITC analysis for drug-excipient interactions.

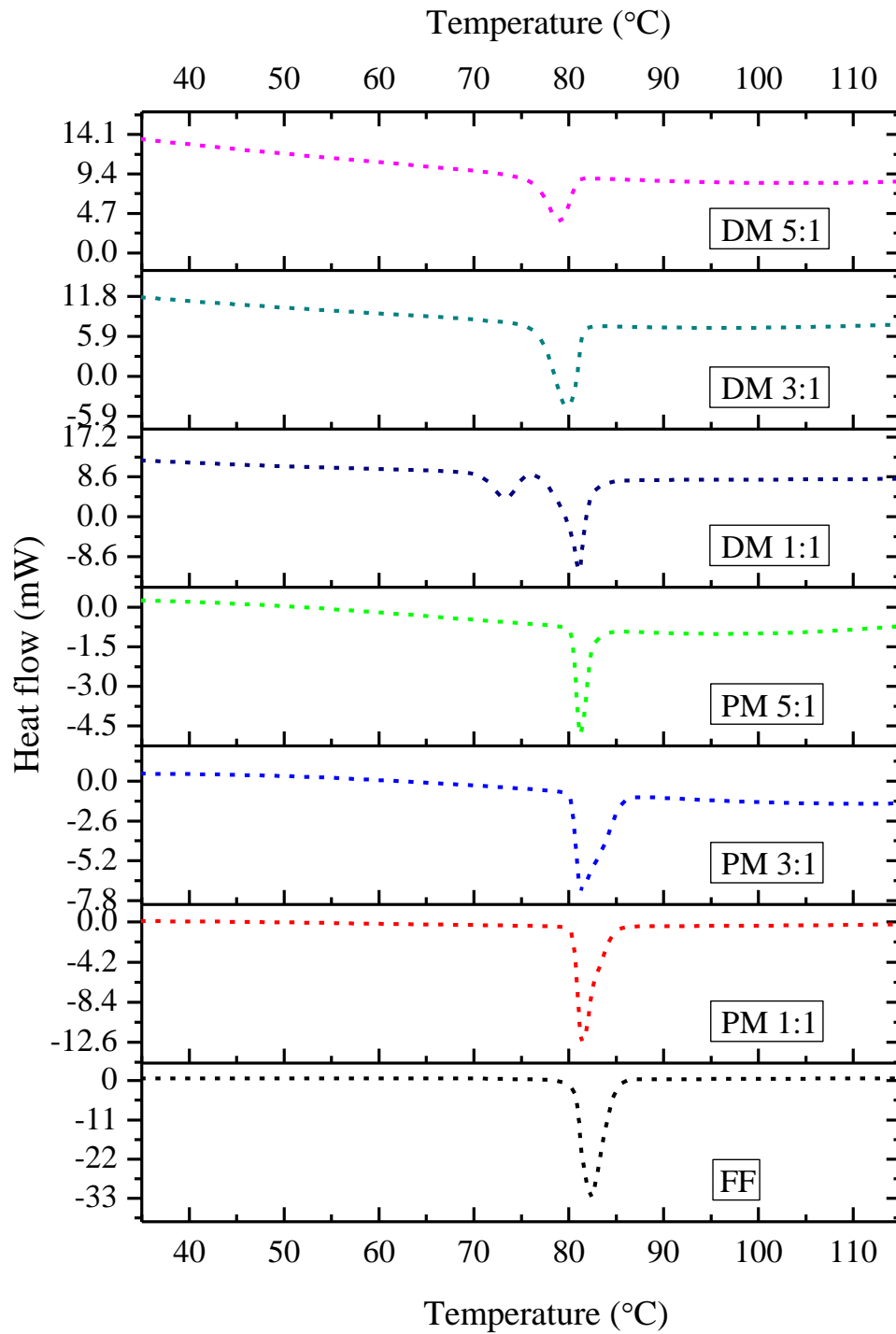
Appendix 1: DSC curves of Core Shell (CS), Core Shell rehydrox (CSR) and silica gel (SG) based dry microwave formulations all at silica / drug ratios of 1:1, 3:1 and 5:1



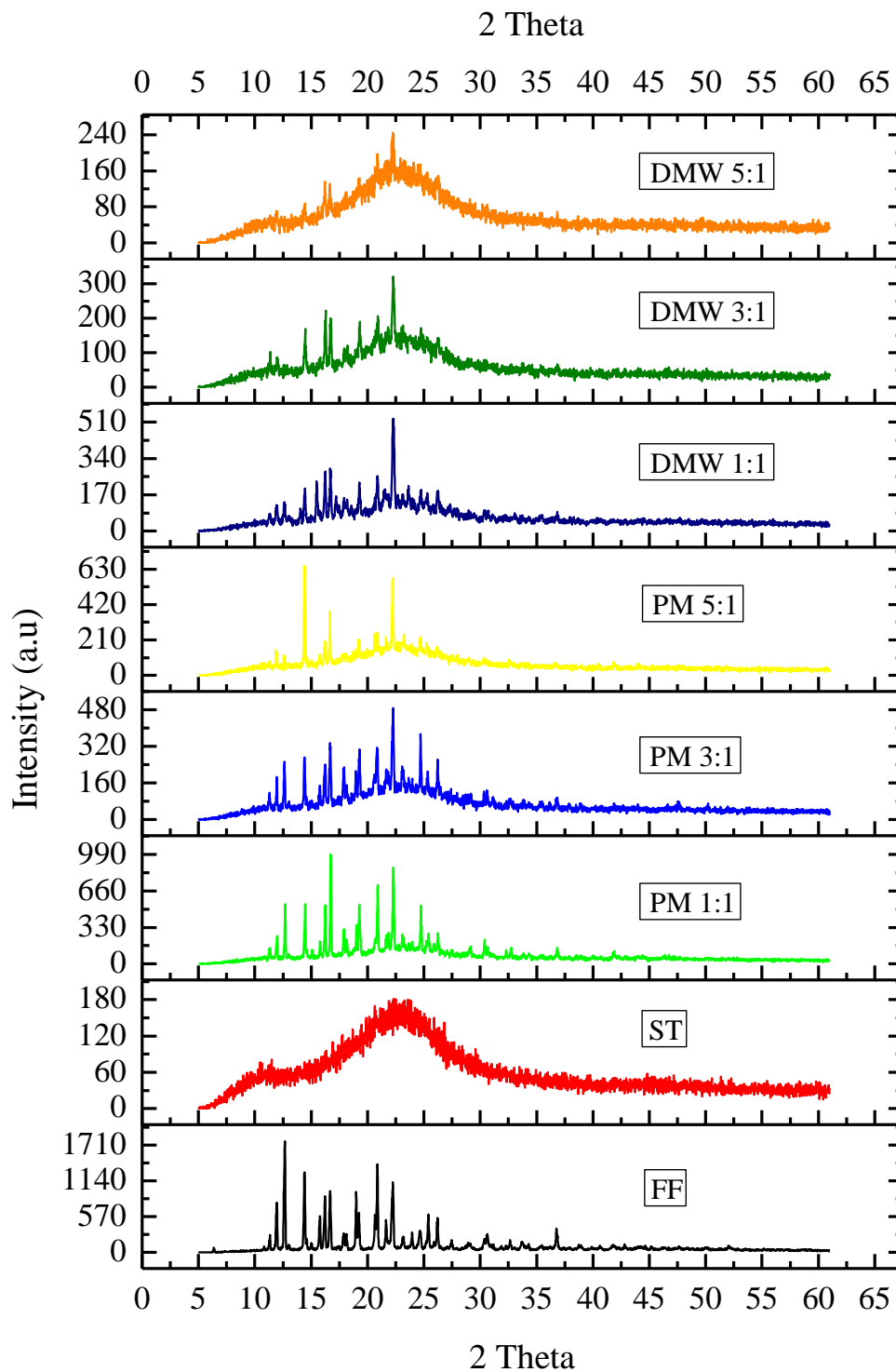
Appendix 2: XRD Patterns for fenofibrate along with Core shell (CS), Core Shell rehydrox (CSR) and silica gel (SG) based dry microwave formulations all at silica / drug ratios of 1:1 and 3:1



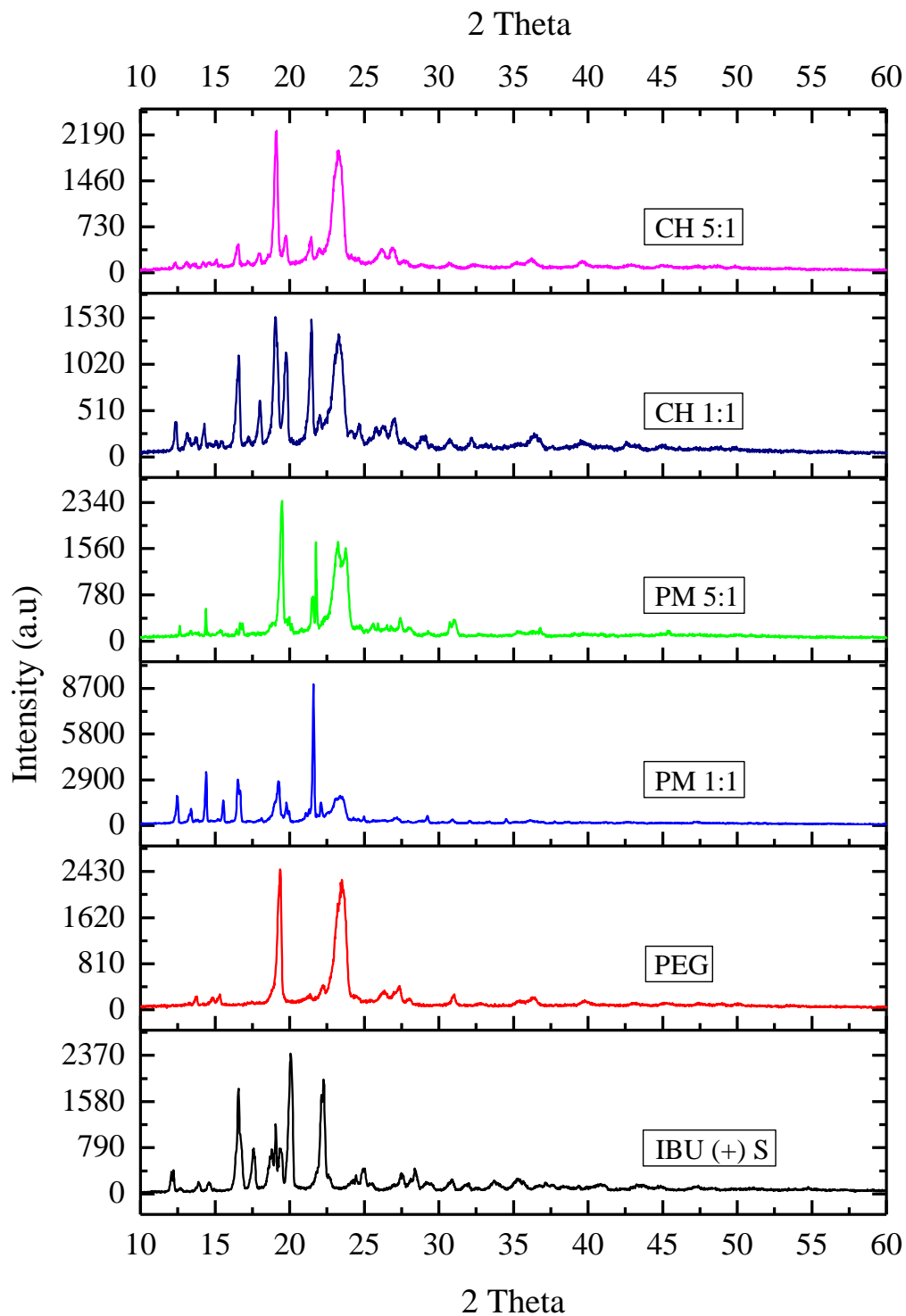
Appendix 3: DSC curves of fenofibrate (FF) along with Stober (ST) based physical mixtures and dry microwave (DM) formulations all at silica / drug ratios of 1:1, 3:1 and 5:1



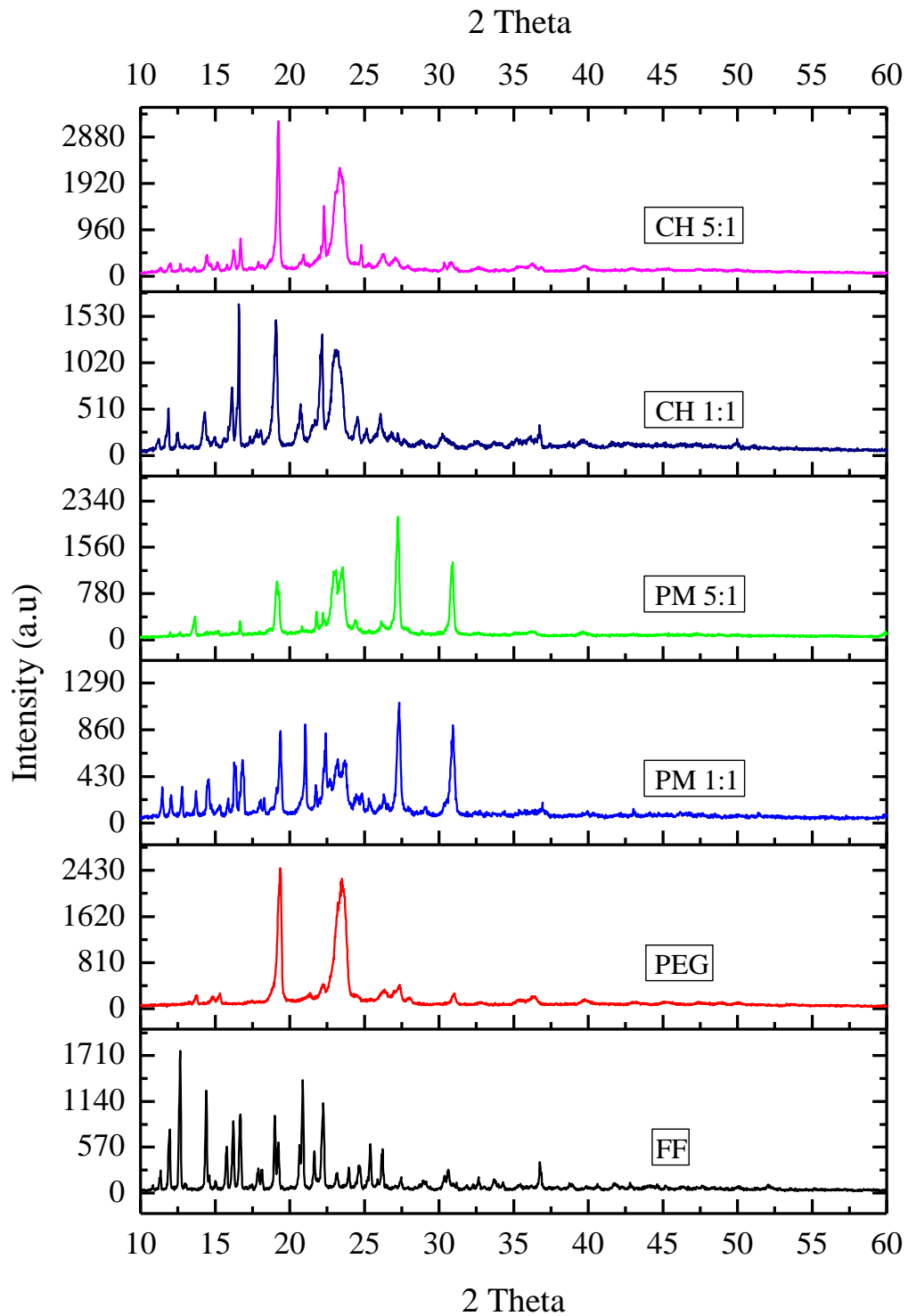
Appendix 4: XRD Patterns for fenofibrate along with Stober (ST) based physical mixtures (PM) and dry microwave (DM) formulations all at silica / drug ratios of 1:1, 3:1 and 5:1



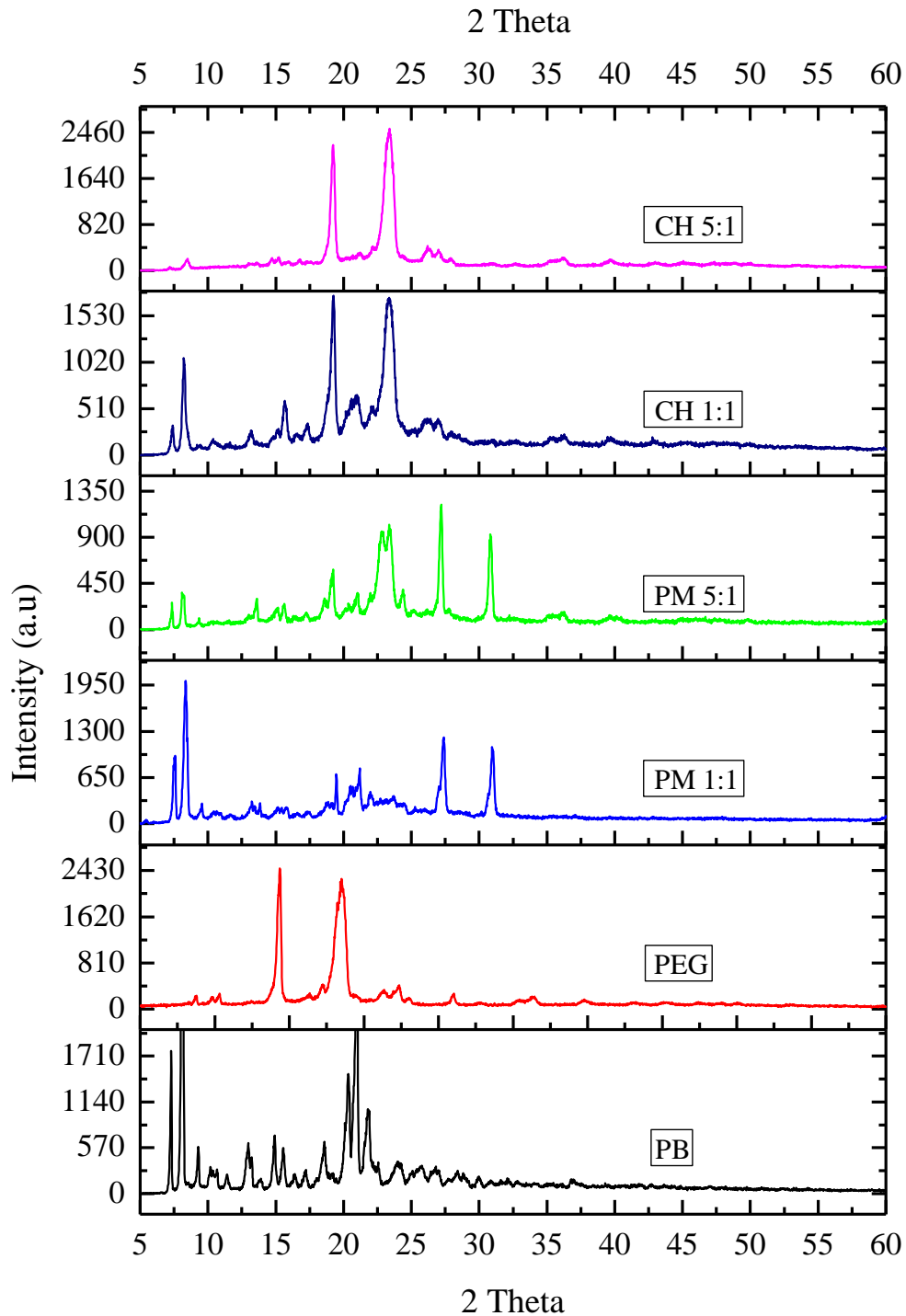
Appendix 5: XRD Patterns for ibuprofen IBU (+) S along with PEG based physical mixtures (PM) and conventionally heated (CH) formulations all at PEG / drug ratios of 1:1 and 5:1



Appendix 6: XRD Patterns for fenofibrate (FF) along with PEG based physically mixtures (PM) and conventionally heated (CH) formulations all at PEG / drug ratios of 1:1 and 5:1



Appendix 7: XRD Patterns for phenylbutazone (PB) along with PEG based physically mixtures (PM) and conventionally heated (CH) formulations all at PEG / drug ratios of 1:1 and 5:1



Appendix 8

Peer reviewed Publications

1. Titration calorimetry of surfactant-drug interactions : Micelle formation and saturation studies
LJ Waters, T Hussain, G.M.B Parkes
Journal of Chemical Thermodynamics, Vol. 53, 36-41, 2012
2. Inclusion of fenofibrate in a series of mesoporous silica using microwave irradiation
LJ Waters, T Hussain, G.M.B Parkes, J P Hanrahan, J.M Tobin
European Journal of Pharmaceutics and Biopharmaceutics, Vol. 85 (3-B), 936-941, 2013
3. Thermodynamics of micellisation: Sodium dodecyl sulfate/sodium deoxycholate with polyethylene glycol and model drugs
LJ Waters, T Hussain, G.M.B Parkes
Journal of Chemical Thermodynamics, Vol. 77, 77-81, 2014

Additional Outputs Not Included

Oral presentation

Controlled microwave assisted hot-melt solid dispersions to enhance solubility of poorly water soluble drugs
UKPharmSci, Edinburgh, 2013

Poster presentation

Pharmaceutical analysis: Drug-Micelle interactions
Swiss Pharma Science Day, Bern, Switzerland, 2011
Conference proceedings published in Swiss Pharma, Vol. 33 (10), p. 36, 2011

Controlled microwave assisted hot-melt solid dispersions to enhance solubility of poorly water soluble drugs
UKPharmSci, Edinburgh, 2013